UNIVERSITY OF CALIFORNIA SAN DIEGO

# Visible Light-Absorbing Polymers

A dissertation submitted in partial satisfaction of the
requirements for the degree Doctor of Philosophy

in

Chemistry

by

Vincent Tran

Committee in charge:

Professor Adah Almutairi, Chair
Professor Ulrich F. Muller, Co-Chair
Professor Adam J. Engler
Professor James A. McCammon
Professor Jerry Yang

2021

The Dissertation of Vincent Tran is approved, and it is acceptable in quality and form for publication on microfilm and electronically.

University of California San Diego

2021

# DEDICATION

I dedicate this doctoral dissertation to my parents, Trung Tran and Thuy Phan, my sister, Lynn Tran, and my girlfriend, Jessica Phan who have always shown me unyielding support and love during this process. I hope I have made you proud.

TABLE OF CONTENTS

# LIST OF ABBREVIATIONS

## Introduction

ONB, *o*-nitrobenzyl; DDS, drug delivery system; PNM, polymeric nanomaterials; ROP, ring-opening polymerization; PEG, polyethylene glycol; DASA, Donor-acceptor Stenhouse Adducts; Dex, dextran; AB, azobenzene; SP, spiropyran; GFP, green fluorescent protein; UV, Ultraviolet; NIR, near-infrared; Vis, visible; DOX, doxorubicin; SPN, semiconducting polymer nanomaterials; SP, semiconducting polymer; BBT, Bis[5-bromo-4-(2-octyldodecyl)-2-thienyl]-benzo[1,2-c:4,5-c']bis[1,2,5]thiadiazole; CPDT, 2,6-dibromo-4,4-bis(6-bromohexyl)-4H-cyclopenta[2,1-b:3,4-b']dithiophene; DT, 2,5-Bis(trimethylstannyl)thieno[3,2-b']thiophene; VIPA, vipadenant; DPPC, Dipalmitoylphophatidylcholine; DSPE-PEG, 1, 2-Distearoyl-sn-glycero-3-phosphoethanolamine-Poly(ethylene glycol); UCNP, upconverting nanoparticles; DNQ, 2-diazo-1,2-naphthoquinone.

## Chapter 1

ANBB, 2-(4'-N-dimethyl**a**mino-4-**n**itro-[1,1'-**b**iphenyl]-3-yl)**b**utane-1,4-diyl dicarbonyl; BODIPY, boron-dipyrromethene; UV, Ultraviolet; NIR, near-infrared; Vis, visible; MOIC, **MO**lecular **I**onic **C**ircuits; MOSAIC, MOIC added with **S**upr**A**molecular **I**onic **C**ircuit; DIBAL-H, Diisobutylammonium hydride; DMF, Dimethylformamide; DDQ, 2,3-Dichloro-5,6-dicyano-1,4-benzoquinone; TFA, Trifluoroacetic acid; NMR, nuclear magnetic resonance; GPC, gel permeation chromatography; THF, tetrahydrofuran; DIPEA, N,N-Diisopropylethylamine; TLC; thin layer chromatography.

Chapter 2

ONB, *o*-nitrobenzyl; UV, Ultraviolet; NIR, near-infrared; Vis, visible; Dex, dextran; ROS, reactive oxygenated species; BIST, dinitro derivative of bisstyrylthiophene; MeBIST, methyl derivative of the dinitro derivative of bisstyrylthiophene; ANBB, 2-(4′-*N*-dimethylamino-4-nitro-[1,1′-biphenyl]-3-yl)butane-1,4-diyl dicarbonyl; TBDMS-Cl, tert-Butyldimethylsilyl chloride; TBAF, tetra-n-butylammonium fluoride; DCM, dichloromethane; DME, dimethoxyethane; TBACl, tetrabutylammonium chloride; DMF, dimethyl formamide; THF, tetrahydrofuran, LC-MS, liquid chromatography-mass spectroscopy; NMR, nuclear magnetic resonance; DBU, 1,8-Diazabicyclo[5.4.0]undec-7-ene; GPC, gel permeation chromatography; DMSO, dimethyl sulfoxide; PMMA, poly(methyl methacrylate); PVA, polyvinyl alcohol; DLS, dynamic light scattering; ANBP, (2-(40-(N,N-dimethylamino)-4-nitro-[1,10-biphenyl]-3-yl) propyl carbonyl); CDI, 1,1′-carbonyldiimidazole; PBS, phosphate buffered saline

Chapter 3

UV, ultraviolet; VL, visible light; IR, infrared; ROS, reactive oxygenated species; DNA, deoxyribonucleic acid; IPD, immediate pigment darkening; PPD, persistent pigment darkening; DT, delayed tanning; BVL, blue visible light; MELASQoL, melasma quality of life scale; MASI, melasma area and severity index; FDA, Food and Drug Administration; ANBB, 2-(4′-*N*-dimethylamino-4-nitro-[1,1′-biphenyl]-3-yl)butane-1,4-diyl dicarbonyl; ANBP, (2-(40-(N,N-dimethylamino)-4-nitro-[1,10-biphenyl]-3-yl) propyl carbonyl); MB-1-P, methyl BIST polymer; BIST, dinitro derivative of bisstyrylthiophene; DLS, dynamic light scattering; TBDMS-Cl, tert-Butyldimethylsilyl chloride; TBAF, tetra-n-butylammonium fluoride; DCM, dichloromethane; DME, dimethoxyethane; TBACl, tetrabutylammonium chloride; DMF, dimethyl formamide; THF,

tetrahydrofuran, LC-MS, liquid chromatography-mass spectroscopy; NMR, nuclear magnetic resonance; NP, nanoparticle; PVA, polyvinyl alcohol; CDI, 1,1′-carbonyldiimidazole; PBS, phosphate buffered saline; DI, deionized; MALDI-TOF, matrix-assisted laser desorption ionization time-of-flight;

LIST OF FIGURES

LIST OF SCHEMES

LIST OF TABLES

ACKNOWLEDGEMENTS

I would like to acknowledge Prof. Adah Almutairi for her guidance in my doctoral work and for giving me the opportunity to explore new research fields.

I would also like to acknowledge the other members of my doctoral committee: my co-advisor Prof. Uli Muller, Prof. Jerry Yang, Prof. Andrew McCammon, and Prof. Adam Engler, as well as former committee members in my departmental exam: Prof. Emmanual Theodorakis and Prof. Seth Cohen. Their support, encouragement, and feedback were much appreciated

I would like to express gratitude to my old lab mates: Dr. Peng-Hao Hsu, Dr. Carina Arboleda, Prof. Alexandra Stubelius, and Dr. Sangeun Lee. Their guidance and support have been invaluable to me. I also thank the other former member in the lab: Dr. Amy Moore, Dr. Viet Anh Nguyen Huu, Dr. Sha He, Dr. Wangzhong Sheng, for their help and for providing an environment where I felt welcomed. I would also like to extend my gratitude to the undergraduate students who have helped with me with my research, especially Kimi SooHoo and Rachel Strons. I would also like to thank my undergraduate professor, Dr. Minehan, for his invaluable advice and for teaching me my love for chemistry. I also want to thank Kevin Ng and Dr. Xiao Cai for all the chemistry discussions and feedback. I would like to thank my close friend, Angie Truong, for her words of encouragement and for always talking me through my most stressful times. Lastly, I would like to thank my girlfriend, Jessica Phan, for all her love and support, and for believing in me even when I didn't.

Chapter 1 is coauthored with Dr. Adah Almutairi. The dissertation author was the primary author of chapter 1. Chapter 2 is coauthored with Dr. Peng-Hao Hsu and Dr. Adah Almutairi. The dissertation author was the primary author of chapter 2. Chapter 3 is coauthored with Dr. Adah Almutairi and the dissertation author was the primary author of this chapter.

## VITA

| | |
|---|---|
| 2013 | Bachelor of Science, California State University Northridge |
| 2017 | Master of Science, University of California San Diego |
| 2015–2021 | Teaching Assistant, University of California San Diego |
| 2021 | Doctor of Philosophy, University of California San Diego |

## FIELDS OF STUDY

Major Field: Chemistry

Studies in Polymer Synthesis and Materials Science
Professor Adah Almutairi

ABSTRACT OF THE DISSERTATION

Visible Light-Absorbing Polymers

by

Vincent Tran

Doctor of Philosophy in Chemistry

University of California San Diego, 2021

Professor Adah Almutairi, Chair

Professor Ulrich F. Muller, Co-Chair

Polymeric nanomaterials have been well established as drug delivery systems as they can protect therapeutic payloads from the harsh *in vivo* environment, minimize degradation of therapeutics upon administration, allow for delivery of higher concentrations, and minimize unwanted side effects. These materials can be tailored to respond to a variety of external and biological stimuli such as pH, enzymes, redox molecules, light, and heat. Light is an attractive trigger because it is not limited by physiological conditions and can be controlled remotely. This provides great spatial and temporal control of the triggered reaction. In the past decades, most light-responsive materials have utilized UV due to the large library of molecules that absorb that wavelength and its efficient one-photon absorption mechanism. However, its poor penetration depth and deleterious health effects has made it less attractive. As an alternative, near-infrared (NIR) responsive materials have been explored. Although NIR is biologically benign and can penetrate much deeper than UV, it can be disadvantageous as it is much lower in energy and would require materials to upconvert or undergo inefficient two-photon absorption to trigger its photochemistry. Visible light provides a great middle ground as it is higher in energy than NIR and much less deleterious than UV. However, despite the decades of research, very few materials have been developed that utilize visible light for polymeric nanomaterials. To further advance this field, research into visible light responsive polymers is described in this dissertation. In chapter 1, a fluorescent dye was conjugated onto an established visible light polymer to allow for *in vivo* tracking and monitoring. In chapter 2, a dinitro derivative of bisstyrylthiophene was explored as a potential visible light polymer. Additionally, a biphenyl visible light chromophore was conjugated onto dextran to be explored as a visible light responsive polymer. In chapter 3, the visible light responsive materials that were developed are used to assess their absorption of blue visible light from ambient sunlight.

# INTRODUCTION

Photo-triggered Polymeric Nanomaterials for Controlled Release

## 0.1 Abstract

The incorporation of nanotechnology for drug delivery systems (DDS) has garnered a considerable amount of research interest in the past few years. The use of stimuli-responsive polymeric nanomaterials (PNMs) has been especially popular because they provide a controlled release of therapeutics, which will allow a more controlled biodistribution and lower doses, thereby decreasing undesired side effects. Throughout the years, several endogenous (pH, redox, enzymes) and exogenous (temperature, light, electrical or magnetic field) triggers have been harnessed to develop materials for the release of a drug cargo. Of these stimuli. light is especially attractive as it can be applied remotely and activates chemistries on-demand independently of biological environment unlike other chemical systems that rely on biological stimuli. Additionally, a wide range of parameters (wavelength, light intensity, exposure time, and irradiation area) can be adjusted for spatial and temporal control thus controlling release. Here, we discuss the many ways light has been utilized in the development of materials for DDSs.

## 0.2 Introduction

Nanomedicine is a growing field of research that utilizes nanotechnology towards the diagnosis and treatment of diseases. Polymeric nanomaterials have been well established as drug delivery systems as they can protect therapeutic payloads from the harsh *in vivo* environment, minimize degradation of therapeutics upon administration, allow for delivery of higher

concentrations, and minimize unwanted side effects. PNMs can be tailored to respond to specific triggers by utilizing natural and synthetic organic materials. The goal of these stimuli-responsive PNMs is to control the place and time of therapeutic release. This controlled release would allow for lower administration dose and reduce systemic toxicity.

Many PNMs have been developed that respond to a variety of endogenous and exogenous triggers such as pH, temperature, reactive oxygen species, enzymes, magnetic field, and light. Of these triggers, light is a very attractive trigger as it is not limited by physiological parameters which can vary between individuals, often leading to poorly controlled release.[1] Light provides excellent spatial and temporal control because it can be applied externally and tuned to a specific wavelength.[2-7] Additionally, light is non-invasive and provides a wide range of parameters such as wavelength, intensity, and exposure time, which can be adjusted and tuned for a more controlled release. Currently, most photo-triggered PNMs utilize ultraviolet (UV, 100-400 nm), visible (vis, 400-740 nm), and near-infrared (NIR, 740 nm - 1 mm)[8] light as their stimuli, but each wavelength has its own advantages and limitations.

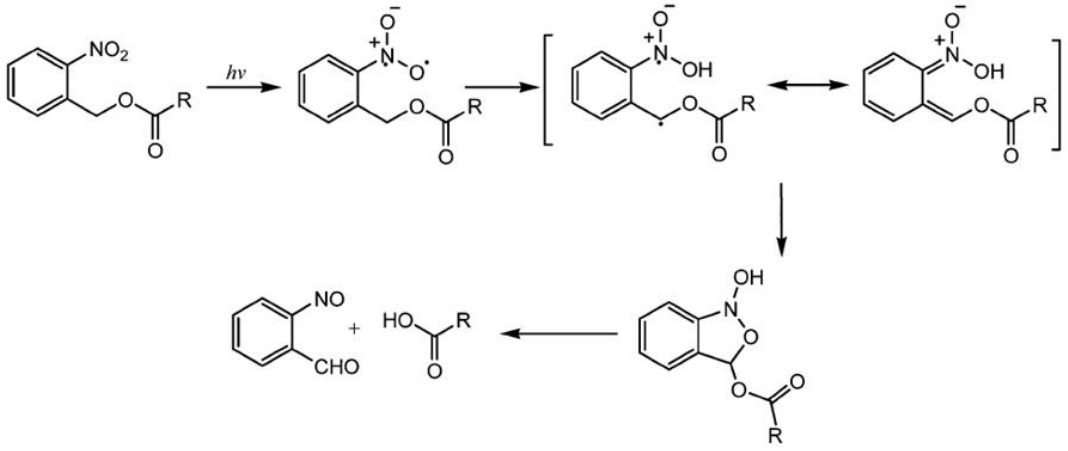


Figure 0.1. The photocleavage mechanism of o-nitrobenzyl derivatives. Reprinted from Ref. 41 with permission from The Royal Society of Chemistry.

Of the photo-triggered PNMs in literature, most utilize UV light due to the large library of organic molecules that absorb those wavelengths.[9] UV wavelengths also provide enough energy

to allow for bond cleavage, isomerization, and rearrangement to release therapeutic agents from PNMs.[10] However, despite the efficiency of their photochemistry, UV light has poor skin penetration[8] and the deleterious health effects from UV exposure are well documented.[11-14] On the contrary, NIR can penetrate much deeper (deeper than 5 mm) into living tissue and is not damaging to tissue and cells.[1,2] However, NIR lacks the energy that UV provides to undergo photochemical reactions. PNMs that utilize NIR generally overcome this disadvantage by i) using IR-sensitive material to generate heat for temperature sensitive materials, ii) utilize two-photon absorbing PNMs, and iii) using lanthanides to convert the NIR to higher energy wavelengths.[10] The two-photon absorption method is inefficient and requires prolonged exposure to high power NIR, which can generate heat that damages biological tissue.[15,16] Although visible light wavelengths are not as damaging as UV and can undergo a more efficient one-photon excitation, they still penetrate poorly into the skin and are limited to subcutaneous applications.[10]

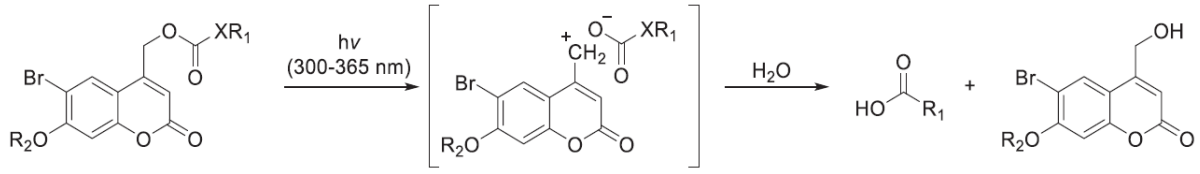


$R_2$ = O-R , NH-R, S-R or R; $R_2$= OH, $NR_2$ or R

Figure 0.2. The photocleavage mechanism of coumarin derivatives. Reprinted from Ref. 10 with permission from John Wiley and Sons.

In this chapter, we will discuss the different ways light can be utilized in DDS. First, we will discuss the photoinduced isomerization / rearrangement and photocleavage caused by direct UV/visible light absorbance. Then we will discuss how the lower energy NIR can be used to release payloads from PNMs.

### 0.3 UV and Visible Light Responsive PNMs

Most materials capable of photorelease in the literature rely on one-photon excitation by UV light, primarily due to the prevalence and synthetic accessibility of photoactive chromophores with direct absorption of UV wavelengths. The chromophores absorb UV light which provide enough energy to undergo photochemical reactions resulting in bond cleavage, isomerization, and rearrangement. Here we discuss a few of the chromophores that can undergo these transformations upon irradiation of UV or visible light.

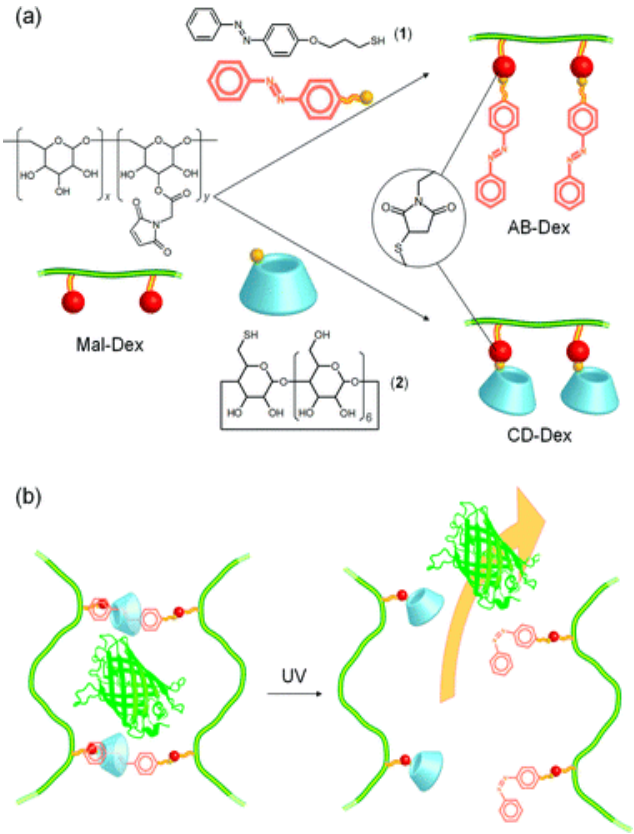


Figure 0.3. (a) preparation of azobenzene conjugated dextran (AB-Dex) and β-cyclodextrin conjugated dextran (CD-Dex). (b) Schematic representation of the photoresponsive release of protein from the gel composed to *trans* AB-Dex and CD-Dex. Upon irradiation with UV light, the *trans*-AB will photoisomerize to the *cis* form, resulting in the dissociation of the crosslinking points, release the protein. Reprinted from Ref. 18 with permission from The Royal Society of Chemistry.

*0.3.1 Photoinduced Isomerization and Rearrangement*

UV/visible light induced photoisomerization is a useful tool for light-responsive PNMs. Upon irradiation, the photosensitive moiety will photoisomerize which will lead to the disassembly of the PNM thereby releasing the payload. Azobenzene (AB) and spiropyran (SP) derivatives are the two most utilized moieties among photoinduced isomerization PNMs. Upon irradiation with UV light, azobenzene isomerizes from the stable *trans* isomer to the metastable *cis* isomer. The process can be reversed by irradiation with visible light or by heat.[10] Wang *et al.* demonstrated that the photoisomerization of azobenzene surfactants lead to the disassembly of block ionomer complex vesicles. They synthesized an azobenzene-containing surfactant and utilized its positive charge to undergo electrostatic complexation with a double-hydrophilic block copolymer of poly(ethylene glycol)-*block*-poly(acrylic acid). They saw that upon irradiation with UV light (365nm for 300s) the AB surfactant underwent the *trans-cis* photoisomerization, leading to a structural change of the block ionomer complexes. This, accompanied by the drastic change in particle size, suggests that the azobenzene isomerization led to the disassembly of the particle. Upon irradiation with visible light (450 nm for 900s), the metastable *trans* isomer reverted back to the more stable *cis* form, which reassembled the vesicle structures.[17] Peng and coworkers conjugated azobenzene onto dextran via the thiol-maleimide reaction (Figure 0.3). This AB-dextran polymer was mixed with β-cyclodextrin conjugated dextran polymers to form a light-triggered supramolecularly cross-linked hydrogel, entrapped with green fluorescent protein (GFP) as a model protein. After irradiation with UV light at 365 nm, the hydrogel dissociated due to the *trans-cis* photoisomerization, leading to the dissolution of the hydrogel and release of GFP (65% released after 2 hours of irradiation).[18]

Spiropyran (SP) is a photoresponsive molecule that can reversibly isomerize from its hydrophobic, non-ionic state to a polar zwitterionic form after UV irradiation. Similar to AB, the SP *trans-to-cis* isomerization is reversible under visible light irradiation or heat. Son and coworkers conjugated SP onto hyperbranched polyglycerols to form UV-responsive micellar PNMs that encapsulated pyrene as a model hydrophobic therapeutic. Upon irradiation at 254 nm, the SP would isomerize to its zwitterionic *cis* form, leading to a hydrophobicity change that destabilized the micelles, releasing the hydrophobic cargo. They found that upon visible light irradiation at 620 nm, SP would revert back to its hydrophobic *trans* form and reform the micellar structure.[19] Recently, Razavi *et al.* developed multi-responsive PNMs that incorporated SP into poly(dimethylaminoethyl methacrylate). Under UV irradiation at 365 nm, the SP incorporated micelles demonstrated the controlled release of doxorubicin.[20]

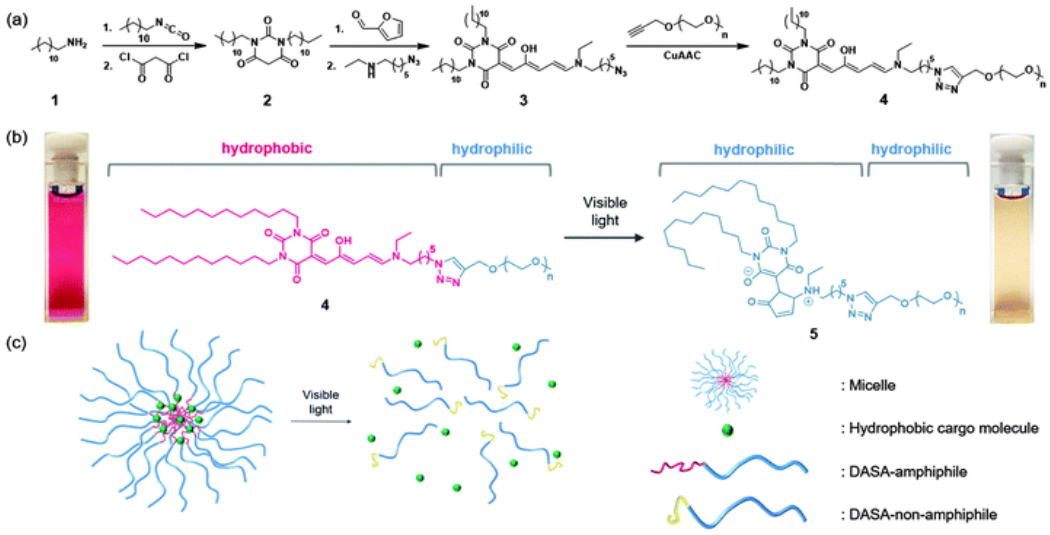


Figure 0.4. (a) The synthesis of the visible light responsive DASA. (b) The hydrophobicity switch of DASAs upon visible light irradiation that leads to (c) the disassembly of the micelle, releasing the hydrophobic cargo molecule. Reprinted from Ref. 21 with permission from The Royal Society of Chemistry.

Donor-acceptor Stenhouse adducts (DASAs) is a relatively new class of molecules that undergo a hydrophilicity switch under visible light irradiation. Poelma *et al*. demonstrated the

self-assembly of a PEG functionalized DASA-amphiphile into micelles, with the hydrophobic DASA as the core. Under visible light irradiation, the DASA would undergo photoisomerization, causing a hydrophilicity switch which leads to the disassembly of the micelle. They demonstrated the controlled delivery of therapeutics by encapsulating paclitaxel, a commonly employed anti-tumor treatment (Figure 0.4). Upon irradiation with visible light, cells treated with paclitaxel loaded DASA-based micelles displayed a decrease in cell viability as opposed to non-irradiated cells, indicating the release of the drug was mediated by the irradiation.[21] More recently, Rifaie-Graham demonstrated the functionalization of block copolymers with different DASAs resulted in the wavelength selective release of enzymes from polymersomes. The DASA polymersomes would either react with red light or green light, depending on the DASA.[22]

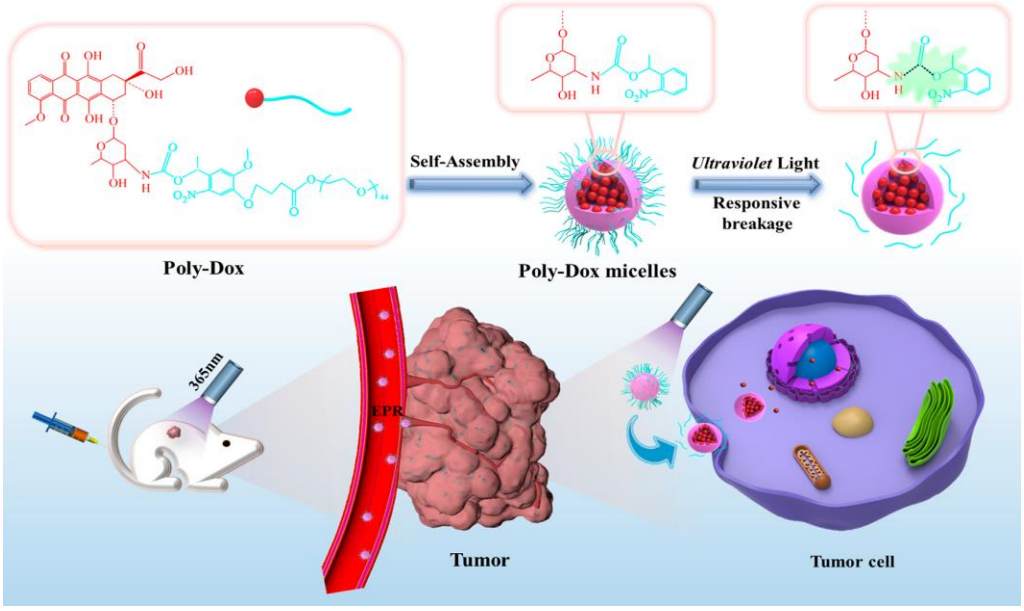


Figure 0.5. The schematic illustration of the self-assembly of Poly-Dox micelles bearing the ONB moiety as a linker. Upon irradiation of UV light, the ONB group photocleaves, releasing DOX from the system. Ref. 26.

### *1.3.2 Photocleavage*

Photocleavable polymers are one of the most studied methods in photoresponsive DDSs. The incorporation of a photolabile bond in the polymer backbone induces the release of therapeutic

payloads upon irradiation of UV or visible light. Two of the most commonly utilized moieties in photocleavable polymers are the *o*-nitrobenzyl (ONB) and coumarin based groups.[10] The ONB group is one of the most studied irreversible photo-responsive molecules in polymer chemistry due to its versatility in being incorporated in different polymer networks. Upon UV light irradiation, the ONB chromophore abstracts a hydrogen from the methylene carbon forming an aci-nitro intermediate. This intermediate then rearranges to form a benzoisoxaline derivative that cleaves to form carboxylic acid and o-nitrosobenzaldehyde as photoproducts (Figure 1).[23] The ONB photolabile group was first incorporated into polymers by Petropoulos in 1977.[24] Recent reports of PNMs utilizing ONB demonstrate how popular the chromophore is. In June of 2021, Yamaguchi and coworkers utilized the ONB chromophore to formulate photodegradable hydrogels consisting of avidin and biotinylated synthetic polymers. In their work, Yamaguchi *et al.* incorporated the ONB chromophore as a linker between the 4armPEG and the biotinylated cell adhesion peptides. The hydrogels were incorporated with NIH3T3 cells and upon irradiation with 405 nm light, the cells were released from the hydrogel.[25] In another recent study, Chen *et al.* utilized ONB to develop light-responsive nano-micelles for the release of doxorubicin (Figure 0.5). In this study, Chen and coworkers conjugated DOX directly onto PEG using the ONB moiety as a linker and formed micelles. After just several minutes of UV irradiation, the ONB group photocleaved, releasing DOX and producing the *o*-nitrosophenone-PEG derivative as a photoproduct.[26]

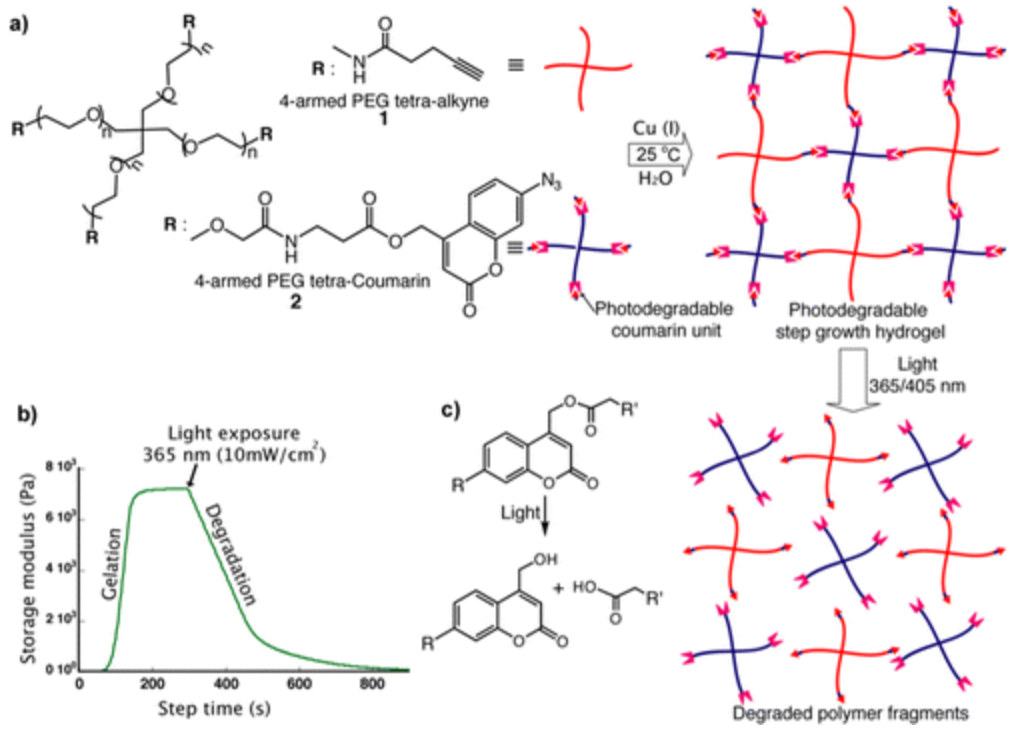


Figure 0.6. (a) Chemical structures of the coumarin conjugated 4armPEG and 4armPEG tetra-alkyne that cross-links to form the photoresponsive hydrogel. (b) the decrease in gelation after UV irradiation at 365 nm. (c) The photodegradation products due to the photocleavage of the coumarin derivative. Reprinted (adapted) with permission from *ACS Macro Lett.* 2014, 3, 6, 515–519. Copyright 2014 American Chemical Society.

The other photocleavable moiety that is often employed in PNMs is coumarin. Coumarin was first explored as a photoactive group in 1984 by Givens and Matuszewski.[27] This photoactive group has a larger molar absorption coefficient than ONB which allows for faster photorelease rate compared to ONB.[1] Upon irradiation with UV light, the carbonyl group on coumarin decomposes into an ionic intermediate which will release the functional group with hydrolysis (Figure 0.2). Many coumarin analogues have been synthesized to improve solubility and increase its absorption wavelengths. Azagarsamy *et al*. reported a new class of photodegradable coumarin-based hydrogels in 2014 (Figure 0.6). They formulated hydrogels using an amine-terminated coumarin azide that was conjugated onto 4armPEG and crosslinked them with a 4armPEG decorated with an alkyne using copper-catalyzed click chemistry. Irradiation with both 365 nm and 405 nm lead

to the rapid photodegradation of the coumarin moieties which eroded the hydrogel.[28] More recently, Karthik and coworkers demonstrated the use of coumarin analogues for the delivery of a cocktail of anticancer drugs. In their work, they utilized a combination of direct conjugation and encapsulation of the therapeutic payloads. Chlorambucil was directly conjugated onto 7-hydroxycoumarin and a photoresponsive polymer was formed by ring-opening polymerization (ROP) with caprolactone. PNMs were formed by nanoprecipitation which encapsulated doxorubicin. In their *in vitro* cytotoxicity studies, the photoresponsive DDSs were less toxic to cancer cells until they were irradiated with UV light, demonstrating the photocleavage of coumarin to release chlorambucil, which would lead to the release of doxorubicin.[29]

**0.4 Near Infrared Responsive PNMs**

Utilization of near-infrared wavelengths (740-1000 nm) would allow for deeper tissue penetration as common endogenous chromophores like heme, melanin, and water do not absorb these wavelengths. However, there are very few photoreactive chromophores that can absorb these wavelengths and undergo the desired photochemistry directly. To overcome this challenge, methods such two-photo excitation and NIR-to-UV upconversion have been utilized to break, isomerize, and rearrange molecules. Here we discuss how PNMs can utilize the low energy NIR wavelengths to obtain the desired photochemistry.

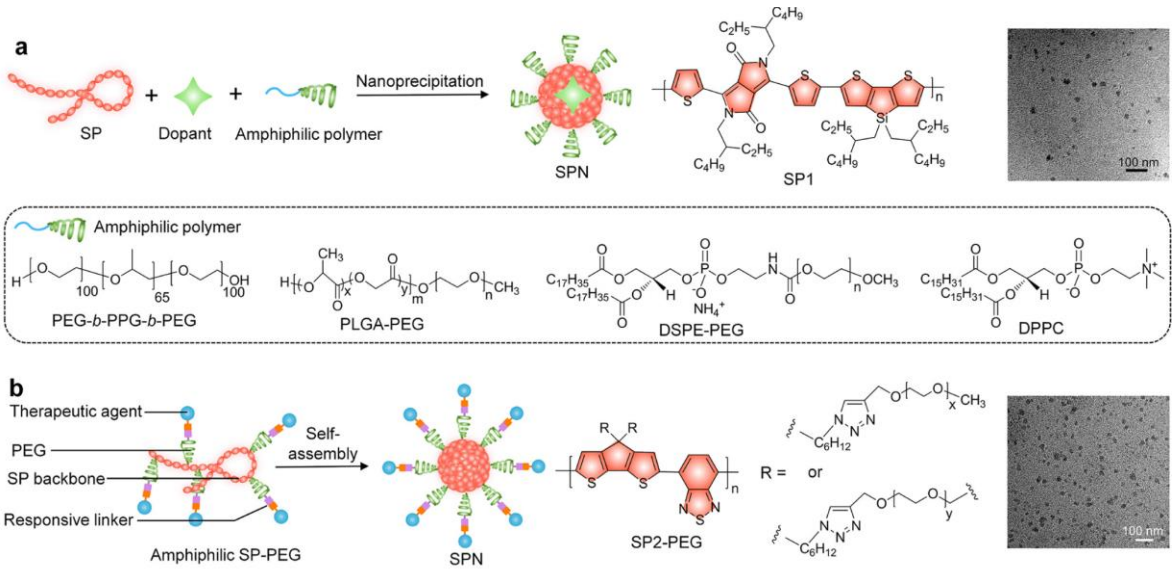


Figure 0.7. The preparation of SPNs utilizing different NIR absorbing photothermal triggered materials. Reprinted (adapted) with permission from *Acc. Chem. Res.* 2020, 53, 4, 752–762. Copyright 2020 American Chemical Society.

### *0.4.1 NIR Induced Thermochemistry*

Despite its deep tissue penetration and minimal cytotoxicity, NIR lacks sufficient energy to undergo photochemical changes. Many organic NIR absorbing materials incorporate cyclopentadithiophene, dikeopyrrolopyrrole, 2,1,3-benzothiodiazole, and indaceno thiophene moeities or a combination of them as copolymers for a variety of applications.[30-32] However, in regard to photo-releasing materials, PNMs generally utilize NIR to generate heat to undergo photothermal triggered release. These semiconducting polymer nanomaterials (SPNs) are an emerging category of optically active PNMs as they possess good biocompatibility and their optical activity is size independent.[32] SPNs generally contain a semiconducting polymer (SP) backbone that is formulated into nanomaterials with thermolabile groups or facilitate a phase change to allow for the release of therapeutic agents. Recently, Pu's group. utilized two SPs in their preparation of SPNs as photoactivatable cancer treatments. The first SP is composed diketopyrrolopyrrole and thiophene units (SP1) while the second SP contained

cyclopentadiothiophene units (SP2) (Figure 0.7). With these two SPs, Li was able to formulate SPNs for a variety of delivery applications. They were able to encapsulate the agonist, capsaicin, through the nanoprecipitation of SP1 and amphiphilic lipids DSPE-PEG and DPPC. Upon irradiation at 808 nm, the SPN would generate heat up to 73 ℃ after 6 mins and allow for the release of the cargo by the melting of the lipid layer. They also demonstrated the ability to conjugate temperature-sensitive protease onto the SP2 backbone to formulate nanoparticles by self-assembly. Upon irradiation at 808 nm, this SPN would generate heat to activate Bromelain enzyme activity. Additionally, Pu's group was also able to develop self-assembled NIR absorbing dendronized SPs that could load plasmids through electrostatic attraction. Here the dendronized SP would deliver the plasmid into the cell nucleus and upon irradiation at 808 nm, raise the local temperature which eventually leads to the expression of target genes.

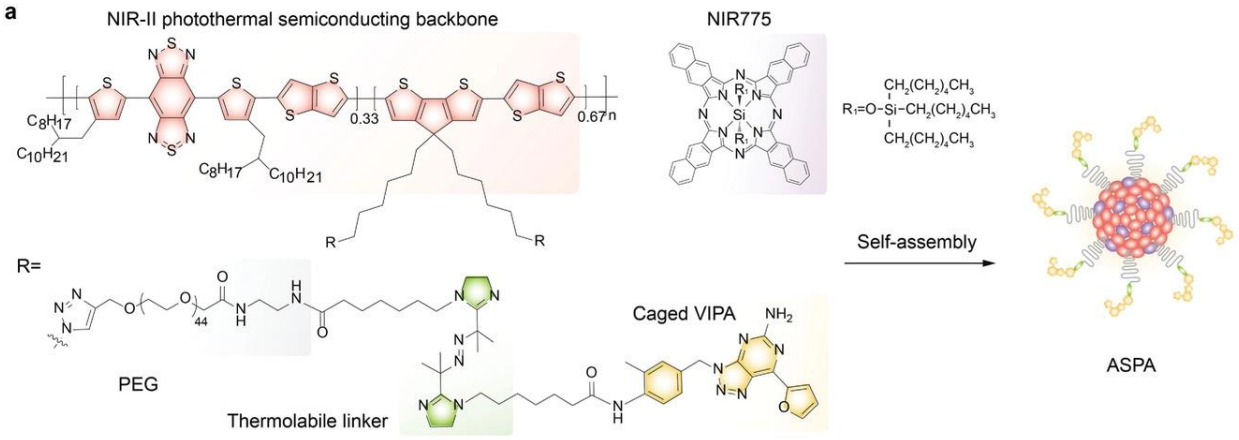


Figure 0.8. The self-assembly of NIR-II absorbing SNPs with PEG conjugated with an azo-based thermolabile linker to form nanoparticles. Reproduced from Ref. 33 with permission from John Wiley and Sons.

While most NIR responsive materials utilize NIR-I (650-950 nm), NIR-II (1000-1500nm) provides deeper tissue penetration. Pu's group developed a SP that can effectively absorb NIR-II wavelengths for the photoregulation of immunometabolism for tumor therapy. The polymer was synthesized by Stille polymerization between Bis[5-bromo-4-(2-octyldodecyl)-2-thienyl]-

benzo[1,2-c:4,5-c']bis[1,2,5]thiadiazole (BBT), 2,6-dibromo-4,4-bis(6-bromohexyl)-4H-cyclopenta[2,1-b:3,4-b']dithiophene (CPDT), and 2,5-Bis(trimethylstannyl)thieno[3,2-b']thiophene (DT). The SP was further conjugated with an adenosine A2A receptor agonist, VIPA, via a AB-based thermolabile linker (Figure 0.8).[33] This SP solution was irradiated at 1064 nm and reached a maximum temperature of 67 °C, with a photothermal conversion efficiency of 85.4%.

*0.4.2 Upconversion of NIR*

Another method of utilizing the low-energy NIR for photocontrolled drug release is using upconverting nanoparticles (UCNPs). UCNPs are crystal matrixes doped with lanthanide ions that have anti-Stokes luminescence properties, allowing them to absorb NIR and emit higher-energy photons with wavelengths ranging from UV to visible.[34] When the lanthanide ions are in the excited state and continue to receive excessive energy, they can reach higher excited states and return to the ground state by releasing a higher energy photon.[35] Here we discuss how these UCNPs can be combined with light-responsive/degradable polymers for drug delivery.

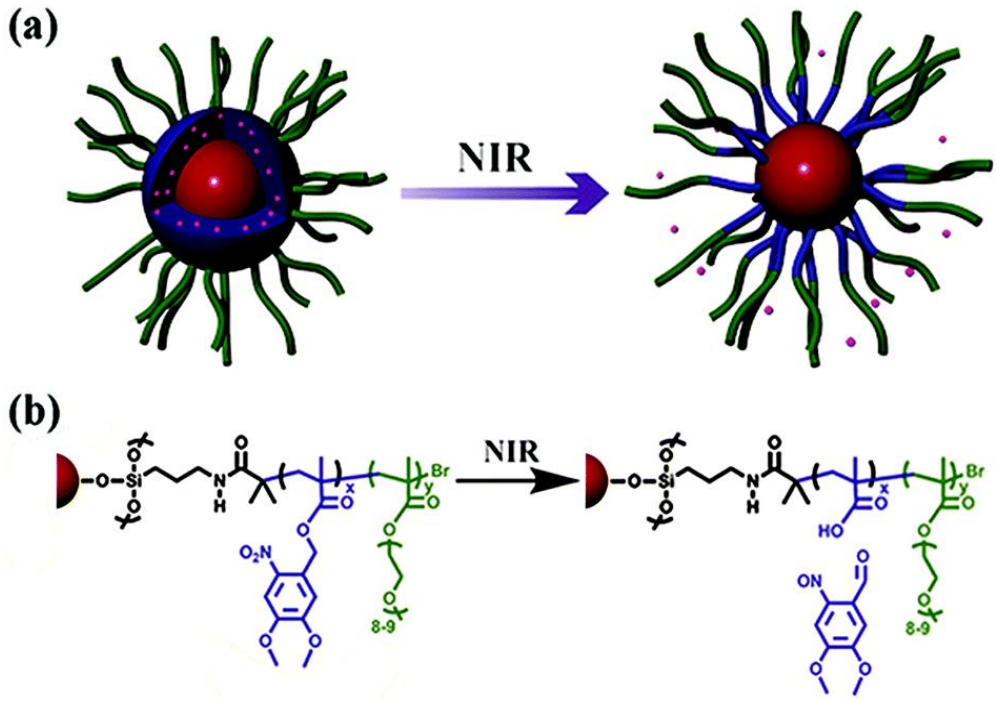


Figure 0.9. (a) A schematic illustration of the self-assembly of UCNP coated with an ONB containing, amphiphilic diblock copolymer. (b) The upconversion of NIR light to UV to photocleave the ONB, leading to a hydrophobicity switch, assembling the micelle. Reproduced from Ref. 37 with permission from The Royal Society of Chemistry.

There are a variety of photoresponsive functional groups that have been incorporated into polymers. These functional groups can undergo irreversible photocleavage such as *o*-nitrobenzyl esters and cumarinyl esters, but can also undergo reversible isomerizations with azobenzene and spiropyran. These functional groups and mechanisms will be further discussed in the following sections. By combining UCNPs with polymers containing photoresponsive functional groups, NIR can be converted to UV/visible light which can induce the photocleavage or isomerization of the polymers. Yan *et al*. demonstrated the viability of this method by loading NaYF4:Tm:Yb UCNP into micelles composed of an amphiphilic photosensitive diblock copolymer consisting of the hydrophilic poly-(ethylene oxide) and hydrophobic polymethacrylate decorated with the *o*-nitrobenzyl group. When irradiated with a 980 nm laser, NaYF4:Tm:Yb nanoparticles absorb the NIR light and emit a photon around 350 nm. The modified ONB moiety on the polymer absorbed

that emitted photon and underwent photocleavage, converting the polymethacrylate block of the copolymer to the hydrophilic poly-(methacrylic acid). This hydrophilicity switch destabilizes the micelle.[36] Recently, Xiang *et al.* demonstrated an approach that confines a single UCNP ($NaYF_4$:18%Yb/0.5%Tm@$NaYF_4$) inside the micelle core. This was done by growing an amphiphilic copolymer from the UCNP with a hydrophobic UV-responsive polymer as the core block and a hydrophilic polymer as the outer block. The anti-tumor drug, doxorubicin, was also encapsulated into this nanoparticle. Upon irradiation at 980 nm, the UCNP emitted a photon at around 350 nm, which again, causes the photocleavage of the ONB moiety inside the hydrophobic block, converting it into a hydrophilic block which releases the drug (Figure 0.9).[37]

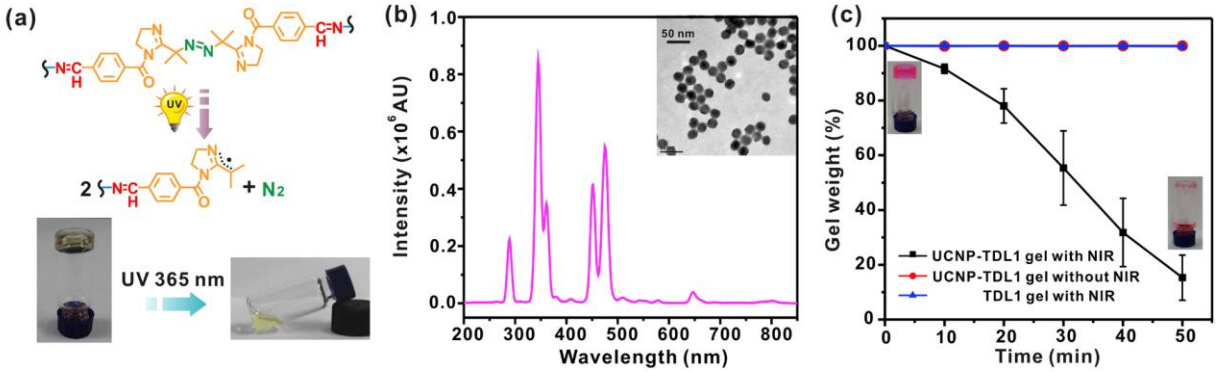


Figure 0.10. The incorporation of UCNPs into a hydrogel composed with UV photocleavable AB-linkers. Upon irradiation with NIR, the encapsulated UCNPs upconvert the incoming photons to UV, causing the AB-moiety to degrade. Reproduced from Ref. 38 with permission from Elsevier.

NIR upconversion is not just limited to micelles with ONB functional groups. Hu and coworkers demonstrated the use of UCNPs in hydrogel formulations with the photolabile AB moiety. They embedded UCNPs (NaYF4:Yb,Tm) in 4arm-PEG-NH2 hydrogels crosslinked by two AB-containing linkers along with doxorubicin. Upon NIR irradiation, the UCNPs emitted UV photons, triggering the photocleavage of the AB-moiety, releasing the anti-tumor agent (Figure 0.10).[38]

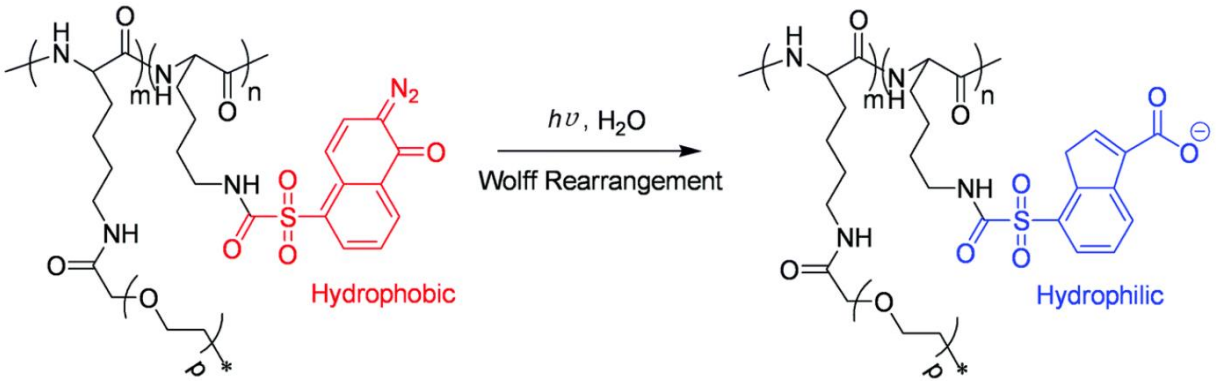


Figure 0.11. The DNQ conjugated PEG polymer that undergoes a hydrophobicity switch via the Wolff Rearrangement after two-photon NIR excitation. Reproduced from Ref. 40 with permission from The Royal Society of Chemistry.

*0.4.3 Two-Photon Absorption*

While the one-photon absorption of NIR is not energetic enough to trigger photo-activated systems, a two-photon excitation approach could be utilized to undergo photochemical changes. Two photon absorption requires simultaneous absorption of two identical or different frequencies. Jiang and coworkers demonstrated the application of two-photon absorption of NIR in polymeric micelles. They synthesized an *o*-nitrobenzyl-containing amphiphilic block copolymer and formulated micelles containing the hydrophobic dye, Nile Red, as a model drug. Upon irradiation at 700 nm, the ONB moiety photocleaved, leading to a hydrophilicity switch, prompting the release of Nile Red which was measured by the quenching of its fluorescence intensity in aqueous media. Although the two-photon excitation of the micelles led to the release of the dye, Jiang *et al.* noted that the irradiation time needed was much longer than what was needed under UV irradiation.[39] More recently, in 2015, Yuan and coworkers reported on the release of doxorubicin from an amphiphilic polymer conjugated with a 2-diazo-1,2-naphthoquinone (DNQ) moiety. They demonstrated that the two-photo absorption of NIR at 800 nm induced a hydrophobicity switch of the hydrophobic DNQ moiety to its hydrophilic rearranged photoproduct via the Wolff

rearrangement. This hydrophobicity switch allowed for the disassembly of the nanoparticle (Figure 0.11).[40]

## 0.5 Conclusion

UV activated photochemistry is rapid and efficient but practical application of these chromophores towards drug delivery in biological systems are limited for a variety of reasons. First, UV light penetration through the skin is limited as many endogenous molecules absorb UV light. Secondly, UV light has a deleterious effect on healthy tissues and cells, causing them to degrade or die. NIR wavelengths can penetrate deeper into the skin and are much less harmful compared to UV. However, materials that harness NIR require either upconversion to UV wavelengths or two-photon absorption. These non-linear optical phenomena are inefficient and require high-powered, focused lasers to occur. In addition to these limitations, *in vivo* of NIR drug delivery systems would also be limited because mammalian tissue scatters and defocuses NIR laser light, lowering the power density that would reach an affected area. The shortcomings of UV and NIR absorbing photosystems clearly display a need for the development of a chromophore that can undergo one-photon absorption of a biologically innocuous wavelength of light. By incorporating visible light (400-750 nm) absorbing chromophores, we can develop polymers that can efficiently photoreact upon one-photon absorption. Though the wavelength penetration of visible light is lower than NIR, it is still less damaging than UV and would therefore provide the perfect middle ground between the two wavelengths.

## 0.6 Abbreviations

ONB, *o*-nitrobenzyl; DDS, drug delivery system; PNM, polymeric nanomaterials; ROP, ring-opening polymerization; PEG, polyethylene glycol; DASA, Donor-acceptor Stenhouse Adducts; Dex, dextran; AB, azobenzene; SP, spiropyran; GFP, green fluorescent protein; UV, Ultraviolet; NIR, near-infrared; Vis, visible; DOX, doxorubicin; SPN, semiconducting polymer nanomaterials; SP, semiconducting polymer; BBT, Bis[5-bromo-4-(2-octyldodecyl)-2-thienyl]-benzo[1,2-c:4,5-c']bis[1,2,5]thiadiazole; CPDT, 2,6-dibromo-4,4-bis(6-bromohexyl)-4H-cyclopenta[2,1-b:3,4-b']dithiophene; DT, 2,5-Bis(trimethylstannyl)thieno[3,2-b']thiophene; VIPA, vipadenant; DPPC, Dipalmitoylphophatidylcholine; DSPE-PEG, 1, 2-Distearoyl-sn-glycero-3-phosphoethanolamine-Poly(ethylene glycol); UCNP, upconverting nanoparticles; DNQ, 2-diazo-1,2-naphthoquinone.

## 0.7 References


1) Beaute, L., McClenaghan, N., Lecommandoux, S.; *Adv. Drug Deliv. Rev.,* **2019**, 138, 148 166.

2) Fomina, N., Sankaranarayanan, J., Almutairi, A.; *Adv. Drug Deliv. Rev.,* **2012**, 64, 1005.

3) Menon, J.U., Jadeja, P., Tambe, P., Vu, K., Yuan, B.H., Nguyen, K.T.; *Theranostics,* **2013**, 3, 152.

4) Zhao, Y., *Macromolecules,* **2012**, 45, 3647.

5) Liu, G., Liu, W., Dong, C.M.; *Polym. Chem.-UK.*, **2013**, 4, 3431.

6) Tong, R.., Kohane, D.S.; *Wires Nanomed. Nanobiotechnol.*, **2012**, 4, 638.

7) Bansal, A., Zhang, Y.; *Acc. Chem. Res.*, **2014**, 47, 3052.

8) Krutmann, J., Bouloc, A., Sore, G., Bernard, B.A., Passeron, T.; *J. Dermatol. Sci.*, **2017**, 85, 152-161.

9) Klan, P., Solomek, T., Bochet, C.G., Blanc, A., Givens, R., Rubina, M., Popik, V., Kostikov, A., Wirz, J.; *Chem. Rev.*, **2013**, 113, 119-191.

10) Zhao, W., Zhao, Y., Wang, Q., Liu, T., Sun, J., Zhang, R.; *Small*, **2019**, 15, 1903060

11) Cadet, J., Douki, T., *Photochem. Photobiol. Sci.*, **2018**, 17, 1816

12) Liebmann, J., Born, M., Kolb-Bachofen, V. *J. Invest. Dermatol.*, **2010**, 130, 259-269

13) Tonoli, P.N., Chiarelli-Neto, O., Santacruz-Perez, C., Junqueira, H.C., Watanabe, I.S., Ravagnani, F.G., Martins, W.K., Baptista, M.S.; *J. Invest. Dermatol.*, **2017**, 137, 2447-2450.

14) Zastrow, L., Meinke, M.C., Albrecht, S., Patzelt, A., Lademann, J.; *Adv. Exp. Med. Biol*., **2017**, 996, 311-318.

15) Carling, C.J., Viger, M.L., Huu, V.A.N., Garcia, A.V., Almutairi, A.; Chem. Sci., **2015**, 6, 335-34.

16) Fomina, N., McFearin, C.L., Sermsakdi, M., Morachis, J.M., Almutairi, A.; *Macromolecules*, **2011**, 44, 8590-8597.

17) Wang, Y., Han, P., Xu, H., Wang, Z., Kabanov, A.V.; *Langmuir*, **2010**, 26, 709-715.

18) Peng, K., Tomatsu, I., Kros, A.; *Chem. Commun.*, **2010**, 46, 4094-4096.

19) Son, S., Shin, E., Kim, B.S.; *Biomacromolecules*, **2014**, 15, 628-634.

20) Razavi, B., Abdollahi, A., Roghani-Mamaqani, H., Salami-Kalajahi, M.; *Mater. Sci. Eng. C* ., **2020**, 109, 110524.

21) Poelma, S.O., Oh, S.S., Helmy, S., Knight, A.S., Burnet, G.L., Soh, H.T., Hawker, C.J., Read de Alaniz, J.; *Chem. Commun.*, **2016**, 52, 10525-10528.

22) Rifaie-Graham, O., Ulrich, S., Galensowske, N.F.B., Balog, S., Chami, M., Rentsch, D., Hemmer, J.R., Read De Alaniz, J., Boesel, L.F., Bruns, N.; *J. Am. Chem. Soc.*, **2018**, 140, 8027-8036.

23) Romano, A., Roppolo, I., Rossegger, E., Schlogl, S., Sangermano, M.; *Materials*, **2020**, 13, 2777.

24) Peteropoulos, C.C; *J. Polym. Sci., Part A: Polym. Chem.*, **1977**, 15, 1637-1644.

25) Yamaguchi, S., Ohashi, N., Minamihata, K., Nagamune, T.; *Biomater. Sci.*, **2021**, Advance Article.

26) Chen, J., Qian, C., Ren, P., Yu, H., Kong, X., Huang, C., Luo, H., Chen, G.; *Front. Pharmacol.*, **2021**, 12, 679610.

27) Givens, R.S., Matuszewski, B., *J. Am. Chem. Soc.*, **1984**, 106, 6860.

28) Azagarsamy, M.A., McKinnon, D.D., Alge, D.L., Anseth, K.S.; *ACS Macro. Lett.*, **2014**, 3, 515-519.

29) Karthik, S., Jana, A., Selvakumar, M., Venkatesh, Y., Paul, A., Shah, S.S., Singh, N.D.P.; *J. Mater. Chem. B*, **2017**,5, 1734-1741.

30) Chen, H., Wang, F., Qian, M., Zhou, X., Li, Z., Cheng, T., Qin, G.; *J. Mater. Chem. C.*, **2020**, 8, 4919.

31) Yin, C., Wen, G., Liu, C., Yang, B., Lin, S., Huang, J., Zhao, P., Wong, S.H.D., Zhang, K., Chen, X., Li, G., Jiang, X., Huang, J., Pu, K., Wang, L., Bian, L.; *ACS Nano*, **2018**, 12, 12201-12211.

32) Li, J., Pu, K.; *Acc. Chem. Res.*, **2020**, 53, 752-762

33) Xu, C., Jiang, Y., Huang, Jin., Huang, Jia., Pu, K.; *Adv. Mater.*, **2021**, 2101410.

34) Zhang, L., Jin, D., Stenzel, M.H.; *Biomacromolecules*, **2021**, ASAP.

35) Shen, K.H, Lu, C.H., Kuo, C.Y., Li, B.Y., Yeh, Y.C.; *J. Mater. Chem. B.*, **2021**, Advance Article.

36) Yan, B., Boyer, J.C., Branda, N.R., Zhao, Y.; *J. Am. Chem. Soc.*, **2011**, 133, 19714-19717.

37) Xiang, J., Tong, X., Shi, F., Yan, Q., Yu, B., Zhao, Y., *J. Mater. Chem. B.*, **2018**, 6, 3531-3540.

38) Hu, J., Chen, Y., Li, Y., Zhou, Z., Cheng, Y.; *Biomaterials*, **2017**, 112, 133-140.

39) Jiang, J., Tong, X., Morris, D., Zhao, Y.; *Macromolecules*, **2006**, 39, 4633-4640.

40) Yuan, Y., Wang, Z., Cai, P., Liu, J., Liao, L.D., Hong, M., Chen, X., Thakor, N., Liu, B.; *Nanoscale*, **2015**, 7, 3067-3076.

41) Edler, M., Mayrbrugger, S., Fian, A., Trimmel, G., Radl, S., Kern, W., Griesser, T.; *J. Mater. Chem. C*, **2013**, 1, 3931-3938.

# CHAPTER 1

Modification of the Visible Light Degradable Polymer, ANBB

## 1.1 Abstract

The blue visible light responsive polymer, ANBB, was developed and studied for the application of *in vivo* drug release by the Almutairi lab. The ANBB monomer was successfully polymerized using the cyclic-diamine, piperazine, as a linker. However, in their work, Carling and coworkers required the encapsulation of the NIR fluorescent probe, IR780, to allow for the *in vivo* monitoring of the nanoparticles. In this study, we explore how variations in the molar amounts of the polymer linker, the BODIPY dye, and addition time affect the polymer length and photochemistry. Polymer formulations that introduced less piperazine and early additions of BODIPY formed much shorter polymers but a stronger fluorescence intensity. Conversely, polymer formulations that introduced BODIPY later in the reaction process produced longer polymers but exhibited much weaker fluorescence intensities.

## 1.2 Introduction

In 2015, the Almutairi group published a paper on a visible light degradable polymer in *Chemical Science.* The polymer employed a butane-diol derivative of 2-(4'-N-dimethyl**a**mino-4-**n**itro-[1,1'-**b**iphenyl]-3-yl)**b**utane-1,4-diyl dicarbonyl (ANBB). The diols were further decorated with acrylates and was polymerized with piperazine by the Michael addition to yield the ANBB polymer ($M_w$ = 31.7 kDa, PDI = 2.7) (Scheme 1.1). Conjugating the biphenyl chromophore with the photolabile bond directly into the polymer backbone would enhance the photodegradation kinetics. The goal of this paper was to demonstrate the viability of the ANBB as a photo-triggered drug delivery system. Dexamethasone was encapsulated into the photoresponsive particles by electrospray with 1% w/w loading with a hydrodynamic size of 0.95 ± 0.5 μm. However, in their

*in vivo* studies, the NIR fluorescent probe IR-780, also needed to be encapsulated so the particles could be monitored in real time, demonstrating the lack of fluorescence from the polymers themselves.[1]

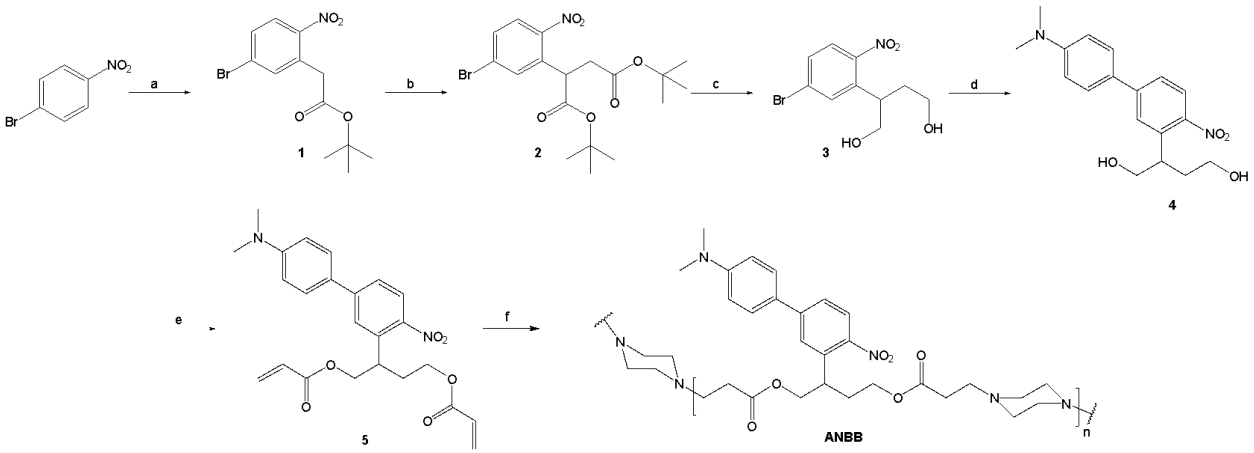


Scheme 1.1. Synthetic route of the ANBB polymer.[1]

Later, the Almutairi group joined in a collaboration with the Rolandi and Khademhosseini groups for the "Intracellular Delivery of Molecular and Supramolecular Ionic Circuits for CyborgTissue." The ultimate goal of the collaboration was to develop **Mo**lecular **I**onic **C**ircuits (MOIC) and MOIC added with **S**upr**A**molecular **I**onic **C**ircuit (MOSAIC) which could deliver $Ca^{2+}$ and $OH^-$ ions to cyborgmyocytes and cyborgneurons to elicit a response. The MOICs consist of either a $Ca^{2+}$ or $OH^-$ ion cage attached to the hydrophobic dye IR-780. The MOSAIC consists of the MOIC encapsulated in the Almutairi lab's polymeric particles, to provide an on-demand delivery of the cages into the cyborg cells. One of the polymers chosen to encapsulate the MOICs was ANBB due to its blue visible light trigger which differed from the UV-light stimulus used to release the $Ca^{2+}$ and $OH^-$ ions from the cages. However, due to ANBB's lack of fluorescence, a dye needs to be conjugated onto ANBB to provide fluorescence for *in vivo* tracking. A boron-dipyrromethene (BODIPY) dye was chosen because it fluoresces at a different wavelength compared to the IR-780 already incorporated in the MOICs.

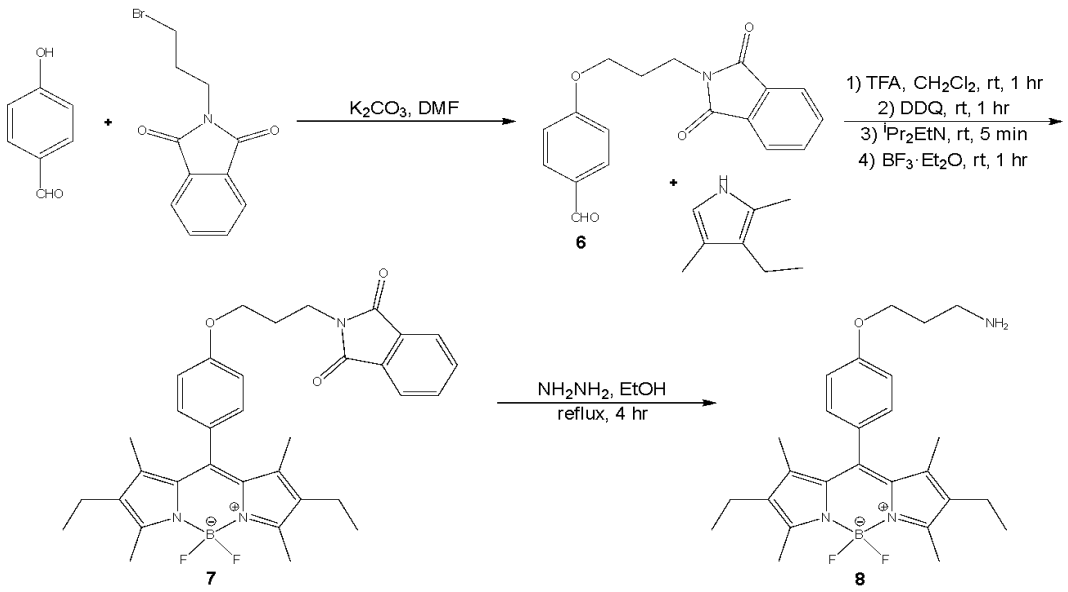


Scheme 1.2. Synthetic route of a modified boron-dipyrromethene (BODIPY) dye.[4]

In this chapter, the synthesis of a modified BODIPY dye and its polymerization with ANBB is discussed. Formulations using different molar amounts of BODIPY and addition times will be explored and compared. We hope that by incorporating BODIPY, ANBB will see an improvement in fluorescence intensity, which will be useful in the application for on-demand release of biological effectors which can be tracked.

### 1.3 Results and Discussion

The ANBB polymer was prepared following the procedure published by the Almutairi lab.[1] To start, compound **1** was prepared following a procedure by Zhao *et al*.[3] The benzyl carbon on **1** was decorated with another *tert*-Butyl acetate moiety for form compound **2**. The two *tert*-butyl acetate moieties were reduced with DIBAL-H to yield diols, **3**. The title compound **3** was coupled with 4-Dimethylaminophenylboronic acid via the Suzuki Coupling to form the biphenyl chromophore, **4**. Finally, the ANBB monomer (**5**) was synthesized by decorating the diols with acryloyl chloride to yield the diacrylate monomer. The ANBB polymer was also prepared for

comparison by polymerizing **5** with piperazine via the Michael addition to yield an orange solid ($M_w$ = 24.8 kDa, PDI = 2.2) (Figure 1.3). ANBB exhibited an absorption at $\lambda_{max}$ = 400 nm (Figure 1.2).

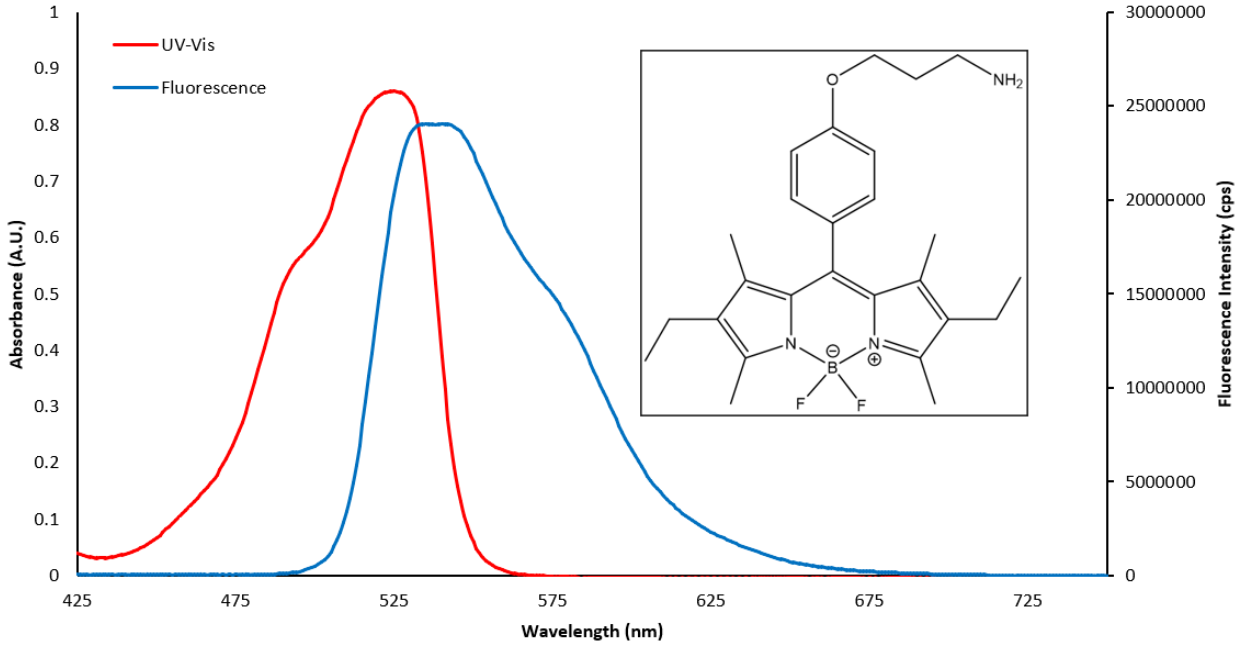


Figure 1.1. The UV-Vis absorbance (red) and the fluorescence (blue) profiles of BODIPY-$NH_2$.

In order to incorporate BODIPY onto ANBB, it must first be modified with an amine (BODIPY-$NH_2$) to allow for the Michael addition with the acrylate moiety on the ANBB monomer. BODIPY-$NH_2$ was synthesized following a procedure by Galeotti *et. al.* which incorporated a primary amine on a phenoxy propyl tether (Scheme 1.2).[4] To start, the precursor **6** was synthesized by substituting the bromine on (3-bromopropyl)-phthalimide with 4-hydroxybenzaldehyde.[5] Compound **6** was then reacted with 3-Ethyl-2,4-dimethyl-1*H*-pyrrole and $BF_3 \cdot Et_2O$ to form the BODIPY core, **7**. The phthalimide was reduced to the primary amine using the Ing-Manske procedure to finally produce compound **8**, BODIPY-$NH_2$ and exhibited an absorption at $\lambda_{ebs}$ = 525 nm and a fluorescent signal at $\lambda_{em}$ = 535 nm (Figure 1.1).

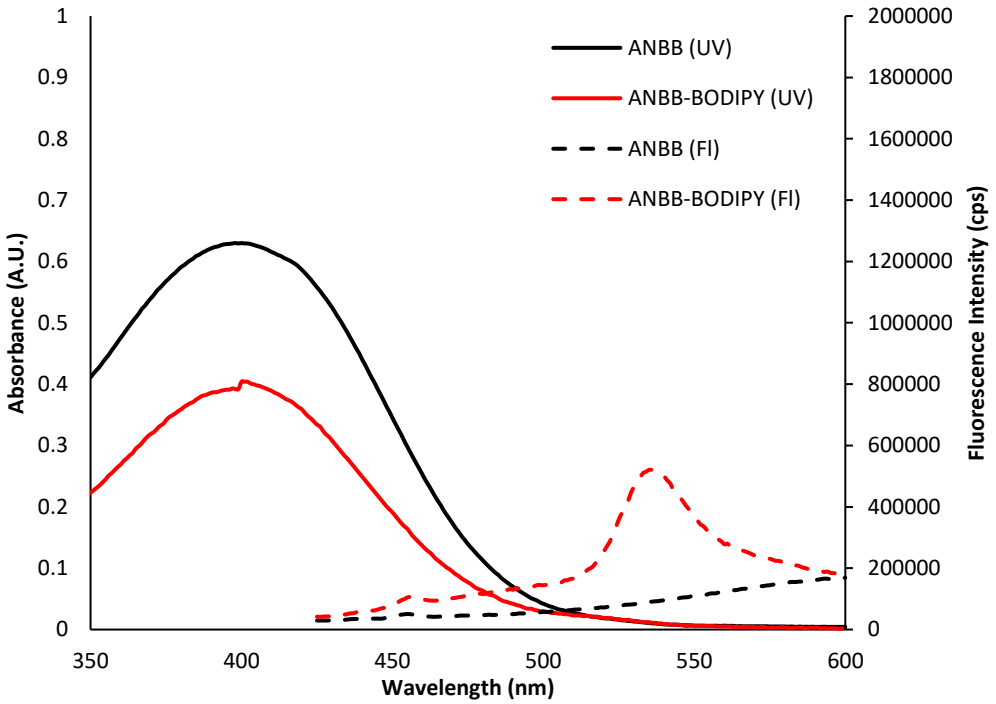


Figure 1.2. The UV-Vis absorbance profiles (solid) with their fluorescence profiles (dashed) of ANBB (black) and AB-1 (red).

The first attempt to incorporate BODIPY with ANBB was done using equal molar amounts of ANBB monomer and piperazine and half an equivalent of BODIPY-$NH_2$ (**AB-1**). The photoproperties of AB-1 were analyzed by UV-Vis (Shimadzu UV-3600) and Fluorescence (Horiba Jobin Yvon FluoroLog3) spectroscopy. This formulation exhibited a $\lambda_{abs}$ = 400 nm and a fluorescent signal at $\lambda_{em}$ = 535nm, which corresponds to the BODIPY (Figure 1.2). However, AB-1 produced a very short polymer with an $M_w$ = 1.2 kDa but very monodispersed with a PDI = 1.1. Due to its short length, a 10:1 blend of the ANBB polymer and AB-1 was used to encapsulate the $OH^-$ MOIC. This was done using a high-pressure homogenizer emulsion technique that effectively formed nano-sized particles in the 500 nm range. These particles were sent to the collaborators for testing but ultimately, they decided to move forward with polymers utilizing a different stimulus.

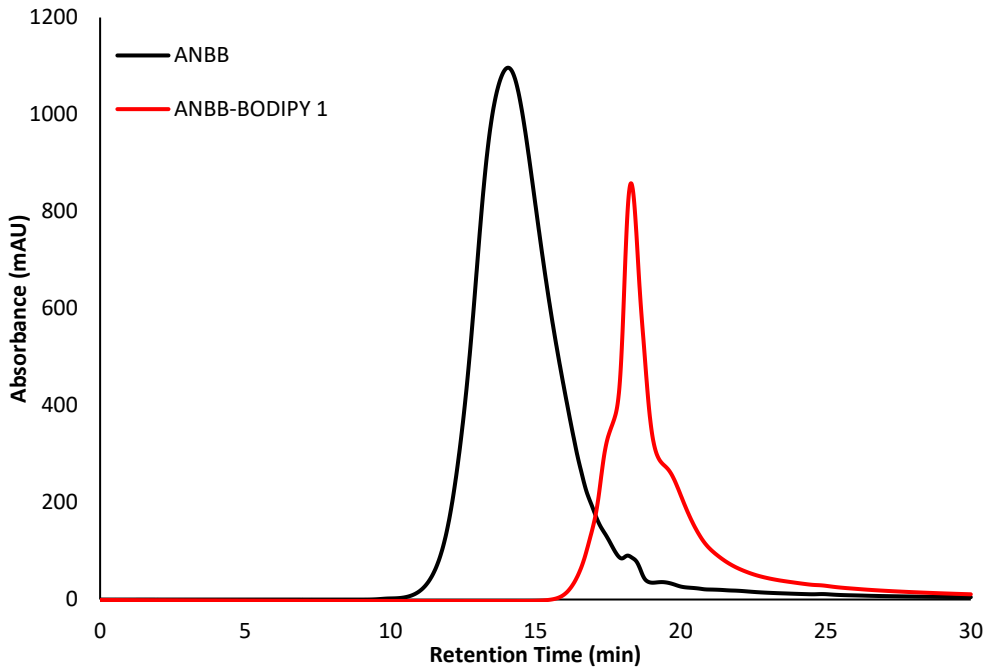

Figure 1.3. The GPC chromatogram of ANBB (black) and AB-1 (red).

Despite this, modifications to the polymerization method were explored to see if ANBB-BODIPY could form longer polymers while still exhibiting fluorescence. These following formulations were all analyzed uniformly using both UV-Vis at 0.05 mg $mL^{-1}$ and Fluorescence spectroscopy at 0.01 mg $mL^{-1}$. To do this, different molar amounts and addition times were done (Table 1.1). **AB-2** was prepared by mixing the monomer, **5** (0.288 mmol, 1 eq.), with piperazine (0.205 mmol, 0.9 eq.) together first. After one day of stirring at room temperature, half of the BODIPY-NH2 was added to the solution, stirring at room temperature. After one more day of stirring, the other half of the BODIPY-NH2 was added, totaling 0.022 mmol (0.1 eq.). The polymer solution was precipitated out in cold hexanes and produced very polydisperse polymers with a $M_w$ = 12.7 kDa and PDI of 5.24. AB-2 exhibited $\lambda_{abs}$ = 400 nm and a fluorescent signal $\lambda_{em}$ = 535 nm (148,320 cps). **AB-3** was polymerized by mixing 1 eq. of ANBB and 0.75 eq of piperazine together on the first day with the addition of BODIPY-NH2 (0.25 eq.) in one batch after the second day. After another 2 days of stirring, the solution was precipitated out in cold EtOH to

produce AB-3. GPC analysis of AB-3 showed a shorter chain polydisperse polymer with a Mw = 6.8 kDa and PDI = 2.47. The absorbance of AB-3 exhibited $\lambda_{abs}$ = 400 nm with a new, smaller absorbance at 525 nm, which corresponds to the absorbance of BODIPY-$NH_2$. AB-3 also displays fluorescence at $\lambda_{em}$ = 535 nm (1,088,653 cps).

Table 1.1. Various synthetic conditions for the synthesis of ANBB-BODIPY.

| Sample | ANBB Monomer | Piperazine | BODIPY-$NH_2$ | Day Added |
|---|---|---|---|---|
| **AB-1** | 0.288 mmol (1 eq.) | 0.288 mmol (1 eq.) | 0.114 mmol (0.50 eq) | 1 |
| **AB-2** | 0.288 mmol (1 eq.) | 0.205 mmol (0.90 eq) | 0.022 mmol (0.10 eq) | 2 and 3 |
| **AB-3** | 0.288 mmol (1 eq.) | 0.171 mmol (0.75 eq) | 0.057 mmol (0.25 eq) | 2 |
| **AB-4** | 0.288 mmol (1 eq.) | 0.182 mmol (0.80 eq) | 0.091mmol (0.40 eq) | 1 |
| **AB-5** | 0.288 mmol (1 eq.) | 0.205 mmol (0.90 eq) | 0.057 mmol (0.25 eq) | 3 |

**AB-4** was polymerized by mixing ANBB (1 eq.), piperazine (0.80 eq.), and BODIPY-NH2 (0.40 eq.) added all on the same day. After 4 days of stirring, the solution was precipitated out in cold EtOH. GPC analysis showed that the synthesis of AB-4 produced a short chain, polydisperse polymer with $M_w$ = 7.8 kDa and PDI of 2.42. This formulation exhibited $\lambda_{abs}$ = 400 nm and also exhibited the smaller absorbance at 525 nm, similar to AB-3. The fluorescence of AB-4 with an intensity of 1,104,980 cps. Finally, **AB-5** was polymerized by mixing ANBB (1 eq.) with piperazine (0.90 eq.). BODIPY-NH2 (0.25 eq.) was added in one batch on the third day of the reaction. After one more day of stirring, the polymer solution was precipitated out in cold EtOH to produce a polydisperse polymer (Mw = 19.8 kDa, PDI = 5.52). This formulation again showed the larger absorbance peak at 400 nm but the smaller peak at 525 nm was much smaller than AB-3 and AB-4. AB-5 exhibited a fluorescence intensity of 387,863 cps at 535 nm.

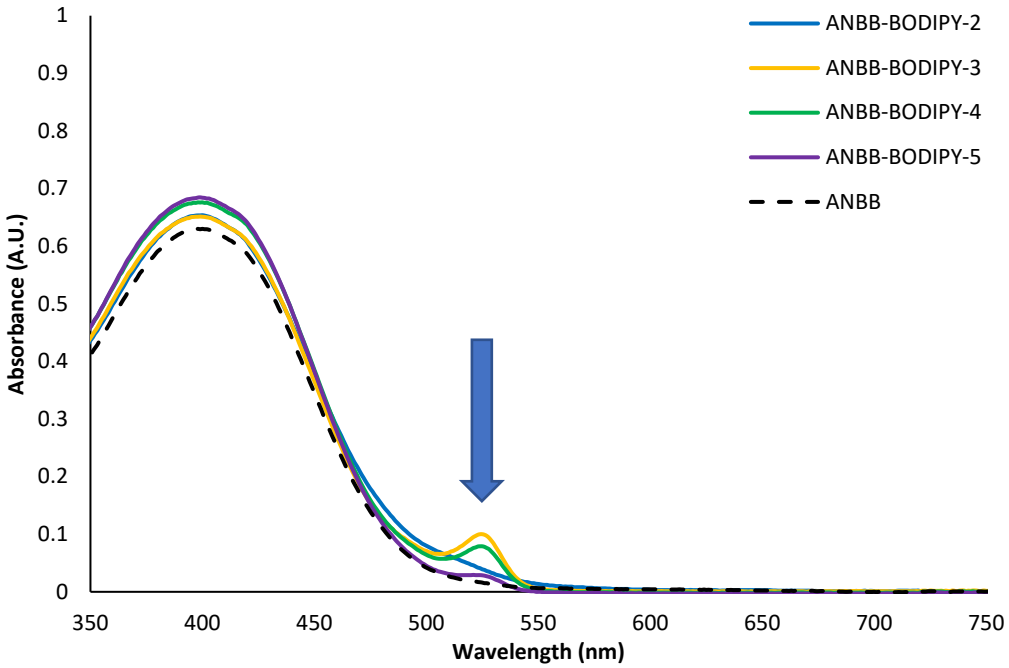


Figure 1.4. UV-Vis absorbance profiles of the various AB polymers with ANBB (dashed). The peak at 525 nm (blue arrow) corresponds to the BODIPY dye at 0.05 mg $mL^{-1}$.

When comparing the characteristics of the polymer, the syntheses that added BODIPY-$NH_2$ later (AB-2 and AB-5) created much longer polymer chains and exhibited much lower fluorescence intensities. AB-3 and AB-4 produced much more monodisperse polymers relative to the other formulations but also much shorter polymers, while exhibiting much stronger fluorescence intensities. This can be attributed to how BODIPY-$NH_2$ is incorporated into the ANBB polymer. When the ANBB monomer is polymerized, the diacrylates undergo a Michael addition with the cyclic-diamine, piperazine. The two secondary amine moieties in the 6-member ring make it a suitable linker for between monomer units. BODIPY-$NH_2$ has a primary amine tethered to the dyes core. The single primary amines would effectively cap one of the tethers on ANBB, stopping it from elongating the polymer chain. We can see that when BODIPY-$NH_2$ is introduced later, as with AB-2 (day 2 and 3) and AB-5 (day 3), the polymers produced are much longer, but because they are longer, the fluorescence intensity is much lower. Conversely, when

BODIPY-NH2 is introduced early in the reaction process (AB-3 on day 2 and AB-4 on day 1), shorter polymer chains are made but the fluorescence signal is much more intense compared to their longer counterparts.

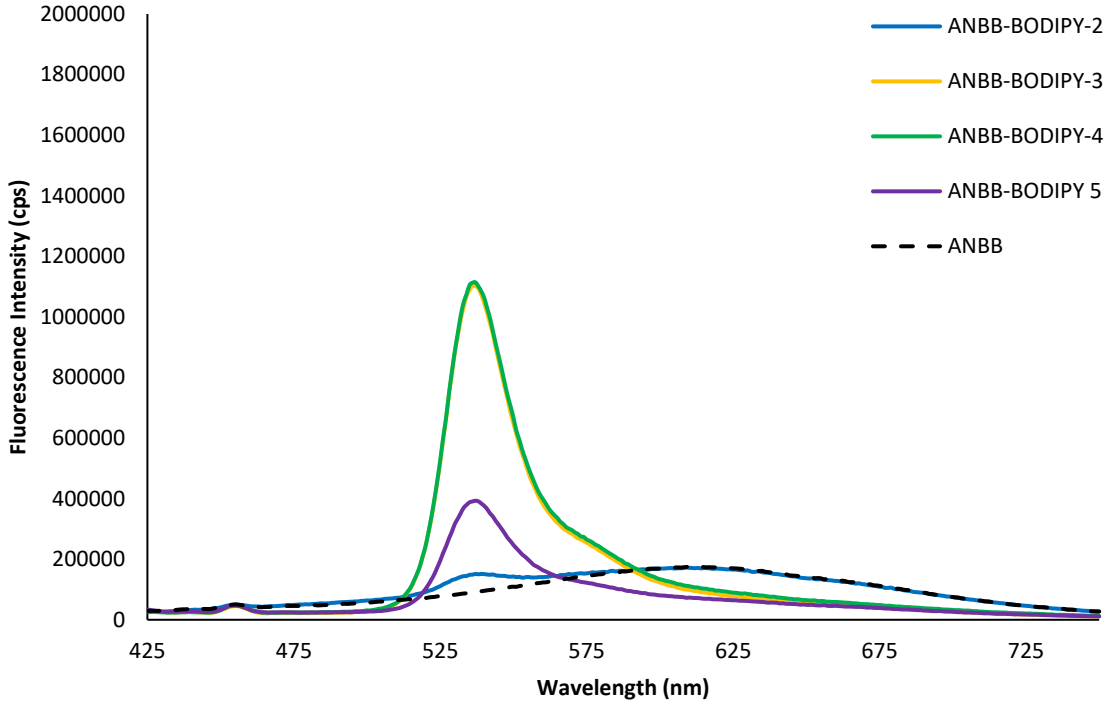


Figure 1.5. The fluorescence profiles of the various ANBB-BODIPY polymers with ANBB (dashed) at 0.01 mg $mL^{-1}$.

When comparing the absorbance profiles, all the formulations produce a strong absorbance at $\lambda_{abs}$ = 400 nm. This absorbance corresponds to the ANBB chromophore and does not seem to be affected by the difference in polymer length. However, the absorbance profiles of AB-3, 4, and 5 also show a smaller peak at $\lambda_{abs}$ = 525 nm, corresponding to the absorbance of the dye. The absorbance at 525 nm is much stronger in AB-3 and AB-4 then in AB-5. AB-2 did not exhibit a defined peak at this wavelength.

Table 1.2. Table of results from the analysis of the various AB polymers.

| Sample | Mw | PDI | Abs @ 400 nm | Abs @ 525 nm | Fluorescence @ 535 nm |
|---|---|---|---|---|---|
| **AB-2** | 12,652 | 5.24 | 0.654 | N/A | 148,320 |
| **AB-3** | 6,804 | 2.47 | 0.641 | 0.100 | 1,088,653 |
| **AB-4** | 7,754 | 2.42 | 0.676 | 0.079 | 1,104,980 |
| **AB-5** | 19,833 | 5.52 | 0.684 | 0.029 | 387, 863 |

When comparing AB-2 and AB-5, both formulations had equal amounts of piperazine and only varied in the amount of BODIPY-$NH_2$ and time of addition. AB-2 had less than half the molar amount of BODIPY-$NH_2$ and the addition was split among two days. The earlier introduction of BODIPY-$NH_2$ may have resulted in the shorter polymer length, however due to the molar amount that was added, resulted in a lower fluorescence intensity as seen by the lack of absorption at 525 nm. A comparison of AB-3 and AB-4 showed that despite the differing amounts of BODIPY-$NH_2$ introduced into the polymer chain, there was no noticeable difference in their fluorescence nor the absorbance profiles. Interestingly, although AB-4 had more BODIPY-$NH_2$ added earlier compared to AB-3, the polymer length of AB-4 was longer than AB-3. This can be attributed to the amounts of piperazine that was added as AB-3 had slightly less.

### 1.4. Conclusions

In this work, we describe the integration of a fluorescent BODIPY analogue into the established ANBB polymer. The primary amine tether on the modified BODIPY was incorporated through the Michael addition, however, due to the presence of a single amine, the BODIPY acted as an end cap instead of being copolymerized with ANBB, forming an oligomer. Utilizing different molar amounts of piperazine, BODIPY-NH2, and various addition times generated polymers of various lengths and fluorescence. The synthesis of AB-3 and AB-4 introduced BODIPY-NH2 early in the reaction and generally formed shorter polymers but exhibited strong fluorescence intensities. AB-2 and AB-5 introduced the dye later in the reaction and produced

longer polymers but were much more polydisperse and their fluorescence compared to their shorter counterparts were much lower.

Future work on this study could result in a more uniform comparison, using equal amounts of piperazine and BODIPY-NH2 while varying just the addition times. Additionally, testing different formulations while just varying the amount of piperazine would also give a clear answer as to which has more of an effect on polymer length, the piperazine or the addition time of BODIPY-NH2. Lastly, utilizing BODIPY-NH2 as a copolymer in the absence of piperazine would be worthwhile to explore. To do this, a second primary amine tether should be incorporated onto BODIPY.

### 1.5. Abbreviations

ANBB, 2-(4'-N-dimethyl**a**mino-4-**n**itro-[1,1'-**b**iphenyl]-3-yl)**b**utane-1,4-diyl dicarbonyl; BODIPY, boron-dipyrromethene; UV, Ultraviolet; NIR, near-infrared; Vis, visible; MOIC, **MO**lecular **I**onic **C**ircuits; MOSAIC, MOIC added with **S**upr**A**molecular **I**onic **C**ircuit; DIBAL-H, Diisobutylammonium hydride; DMF, Dimethylformamide; DDQ, 2,3-Dichloro-5,6-dicyano-1,4-benzoquinone; TFA, Trifluoroacetic acid; NMR, nuclear magnetic resonance; GPC, gel permeation chromatography; THF, tetrahydrofuran; DIPEA, N,N-Diisopropylethylamine; TLC; thin layer chromatography

### 1.6. Acknowledgements

NMR spectra were acquired at the UCSD Skaggs School of Pharmacy and Pharmaceutical Sciences NMR Facility. Mass spectroscopy data was acquired at the UCSD Department of Chemistry and Biochemistry Molecular Mass Spectrometry Facility. Gel Permeation

Chromatography data was acquired at the UCSB Materials Research Laboratory Polymer Characterization Facility.

This chapter was coauthored with Dr. Adah Almutairi. The dissertation author was the principal researcher and primary author of this chapter.

## 1.7. References


1) Carling, C.J., Viger, M.L., Huu, V.A.N., Garcia, A.V., Almutairi, A.; *Chem. Sci.*, **2015**, 6, 335-34.

2) Rolandi, M. Almutairi, A., Khademhosseini, A.; "CybrogCell: Instracellular Delivery of Molecular and Supramolecular Ionic Circuits for CyborgTissue." Air Force Office of Scientific Research / Energy, Power and Propulsion Sciences.

3) Zhao, H., Sterner, E.S., Coughlin, E.B., and Theato, P., *Macromolecules*, **2012**, 45, 1723−1736.

4) Galeotti, F., Calabrese, V., Cavazzini, Quici, S., Poleunis, C., Yunus, S., Bolognesi, A., *Chem. Mater.*, **2010**, 22, 2764–2769.

5) Dick, D.L., Rao, S.V.T., Sukumaran, D., Lawrence, D.S., *J. Am. Chem. Soc.*, 1992, 114, 2664-9.


## 1.8. Supplementary

**General Methods and Instrumentation.** All reactions requiring anhydrous conditions were performed under an argon atmosphere. Flash chromatography was performed using a CombiFlash Companion system. $^{1}$H NMR spectra were acquired using a Bruker 600 MHz. Chemical shifts are reported as δ in units of part per million (ppm) relative to chloroform (δ 7.26, s). Multiplicities are reported as follows: s (singlet), bs (broad singlet), d (doublet), t (triplet), q (quartet), sex (sextet), dd (doublet of doublets), m (multiplet), br (broadened). Coupling constants are reported as J values in Hertz (Hz). The number of protons (n) for a given resonance is indicated as nH and is based on

spectral integration values. UV spectra were acquired using a dual beam Shimadzu UV-3600 UV-Vis-NIR Spectrophotometer. Fluorescence measurements were conducted on a Horiba Jobin Yvon FluoroLog3 and a Hitachi F-2700 fluorescence spectrophotometer. Ultracentrifucation was performed on a Beckman Coulter Allegra 64R centrifuge.

*Synthesis of tert-butyl 2-(5-bromo-2-nitrophenyl)acetate (**1**)*

A flame-dried round-bottom flask under argon was charged with 4-bromonitrobenzene (19.8 mmol, 1 eq.), *tert*-Butyl chloroacetate (30.7 mmol, 1.55 eq.), and DMF (30 mL) and was stirred at 0 °C. In a separate flask, *t*-BuOK (123 mmol, 6.26 eq.) was dissolved in DMF (70 mL) and was added to the reaction flask via cannula and was left to stir overnight at room temperature. The reaction mixture was cool to 0 °C and was quenched with 5% HCl and extracted with EtOAc. The combined organic extracts were washed with brine and dried over $MgSO_4$ and were concentrated under vacuum. The product was purified by silica gel column chromatography (80g, EtOAc in hexanes, 10%) to afford a light-yellow solid (57% yield).

$^{1}$H NMR (600 MHz, $CDCl_3$) δ 7.99 (d, *J*: 8.8 Hz, 1H), 7.60 ppm (dd, *J*: 8.8, 2.6 Hz, 1H), 7.51 (d, *J*: 1.8 Hz, 1H), 3.92 (s, 2H), 1.45 (s, 9H)

$^{13}$C NMR (150 MHz, $CDCl_3$) δ 193.55, 168.47, 136.14, 132.35, 131.50, 128.19, 126.65, 82.21, 40.79, 27.93.

*Synthesis di-tert-butyl 2-(5-bromo-2-nitrophenyl)succinate **(2)***

A flame-dried round-bottom flask was charged with **1** (3.16 mmol, 1 eq.), $Bu_4NBr$ (0.63 mmol, 0.2 eq.) and anhydrous $K_2CO_3$ (9.49 mmol, 3 eq.). The system was purged and backfilled with argon. Anhydrous $CH_3CN$ (35 mL) was added and the reaction was heated to 84 °C. The solution gradually turned dark purple. After 10 minutes, t-butyl bromoacetate (6.32 mmol, 2 eq.)

was added and the reaction changed from purple to clear. The reaction was refluxed overnight. The resulting solution was allowed to cool and was vacuum filtered. The yellow solid was washed with EtOAc several times and the supernatant was concentrated. The crude oil was purified by silica gel column chromatography (24g, 5% EtOAc in hexanes) to yield a yellow oil (87% yield). The compound was stored at ambient temperature.

$^{1}$H NMR (600 MHz, $CDCl_3$) δ 7.85 (d, *J*: 8.8 Hz, 1H), 7.60 (d, *J*: 2.6 Hz, 1H), 7.56 (dd, *J*: 2.2, 8.3 Hz, 1H), 4.51 (t, *J*: 7.5 Hz, 1H), 3.13 (dd, *J:*7.9, 16.7 Hz, 1H), 2.74 (dd, *J*: 7.0, 16.7 Hz, 1H), 1.40 (s, 9H), 1.38 (s, 9H)

$^{13}$C NMR (150 MHz, $CDCl_3$) δ 170.24, 169.98, 147.93, 134.03, 131.59, 128.17, 126.80, 82.62, 81.53, 45.15, 38.15, 28.15, 27.95

*Synthesis of 2-(5-bromo-2-nitrophenyl)butane-1,4-diol **(3)***

A flame-dried round-bottom flask was charged with compound **2** (2.64 mmol, 1 eq.) and dissolved in anhydrous THF (23 mL) and the resulting solution was cool to 0 °C. DIBAL-H (18.46 mmol, 7 eq., 1M in THF) was added dropwise to the reaction over 30 minutes. The reaction continued to stir at 0 °C for 3.5 hours. The mixture was then poured into ice cold $H_2O$ which led to gas and heat evolution and the formation of Al salts. HCl (5 mL, 1M) was added to dissolve the salts and the solution was extracted with EtOAc. The combined organic extracts were washed with brine, dried over $MgSO_4$, filtered, and concentrated. The crude compound **3** was purified by silica gel column chromatography (24g, gradient 20% → 50% EtOAc in hexanes) to yield a yellow solid (27% yield). The product was stored at ambient temperature in a foil-wrapped vial.

$^{1}$H NMR (600 MHz, CD3OD) δ 7.78 (d, *J*: 2.6 Hz, 1H), 7.69 (d, *J*: 8.8 Hz, 1H), 7.59 (dd, *J*: 2.1, 8.8 Hz, 1H), 3.75 (d, *J*: 6.1 Hz, 2H), 3.47 (m, 3H), 2.05 (m, 1H), 1.88 (m, 1H)

$^{13}$C NMR (150 MHz, CD3OD) δ 140.69, 133.47, 131.76, 127.85, 126.79, 66.51, 60.89, 40.37, 35.85

*Synthesis of 2-(4'-(dimethylamino)-4-nitro-[1,1'-biphenyl]-3-yl)butane-1,4-diol* ***(4)***

A flame-dried two-neck round-bottom flask equipped with a condenser was charged with **3** (0.97 mmol, 1 eq.), 4-Dimethylaminophenylboronic acid (1.02 mmol, 1.05 eq.), $Na_2CO_3$ (9.70 mmol, 10 eq.), and dissolved in toluene (5 mL), EtOH (0.94 mL), and $H_2O$ (1.6 mL). The reaction mixture was degassed by bubbling argon for 25 minutes. $Pd(PPh_3)_4$ (0.05 mmol, 0.05 eq.) was added, the system purged, covered in foil, and the reaction was heated to 90 °C in an oil bath. After 19 hours, the reaction was cooled and diluted with $H_2O$. The resulting solution was extracted with EtOAc. The organic extracts were washed with brine, dried over $MgSO_4$, filtered, and concentrated. The crude product was purified by silica gel column chromatography (12g, 40% → 80% EtOAc in hexanes) to yield a light orange solid (90% yield). The product was stored in a foil-wrapped vial at room temperature.

$^{1}$H NMR (600 MHz, $CDCl_3$) δ 7.86 (d, *J*: 8.8 Hz, 1H), 7.63 (d, *J*:1.8 Hz, 1H), 7.52 (m, 3H), 6.81 (d, *J*: 7.9 Hz, 2H), 3.93 (d, *J*:6.2 Hz, 2H), 3.77 (m, 1H), 3.67 (m, 2H), 3.04 (s, 6H), 2.16 (m, 1H), 2.03 (m, 1H)

$^{13}$C NMR (150 MHz, $CDCl_3$) δ 137.83, 128.03, 126.02, 125.69, 125.22, 124.52, 112.50, 67.02, 61.05, 40.32, 39.89, 35.85

*Synthesis of 2-(4'-(dimethylamino)-4-nitro-[1,1'-biphenyl]-3-yl)butane-1,4-diyl Diacrylate* ***(5)***

In a flame dried round bottom flask, **4** (2.09 mmol, 1 eq.) was dissolved in anhydrous DMF (7.8 mL) and then diluted with anhydrous DCM (27.4). The solution was cooled to 0 °C. Et3N (6.26 mmol, 3 eq.) was added and acryloyl chloride (4.59 mmol, 2.2 eq.) was added drop wise.

The reaction was brought up to room temperature and stirred overnight. The resulting solution was poured into H2O and extracted with DCM. The combined organic extracts were washed with brine, dried over MgSO4, filtered, and concentrated *in vacuo*. The crude product was purified twice by silica gel column chromatography (40% EtOAc in Hexanes) to yield an orange solid (58% yield). The compound was wrapped in foil and stored at ambient temperature.

$^{1}$H NMR (600 MHz, $CDCl_3$) δ 7.86 (d, *J*: 8.8 Hz, 1H), 7.58 (d, *J*:1.8 Hz, 1H), 7.52 (dd, *J*: 1.8, 7.9 Hz, 1H), 7.50 (d, *J:* 8.8 Hz, 2H), 6.80 (d, *J*: 8.8 Hz, 2H), 6.34 (t, *J*: 17.1 Hz, 2H), 6.06 (m, 2H), 5.80 (dd, *J*: 16.7 Hz, 2H), 4.47 (m, 1H), 4.40 (m, 1H), 4.22 (m, 1H), 4.11 (m, 1H), 4.01 (m, 1H), 3.03 (s, 6H), 2.26 (m, 1H), 2.20 (m, 1H)

$^{13}$C NMR (150 MHz, $CDCl_3$) δ 165.88, 165.73, 150.78, 148.16, 145.94, 135.63, 131.19, 130.88, 128.02, 127.95, 127.93, 125.49, 125.36, 124.90, 112.42, 67.37, 62.03, 40.23, 35.58, 30.94

*Synthesis of 4-(3-(1,3-dioxoisoindolin-2-yl)propoxy)benzaldehyde (**6**)*

A flame-dried round-bottom flask was charged with 4-hyroxybenzaldehyde (12.3 mmol, 1 eq.), (3-bromopropyl)-phthalimide (12.3 mmol, 1 eq.) and $K_2CO_3$ (15.9 mmol, 1.3 eq.) were dissolved in anhydrous DMF (15 mL) and allowed to stir at 65 °C for 2 hours. The resulting solution was diluted with DCM and concentrated to remove DMF. The resulting solid was dissolved again in DCM and extracted with 1M NaOH. The combined organic extracts were combined and washed with brine, dried over $MgSO_4$, filtered, and concentrated. The crude solid was recrystallized from hot EtOAc and allowed to dry overnight producing a white crystal (61% yield). The product was stored at room temperature.

$^{1}$H NMR (600 MHz, $CDCl_3$) δ 9.85 (s, 1H), 7.83 (dd, *J*: 3.1, 5.7 Hz, 2H), 7.78 (d, *J*: 8.8 Hz, 2H), 7.72 (dd, *J*: 2.6, 5.3 Hz, 2H), 6.88 (d, *J*: 8.8 Hz, 2H), 4.11 (t, *J*: 6.1 Hz, 2H), 3.92 (t, *J*: 6.6 Hz, 2H), 2.22 (quintet, *J*: 6.4 Hz, 2H),

$^{13}$C NMR (150 MHz, $CDCl_3$) δ 190.56, 168.11, 163.45, 133.78, 131.83, 131.69, 129.74, 123.05, 114.42, 65.80, 35.06, 27.90

*Synthesis of 2-(3-(4-(2,8-diethyl-5,5-difluoro-1,3,7,9-tetramethyl-5H-4l4,5l4-dipyrrolo[1,2-c:2',1'-f][1,3,2]diazaborinin-10-yl)phenoxy)propyl)isoindoline-1,3-dione (7)*

A flame-dried round-bottom flask was charged with **6** (1.49 mmol, 1 eq.) and 3-Ethyl-2,4-dimethyl-1*H*-pyrrole (2.97 mmol, 2 eq.) were dissolved in anhydrous DCM (90 mL) under argon. One drop of trifluoracetic acid was added and the solution was allowed to stir at room temperature for 1 hour. The resulting solution was diluted with anhydrous DCM (45 mL) and 2,3-dichloro-5,6-dicyanobenzoquinone (DDQ) (2.97 mmol, 2 eq.) was added and stirred at room temperature for 1 hour. DIPEA (22.28 mmol, 15 eq.) and $BF_3 \cdot Et_2O$ (29.70 mmol, 20 eq.) were added to the solution and allowed to stir for an hour. The reaction mixture was quenched with $H_2O$ and the two-phase solution was filtered over Celite. The organic phase was separated and extracted again with water, dried over $MgSO_4$, filtered, and concentrated. The crude product was purified by silica gel column chromatography with DCM as an eluent to give a red-orange solid (67% yield). The compound was stored at ambient temperature.

$^1$H NMR (600 MHz, $CDCl_3$) δ 7.85 (m, 2H), 7.73 (m, 2H), 7.11 (d, *J*: 7.9 Hz, 2H), 6.89 (d, *J*: 8.8 Hz, 2H), 4.11 (t, *J*: 6.1 Hz, 2H), 3.96 (t, *J*: 6.6 Hz, 2H), 2.52 (s, 6H), 2.26 (m, 6H), 1.31 (s, 6H), 0.98 (t, *J*: 7.5 Hz, 6H)

$^{13}$C NMR (150 MHz, $CDCl_3$) δ 168.34, 159.06, 153.42, 140.22, 138.42, 133.95, 132.58, 132.13, 131.11, 129.35, 127.92, 123.22, 114.88, 65.84, 35.50, 30.90, 28.24, 17.05, 14.61, 12.44, 11.81

*Synthesis of 3-(4-(2,8-diethyl-5,5-difluoro-1,3,7,9-tetramethyl-5H-4l4,5l4-dipyrrolo[1,2-c:2',1'-f][1,3,2]diazaborinin-10-yl)phenoxy)propan-1-amine (**8**)*

A flame-dried two-neck round-bottom flask attached with a condenser was charged with **7** (0.26 mmol, 1 eq.) and dissolved in EtOH (20 mL). Hydrazine monohydrate (12.42 mmol. 47.46 eq.) was added dropwise and the reaction was allowed to stir at 80 °C. The reaction was monitored by TLC (silica, 50% EtOAc in hexanes) to check for the disappearance of the starting material. The reaction was cooled to room temperature and a white solid was formed in solution. The supernatant was concentrated and diluted using DCM. Again, the white solids were filtered off and the dark red solution was concentrated. The crude product was purified by silica gel column chromatography (10% MeOH in DCM) to yield a dark red solid (80% yield).

$^{1}$H NMR (600 MHz, $CDCl_3$) δ 7.16 (d, *J*: 8.8 Hz, 2H), 7.01 (d, *J*: 8.8 Hz, 2H), 4.13 (t, *J*: 6.1 Hz, 2H), 3.04 (t, *J*: 6.6 Hz, 2H), 2.52 (s, 6H), 2.32 (q, *J*: 7.9 Hz, 4H), 2.08 (quintet, *J*: 6.2 Hz, 2H), 1.33 (s, 6H), 0.99 (t, *J*: 7.5 Hz, 6H)

$^{13}$C NMR (150 MHz, $CDCl_3$) δ 138.42, 133.96, 132.60, 132.13, 131.13, 129.35, 127.92, 114.88, 65.84, 35.49, 30.90, 28.23, 17.05, 14.61, 12.44, 11.81

ESI-MS calc. mass $(C_{26}H_{34}BF_2N_3O)^+$ $[M+H]^+$ 454.29 g/mol, experimental mass $[M+H]^+$ 454.35 g/mol, $[M-F]^+$ 434.50 g/mol

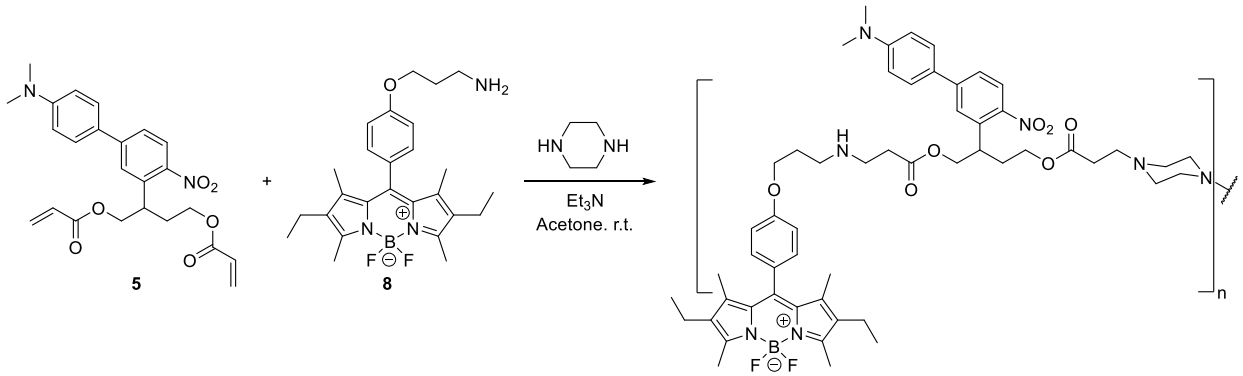


Scheme 1.S1. The schematic illustration of the polymerization of ANBB-BODIPY.

*Synthesis of ANBB-BODIPY-**1 (AB-1)***

A flame-dried 1 dram vial charged with **5** (0.288 mmol, 1eq.), piperazine (0.288 mmol, 1 eq.), and **8** (0.114 mmol, 0.5 eq.) and was dissolved in anhydrous acetone (1.25 mL) under argon. $Et_3N$ (1.14 mmol, 5 eq.) was added, and the reaction was allowed to stir at room temperature for 4 days. The solution was dissolved in DCM (1 mL) and precipitated out in cold hexanes (50 mL). The resulting solution was centrifuged for 15 minutes at 20k rpm at 4 °C. The pellet was collected, and the purification process was repeated 3x to yield an orange solid (100 mg) (Mw = 1.2 kDa

*Synthesis of ANBB-BODIPY-**2 (AB-2)***

A flame-dried 1 dram vial charged with **5** (0.288 mmol, 1eq.) and piperazine (0.21 mmol, 0.9 eq.) was dissolved with anhydrous acetone (1.25 mL) under argon. $Et_3N$ (1.14 mmol, 5 eq.) was added and the reaction was allowed to stir at room temperature. After 1 day, compound **5** (0.011 mmol, 0.05 eq) was added to the reaction mixture and continued to stir at room temperature. After 24hrs, more **5** (0.011 mmol, 0.05 eq) was added and the reaction stirred for another 24 hours. The solution was dissolved in DCM (1 mL) and precipitated out in cold hexanes (50 mL). The resulting solution was centrifuged for 15 minutes at 20k rpm at 4 °C. The pellet was collected, and the purification process was repeated 3x to yield an orange solid.

*Synthesis of ANBB-BODIPY-**3 (AB-3)***

A flame-dried vial charged with **5** (0.288 mmol, 1eq.) and piperazine (0.17 mmol, 0.75 eq.) was dissolved with anhydrous acetone (1.25 mL) under argon. $Et_3N$ (1.14 mmol, 5 eq.) was added, and the reaction was allowed to stir at room temperature. After 1 day, compound **5** (0.057 mmol, 0.25 eq) was added to the reaction mixture and continued to stir at room temperature for another 3 days. The resulting solution was dissolved in DCM (1 mL) and precipitated out in cold EtOH

(50 mL). The resulting solution was centrifuged for 15 minutes at 20k rpm at 4 °C. The pellet was collected, and the purification process was repeated 3x to yield an orange solid (41.7 mg).

*Synthesis of ANBB-BODIPY-**4 (AB-4)***

A flame-dried vial charged with **5** (0.288 mmol, 1eq.), piperazine (0.18 mmol, 0.8 eq.), and **5** (0.09 mmol, 0.4 eq.) was dissolved with anhydrous acetone (1.25 mL) under argon. $Et_3N$ (1.14 mmol, 5 eq.) was added, and the reaction was allowed to stir at room temperature. After 4 days, the resulting solution was dissolved in DCM (1 mL) and precipitated out in cold EtOH (50 mL). The resulting solution was centrifuged for 15 minutes at 20k rpm at 4 °C. The pellet was collected, and the purification process was repeated 3x to yield an orange solid (33.7 mg).

*Synthesis of ANBB-BODIPY-**5 (AB-5)***

A flame-dried vial charged with **5** (0.288 mmol, 1eq.) and piperazine (0.21 mmol, 0.9 eq.) was dissolved with anhydrous acetone (1.25 mL) under argon. $Et_3N$ (1.14 mmol, 5 eq.) was added, and the reaction was allowed to stir at room temperature. After 3 days, compound **5** (0.06 mmol, 0.25 eq.) was added to the reaction solution and stirred at room temperature for another 24 hours. The resulting solution was dissolved in DCM (1 mL) and precipitated out in cold EtOH (50 mL). The resulting solution was centrifuged for 15 minutes at 20k rpm at 4 °C. The pellet was collected, and the purification process was repeated 3x to yield an orange solid (37.1 mg).

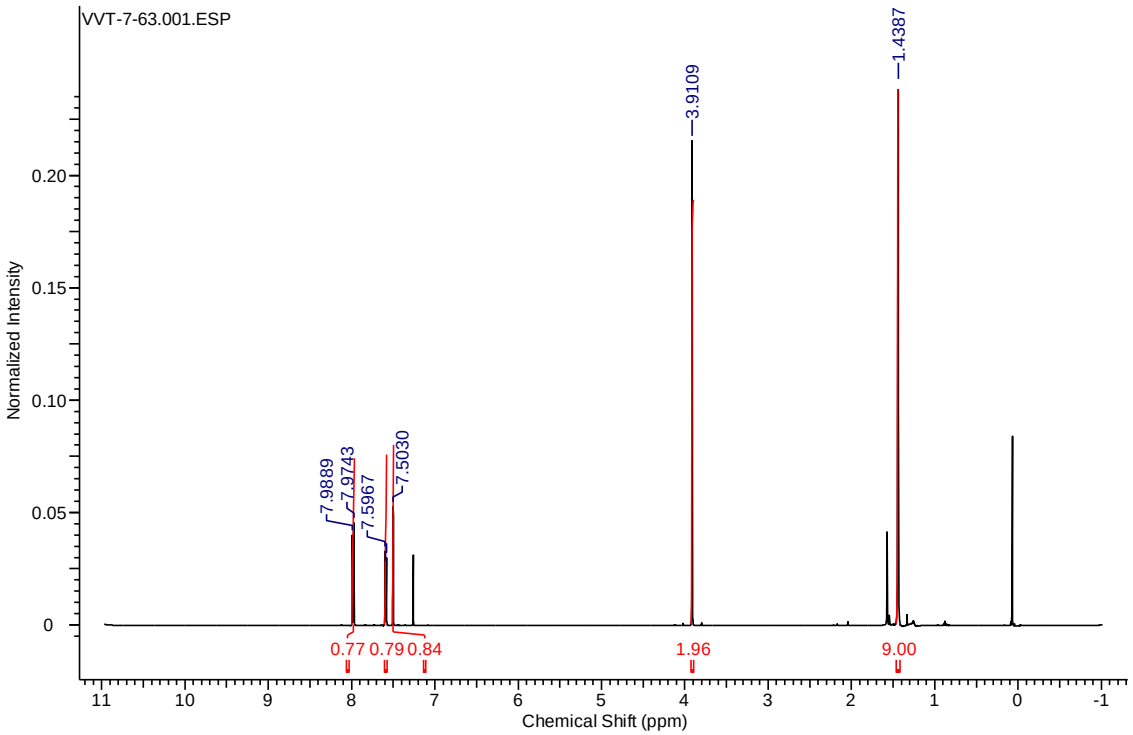


Figure 1.S2. $^{1}$H NMR spectrum of compound **1** in $CDCl_3$.

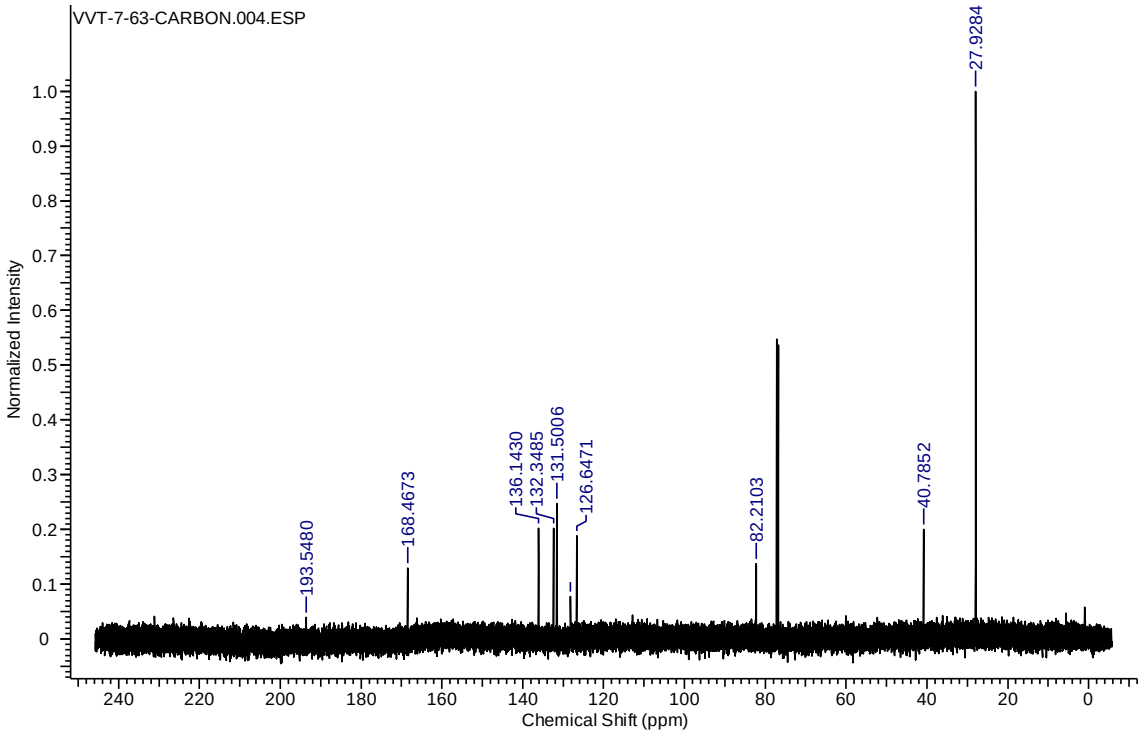


Figure 1.S3. 13C HNMR spectrum of compound **1** in CDCl3.

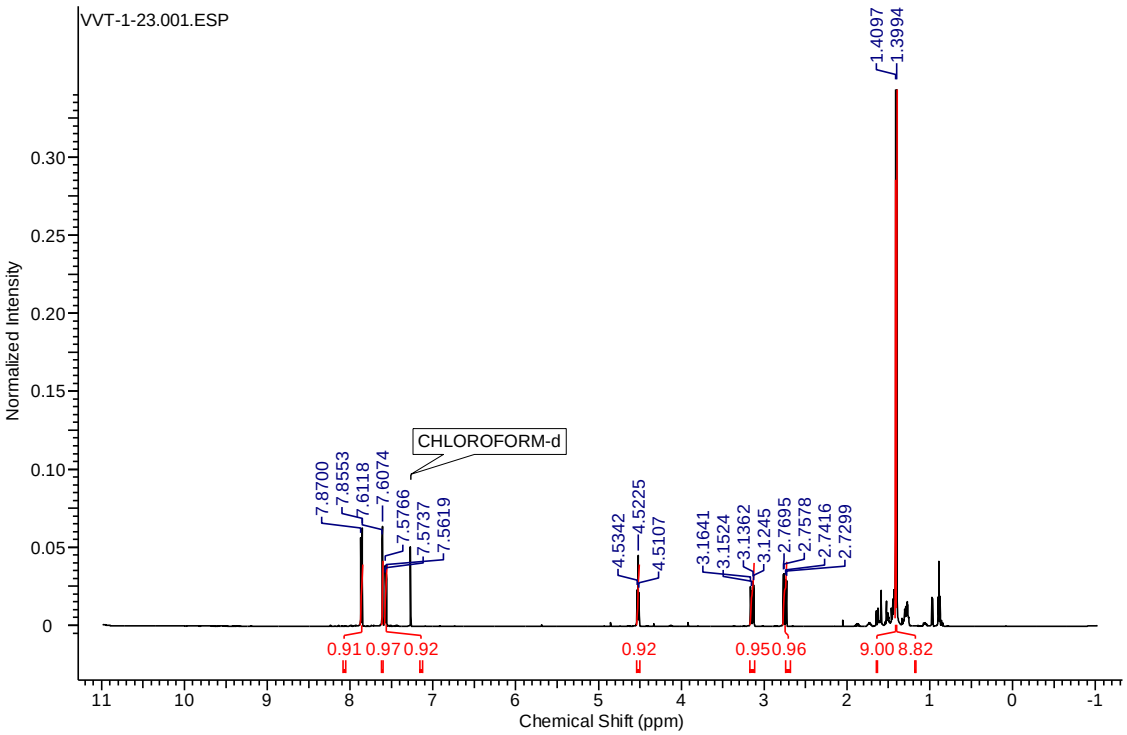


Figure 1.S4. $^{1}$H NMR spectrum of compound **2** in $CDCl_3$.

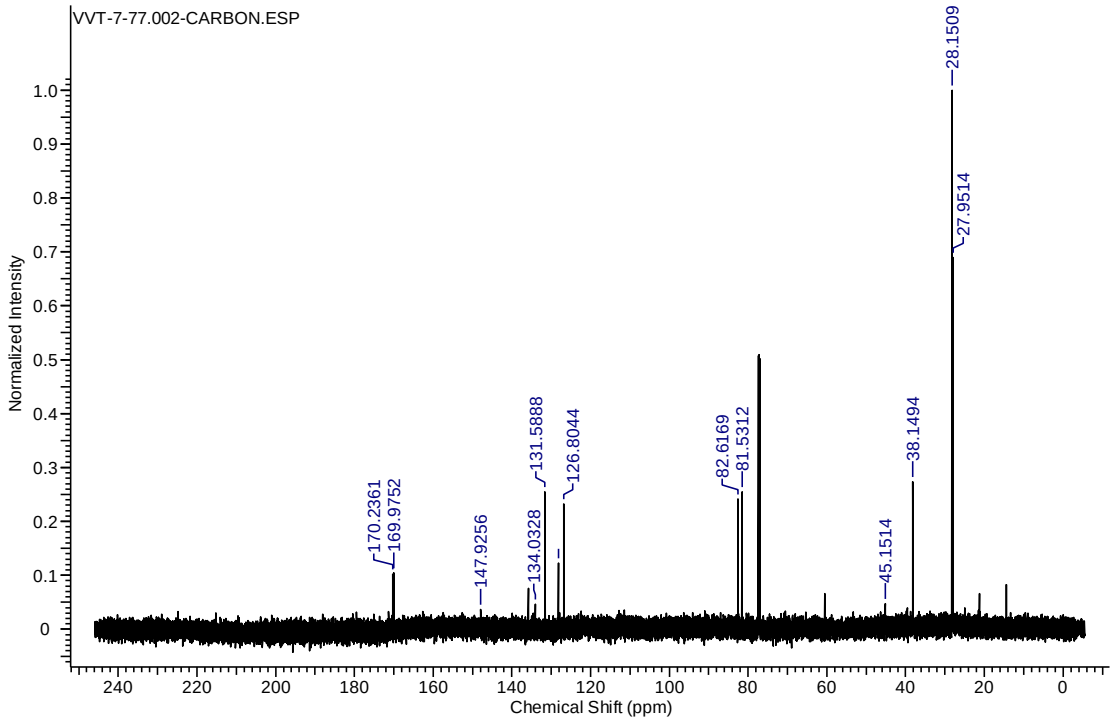


Figure 1.S5. $^{13}$C NMR spectrum of compound **2** in $CDCl_3$.

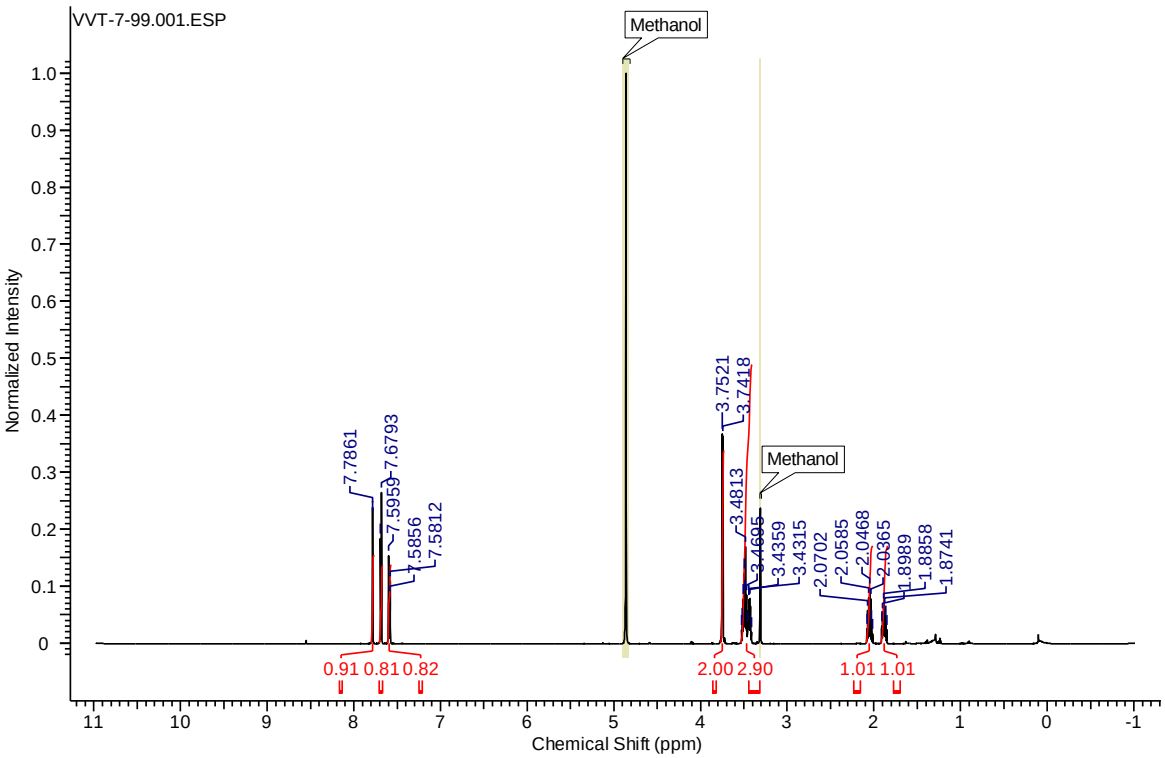


Figure 1.S6. $^{1}$H NMR spectrum of compound **3** in MeOD.

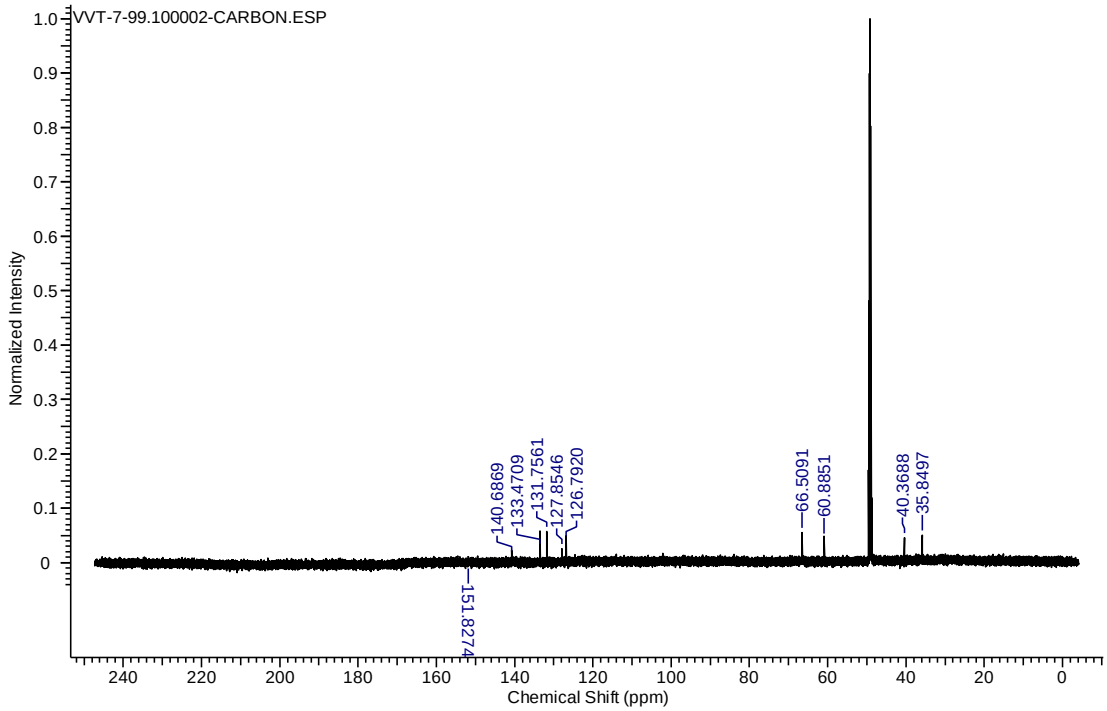


Figure 1.S7. $^{13}$C NMR spectrum of compound **3** in MeOD.

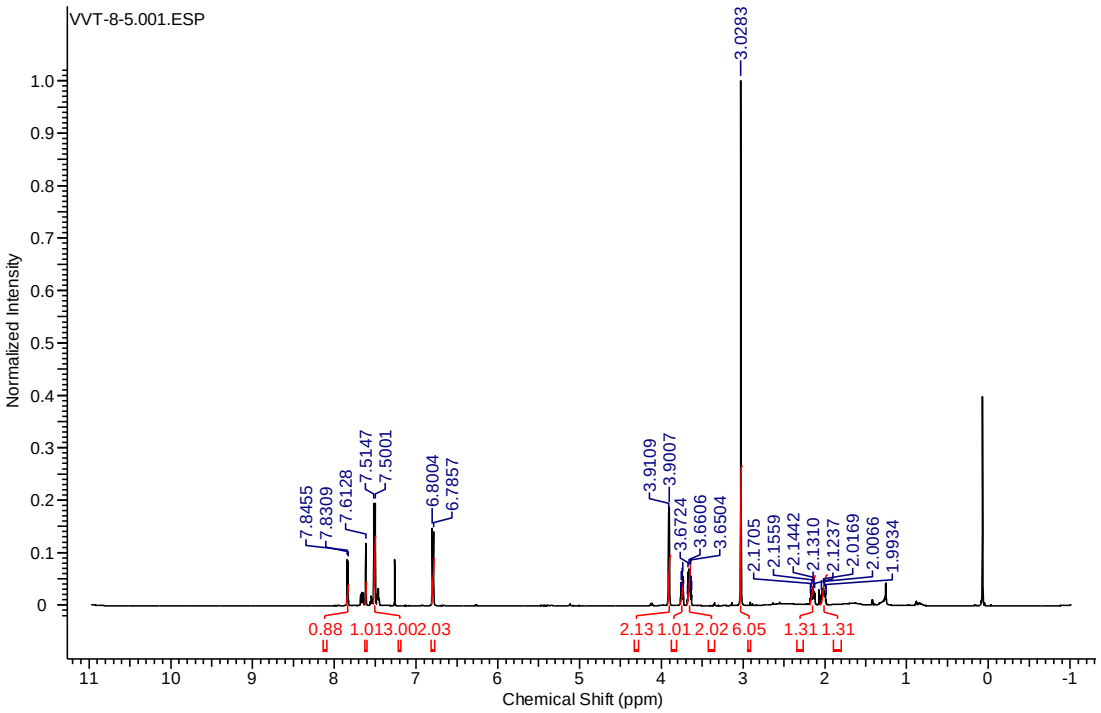


Figure 1.S8. $^{1}H$ NMR spectrum of compound **4** in $CDCl_3$.

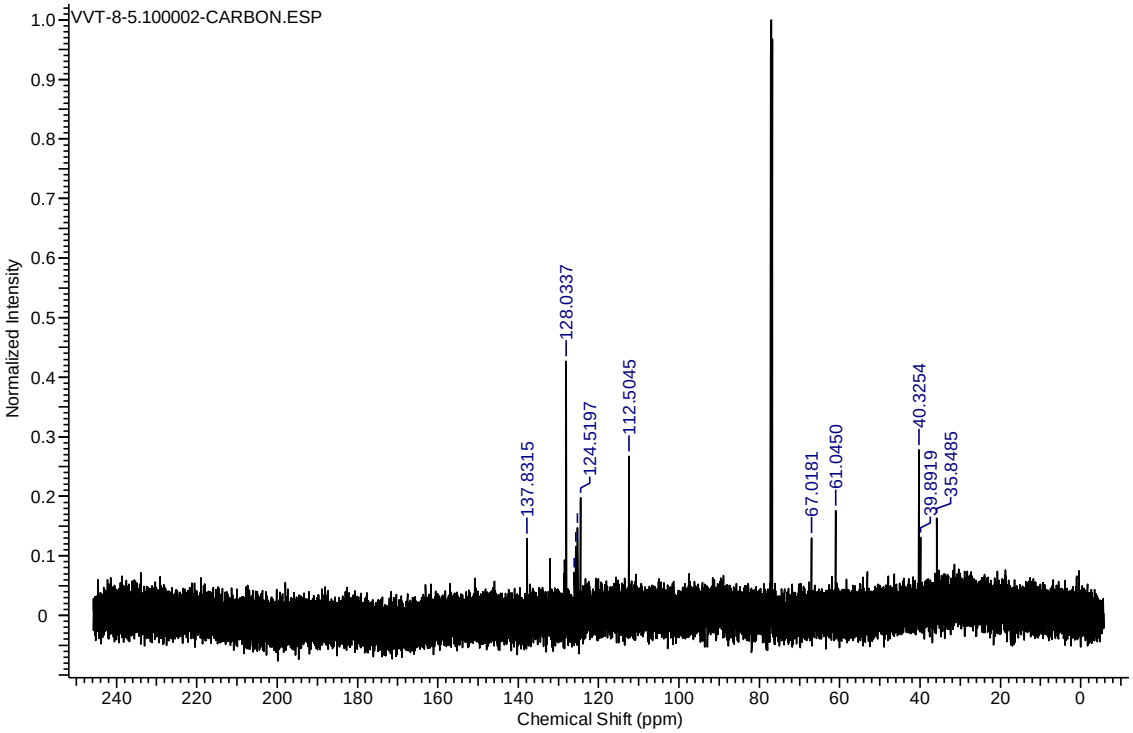


Figure 1.S9. $^{13}C$ NMR spectrum of compound **4** in $CDCl_3$.

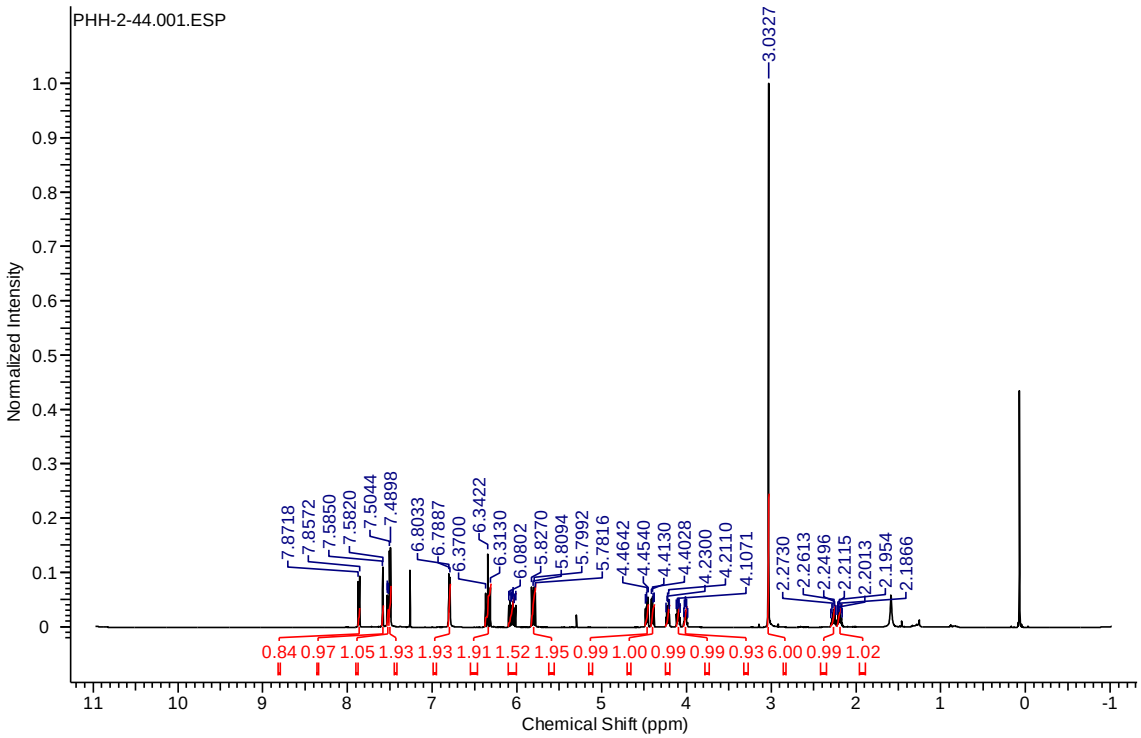


Figure 1.S10. $^{1}$H NMR spectrum of compound **5** in $CDCl_3$.

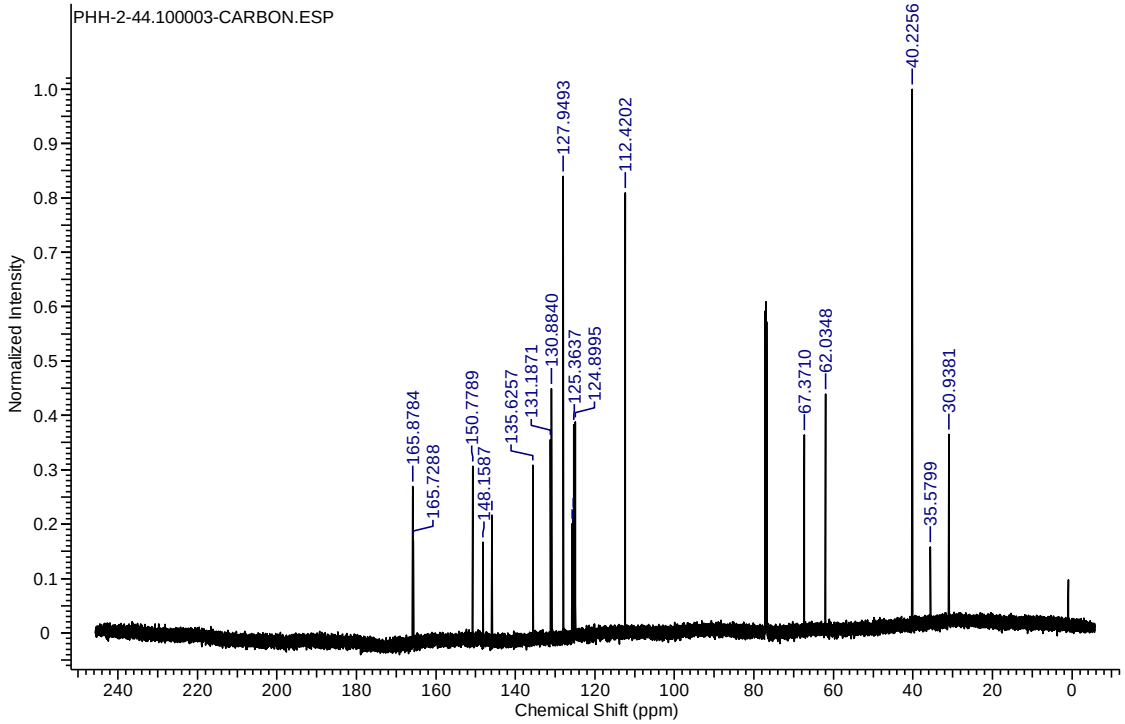


Figure 1.S11. $^{13}$C NMR spectrum of compound **5** in $CDCl_3$.

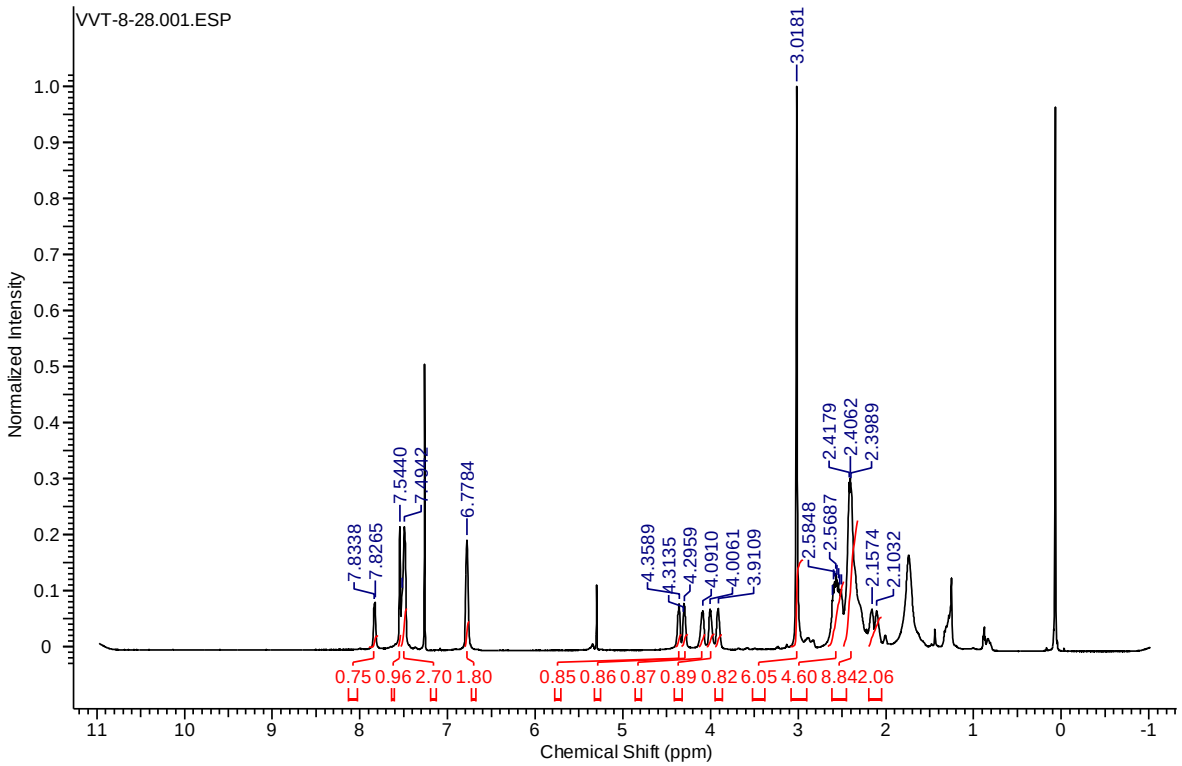


Figure 1.S12. $^{1}$H NMR spectrum of polymer ANBB in $CDCl_3$.

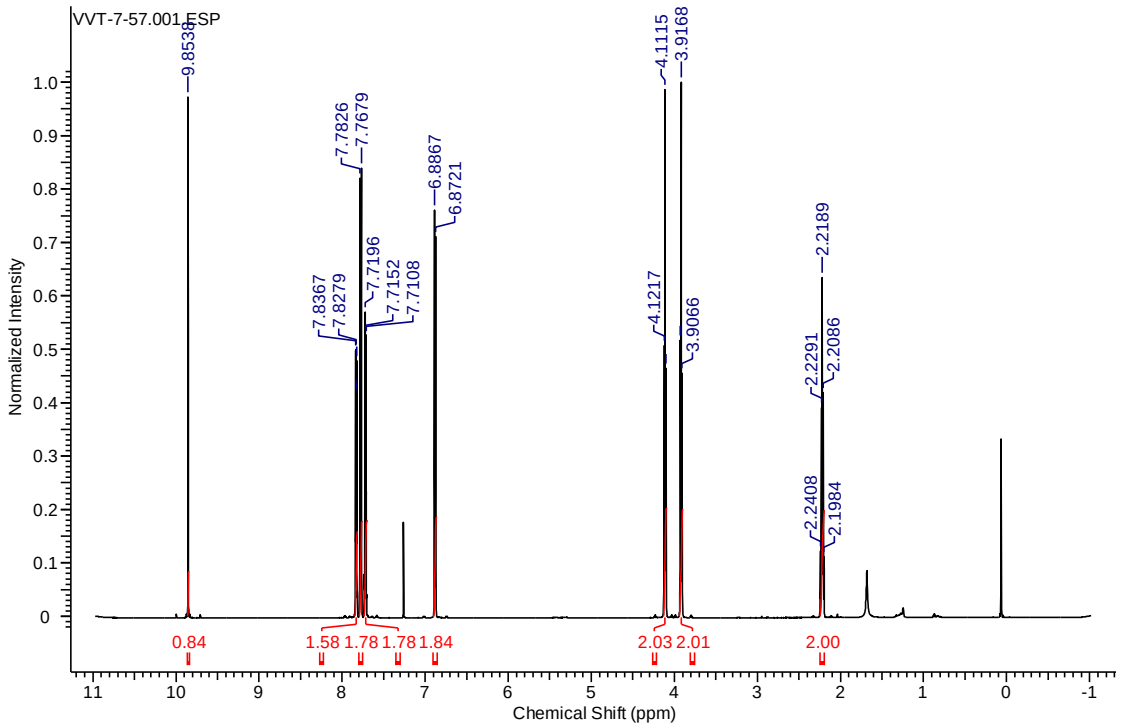


Figure 1.S13. $^{1}$H NMR spectrum of compound **6** in $CDCl_3$.

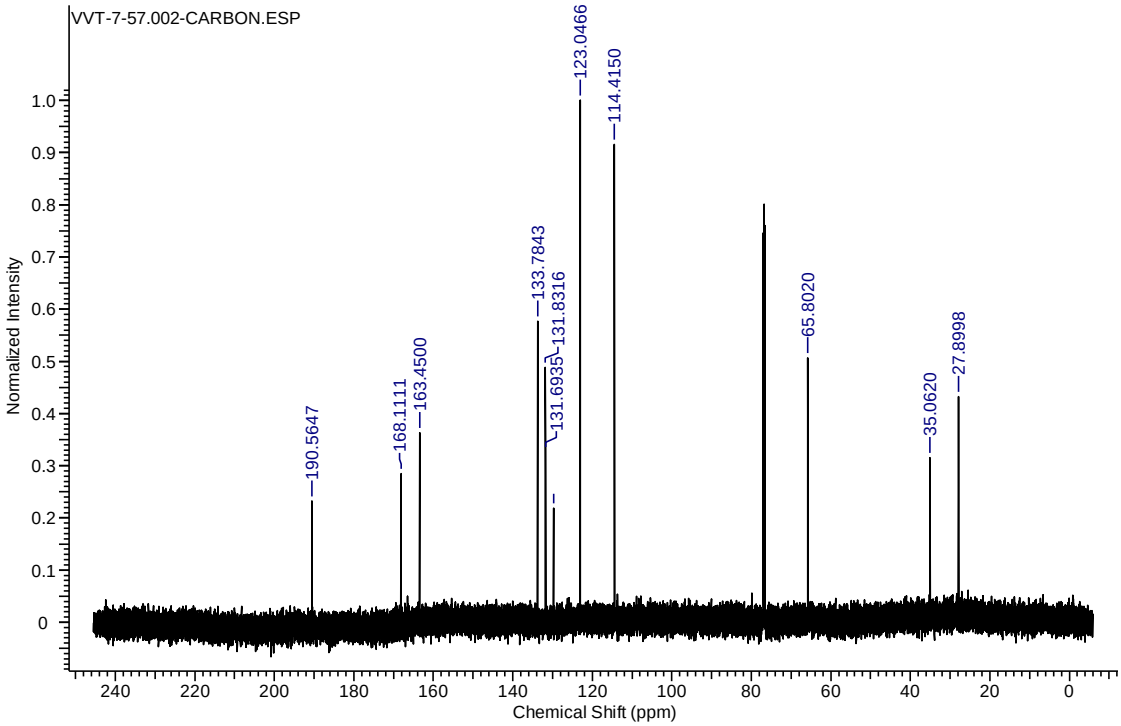


Figure 1.S14. $^{13}$C NMR spectrum of compound **6** in $CDCl_3$.

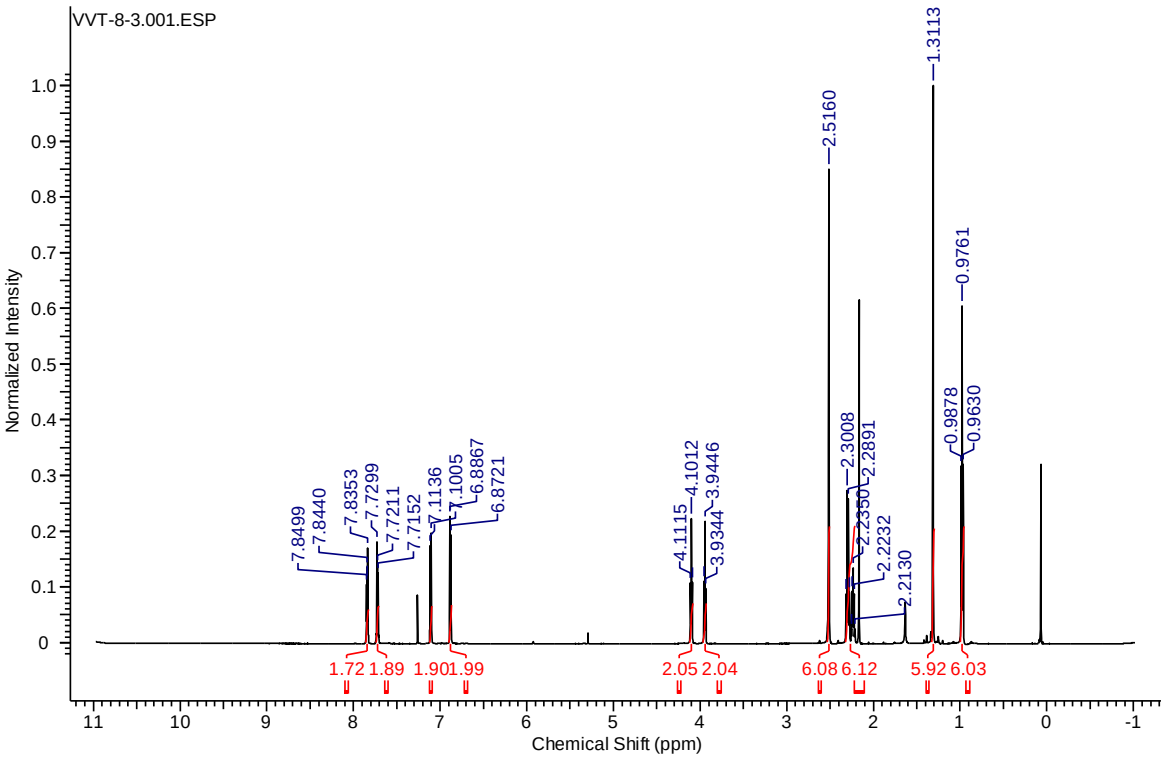


Figure 1.S15. $^{1}$H NMR spectrum of compound **7** in $CDCl_3$.

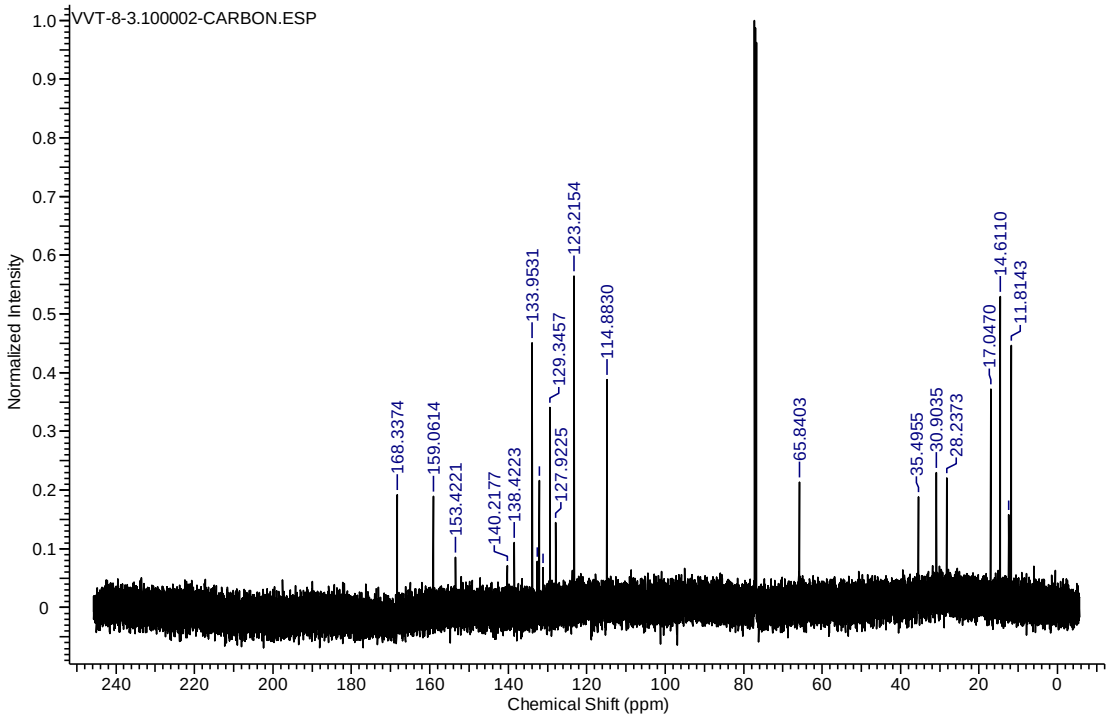


Figure 1.S16. $^{13}$C NMR spectrum of compound **7** in $CDCl_3$.

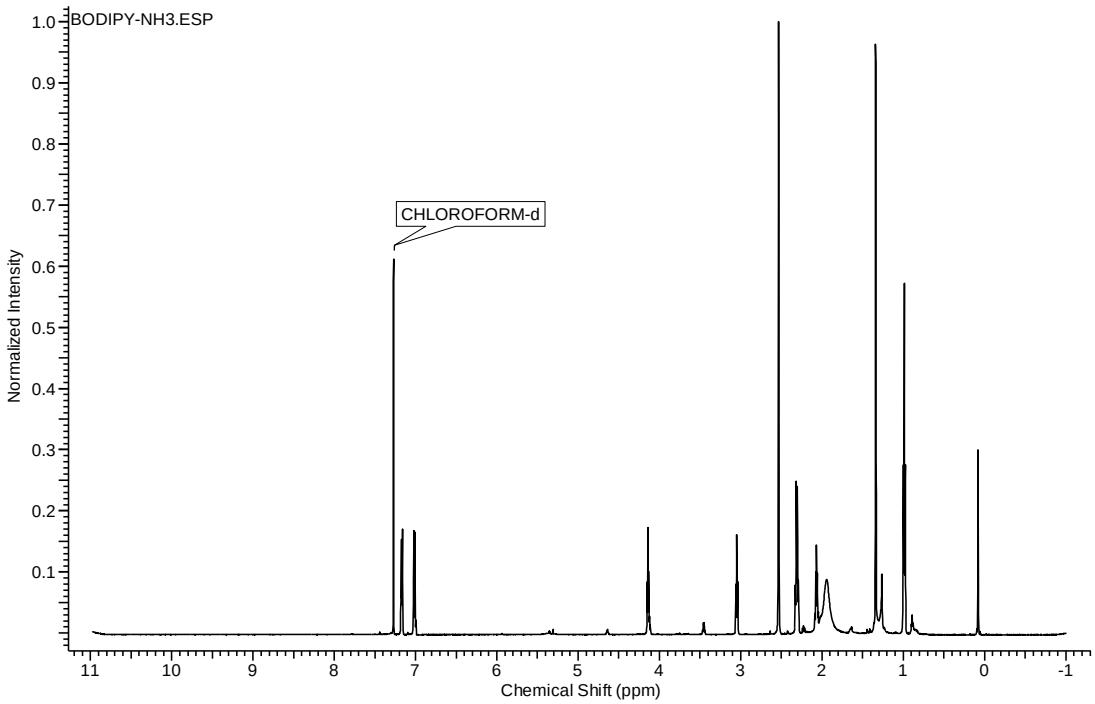


Figure 1.S17. $^{1}$H NMR spectrum of compound **8** in $CDCl_3$.

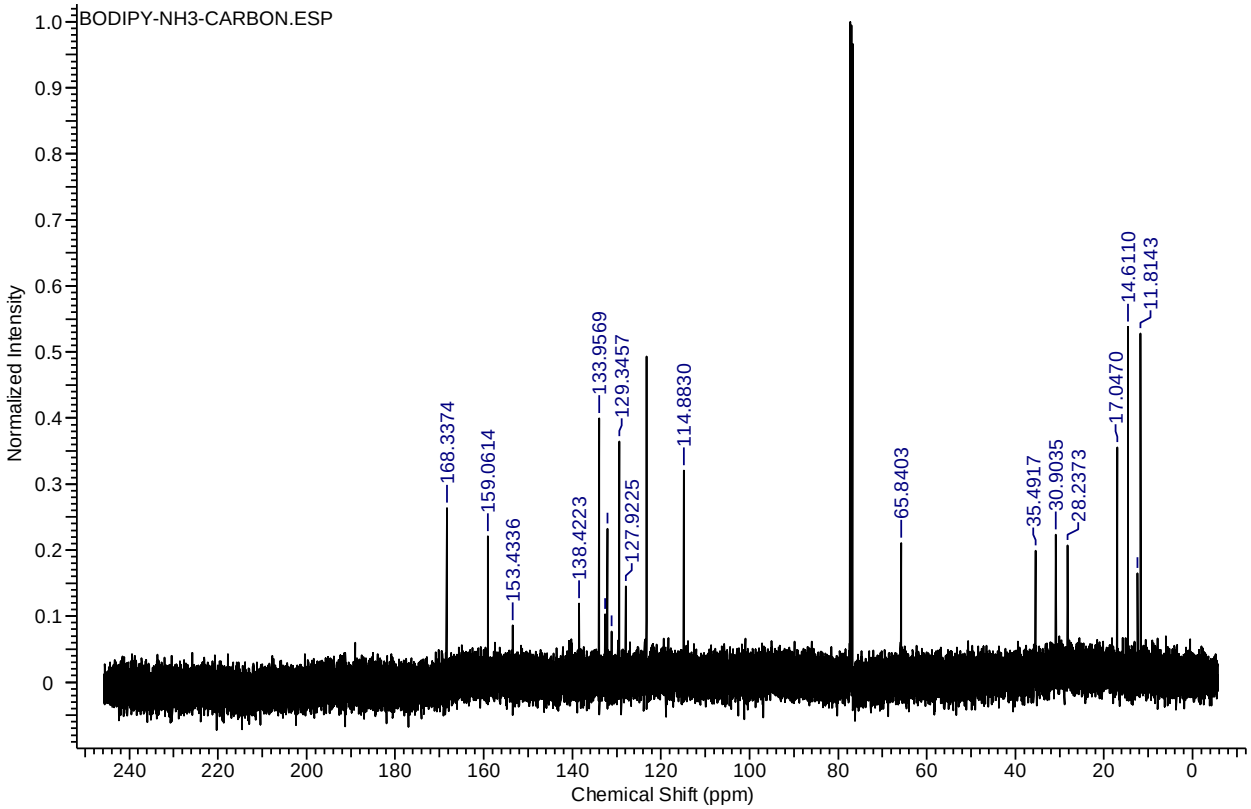


Figure 1.S18. $^{13}$C NMR spectrum of compound **8** in $CDCl_3$.

# CHAPTER 2

Exploration of Visible Light Responsive Chromophores as Potential Polymers

## *2.1 Abstract*

Spatial and temporal control of chemistry has opened the door to more precise stimuli-responsive drug-delivery systems. The majority of these systems utilize biological cues such as ROS, pH, or other endogenous chemicals to activate the chemistry of the delivery system to release their drug cargo. Light, however, provides more precise control as it can be externally applied while manipulating the irradiation time, power density, and beam size. Very few systems utilize innocuous blue visible light as a stimulus. Here we utilize two chromophores and explore their potential as blue visible light responsive polymers and possibly drug-delivery systems.

## *2.2 Introduction*

Light is widely used as an exogenous trigger to release a desired payload from stimuli responsive small molecules or nanomaterials. External application allows for the application of a desired wavelength of light and spatiotemporal control over photoactive systems.[1-6] The utilization of light as a stimulus allows for on-demand activation of photochemistry which provides a higher level of control compared to systems that rely on biological cues such as pH[7-10], reactive oxygen species (ROS)[11-16], and enzymes[17-23]. This enhanced level of control has made light-responsive materials a very attractive platform for effective drug delivery, for example to trigger the release of payloads from photocages. Photocages are an approach to protect the payload from off-target interactions – because the localization of light – and from degradation – because the payload will remain stable within the cages.

To be truly effective in biological applications, light responsive materials should utilize wavelengths that allow for penetration deep into tissue and are innocuous in biological systems. Currently, the majority of light responsive materials utilize ultraviolet (UV)[24] and near-infrared (NIR) wavelengths as an excitation source, but these wavelengths have substantial limitations for *in vivo* and *in vitro* application. Although UV light can stimulate a one-photo excitation to activate photochemistry, the deleterious effects of UV light have been well documented as it is the primary suspect in causing skin cancer. Additionally, many biological molecules absorb UV light resulting in poor tissue penetration and undesired photochemical reactions.[24] The longer wavelengths of NIR light provide deeper tissue penetration and its lower energy allows for bio-benign interactions.[25-28] However, systems utilizing NIR use multi-photon methods such as two-photon excitation[29-31] and NIR-to-UV upconversion[32-34] are inefficient compared to single photon systems. Two-photon excitation requires extended irradiation at high laser outputs, which is inefficient and may lead to heat-induced damage of biological tissue while upconversion still exposes cells to UV wavelengths.

The utilization of visible light absorbing chromophores offers the perfect middle ground to both UV and NIR-responsive materials. Visible light is energetic enough to activate quick and efficient photochemistry triggered by one-photon excitation, requiring shorter irradiation times at lower powers densities.[35] Additionally, visible light is less harmful to biological tissue than UV[36,38] and has a greater penetration depth compared to UV due to the low number of biological molecules that absorb this particular wavelength.[39] However, the number of single-photon absorbing, visible light-responsive materials capable of releasing molecules is limited. Recent studies[36,37] have demonstrated the efficacy of photocages utilizing visible blue light-absorbing

chromophores. Inspired by these studies, we incorporated these chromophores to synthesize monomers for the development of blue light photoresponsive polymeric materials as drug carriers.

The first pair of visible light responsive monomers were inspired by a blue visible light absorbing chromophore developed by Agarwal *et al*.[37] Their chromophore consisted of a dinitro derivative of bisstyrylthiophene (BIST) that absorbed light effectively (extinction coefficient, $\varepsilon_{440}$ = 66,000 $M^{-1}$ $cm^{-1}$) to undergo *ortho*-nitrobenzyl[40] (ONB) photochemistry to release $Ca^{2+}$ ions. Here, two monomers were designed and synthesized that utilized the BIST chromophore with varying functional groups tethered off the terminal benzenes (Scheme 2.1). The first monomer, form **1** (BIST), consists of a benzylic acrylate on the terminal ends of the chromophore to serve as a site to polymerize the monomer using Michael Addition. The other BIST monomer, **2** (MeBIST), consists of a methylated benzylic alcohol that serves as the polymeric linkage through nucleophilic reactions with potential linkers. By polymerizing these dinitro BIST chromophores, the resulting polymers is predicted to undergo complete degradation upon irradiation of light stimuli via ONB photochemistry (Figure 2.1a). This would be the most ideal when utilizing these light absorbing polymers as drug carriers, as it should allow for complete, on-demand drug release.

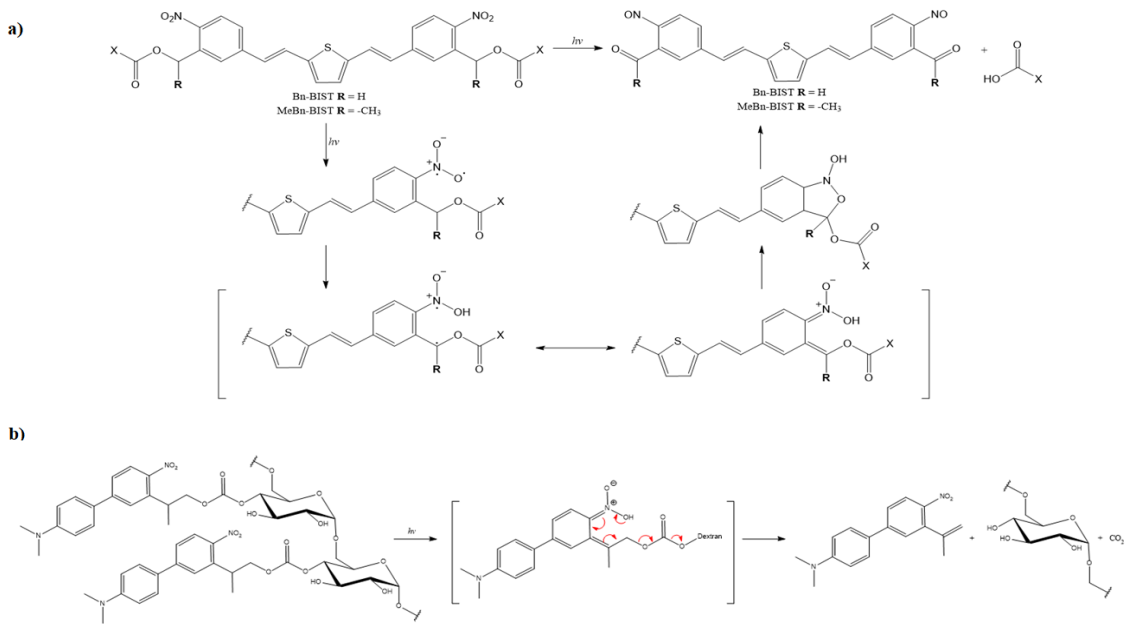


Figure 2.1. The expected mechanisms of degradation of chromophores utilizing (a) BIST/MeBIST and (b) ANBP. (a) The BIST chromophores utilize the *o*-nitrobenzyl photodegradation forming a carbonyl functional group at the terminal ends. (b) The ANBP is expected to degrade through a photoinduced *aci*-nitro intermediate previously explored by our group.

The second chromophore utilized is inspired by the work of Donato *et al*.[36] Their work demonstrated that their diphenyl chromophores could undergo photolysis under irradiation of blue visible light ($\varepsilon_{397}$ =7,500 $M^{-1}$ $cm^{-1}$) while in a hydrophobic environment, which is crucial as most polymer-based carriers have a hydrophobic interior. Our lab previously synthesized a polymer using a modified version of this chromophore.[38] The polymer was made of a 2-(4′-*N*-dimethyl**a**mino-4-**n**itro-[1,1′-**b**iphenyl]-3-yl)**b**utane-1,4-diyl dicarbonyl (ANBB) chromophore, linked together with piperazine using Michael Addition. The degradation mechanism of this polymer starts with the formation of a photo-induced *aci*-nitro intermediate. The deprotonation of the intermediate leads to photocleavage by a β-elimination pathway to break apart the polymeric linkages, yielding a nitro-alkene derivative.[38] However, in this current study, instead of incorporating the chromophore directly into the polymer backbone, we aim to conjugate it onto

the FDA-approved biopolymer, dextran. By conjugating onto an existing polymer, varying lengths of blue light-responsive polymers is easier to prepare. To achieve this, the synthetic route was modified to allow for a single alcohol tether rather than two and the benzyl position was methylated (ANBP) (Scheme 2.2). Upon irradiation with blue visible light, the chromophore should undergo photolysis through the same *aci*-nitro intermediate (Figure 2.1b) and form biocompatible free dextran as a byproduct.

## 2.3 Results and Discussion

The synthesis of monomer **1** (Scheme 1.1) started with the nitration of 3-bromobenzaldehyde, synthesized following the previously published procedure.[41] 5-Bromo-2-nitrobenzaldehyde (**4**) was reduced using $NaBH_4$ to the benzylic alcohol, compound **5.** The alcohol was then protected using TBDMS-Cl to form **6**. The protected alcohol was then vinylated using $Pd(PPh_3)_4$ and 2,4,6-trivinyl-boronxin pyridine complex following a procedure by Agarwal *et al*[37] to the styrene derivative, **7**. The BIST chromophore was synthesized by Heck coupling of **7** with dibromothiophene to give **8**. The chromophore was deprotected using TBAF to yield the terminal diol **9**. The diols were then transformed to acrylates using acryloyl chloride and $Et_3N$ to yield monomer **1.**

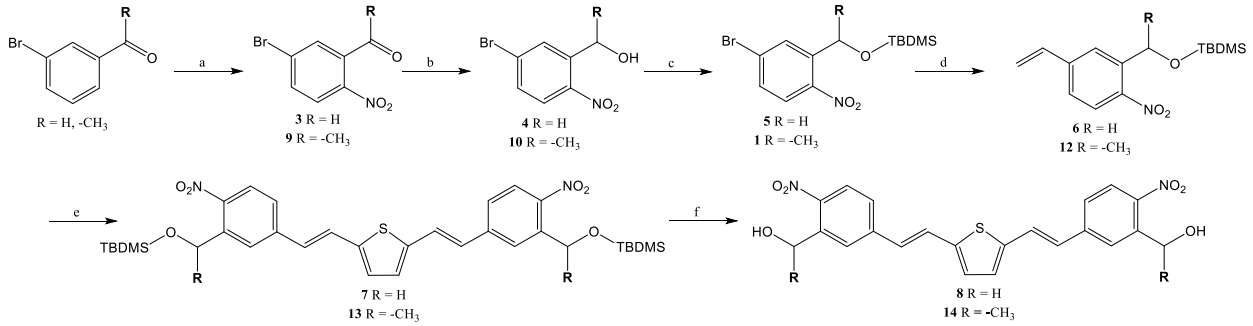


Scheme 2.1. Synthesis of BIST chromophores. (a) $HNO_3$, $H_2SO_4$; (b) $NaBH_4$, MeOH, 0 °C; (c) TBDMS-Cl, imidazole, DCM; (d) $Pd(PPh_3)_4$, 2,4,6-trivinyl-boroxin pyridine complex, $K_2CO_3$, DME, $H_2O$, 100 °C; (e) dibromothiophene, $Pd(OAc)_2$, LiCl, TBACl, $NaHCO_3$, DMF, 110 °C; (f) TBAF, THF

Monomer **1** exhibited a UV-Vis absorbance of 430 nm and fluorescence emission at 580 nm, which may be beneficial in drug delivery systems as it would allow for particles incorporating this monomer to be visualized and traced (Figure 2.2a). Preliminary degradation studies were done on monomer **1** using nuclear magnetic resonance (NMR) and liquid chromatography – mass spectroscopy (LC-MS) (Figure 2.2b). After 15 min of blue light irradiation, the monomer sample was purified using flash chromatography. NMR analysis of the purified irradiated sample showed

a new peak at 10.3 ppm, indicative of an aldehyde (Figure 2.2c). LC-MS data showed a large peak at *m/z* = 457.2 which matches the mass of the predicted degraded product with a sodium ion.

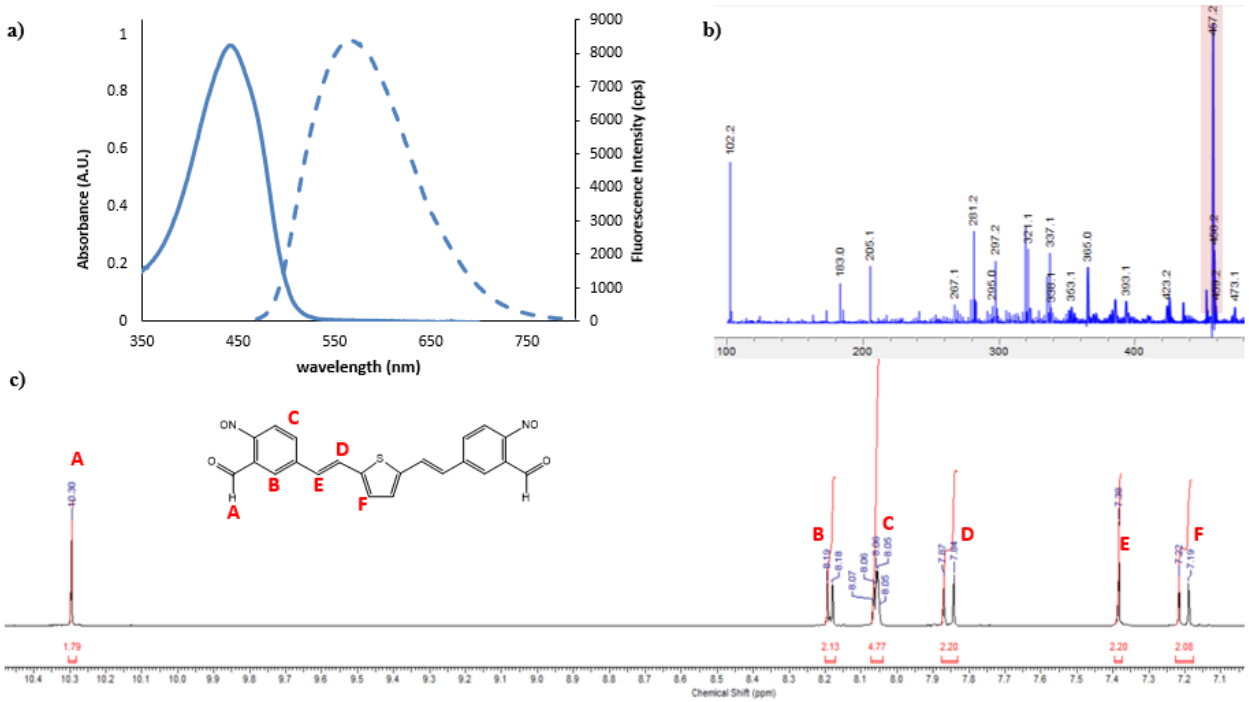


Figure 2.2. Preliminary Analysis of Monomer 1. (a) Absorption and emission spectra of monomer 1 exhibiting an absorbance at 430 nm and emission at 580 nm. (b) Initial LC-MS chromatogram of Monomer 1 after 15 min of irradiation and purification using column chromatography (c) $H^1$ NMR spectra shows the monomer 1 in DMSO-$d_6$ after 15 min. of BVL irradiation and purification by silica gel column chromatography.

With this preliminary result, it appeared as though polymerization of monomer **1** would result in photodegradable organic polymers with an ester linkage. Thus, a few attempts were made to polymerize monomer **1** using the Michael addition, similar to a previous method done in the group.[32] Attempts with piperazine and other linkers bearing amines unsuccessful. Finally, monomer **1** was polymerized with 4,4′-trimethylenedipiperidine using DBU as a base, forming **polyBIST-1**. However, upon analysis of this polymer using gel permeation chromatography (GPC), it was found to be very short (*Mw*: 2.2 kDa) and very polydisperse (PDI: 2.4). The

polyBIST-1 oligomer exhibited an absorbance at $\lambda_{ex}$ = 440nm and a $\lambda_{em}$ = 595nm (Figure 2.3a). Despite polyBIST-1's short length, a preliminary degradation study was done on three samples of the oligomer (5 mg $mL^{-1}$) by GPC. One sample was left in the absence of light as a control while the other two were irradiated for 30 min and 60 min, respectively. The GPC results did not exhibit an obvious degradation process as the irradiated signals did not show any shifts in retention times when compared to the control (Figure 2.3b). Although the UV absorbance clearly decreased over time indicating photophysical process change, the polymer degradation could not be confirmed without a broadening or shift of the GPC retention time. UV-Vis absorbance of polyBIST-1 before and after 60 min (Figure 2.3c). of blue light exposure showed a dramatic decrease but NMR analysis of the crude irradiated polymers did not how the presence of the aldehyde.

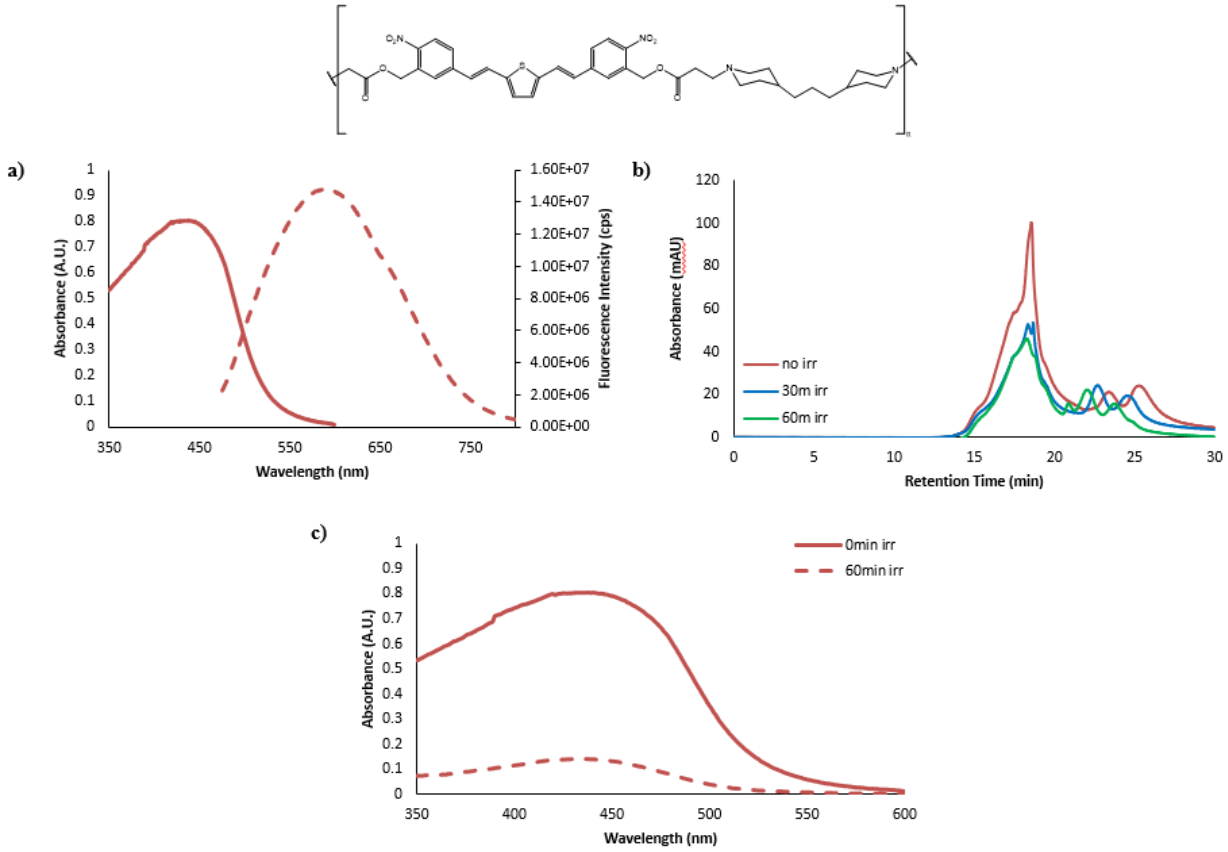


Figure 2.3. (a) UV-Vis absorbance (solid) and fluorescence (dash) profiles for polyBIST-1. (b) GPC analysis of a polymer utilizing Monomer **1** with 4,4'-Trimethylenedipiperidine as a linker under varying blue light exposure time. (5 mg $mL^{-1}$). (c) The absorbance of polyBIST-1 before (solid) and after (dash) 60 min. irradiation of blue visible light.

The lack of degradation after polymerization prompted the re-evaluation of monomer **1**'s photodegradation. This time, the purified monomer **1** was dissolved in DMSO-$d_6$ and irradiated with blue visible light (400-500nm). However, the monomer was not subjected to column chromatography after irradiation. Monomer **1** was irradiated for 20 minutes and then checked by NMR. There was noticeable change in NMR spectra nor was there an appearance of a new peak. The sample was then allowed to incubate overnight at 37 °C and then irradiated the following day for an additional 60 minutes. Again, the NMR did not show any peaks corresponding to the expected aldehyde (Figure 2.4). Additionally, attempts to synthesize more monomer **1** proved to be too tedious, consistently giving low yields and requiring multiple purifications.

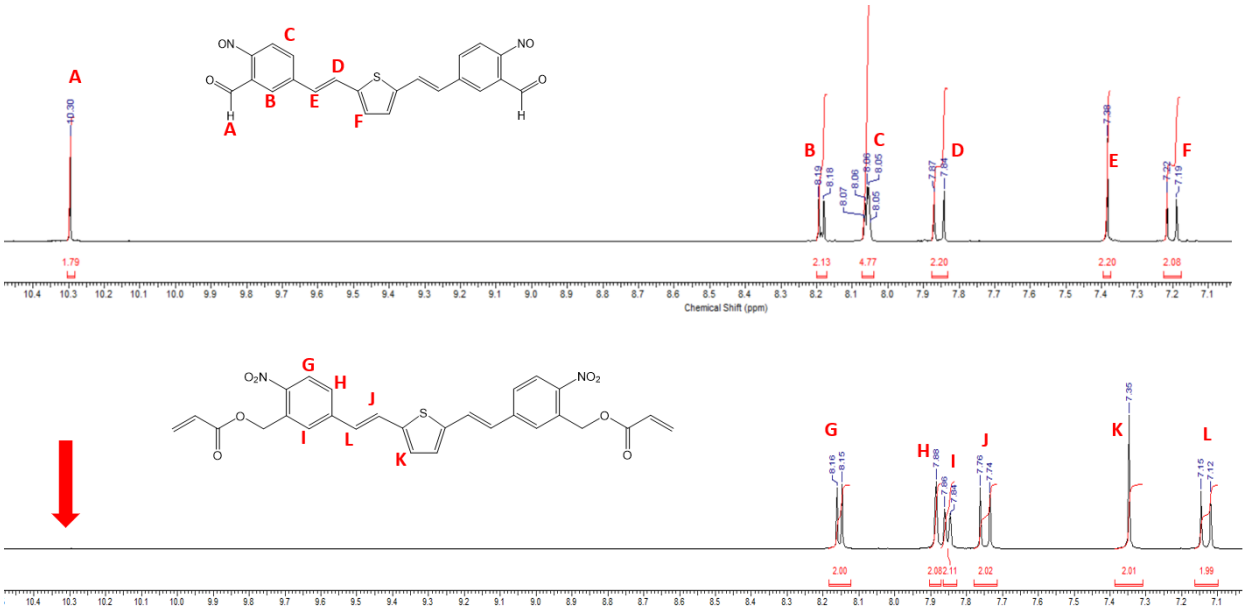


Figure 2.4. A comparison of the NMR spectra of two different samples of monomer 1 subjected to blue light irradiation. The top spectrum represents the degradation study (15 min irr) done on the same sample as Figure 2b. The spectrum on the bottom is from crude degradation studies without column separation (80 min irr).

Alongside the synthesis and analysis of the BIST chromophore, MeBIST was also being studied. The synthesis of MeBIST (Scheme 2.1) was done following a similar synthetic route as **1** but starting with 3-bromoacetophenone instead to position a methyl group in the benzylic position. The absorbance emission profiles for MeBIST were done using the TBDMS protected analog (**13**). TBDMS-protected MeBIST exhibited $\lambda_{ex}$ = 440nm and a $\lambda_{em}$ = 573nm (Figure 2.5a). Crude degradation studies were done on compound **13** using UV-Vis spectroscopy and NMR. The UV-Vis absorbance profile did exhibit a shift in absorbance from 440 nm to 477 nm after 30 mins of irradiation (Figure 2.5b). NMR analysis on **13** did not show the disappearance of the benzyl peak at 5.59 ppm nor did the peak integration decrease as expected (Figure 2.6c). Therefore, the bathochromic shift in the UV-Vis absorbance maxima may not have been due to photodegradation, similar to BIST.

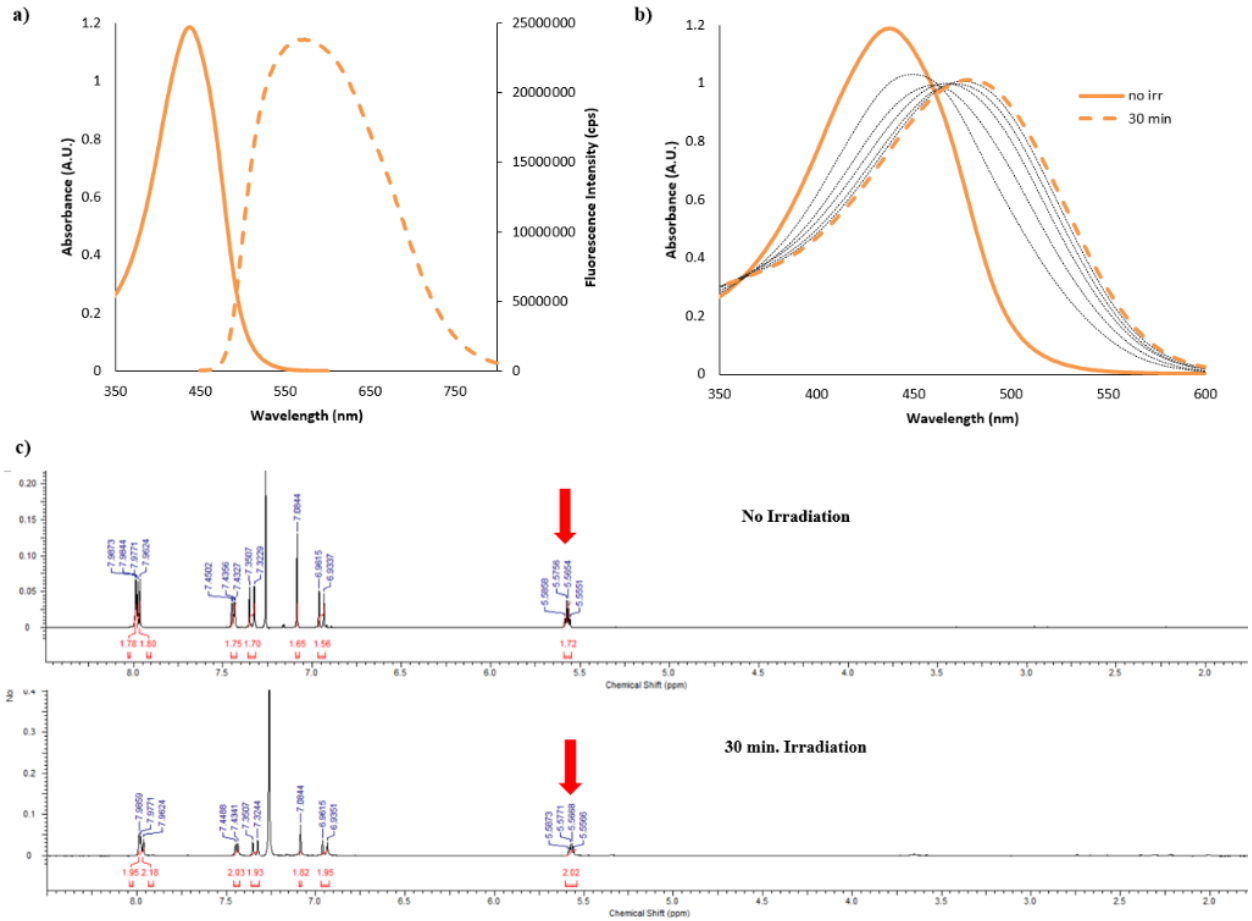


Figure 2.5. Analysis of the TBDMS protected analog of MeBIST (13). (a) The absorbance and emission profiles of 13. (b) Change in absorbance of 13 after subsequent exposure to blue visible light. (c) NMR analysis before and after irradiation.

Although the MeBIST chromophore does not exhibit the desired photodegradation, there were still attempts to polymerize it. The first attempt was to directly polymerize **14** with adipoyl chloride, to form **MB**. However, the GPC analysis showed that the polymer revealed that MB had a *Mw* = 15.4 kDa with a very large polydispersity of 24.4. The GPC results and the lack of peak broadening in the NMR are indicative a failed polymerization.

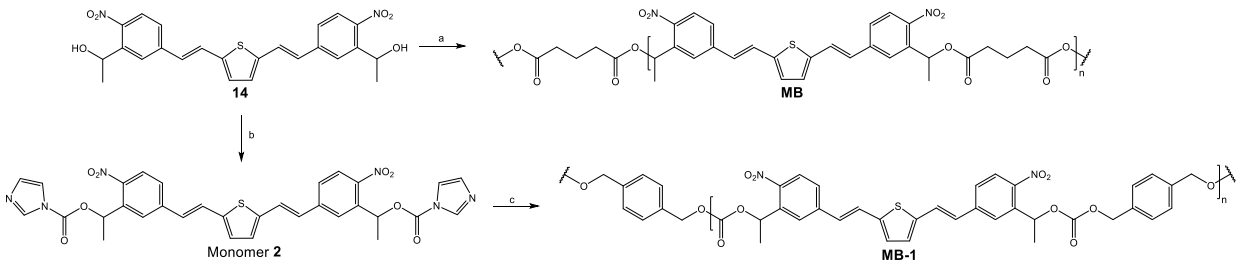

Scheme 2.2. Two different polymerization methods for the MeBIST chromophore.

Another polymerization method was attempted that utilized CDI coupling of monomer **2** with 1,4-benzenedimethanol, forming **MB-1** (Scheme 2.2). GPC analysis of the polymer displayed a *Mw* of 2.2 kDa (calculated by PMMA standard) which equates to about three repeating units, with a polydispersity of 2.1. The oligomer was subjected to blue light irradiation for varying durations up to 120 min. The MeBIST polymer displayed an absorbance at 436nm that shifted to 443 nm after 120 m of irradiation (Figure 2.6) and displayed a considerable decrease in the $Abs_{max}$. Characterization of the photoproperties and degradation of the oligomer still need to be done more thoroughly. However, the MB-1 was formulated into empty particles using a single emulsion method with polyvinyl alcohol (PVA) as a surfactant which resulted 165 ± 0.32 nm nanoparticles with a PdI of 0.107, measured by Dynamic Light Scattering (DLS). The nanoparticles were prepared for a separate project.

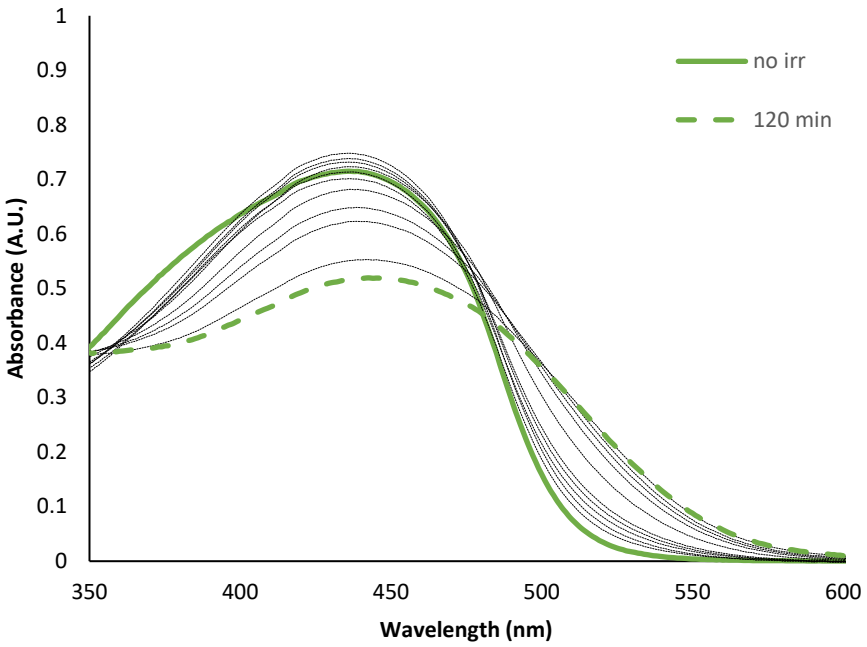


Figure 2.6. UV-Vis analysis of MB-1 with subsequent irradiation times up to 120 mins.

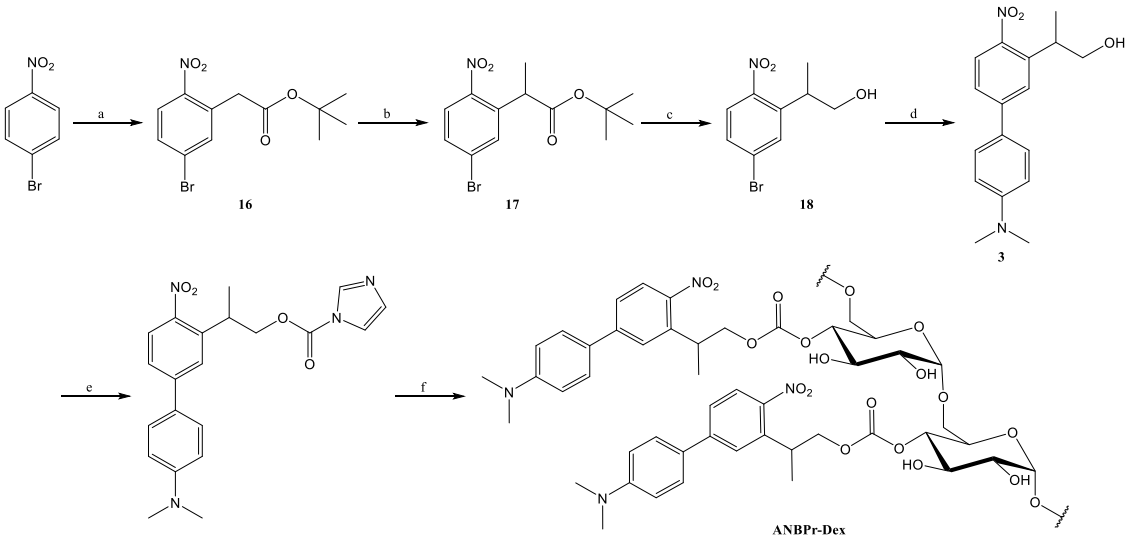


Scheme 2.3. Synthesis of ANBP. (a) 4-bromonitrobenzene, *t*-BuOK, *t*-Butyl chloroacetate, DMF, 0 °C to rt; (b) NaH, MeI, DMF; (c) DIBAL-H, THF, 0 °C; (d) 4-(Dimethylamino)phenylboronic acid, $Pd(PPh_3)_4$, $Na_2CO_3$, toluene, EtOH, $H_2O$, 90 °C; (e) CDI, DCM; (f) dextran, DMAP, DMSO, 80 °C.

The synthesis of ANBP (compound **3**) was done following a procedure by Donato *et al.* (Scheme 2.3).[37] To start, compound **16** was synthesized according to a published procedure.[40] **16** was then methylated using NaH and methyl iodide to form **17**. The *t*-butyl acetate group was

reduced using DIBAL-H to form alcohol **18**. The final chromophore **3** was synthesized by Suzuki coupling of **18** with $Pd(PPh_3)_4$ and 4-dimethylphenylboronic acid. **3** was conjugated onto dextran through a carbonate linker using the 1,1′-carbonyldiimidazole (CDI) coupling following a procedure like Broaders *et al*.[15] To evaluate the photodegradation of ANBP, a small molecule was synthesized using the CDI coupling with benzyl alcohol, **ANBP-Bn**. The molecule was irradiated under blue visible light (400-500nm) in $CH_2Cl_2$ for 1hour. After irradiation, the solution was concentrated *in vacuo* and the dried product was evaluated by NMR and LC-MS. An NMR comparison of ANBP-Bn and the unpurified irradiated product showed the appearance of new peaks but because the NMR is of a crude sample, a conclusion that ANBP-Bn photodegrades could not be made. If **ANBP-Bn** (*m/z* = 434.18) undergoes photodegradation through the *aci-nitro* intermediate, then the expected photoproduct should have a mass *m/z* = 282.14. The LC-MS data shows the presence of a peak at $[M+H]^+ = 282.29$ (Figure 2.7) but the major peak still corresponds to ANBP-Bn at $[M+H]^+ = 435.27$. LC-MS data combined with NMR analysis led us to believe that ANBP will photodegrade under blue visible light but would require more irradiation time with the laser employed in this study.

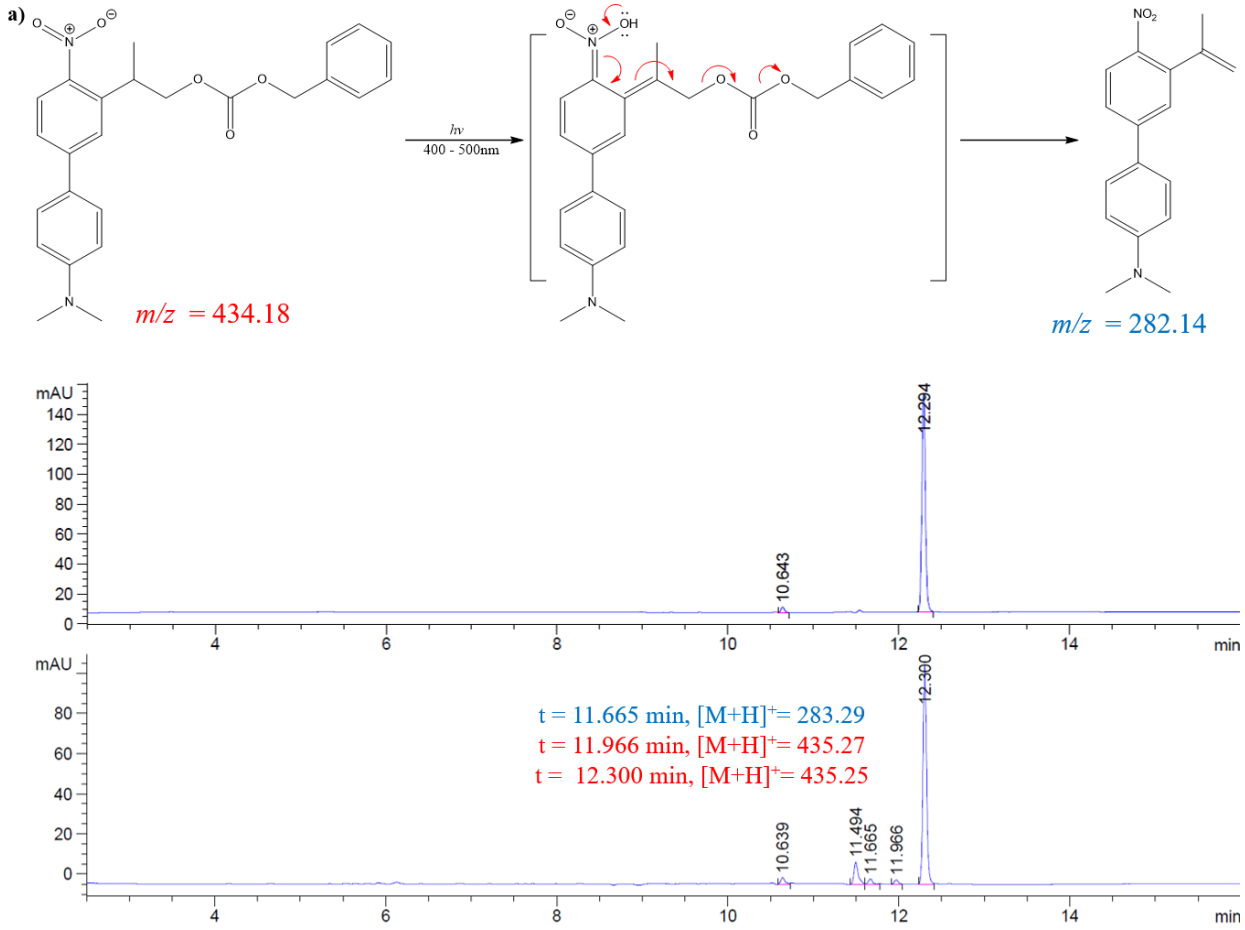


Figure 2.7. LC-MS analysis of ANBP-Bn and a crude sample after 1 hour of irradiation.

The ANBP monomer shows a strong absorbance at $\lambda_{max}$ = 400 nm with a bathochromic shift to 468 nm in $CH_2Cl_2$ after 90 min of irradiation with blue light (Figure 2.8a). The polymer was then formed into empty nanoparticles using a single emulsion formulation using sonication with PVA as a surfactant. After purification using tangential flow, the particles were lyophilized with mannitol as a cryoprotectant. The particles were taken up in phosphate buffered saline (PBS, pH 7.4) at 0.05 mg $mL^{-1}$ and characterized by dynamic light scattering (DLS) and displayed an average diameter of about 278 nm. Preliminary degradation studies were done on empty particles with non-irradiated particles as the control. The irradiated samples were exposed to blue visible light for an hour and incubated in the dark for 30 minutes. DLS data was collected immediately

after incubation. The control sample was left in the dark at room temperature and measured alongside the irradiated sample. The irradiated samples showed a significant decrease in normalized count rate while the control did not (Figure 2.8b). The drastic decrease in the count rate along with the greater decrease in particle size (Figure 2.S1) indicate particle degradation with irradiation. Additionally, it was previously demonstrated[38] that introducing a tertiary amine group in the ANBB polymer would assist in the deprotonation of the *aci*-nitro intermediate and mediate the photocleavage of the polymer. In hopes of seeing a more definitive degradation, the same irradiation study was also done under basic conditions with the particles taken up in sodium phosphate buffer solution (pH 8.5) at 0.05 mg $mL^{-1}$. Again, the irradiated sample showed greater change in particle size and count rate over time (Figure 2.8b). When the degradation at pH 7.4 is compared to pH 8.5, the difference is minimal and not significant enough to conclude that the ANBP-Dex particles degrade better under basic conditions. This may be due to the lack of interaction between the aqueous base and the conjugated chromophore which sits inside the hydrophobic particle.

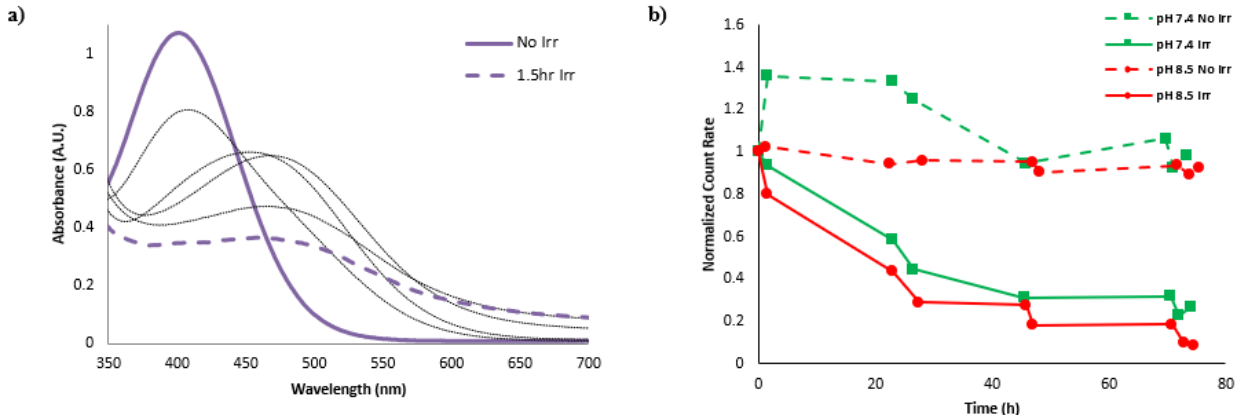


Figure 2.8. The degradation analysis of ANBP and ANBP-Dex. (a) UV-Vis analysis of the ANBP monomer after 90 min. (b) The normalized count rate of ANBP-Dex nanoparticles after irradiation using two different buffers.

To further demonstrate its potential as a drug carrier, the hydrophobic dye, Nile Red, was chosen as a model drug. Nile Red was encapsulated into ANBP-Dex nanoparticles using a single emulsion method, resulting in 9% loading capacity. The particles were taken up in PBS (0.05 mg $mL^{-1}$) and irradiated under blue visible light. Fluorescence was measured after each irradiation period. Since the ANBP-Dex particles do not exhibit fluorescence, any that is measured would be due to Nile Red. The fluorescence intensity of the encapsulated Nile Red decreased as the particles were irradiated with blue visible light (Figure 2.9). Since Nile Red is hydrophobic, when it is released into an aqueous environment, it should aggregate and quench its fluorescence. Therefore, the decrease in fluorescence intensity signifies the release of dye from the hydrophobic particles into the aqueous environment. The results suggest particle photodegradation. To ensure particle degradation, LC-MS studies should be done to ensure the presence of photocleaved byproducts.

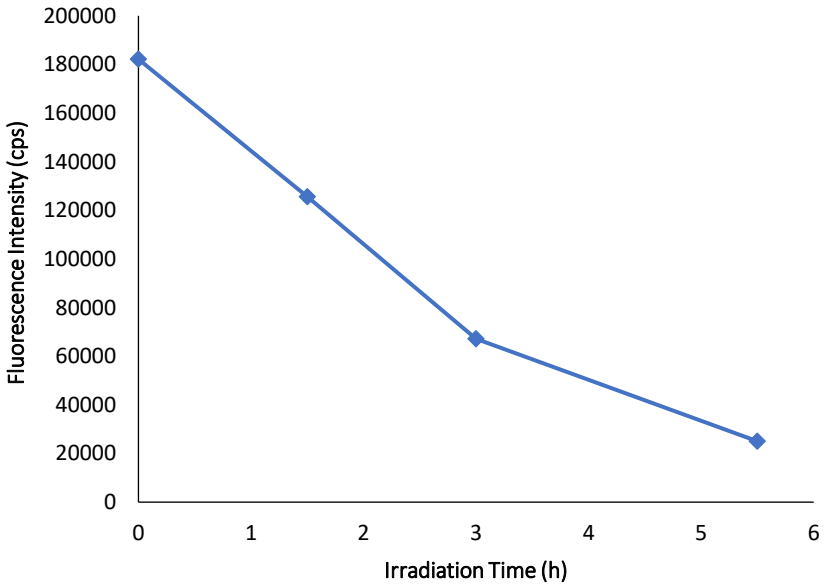


Figure 2.9. Fluorescence intensity Nile Red encapsulated ANBP-Dextran particles. The fluorescence intensity of Nile Red decreases with longer blue light irradiation.

## 2.4 Conclusion

Based on the results, the oligomers utilizing the BIST and MeBist chromophores do not photodegrade as expected. Although the polymers exhibit decreases in absorbance intensities, the lack of changes in the NMR spectra suggest that the polymers are photostable, even under prolonged irradiation times. This may be due to the power density of our blue light laser. A more comprehensive approach to these studies would be to synthesize small molecule models to assess the photodegradation more thoroughly. Additionally, synthesizing the expected photodegradation products and isomers would allow us to make clearer conclusions on the photochemistry of the BIST chromophores under blue visible light.

Studies with ANBP are a bit more promising as LC-MS analysis showed a peak corresponding to the expected photoproduct, although it was much lower in intensity compared peaks corresponding to ANBP. Studies on ANBP could be improved with direct comparison of the crude degradation NMR with synthesized ANBP photoproduct. However, the release of the hydrophobic Nile Red from ANBP-Dex nanoparticles is very encouraging for the prospects of ANBP-Dex as a possible polymeric drug carrier.

## 2.5 Abbreviations

ONB, *o*-nitrobenzyl; UV, Ultraviolet; NIR, near-infrared; Vis, visible; Dex, dextran; ROS, reactive oxygenated species; BIST, dinitro derivative of bisstyrylthiophene; MeBIST, methyl derivative of the dinitro derivative of bisstyrylthiophene; ANBB, 2-(4′-*N*-dimethylamino-4-nitro-[1,1′-biphenyl]-3-yl)butane-1,4-diyl dicarbonyl; TBDMS-Cl, tert-Butyldimethylsilyl chloride; TBAF, tetra-n-butylammonium fluoride; DCM, dichloromethane; DME, dimethoxyethane; TBACl, tetrabutylammonium chloride; DMF, dimethyl formamide; THF, tetrahydrofuran, LC-MS, liquid

chromatography-mass spectroscopy; NMR, nuclear magnetic resonance; DBU, 1,8-Diazabicyclo[5.4.0]undec-7-ene; GPC, gel permeation chromatography; DMSO, dimethyl sulfoxide; PMMA, poly(methyl methacrylate); PVA, polyvinyl alcohol; DLS, dynamic light scattering, ANBP, (2-(40-(N,N-dimethylamino)-4-nitro-[1,10-biphenyl]-3-yl) propyl carbonyl); CDI, 1,1′-carbonyldiimidazole; PBS, phosphate buffered saline.

**2.6. Acknowledgements**

NMR spectra were acquired at the UCSD Skaggs School of Pharmacy and Pharmaceutical Sciences NMR Facility. Mass spectroscopy data was acquired at the UCSD Department of Chemistry and Biochemistry Molecular Mass Spectrometry Facility. Gel Permeation Chromatography data was acquired at the UCSB Materials Research Laboratory Polymer Characterization Facility and the Godula Research Laboratory at UCSD.

This chapter was coauthored with Dr. Peng-Hao Hsu and Dr. Adah Almutairi. The dissertation author was the principal researcher and primary author of this chapter.

**2.5 References**

1) Fomina, N., Sankaranarayanan, J., and Almutairi, A., *Adv. Drug Delivery Rev.*, **2012**, 64, 1005.

2) Gohy, J. F. and Zhao, Y., *Chem. Soc. Rev.*, **2013**, 42, 7117.

3) Liu, G., Liu, W., and Dong, C.-M., *Polym. Chem.*, **2013**, 4, 3431.

4) Pasparakis, G., Manouras, T., Argitis, P. and Vamvakaki, M., *Macromol. Rapid Commun.*, **2012**, 33, 183.

5) Zhao, Y., *Macromolecules*, **2012**, 45, 3647.

6) Tong, R. and Kohane, D. S., *Wiley Interdiscip. Rev.: Nanomed. Nanobiotechnol.*, **2012**, 4, 638.

7) Murthy, N., Xu, M. C., Schuck, S., Kunisawa, J., Shastri, N., Frechet, J. M. J. *Proc. Natl. Acad. Sci. U.S.A.*, **2003**, 100, 4995.

8) Liu, X. M., Wang, L. S. *Biomaterials*, **2004**, 25, 1929.

9) Sankaranarayanan, J., Mahmoud, E. A., Kim, G., Morachis, J. M., Almutairi, A. *ACS Nano*, **2010**, 4, 5930.

10) Xiang, Y. Q., Chen, D. J., *Eur. Polym. J.*, **2007**, 43, 4178.

11) Ma, N.; Li, Y.; Xu, H. P.; Wang, Z. Q.; Zhang, X. *J Am Chem Soc*, **2010**, *132*, 442.

12) Wilson, D. S.; Dalmasso, G.; Wang, L. X.; Sitaraman, S. V.; Merlin, D.; Murthy, N. *Nat Mater*, **2010**, *9*, 923.

13) Lee, S. H.; Gupta, M. K.; Bang, J. B.; Bae, H.; Sung, H. J. *Adv Healthc Mater*, **2013**, *2*, 908.

14) Lux, C. D.; Joshi-Barr, S.; Nguyen, T.; Mahmoud, E.; Schopf, E.; Fomina, N.; Almutairi, A, *J Am Chem Soc*, **2012**, 134, 15758.

15) Broaders, K. E.; Grandhe, S.; Frechet, J. M. J. *J Am Chem Soc*, **2011**, 133, 756.

16) Staff, R. H.; Gallei, M.; Mazurowski, M.; Rehahn, M.; Berger, R.; Landfester, K.; Crespy, D. *Acs Nano*, **2012**, 6, 9042.

17) Veronese, F. M.; Schiavon, O.; Pasut, G.; Mendichi, R.;Andersson, L.; Tsirk, A.; Ford, J.; Wu, G. F.; Kneller, S.; Davies, J.; Duncan, R. *Bioconjugate Chem.*, **2005**, 16, 775.

18) Saez, J. A.; Escuder, B.; Miravet, J. F. *Tetrahedron*, **2010**, 66, 2614.

19) Vemula, P. K.; Cruikshank, G. A.; Karp, J. M.; John, G., *Biomaterials*, **2009**, 30, 383.

20) Khelfallah, N. S.; Decher, G.; Mesini, P. J., *Biointerphases*, **2007**, 2, 131.

21) Romberg, B.; Flesch, F. M.; Hennink, W. E.; Storm, G., *Int. J. Pharm.*, **2008**, 355, 108.

22) Khelfallah, N. S.; Decher, G.; Mesini, P. J., *Macromol. Rapid Commun.*, **2006**, 27, 1004.

23) Igari, Y.; Kibat, P. G.; Langer, R., *J. Controlled Release*, **1990**, 14, 263.

24) P. Klan, T. Solomek, C. G. Bochet, A. Blanc, R. Givens, M. Rubina, V. Popik, A. Kostikov and J. Wirz, *Chem. Rev.*, **2013**, 113, 119.

25) Weissleder, R. *Nat. Biotechnol*. **2001**, 19, 316.

26) Chen, C. C.; Lin, Y. P.; Wang, C. W.; Tzeng, H. C.; Wu, C. H.; Chen, Y. C.; Chen, C. P.; Chen, L. C.; Wu, Y. C. *J. Am. Chem. Soc.*, **2006**,128, 3709.

27) Braun, G. B.; Pallaoro, A.; Wu, G. H.; Missirlis, D.; Zasadzinski, J. A.; Tirrell, M.; Reich, N. O. *ACS Nano*, **2009**, 3, 2007.

28) *Near-Infrared Applications in Biotechnology*; Raghavachari, R.,Ed.; M. Dekker: New York, **2001**; Vol. 25.

29) Goodwin, A. P., Mynar, J. L., Ma, Y. Z., Fleming, G. R. and Frechet, J. M. J., *J. Am. Chem. Soc.*, **2005**, 127, 9952.

30) Fomina, N., McFearin, C., Sermsakdi, M., Edigin, O. and Almutairi, A., *J. Am. Chem. Soc.*, **2010**, 132, 9540.

31) Q. N. Lin, Q. Huang, C. Y. Li, C. Y. Bao, Z. Z. Liu, F. Y. Li and L. Y. Zhu, *J. Am. Chem. Soc.*, **2010**, 132, 10645.

32) C.-J. Carling, F. Nourmohammadian, J.-C. Boyer and N. R. Branda, *Angew. Chem.*, **2010**, 49, 3782.

33) B. Yan, J.-C. Boyer, N. R. Branda and Y. Zhao, *J. Am. Chem. Soc.*, **2011**, 133, 19714.

34) B. Yan, J.-C. Boyer, D. Habault, N. R. Branda and Y. Zhao, *J. Am. Chem. Soc.*, **2012**, 134, 16558.

35) Olejniczak, J., Carling, C.J., Almutairi, A., *J. Con. Rel.*,**2015**, 219, 18-30

36) L. Donato, A. Mourot, C. M. Davenport, C. Herbivo,D. Warther, J. Leonard, F. Bolze, J. F. Nicoud, R. H. Kramer, M. Goeldner and A. Specht, *Angew. Chem.*, **2012**, 51, 1840.

37) Agarwal, H.K., Janicek, R., Chi, S.H., Perry, J.W., Niggli, E., Ellis-Davies, G.C.; *J. Am. Chem. Soc.*, **2016**, 11, 3687-3693.

38) Carling, C.J., Viger, M.L., Huu, V.A.N., Garcia, A.V., Almutairi, A.; Chem. Sci., **2015**, 6, 335-34.

39) Ash, C., Dubec, M., Donne, K., Bashford, T., *Lasers Med Sci*., **2017**, 32, 1909-1918.

40) Zhao, H., Sterner, E.S., Coughlin, E.B., and Theato, P., *Macromolecules*, **2012**, 45, 1723−1736.

41) Boinapally, S., Huang, B., Abe, M., Katan, C., Noguchi, J., Watanabe, S., Kasai, H., Xue, B., and Kobayashi, T., *J. Org. Chem.*, **2014**, 79, 7822−7830.

## 2.6 Supplementary

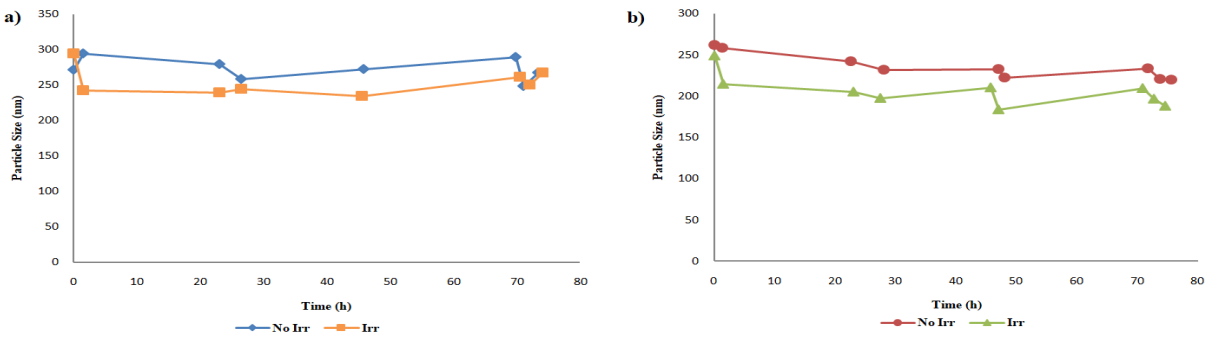


Figure 2.S1. DLS analysis of the change in particle size of ANBP-Dex particles under (a) pH 7.4 and (b) pH 8.5. The irradiated samples were continuously subjected to blue visible light for an hour and allowed to incubate in the dark for 30 min before DLS data was obtained.

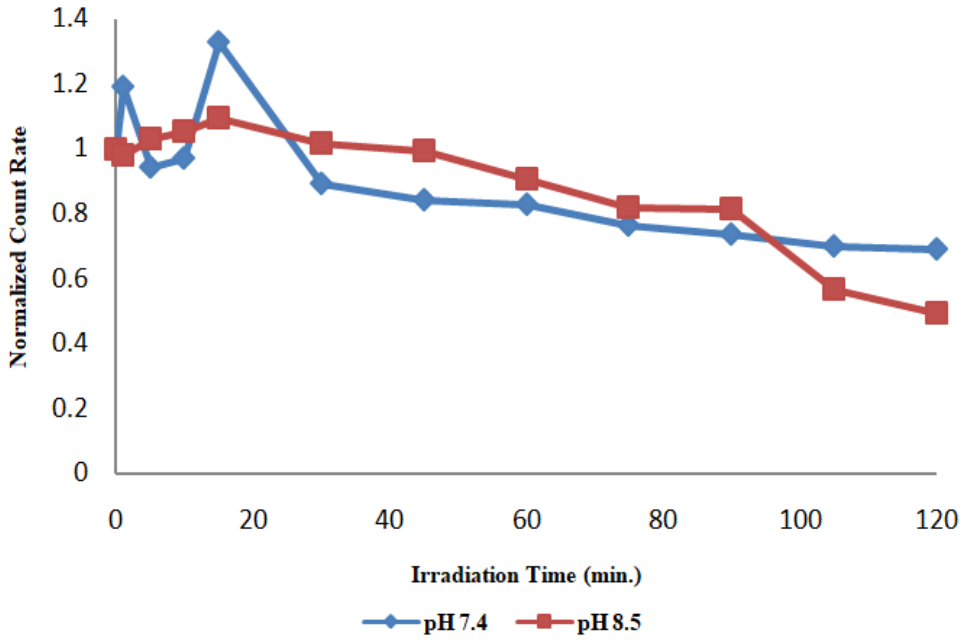


Figure 2.S2. Comparison of the change in normalized count rate after short time periods of blue light irradiation.

**General Methods and Instrumentation.** All reactions requiring anhydrous conditions were performed under an argon atmosphere. Flash chromatography was performed using a CombiFlash Companion system. $^{1}$H NMR spectra were acquired using a Bruker 600 MHz. Chemical shifts are

reported as δ in unites of part per million (ppm) relative to chloroform (δ 7.26, s). Multiplicities are reported as follows: s (singlet), bs (broad singlet), d (doublet), t (triplet), q (quartet), sex (sextet), dd (doublet of doublets), m (multiplet), br (broadened). Coupling constants are reported as J values in Hertz (Hz). The number of protons (n) for a given resonance is indicated as nH, and is based on spectral integration values. UV spectra were acquired using a dual beam Shimadzu UV-3600 UV-Vis-NIR Spectrophotometer. Blank baselines were acquired using the same cuvettes and the same solvent. Samples were irradiated with visible light using an OmniCure s2000 (Lumen Dynamics). A bandpass filter limited the output of the Hg lamp to 320-480 nm. A lens attached to the end of the light guide focused the light ~10 cm away, where the cuvettes were placed.

*Synthesis of 5-bromo-2-nitrobenzaldehyde **(3)***

$HNO_3$ (20 mL) and $H_2SO_4$ (40 mL) were added to a flame-dried round-bottom flask and allowed to cool to 0 °C. 3-bromobenzaldehyde (85.2 mmol, 1 eq) was added dropwise to the reaction, forming a yellow/orange precipitate. The reaction was allowed to stir at 0 °C for 30 minutes and was brought up to RT to stir overnight. The resulting solution was cooled to 0 °C and quenched with saturated $NaHCO_3$ and extracted with EtOAc. The organic extracts were combined and washed with brine, dried over $MgSO_4$, filtered, and concentrated *in vacuo*. Compound **3** was purified by silica gel column chromatography (40g, 10% EtOAc in hexanes) to yield and off-white solid (37% yield). The compound was store at ambient temperature.

$^1$H NMR (600 MHz, $CDCl_3$) δ 10.41 (s, 1H), 8.07 (d, *J*: 1.8 Hz, 1H), 8.03 (d, *J*: 8.8, 1H), 7.88 (dd, *J*: 8.3 Hz, 1H)

$^{13}$C NMR (150 MHz, $CDCl_3$) δ 186.53, 136.27, 132.38, 132.34, 129.31, 125.88

*Synthesis of (5-bromo-2-nitrophenyl)methanol **(4)***

To a flame-dried round-bottom flask, compound **3** (8.93 mmol, 1 eq.) was dissolved in anhydrous MeOH (38 mL) and allowed to stir at 0 °C for 15 minutes. $NaBH_4$ (8.93, 1 eq.) was added slowly to the solution as two portions and continued to stir at 0 °C for 3 hours. The resulting mixture was concentrated *in vacuo* and was dissolved in EtOAc and extracted with $H_2O$. The combined organic extracts were washed with brine, dried over $MgSO_4$, filtered, and concentrated. The crude compound **4** was purified via silica gel column chromatography (40g, 10% EtOAc in hexanes) to yield a yellow solid (92% yield). The compound was stored at ambient temperature.

$^1$H NMR (600 MHz, $CDCl_3$) δ 8.00 (d, *J*: 8.8 Hz, 1H), 7.98 (d, *J:* 1.8 Hz, 1H), 7.60 (dd, *J*: 8.8 Hz, 1H), 5.01 (s, 2H), 2.44 (s, 1H)

$^{13}$C NMR (150 MHz, $CDCl_3$) δ 138.78, 132.20, 131.18, 129.30, 126.26, 61.68

*Synthesis of ((5-bromo-2-nitrobenzyl)oxy)(tert-butyl)dimethylsilane **(5)***

A flame-dried round-bottom flask was charged with compound **4** (5.39 mmol, 1 eq.) and imidazole (10.78 mmol, 2 eq.) were dissolved in anhydrous DCM (20 mL) and allowed to stir at 0 °C. In a separate flask, tert-Butyldimethylsilyl chloride (8.09 mmol, 1.5 eq) was dissolved in anhydrous DCM (32 mL) and was added dropwise to the reaction flask at 0 °C. The solution became turbid upon addition of the TBDMS-Cl. The reaction was brought up to room temp and allowed to stir overnight. The resulting solution was quenched with $H_2O$ and extracted with DCM. The combined organic extracts were washed with brine, dried over $MgSO_4$, filtered, and concentrated to yield brown/yellow oil. The crude product of **5** was purified by silica gel column chromatography (12g, 5% EtOAc in hexanes) to yield a yellow oil (54% yield). The compound was stored at ambient temperature.

$^{1}$H NMR (600 MHz, $CDCl_3$) δ 8.08 (s, 1H), 7.99 (d, *J*: 8.8, 1H), 7.55 (dd, *J*: 8.8, 1H), 5.09 (s, 2H), 0.98 (s, 9H), 0.16 (s. 6H)

$^{13}$C NMR (150 MHz, $CDCl_3$) δ 144.82, 140.24, 131.06, 130.35, 129.22, 125.89, 61.56, 25.66, 18.13, -5.63

*Synthesis of tert-butyldimethyl((2-nitro-5-vinylbenzyl)oxy)silane* ***(6)***

In a flame-dried two neck round-bottom flask equipped with a condenser, compound **5** (3.30 mmol, 1 eq.), vinylboronic anhydride pyridine complex (1.65 mmol, 0.5 eq.) was dissolved in dimethoxyethane (25 mL). A solution $K_2CO_3$ (3.30 mmol, 1 eq.) in $H_2O$ (0.3 mL) was added to the reaction mixture and was deoxygenated by bubbling argon over 15 min. $Pd(PPh_3)_4$ (0.083 mmol, 0.025 eq.) was added and the system was purged, wrapped in foil, and refluxed overnight. The resulting reaction mixture was concentrated and brought up in $H_2O$ and the suspension was extracted with EtOAc. The combined organic extracts were washed with brine, dried over $MgSO_4$, filtered, and concentrated. The crude product was purified by silica gel column chromatography (24g, 5% EtOAc in hexanes) to produce a yellow oil (40% yield). The purified compound was stored at ambient temperature.

$^{1}$H NMR (600 MHz, $CDCl_3$) δ 8.10 (d, *J*: 8.8 Hz, 1H), 7.96 (s, 1H), 7.41 (m, 1H), 6.79 (dd, *J*: 17.5 Hz, 1H), 5.93 (d, *J*: 17.5 Hz, 1H), 5.48 (d, *J*: 11.4 Hz, 1H), 5.11 (s, 2H), 0.99 (s, 9H), 0.15 (s, 6H)

$^{13}$C NMR (150 MHz, $CDCl_3$) δ 145.44, 143.13, 139.13, 135.61, 125.70, 125.44, 125.03, 118.38, 62.38, 26.10, 18.56, -5.20

*Synthesis of 2,5-bis((E)-3-(((tert-butyldimethylsilyl)oxy)methyl)-4-nitrostyryl)thiophene* ***(7)***

In a flame-dried two neck round-bottom flask equipped with a condenser, compound **6** (1.32 mmol, 3 eq.), LiCl (3.08 mmol, 7 eq.), $NaHCO_3$ (3.96 mmol, 9 eq.), and TBACl (0.88 mmol,

2 eq.) were dissolved in anhydrous DMF (20 mL). 2,5-dibromothiophene (0.66 mmol, 1.5 eq.) was added and the system was degassed for 30 minutes. Pd(OAc)2 (0.22 mmol, 0.5 eq.) was added and the reaction flask was purged and allowed to reflux overnight. The reaction was quenched with DI $H_2O$ and the precipitate was filtered and dissolved in DCM and extracted with DI $H_2O$. The combined organic extracts were washed with brine, dried over $MgSO_4$, filtered, and concentrated. The crude product was purified by silica gel column chromatography (12g, 10% EtOAc in hexanes) to yield a dark orange/red solid (40% yield). The purified product was wrapped in foil and stored at ambient temperature.

$^1$H NMR (600 MHz, $CDCl_3$) δ 8.14 (d, *J*: 8.8 Hz, 1H), 8.01 (s, 1H), 7.47 (d, *J*: 8.8. 1H), 7.35 (d, *J*: 15.8 Hz, 1H), 7.09 (s, 1H), 6.97, (d, *J*: 16.7 Hz, 1H), 5.14 (s, 2H), 1.03 (s, 9H), 0.19 (s, 6H)

$^{13}$C NMR (150 MHz, $CDCl_3$) δ 144.63, 142.17, 142.11, 139.08, 128.85, 126.86, 125.41, 125.37, 125.22, 124.51, 62.06, 25.77, 18.23, -5.54

APCI-MS calc. mass $(C_{34}H_{46}N_2O_6SSi_2)^-$ $[M]^-$ 666.26 g/mol, experimental mass $[M]^-$ 666.39 g/mol

*Synthesis of (((1E,1'E)-thiophene-2,5-diylbis(ethene-2,1-diyl))bis(6-nitro-3,1-phenylene))dimethanol* ***(8)***

In a flame-dried round-bottom flask, compound **7** (0.12 mmol, 1 eq.) was dissolved in anhydrous THF (5 mL). TBAF (0.37 mmol, 3 eq.) was added to the reaction flask and allowed to stir at room temperature overnight. The reaction solution was quenched with water and the precipitate was filtered out. The precipitate was dried yielding a dark orange/red solid (82% yield.) The product was covered with foil and stored at ambient temperature.

$^1$H NMR (600 MHz, DMSO-$d_6$) δ 8.08 (d, *J*: 8.8 Hz, 1H), 8.00 (s, 1H), 7.72 (d, *J*: 8.8 Hz, 1H), 7.69 (d, *J*: 15.8 Hz, 1H), 7.36 (s, 1H), 7.11 (d, *J*: 15.8 Hz, 1H), 5.60 (br. S, 1H), 4.86 (d, *J*: 2.6 Hz, 2H)

$^{13}$C NMR (150 MHz, DMSO-$d_6$) δ 145.13, 142.13, 142.04, 139.41, 129.87, 126.60, 125.81, 125.36, 125.35, 125.16, 60.13

*Synthesis of (((1E,1'E)-thiophene-2,5-diylbis(ethene-2,1-diyl))bis(6-nitro-3,1-phenylene))bis(methylene) diacrylate (Monomer **1**)*

A flame-dried flask was charged with **8** (1.64 mmol, 1 eq.) and dissolved with anhydrous THF (21.5 mL). The dark orange solution was cooled to 0 ℃ before $Et_3N$ (4.92 mmol, 3 eq.). Acryloyl chloride (4.11 mmol, 2.5 eq.) was added to the solution drop wise and continued to stir at 0 ℃ for an additional 15 minutes. The reaction was brought up to room temperature and allowed to stir overnight. The reaction mixture was quenched with $H_2O$ and extracted with EtOAc. The combined organic extracts were dried over $MgSO_4$, filtered, and concentrated. Monomer **1** was purified by silica gel column chromatography (EtOAc in hexanes) multiple times to yield an orange solid (6%). The compound was stored at ambient temperature in a foil-wrapped vial.
$^1$H NMR (600 MHz, $CDCl_3$) δ 8.17 (d, *J:* 8.8 Hz, 2H), 7.61 (s, 2H), 7.58 (d, *J:* 6.2 Hz, 2H), 7.34 (d, *J*: 15.8 Hz, 2H), 7.12 (s, 2H), 6.94 (d, *J*: 16.7 Hz, 2H), 6.55 (d, *J*: 18.5 Hz, 2H), 6.28 (dd, *J*: 10.6, 17.6 Hz, 2H), 5.98 (d, *J*: 10.6 Hz, 2H), 5.67 (s, 4H)

*Synthesis of **polyBIST-1***

In a flame dried 1-dram vial, monomer **1** (0.055 mmol, 1 eq.) and 4,4'-trimethylene dipiperidine (0.055 mmol, 1 eq.) were dissolved in anhydrous DCM (0.25 mL) and charged with argon. DBU (0.274 mmol, 5 eq.) was added and the reaction stirred at room temperature for 72 hours. The resulting solution was dissolved in DCM (1 mL) and precipitated out in cold hexanes. The solution was centrifuged (20k rpm, 15 min., 4 °C) and the resulting orange pellet was dissolved again with DCM. The process was repeated three times to yield **polyBIST-1** as an orange solid.

*Synthesis of **polyBIST-2***

In a flame dried 1-dram vial, **8** (0.037 mmol, 1 eq.) and was dissolved in anhydrous THF (1.8 mL) and charged with argon. $Et_3N$ (0.184 mmol, 5 eq.) was added and the reaction stirred at room temperature for 15 minutes. Adipoyl chloride was added drop-wise and the reaction stirred at room temperature for 93 hours. The resulting solution was concentrated *in vacuo*, dissolved in DCM (1 mL), and precipitated out in cold hexanes. The solution was centrifuged (20k rpm, 15 min., 4 °C) and the resulting orange pellet was dissolved again with DCM. The process was repeated three times to yield **polyBIST-2** as an orange solid.

*Synthesis of 1-(5-bromo-2-nitrophenyl)ethan-1-one **(9)***

A flame-dried round-bottom flask under argon was charged with $KNO_3$ (2.76 mmol. 1.1 eq.) and $H_2SO_4$ (50 mL) and allowed to stir at 0 °C for 30 minutes. A solution of 3-bromoacetophenone (2.51 mmol, 1 eq.) in anhydrous DCM (50 mL) was added drop wise of the acid solution and began to turn orange. The mixture was stirred at room temperature overnight. The reaction mixture was poured over ice, which led to heat and gas evolution. The resulting mixture was extracted with DCM washed with brine. The combined organic extracts were dried over $MgSO_4$, filtered, and concentrated. Compound **9** was purified by silica gel column chromatography (80g, EtOAc in hexanes) to yield a white solid (34% yield). The compound was stored at ambient temperature in a foil-wrapped vial.

$^1$H NMR (600 MHz, $CDCl_3$) δ 8.01 (d, *J*: 8.8 Hz, 1H), 7.74 (dd, *J*: 1.8, 8.8 Hz, 1H), 7.55 (d, *J*: 1.8 Hz, 1H), 2.56 (s, 3H)

$^{13}$C NMR (150 MHz, $CDCl_3$) δ 198.14, 139.54, 133.62, 130.35, 129.60, 125.92, 30.20

*Synthesis of 1-(5-bromo-2-nitrophenyl)ethan-1-ol **(10)***

A flame-dried round-bottom flask under argon was charged with **9** (8.49 mmol, 1 eq.) and dissolved in MeOH (37.7 mL) and DCM (3 mL). The reaction flask stirred at 0 °C for 30 minutes. $NaBH_4$ (8.49 mmol, 1 eq.) was added slowly in three portions at 0 °C, resulting in an opaque peachy solution. The reaction stirred at 0 °C for an hour. The reaction mixture was concentrated in vacuo and the resulting solid was dissolved in EtOAc and then washed with $H_2O$ and brine. The combined organic extracts were dried over $MgSO_4$, filtered, and concentrated. Compound **10** was purified by silica gel column chromatography (40g, EtOAc in hexanes) to yield a yellow oil (80% yield). The compound was stored at ambient temperature in a foil-wrapped vial.

$^1H$ NMR (600 MHz, $CDCl_3$) δ 8.04 (d, *J*: 1.8 Hz, 1H), 7.83 (d, *J*: 8.8 Hz, 1H), 7.56 (dd, *J*: 2.2, 8.4 Hz, 1H), 5.48 (q, *J:* 6.2 Hz, 1H), 1.58 (d, *J*: 6.2, 3H)

$^{13}C$ NMR (150 MHz, $CDCl_3$) δ 145.96, 142.99, 131.00, 130.67, 128.62, 125.76, 65.17, 24.15

*Synthesis of (1-(5-bromo-2-nitrophenyl)ethoxy)(tert-butyl)dimethylsilane **(11)***

A flame-dried round-bottom flask under argon was charged with **10** (8.54 mmol, 1 eq.) and imidazole (17.07, 2 eq.) in anhydrous DCM (10 mL) and allowed to stir at 0 °C. In a separate flask, tert-Butyldimethylsilyl chloride (12.81 mmol, 1.5 eq.) was dissolved in anhydrous DCM (32 mL) and was added dropwise to the reaction flask at 0 °C. The reaction was brought up to room temp and allowed to stir overnight. The reaction mixture was quenched with $H_2O$, extracted with DCM. The combined organic extracts were washed with brine and dried over $MgSO_4$, filtered, and concentrated. Compound **11** was purified by silica gel column chromatography (40g, 1% EtOAc in Hexanes) to yield an orange solid (78% yield). The compound was stored at ambient temperature in a foil-wrapped vial.

$^{1}$H NMR (600 MHz, $CDCl_3$) δ 8.05 (d, *J*: 1.8 Hz, 1H), 7.80 (d, *J*: 8.8, 1H), 7.51 (dd, *J*: 1.8, 8.4, 1H), 5.48 (q, *J*: 6.2, 1H), 1.45 (d, *J*: 6.1, 3H), 0.90 (s, 9H), 0.07 (s, 3H), -0.03 (s, 3H)

$^{13}$C NMR (150 MHz, $CDCl_3$) δ 145.62, 144.97, 131.64, 130.93, 128.82, 125.94, 66.37, 26.59, 25.94, 18.31, -4.73, -4.87

*Synthesis of tert-butyldimethyl(1-(2-nitro-5-vinylphenyl)ethoxy)silane* ***(12)***

A two neck, round-bottom flask equipped with a condenser was charged with **11** (6.69 mmol, 1 eq.), vinylboronic anhydride pyridine complex (3.34 mmol, 0.5 eq.), and dissolved in dimethoxyethane (50 mL). A solution $K_2CO_3$ (6.69 mmol, 1 eq.) in $H_2O$ (3 mL) was added to the reaction mixture and was deoxygenated by bubbling argon over 15 min. $Pd(PPh_3)_4$ (0.167 mmol, 0.025 eq.) was added and the system was purged, wrapped in foil, and heated to 85 °C in an oil bath. After 17.5 hours, the reaction was cooled and concentrated in vacuo. The crude solid was resuspended in DCM and washed with water and brine. The crude product was purified by silica gel column chromatography (40g, EtOAc in hexanes, 5%) to yield an orange solid (84% yield). The compound was stored at ambient temperature in a foil-wrapped vial.

$^{1}$H NMR (600 MHz, $CDCl_3$) δ 7.92 (d, *J*: 1.8 Hz, 1H), 7.92 (d, *J*: 7.9 Hz, 1H), 7.38 (dd, *J*: 1.8, 8.8 Hz, 1H), 6.76 (dd, *J*: 10.5, 17.5 Hz, 1H), 5.91 (d, *J*: 17.5 Hz, 1H), 5.53 (q, *J*: 6.1 Hz, 1H), 5.46 (d, *J*: 10.5 Hz, 1H), 1.46 (d, *J*: 6.1 Hz, 3H), 0.90 (s, 9H), 0.06 (s, 3H), -0.05 (s, 3H)

$^{13}$C NMR (150 MHz, $CDCl_3$) δ 145.79, 143.55, 142.81, 135.53, 125.92, 125.11, 124.96, 118.10, 66.59, 26.68, 25.97, 18.35, -4.76, -4.85

*Synthesis of 2,5-bis((E)-3-(1-((tert-butyldimethylsilyl)oxy)ethyl)-4-nitrostyryl)thiophene* ***(13)***

A two neck, round-bottom flask equipped with a condenser was charged was charged with **12** (5.61 mmol, 3 eq.), 2,5-dibromothiophene (2.81 mmol, 1.5 eq.), LiCl (13.10 mmol, 7 eq.),

$NaHCO_3$ (16.84 mmol, 9 eq.), TBACl ( 3.74 mmol, 2 eq.), and DMF (85 mL). The reaction was degassed with bubbling argon for 30 min. $Pd(OAc)_2$ (0.75 mmol, 0.4 mmol) was added, the reaction was purged and heated at 110 °C in an oil bath. After 18h, the reaction was cooled and quenched with $H_2O$. The precipitate that formed was vacuum filtered and redissolved in DCM. The organic solution was dried over $MgSO_4$ and concentrated in vacuo. The crude product was purified by silica gel column chromatography (40g, EtOAc in hexanes, 10%) to yield a dark red/orange solid (64% yield). The compound was stored at ambient temperature in a foil-wrapped vial.

$^1$H NMR (600 MHz, $CDCl_3$) δ 7.99 (d, *J*: 1.8 Hz, 1H), 7.96 (d, *J*: 7.9 Hz, 1H), 7.44 (dd, *J*: 2.2, 8.4 Hz, 1H), 7.33 (d, *J*: 15.8 Hz, 1H), 7.08 (s, 1H), 6.95 (d, *J*: 15.8 Hz, 1H), 5.58 (q, *J*: 6.2 Hz, 1H), 1.48 (d, *J*: 6.2 3H), 0.93 (s, 9H), 0.09 (s, 3H), -0.01 (s, 3H)

$^{13}$C NMR (150 MHz, $CDCl_3$) δ 145.36, 142.47, 142.31, 129.17, 127.17, 125.87, 125.87, 125.38, 125.06, 66.67, 26.72, 26.05, 18.43, -4.71, -4.77

APCI-MS calc. mass $(C_{36}H_{50}N_2O_6SSi_2)^+$ $[M]^-$ 694.29 g/mol, experimental mass $[M]^-$ 694.27 g/mol

*Synthesis of the methyl-BIST monomer 1,1'-(((1E,1'E)-thiophene-2,5-diylbis(ethene-2,1 diyl))bis(6-nitro-3,1-phenylene))bis(ethan-1-ol) (**14**)*

A flame-dried round-bottom flask under argon was charged with **13** (1.80 mmol, 1 eq.) and THF (41 mL). The reaction solution stirred at room temperature for 15 min. TBAF (5.41 mmol, 3 eq.) was added to the reaction flask and the reaction stirred at RT overnight. The reaction was quenched with $H_2O$ and extracted with DCM. The combined organic extracts were washed with brine and then dried over $MgSO_4$. The crude product was purified by silica gel column chromatography (20g, 1% MeOH in DCM) to produce a dark orange solid (75% yield). The compound was stored at ambient temperature in a foil-wrapped vial.

$^{1}$H NMR (600 MHz, DMSO-$d_6$) δ 7.97 (d, *J*: 8.8 Hz, 2H), 7.93 (d, *J*: 1.8 Hz, 2H), 7.48 (dd, *J*: 1.8, 8.8 Hz, 2H), 7.36 (d, *J*: 15.8 Hz, 2H), 7.10 (s, 2H), 6.96 (d, *J*: 15.8 Hz, 2H), 5.54 (m, 6H), 1.62 (d, *J*: 6.2 Hz, 6H)

$^{13}$C NMR (150 MHz, DMSO-$d_6$) δ 145.67, 143.18, 142.05, 141.71, 129.68, 126.51, 125.70. 125.34, 125.23, 124.76, 63.93, 30.68, 25.02.

*Synthesis of (((1E,1'E)-thiophene-2,5-diylbis(ethene-2,1-diyl))bis(6-nitro-3,1-phenylene))bis(ethane-1,1-diyl) bis(1H-imidazole-1-carboxylate) (Monomer **2**)*

A flame-dried round-bottom flask under argon was charged with **14** (1.36 mmol, 1 eq.), carbonyldiimidazole (5.42 mmol, 4 eq.), and DCM. The reaction was stirred at room temperature overnight. The reaction mixture was quenched with $H_2O$ and extracted with EtOAc. The collected organic extracts were washed with brine and dried over $MgSO_4$. The crude product was purified by silica gel column chromatography (20g, EtOAc in hexanes) to yield an orange solid (91% yield). The compound was stored at ambient temperature in a foil-wrapped vial.

$^{1}$H NMR (600 MHz, $CDCl_3$) δ 8.22 (s, 1H), 8.08 (d, *J*: 7.9 Hz, 1H), 7.61 (s, 1H), 7.60 (d, *J*: 3.5 Hz, 1H), 7.48 (s, 1H), 7.32 (d, *J*: 15.8 Hz, 1H), 7.13 (s, 1H), 7.12 (s, 1H), 6.93 (d, *J*: 15.8 Hz, 1H), 6.68 (m, 1H), 1.88 (d, *J*: 7.0 Hz, 3H)

$^{13}$C NMR (150 MHz, $CDCl_3$) δ 142.75, 142.18, 130.76, 129.51, 126.27, 126.16, 125.87, 125.77, 124.76, 124.69, 124.40, 122.18, 117.22, 110.39, 72.78, 21.95

ESI-MS calc. mass $(C_{32}H_{26}N_6O_8S)^+$ $[M+H]^+$ 655.15 g/mol, experimental mass $[M+H]^+$ 654.80 g/mol, $[M+Na]^+$ 676.91 g/mol

*Synthesis of (((1E,1'E)-thiophene-2,5-diylbis(ethene-2,1-diyl))bis(6-nitro-3,1 phenylene))bis(ethane-1,1-diyl) bis(5-(l1-oxidaneyl)-5-oxopentanoate) (polymer **1**) **(MB)***

In a flame-dried vial, **14** (0.43 mmol, 1 eq.) was dissolved in anhydrous DCM (6 mL) and was charged with Argon. Pyridine (2.57 mmol, 6 eq.) was added to the solution and allowed to stir at room temperature for 15 minutes. Adipoyl chloride (0.43 mmol, 1 eq.) was added drop-wise and the reaction stirred at room temperature for 72 hours, covered with aluminum foil. The resulting solution was precipitated out in cold EtOH and centrifuged (15k rpm, 15 min., 4°C). The supernatant was removed and the resulting pellet was disslolved in DCM (1 mL) and the process was repeated three more time.

*Synthesis of bis(4-((l1-oxidaneyl)methyl)benzyl) ((((1E,1'E)-thiophene-2,5-diylbis(ethene-2,1-diyl))bis(6-nitro-3,1-phenylene))bis(ethane-1,1-diyl)) bis(carbonate) (polymer **2**) **(MB-1)***

In a flame-dried vial, **2** (0.04 mmol, 1 eq.) and 4-Dimethylaminopyridine (***DMAP***) (0.10 mmol, 2.2 eq.) was dissolved with anhydrous DCM (2 mL). The solution was degassed by bubbling argon and stirred at room temperature. 1,4-benzenedimethanol (0.04 mmol, 0.9 eq.) was added and the reaction was purged, covered in foil, and stirred at room temperature for 3 days. The resulting solution was precipitated out into cold $Et_2O$. The suspension was centrifuged (20k rpm, 20 min, 4 °C) and the orange supernatant was discarded. The pellet was dissolved in DCM (1 mL) and purification procedure was repeated 3x. The purified polymer (**MB-1**) was obtained as an orange oil (11% yield, $M_w$: 2.8 kDa (PMMA Standard), PDI: 1.8).

*Synthesis of tert-butyl 2-(5-bromo-2-nitrophenyl)acetate (**15**)*

A flame-dried round-bottom flask under argon was charged with 4-bromonitrobenzene (19.8 mmol, 1 eq.), *tert*-Butyl chloroacetate (30.7 mmol, 1.55 eq.), and DMF (30 mL) and was

stirred at 0 °C. In a separate flask, *t*-BuOK (123 mmol, 6.26 eq.) was dissolved in DMF (70 mL) and was added to the reaction flask via cannula and was left to stir overnight at room temperature. The reaction mixture was cool to 0 °C and was quenched with 5% HCl and extracted with EtOAc. The combined organic extracts were washed with brine and dried over $MgSO_4$ and were concentrated under vacuum. The product was purified by silica gel column chromatography (80g, EtOAc in hexanes, 10%) to afford a light-yellow solid (57% yield).

$^1$H NMR (600 MHz, $CDCl_3$) δ 7.99 (d, *J*: 8.8 Hz, 1H), 7.60 ppm (dd, *J*: 8.8, 2.6 Hz, 1H), 7.51 (d, *J*: 1.8 Hz, 1H), 3.92 (s, 2H), 1.45 (s, 9H)

$^{13}$C NMR (150 MHz, $CDCl_3$) δ 193.55, 168.47, 136.14, 132.35, 131.50, 128.19, 126.65, 82.21, 40.79, 27.93,

*Synthesis of tert-butyl 2-(5-bromo-2-nitrophenyl)propanoate (**16**)*

In a flame-dried round-bottom flask, **15** (11.29 mmol, 1 eq.) and sodium hydride (13.55 mmol, 1.2 eq.) was dissolved in anhydrous DMF (45 mL). The solution was cooled to 0 °C and methyl iodide (22.58 mmol, 2 eq.) was added dropwise. The reaction mixture was stirred at room temperature for 19 h. The reaction was quenched with 5% HCl and extracted with EtOAc. The combined organic extracts were washed with brine, dried over $MgSO_4$, and then concentrated in vacuo. The crude product was purified by silica gel column chromatography (40g, EtOAc in hexanes, 2%) to afford a yellow oil (54% yield). The compound was stored at ambient temperature in a foil-wrapped vial.

$^1$H NMR (600 MHz, $CDCl_3$) δ 7.83 (d, *J*: 8.8 Hz, 1H), 7.64 (d, *J*: 1.8 Hz, 1H), 7.75 (dd, *J*: 8.8, 1.8 Hz, 1H), 4.22 (q, *J*: 7.00 Hz, 1H), 1.58 (d, *J*: 7.9 Hz, 3H), 1.41 (s, 9H)

$^{13}$C NMR (150 MHz, $CDCl_3$) δ 171.44, 137.45, 132.59, 130.75, 127.75, 126.08, 81.62, 42.01, 27.60, 17.14

*Synthesis of 2-(5-bromo-2-nitrophenyl)propan-1-ol (**17**)*

A drop funnel was attached to a flame-dried round-bottom flask under argon and charged with **16** (6.05 mmol, 1 eq.) and dissolved in anhydrous THF (10mL). The resulting solution was cooled to 0 °C. DIBAL-H (18.2 mmol, 3 eq., 1M in THF) was added dropwise to the reaction over 30 min. The reaction was stirred at 0 °C for 4 h. The reaction mixture was quenched with 5N HCl and extracted with EtOAc. The combined organic extracts were washed with brine and dried over $MgSO_4$, filtered, and concentrated. The title compound **17** was purified by silica gel column chromatography (40g, EtOAc in hexanes, 20%) to yield a light yellow solid (60% yield). The compound was stored at ambient temperature in a foil-wrapped vial.

$^1$H NMR (600 MHz, $CDCl_3$) δ 7.66 (d, *J*: 8.8 Hz, 1H), 7.63 (d, *J*: 2.6 Hz, 1H), 7.50 (dd, *J*: 8.3, 2.2 Hz, 1H), 3.78 (m, 2H), 3.55 (m, 1H), 1.33 (d, *J*: 7.0, 3H)

$^{13}$C NMR (150 MHz, $CDCl_3$) δ 149.23, 140.50, 131.50, 130.26, 127.37, 125.61, 67.26, 36.25, 17.28

*Synthesis of 2-(4'-(dimethylamino)-4-nitro-[1,1'-biphenyl]-3-yl)propan-1-ol (**18**)*

A flame-dried round-bottom flask attached with a condenser under argon was charged with **18** (3.59 mmol, 1 eq.), 4-dimenthylaminophenylboronic acid (3.77 mmol, 1.05 eq.), $Na_2CO_3$ (35.9 mmol, 10 eq.), toluene (18.7 mL), EtOH (3.5 mL), and $H_2O$ (6.1 mL). The reaction flask was deoxygenated by bubbling argon for 30 min. $Pd(PPh_3)_4$ (0.18 mmol, 0.05 eq.) was added and the reaction mixture was purged and then heated to 90 °C in an oil bath. The reaction flask was wrapped in foil and stirred for 18 h. After, the reaction was cooled and quenched with $H_2O$ and extracted with EtOAc. The combined organic extracts were washed with brine, dried over $MgSO_4$, and was concentrated. The crude product was purified by silica gel column chromatography (20g,

EtOAc in hexanes, 50%) to yield an orange solid (75% yield). The compound was stored at ambient temperature in a foil-wrapped vial.

$^{1}$H NMR (600 MHz, $CDCl_3$) δ 7.87 (d, *J*: 8.8 Hz, 1H), 7.62 (s, 1H), 7.52-750 (m, 3H), 6.81 (d, *J*: 8.8 Hz, 2H), 3.86 (t, *J*: 6.1 Hz, 2H), 3.71 (m, 1H), 3.04 (s, 6H), 1.39 (d, *J*: 7 Hz, 3H)

$^{13}$C NMR (150 MHz, $CDCl_3$) δ 150.77, 148.04, 145.95, 139.02, 128.03, 126.24, 125.33, 125.23, 124.38, 112.49, 68.06, 40.32, 36.46, 17.61

ESI-MS calc. mass $(C_{17}H_{20}N_2O_3)^+$ $[M+H]^+$ 301.15 g/mol, experimental mass $[M+H]^+$ 301.31 g/mol, $[M+Na]^+$ 323.10 g/mol

*Synthesis of 2-(4'-(dimethylamino)-4-nitro-[1,1'-biphenyl]-3-yl)propyl 1H-imidazole-1-carboxylate (**19**)*

In a flame-dried round-bottom flask charged with argon, **18** (1.66 mmol, 1 eq.) was dissolved in DCM (12 mL). Carbonyldiimidazole (3.33 mmol, 2 eq.) was added and the reaction flask was deoxygenated by bubbling argon over 30 min. The dark orange solution was stirred at room temperature for 18 h. The reaction was quenched with water and extracted with EtOAc (4x the amount the DCM). The combined organic extracts were washed with brine and dried over $MgSO_4$. The concentrated crude solid was purified by silica gel column chromatography (20g, EtOAc in hexanes) to yield an orange solid (63% yield).

$^{1}$H NMR (600 MHz, $CDCl_3$) δ 8.08 (s, 1H), 7.92 (d, *J:* 8.8 Hz, 1H), 7.61 (s, 1H), 7.55 (dd, *J*: 7.9 Hz, 1H), 7.50 (d, *J:* 8.8 Hz, 2H), 7.36 (s, 1H), 7.05 (s, 1H), 6.80 (d, *J:* 8.8 Hz, 2H), 4.64 (dd, *J:* 2.6, 7.0 Hz, 2H), 4.05 (m, 1H), 3.04 (s, 6H), 1.49 (d, *J*: 7.0 Hz, 3H)

$^{13}$C NMR (150 MHz, $CDCl_3$) δ 150.86, 148.44, 147.48, 146.25, 137.00, 130.66, 127.94, 125.65, 125.51, 125.01, 125.00, 117.00, 112.47, 71.91, 40.25, 33.15, 17.70

*Synthesis of benzyl (2-(4'-(dimethylamino)-4-nitro-[1,1'-biphenyl]-3-yl)propyl) carbonate (**ANBP-Bn**)*

In a flame-dried round bottom flask, **19** (0.43 mmol, 2 eq.), DMAP (0.43 mmol, 2 eq.), and benzyl alcohol (0.22 mmol, 1 eq.) were dissolved in anhydrous DCM (2.5 mL). The reaction stirred at 30 °C for 24 hours. The solution was quenched with $H_2O$ and extracted with DCM. The combined organic extracts were washed with brine, dried over $MgSO_4$, filtered, and concentrated by rotary evaporation. The crude product was purified by silica gel column chromatography (EtOAc in hexanes).

$^1$H NMR (600 MHz, $CDCl_3$) δ 7.9 (d, *J*: 7.9 Hz, 1H), 7.6 (s, 1H), 7.51 (d, *J*: 8.8 Hz, 4H), 7.38 (d, *J*: 4.4 Hz, 1H), 7.34 (m, 5H), 6.78 (d, *J*: 8.8 Hz, 2H), 5.13 (s, 2H), 4.41 (d, *J*: 6.2 Hz, 2H), 3.91 (m, 1H), 3.04 (s, 6H), 1.43 (d, *J*: 7.0 Hz, 4H)

*Synthesis of ANBP conjugated dextran polymers (**ANBP-Dex**)*

In a flame-dried 1 dram vial, **19** (0.40 mmol, 2 eq.) was dissolved in anhydrous DMSO (0.5 mL) with gentle heating. Dextran ($M_w$ = 9k -11k g/mol, 0.20 mmol, 1 eq.) and DMAP (0.04 mmol, 0.2 eq). The solution was allowed to stir at 80 °C for 2 days. The solution was cooled and precipitated out in cold $Et_2O$. The resulting suspension was centrifuged (20k rpm, 10min, 10 °C) and the supernatant was discarded. The resulting orange pellet was dissolved in $CH_2Cl_2$ and precipitated out in cold $Et_2O$ two more times. The purified polymer **ANBP-Dex** was obtained as an orange oil. (Mw = 15.6 kDa, PDI, 1.40, PS standard)

*Formulation of ANBP-Dex particles using single emulsion (**ANBP-Dex-P**)*

In a 40 mL vial, **ANBP-Dex** (10.0 mg) was dissolved in DCM (300 µL). A poly(vinyl alcohol) (PVA) (1% w/v, 6 mL) was added to the organic phase and was mixed. The biphasic solution was probe sonicated until it reached 2400 J of applied energy. DCM was removed from

the resulting emulsion by putting the solution under vacuum for 2 hours while stirring. The crude particle suspension was purified by tangential flow using a 500 kDa membrane (Biomax) to remove excess surfactants. The resulting solution was lyophilized with mannitol (100 mg) as a cryoprotectant.

*Formulation of Nile Red encapsulated ANBP-Dex particles using single emulsion (**ANBP-Dex-P-NR**)*

In a 40 mL vial, **ANBP-Dex** (10.0 mg) was dissolved in DCM (300 µL). A poly(vinyl alcohol) (PVA) (1% w/v, 6 mL) was added to the organic phase and was mixed. The biphasic solution was probe sonicated until it reached 2400 J of applied energy. DCM was removed from the resulting emulsion by putting the solution under vacuum for 2 hours while stirring. The crude particle suspension was purified by tangential flow using a 500 kDa membrane (Biomax) to remove excess surfactants. The resulting solution was lyophilized with mannitol (100 mg) as a cryoprotectant.

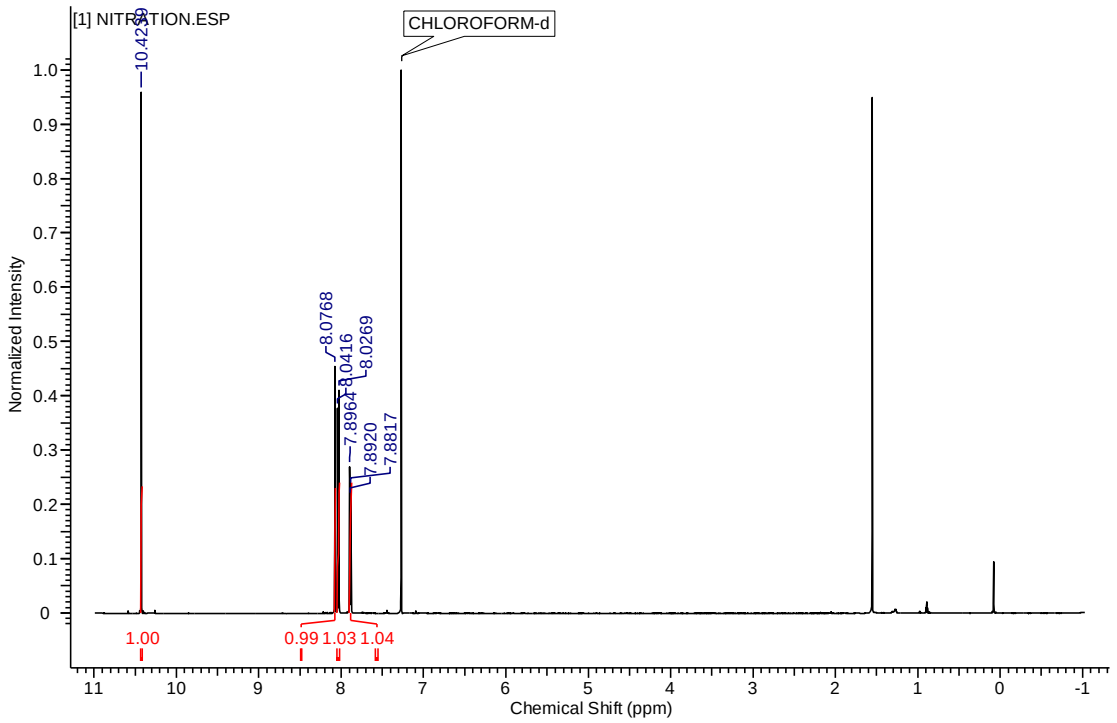


Figure 2.S3. $^{1}H$ NMR spectrum of compound **3** in $CDCl_3$.

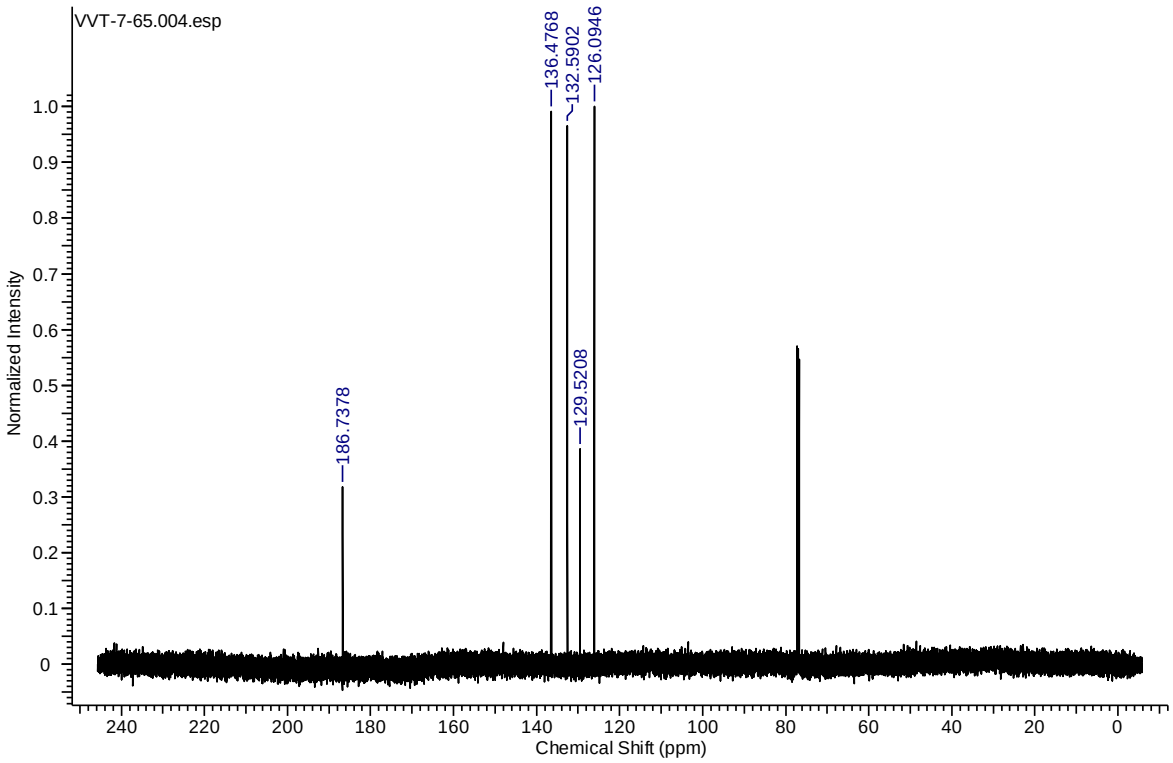


Figure 2.S4. $^{13}C$ NMR spectrum of compound **3** in $CDCl_3$.

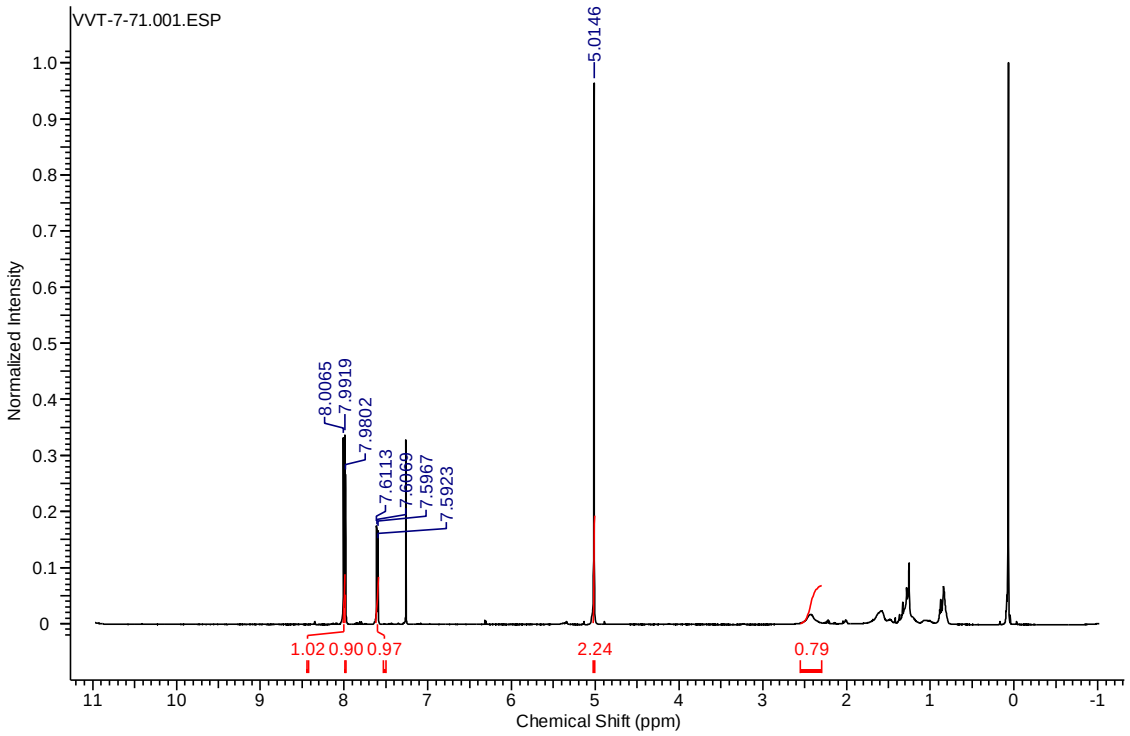


Figure 2.S5. $^{1}$H NMR spectrum of compound **4** in $CDCl_3$.

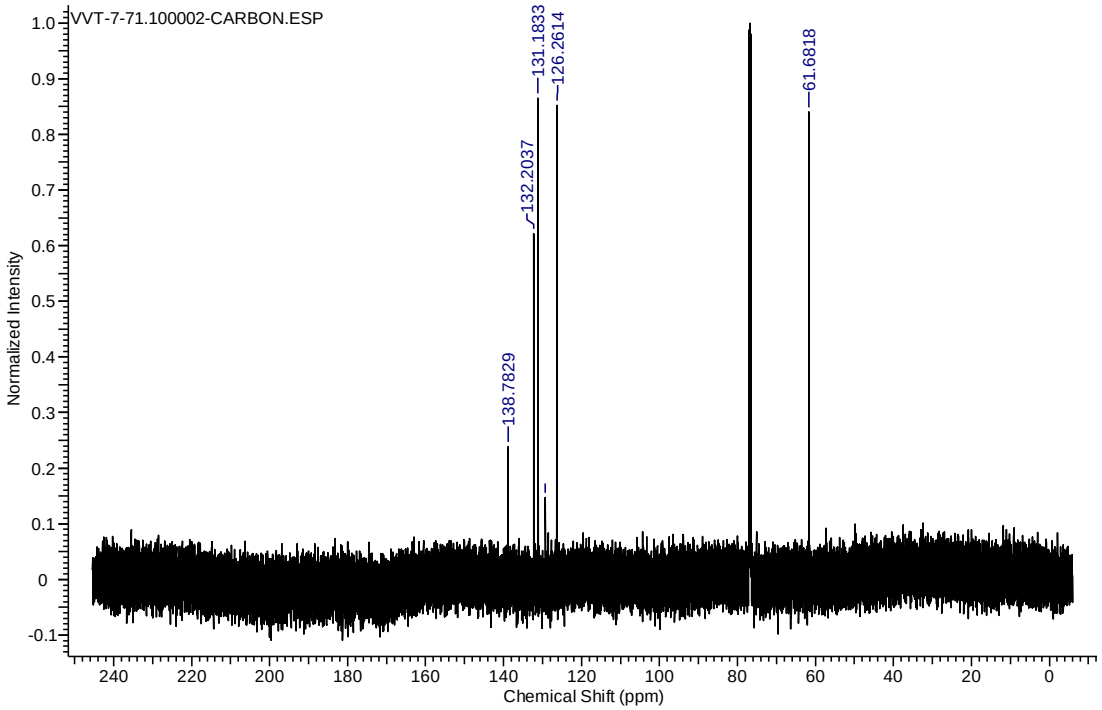


Figure 2.S6. $^{1}$H NMR spectrum of compound **4** in $CDCl_3$.

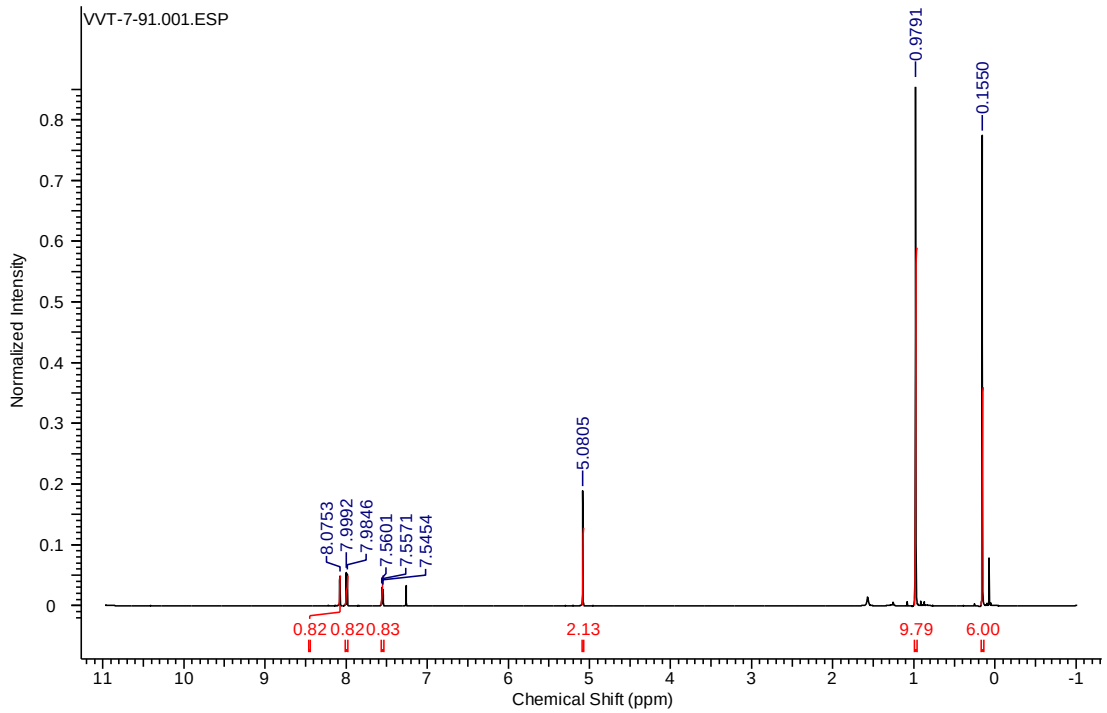


Figure 2.S7. $^{1}$H NMR spectrum of compound **5** in $CDCl_3$.

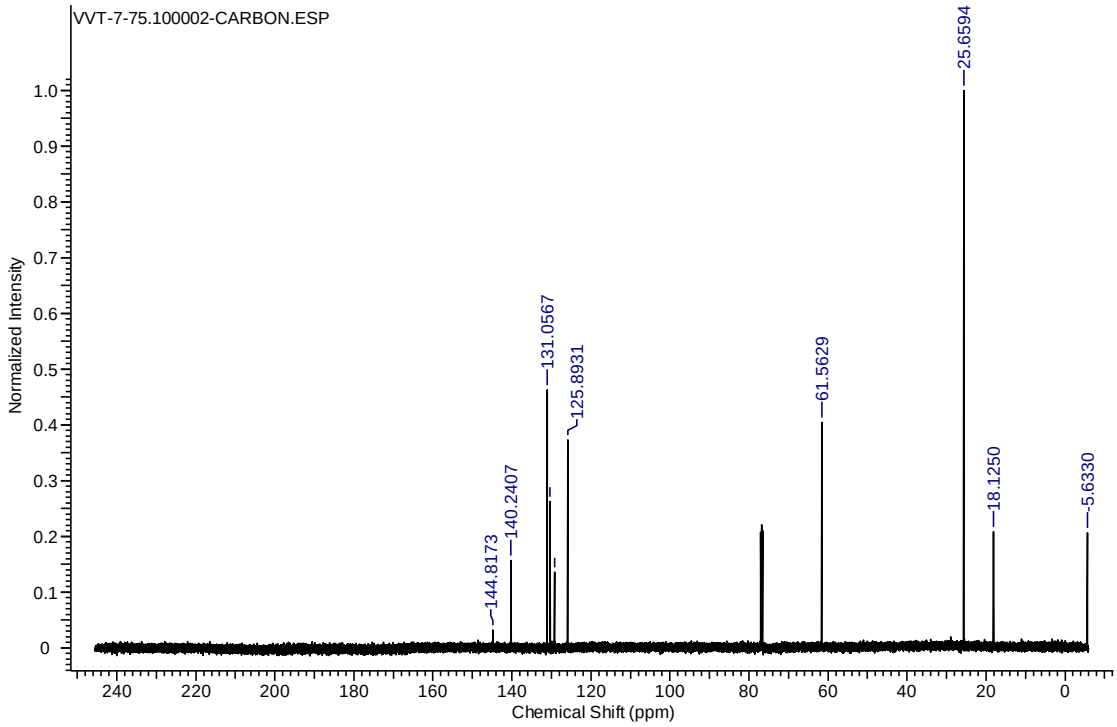


Figure 2.S8. $^{13}$C NMR spectrum of compound **5** in $CDCl_3$.

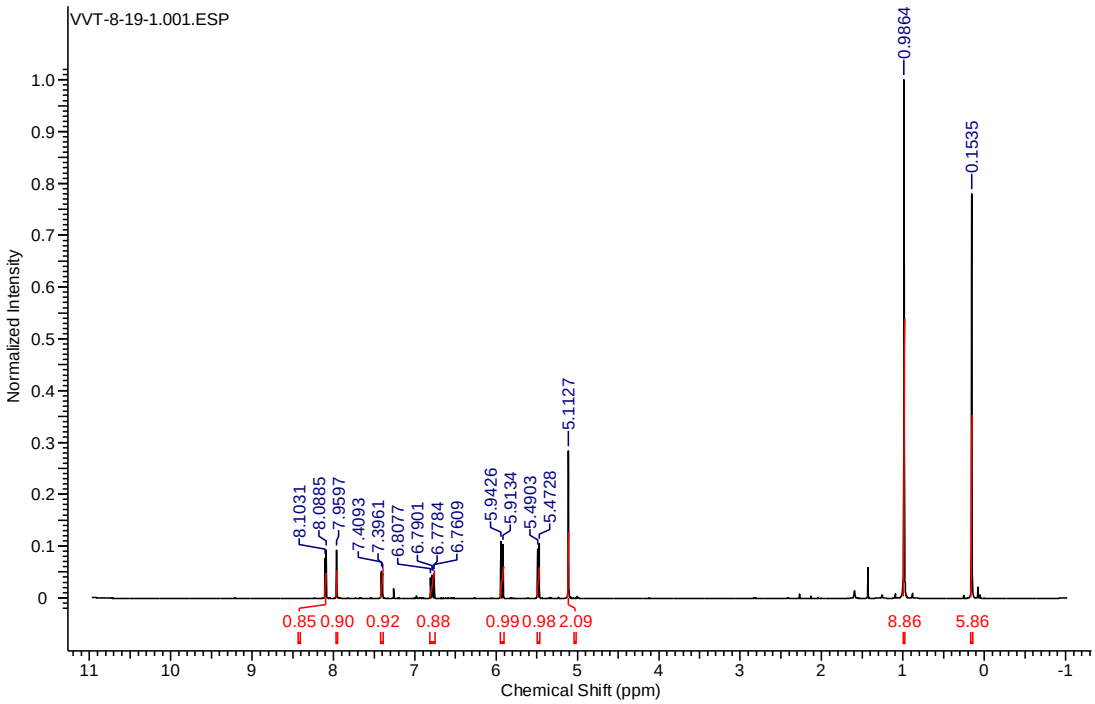


Figure 2.S9. $^{1}$H NMR spectrum of compound **6** in $CDCl_3$.

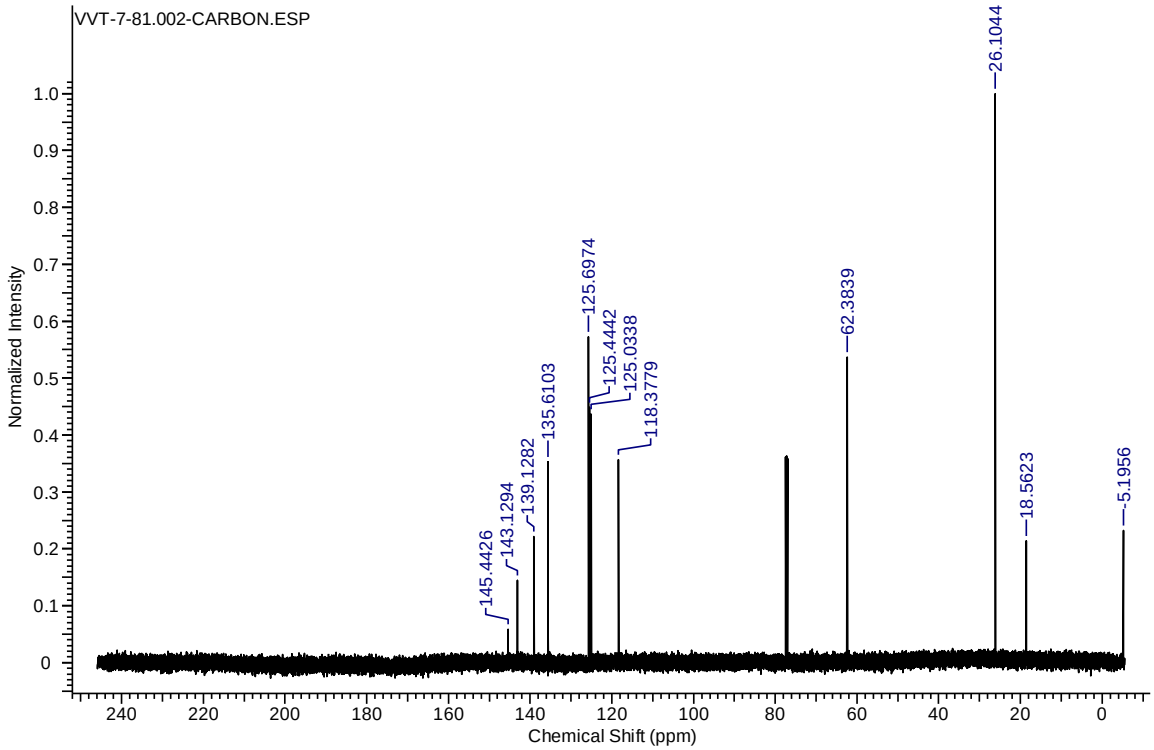


Figure 2.S10. $^{13}$C NMR spectrum of compound **6** in $CDCl_3$.

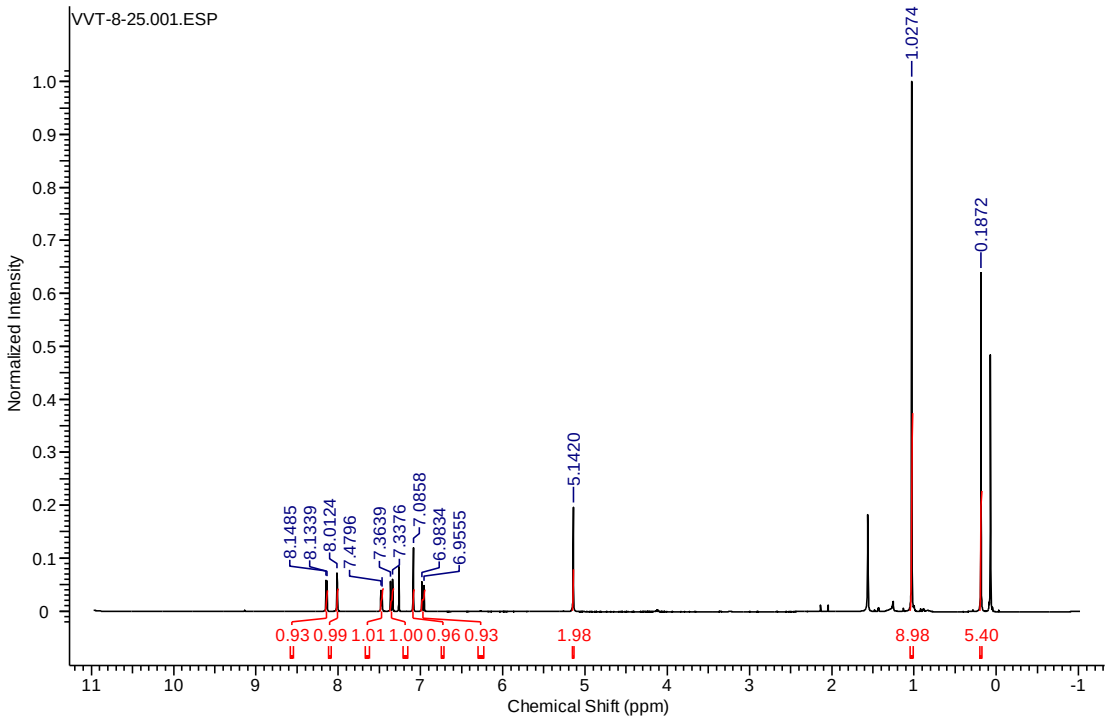


Figure 2.S11. $^{1}$H NMR spectrum of compound **7** in $CDCl_3$.

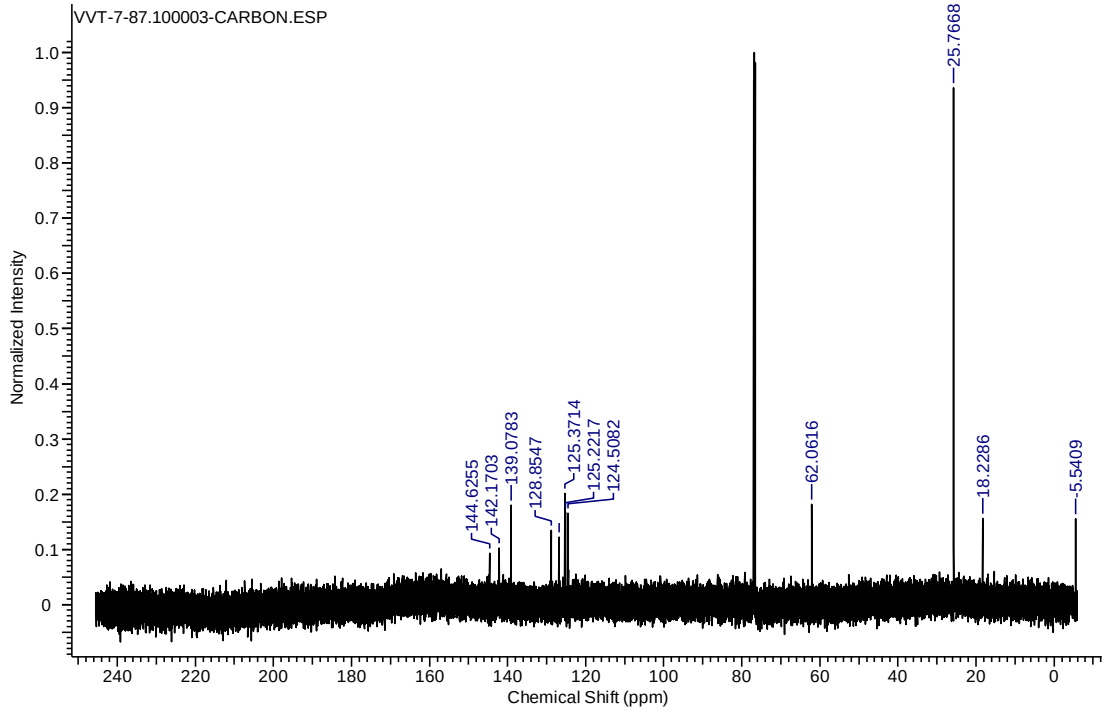


Figure 2.S12. $^{13}$C NMR spectrum of compound **7** in $CDCl_3$.

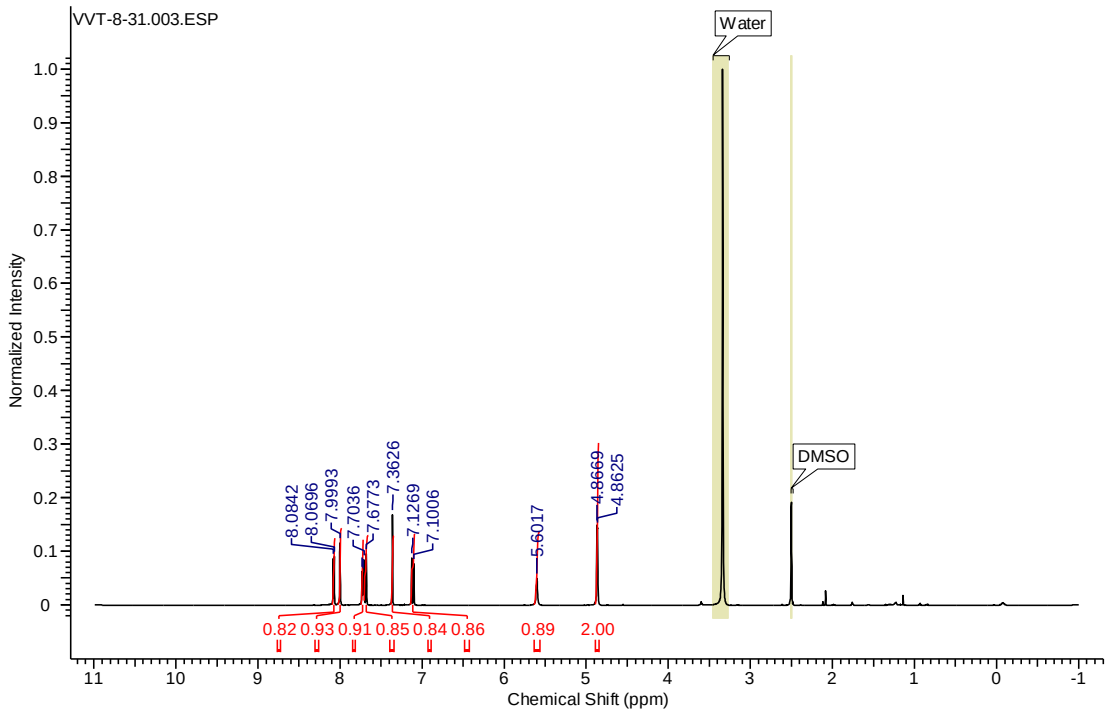


Figure 2.S13. $^{1}$H NMR spectrum of compound **8** in DMSO-$d_6$.

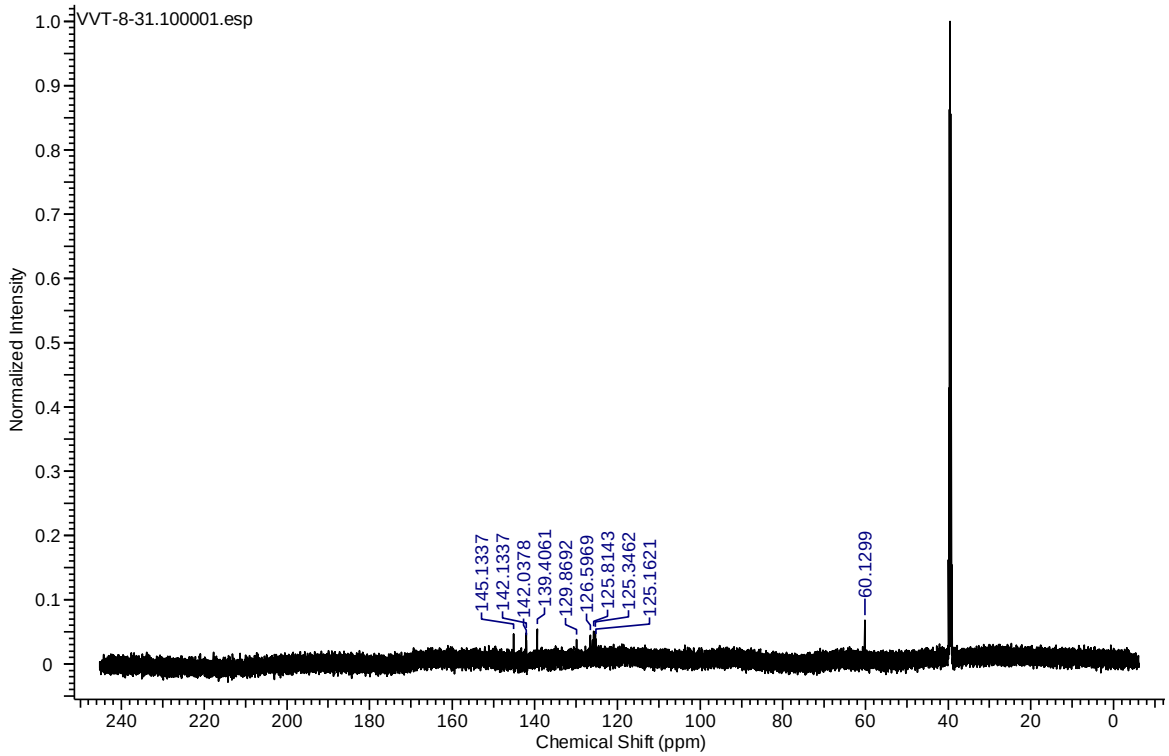


Figure 2.S14. $^{13}$C NMR spectrum of compound **8** in DMSO-$d_6$.

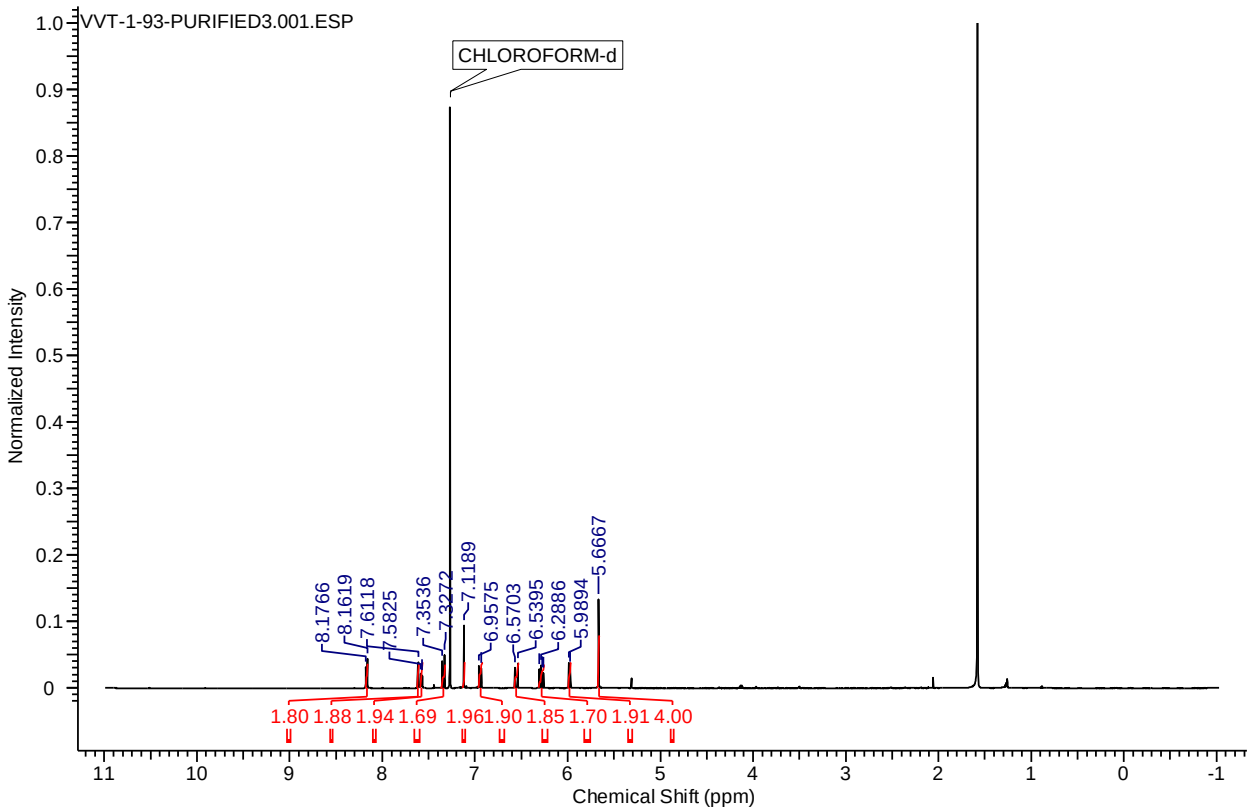


Figure 2.S15. $^{1}$H NMR spectrum of monomer **1** in DMSO-$d_6$.

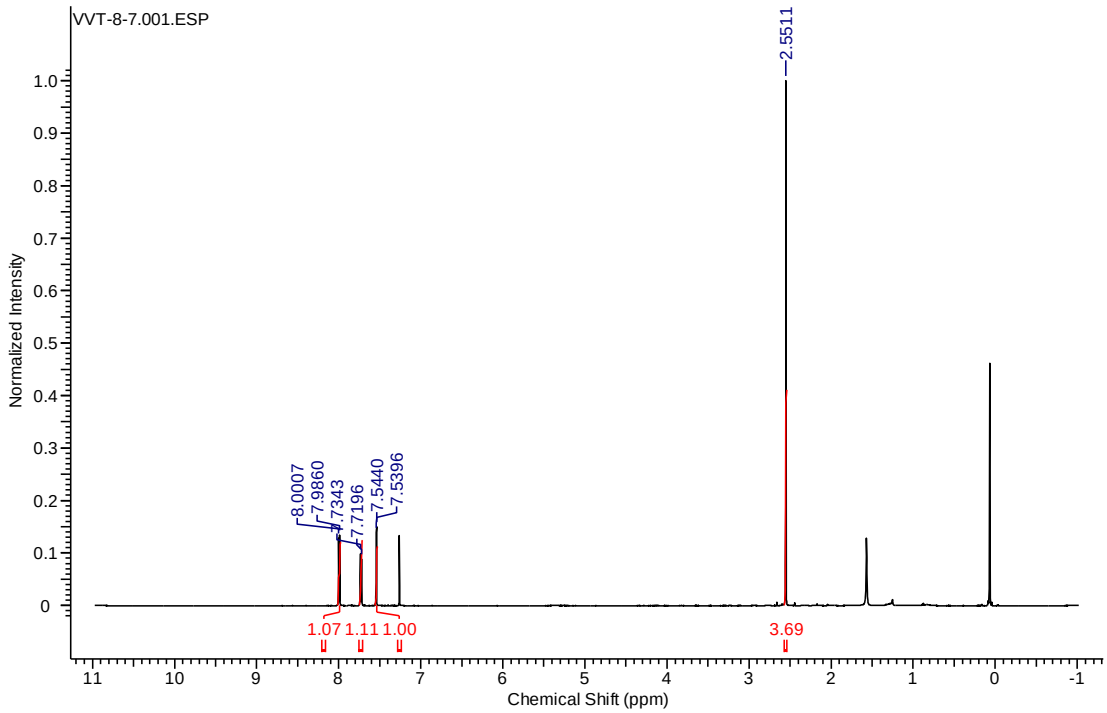


Figure 2.S16. $^{1}$H NMR spectrum of compound **9** in $CDCl_3$.

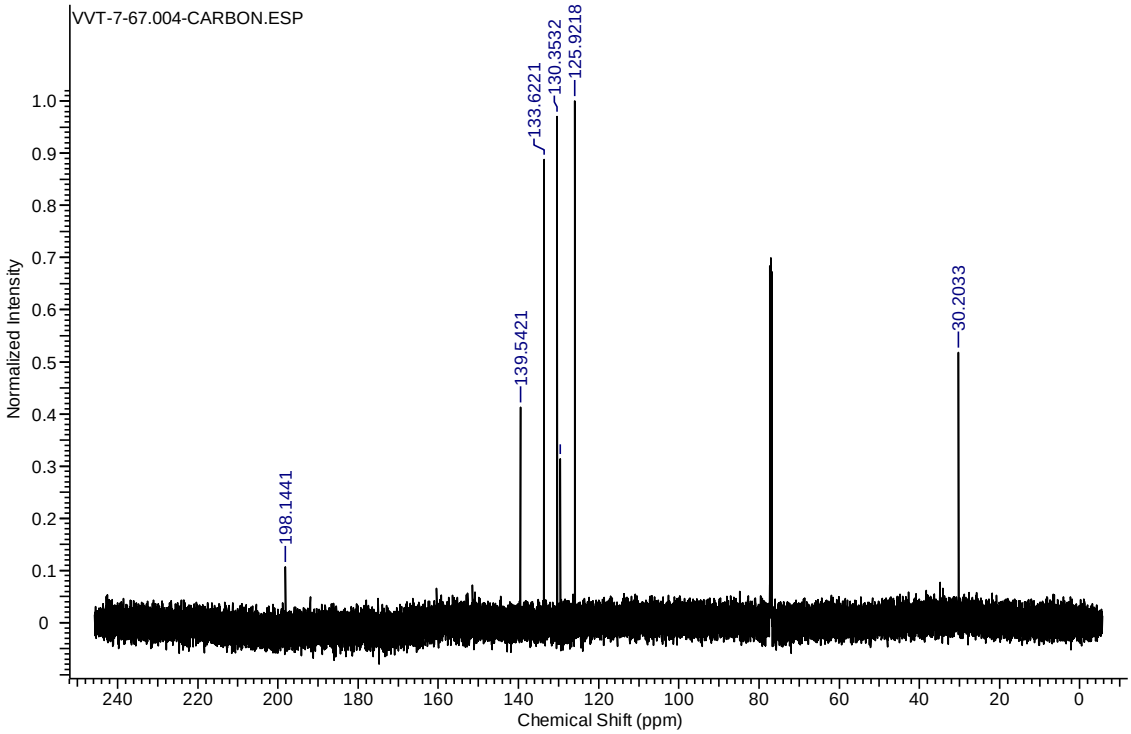


Figure 2.S17. $^{13}$C NMR spectrum of compound **9** in $CDCl_3$.

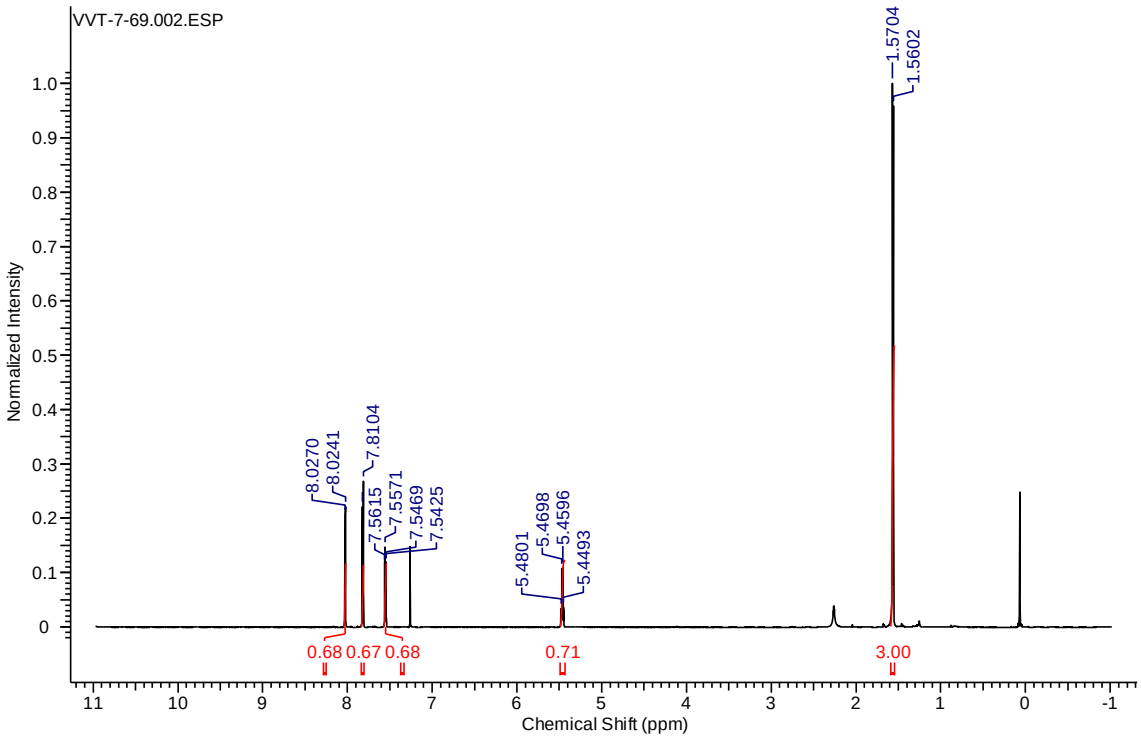


Figure 2.S18. $^{1}$H NMR spectrum of compound **10** in $CDCl_3$.

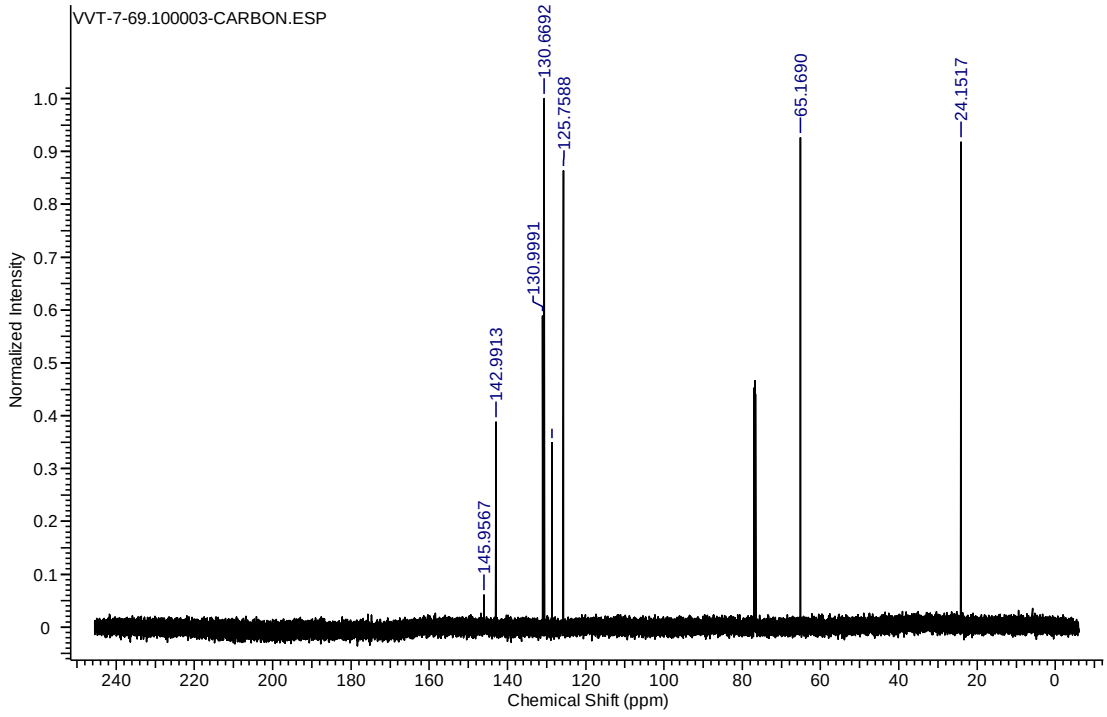


Figure 2.S19. $^{13}$C NMR spectrum of compound **10** in $CDCl_3$.

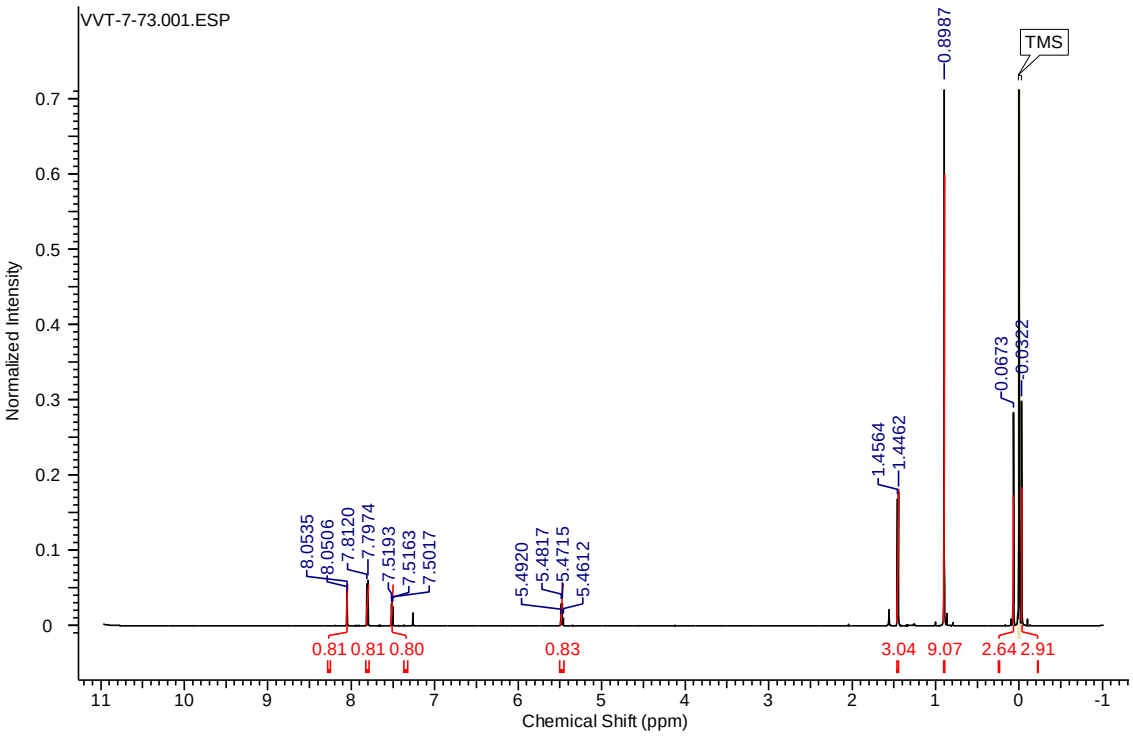


Figure 2.S20. $^{1}$H NMR spectrum of compound **11** in $CDCl_3$.

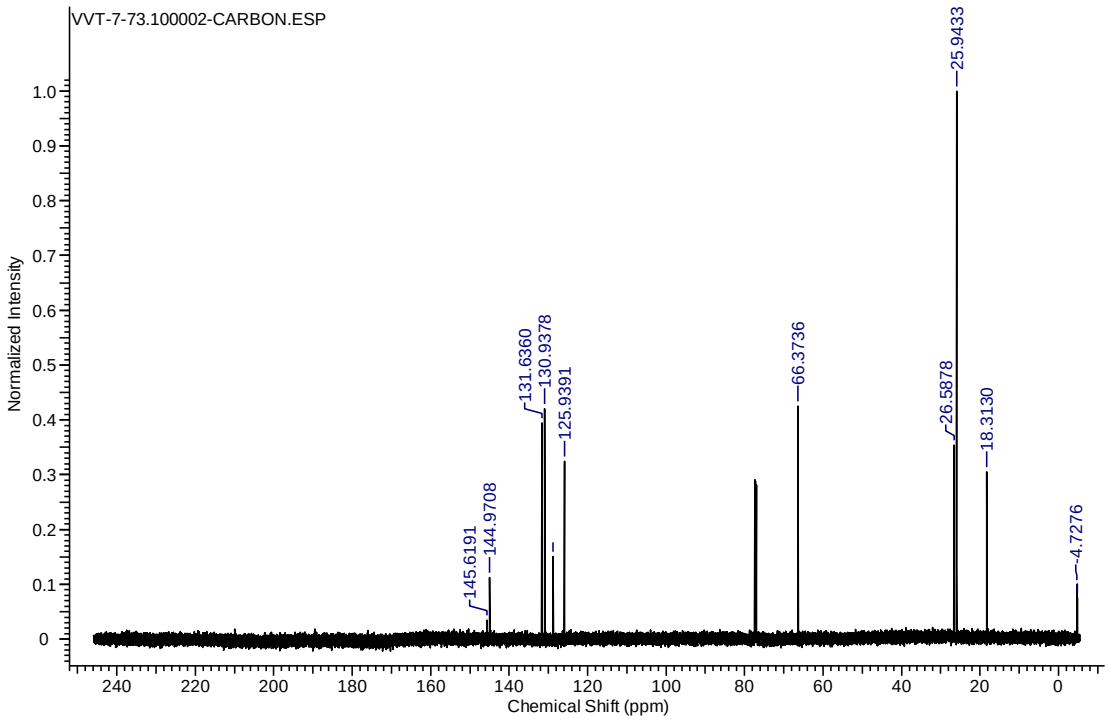


Figure 2.S21. $^{13}$C NMR spectrum of compound **11** in $CDCl_3$.

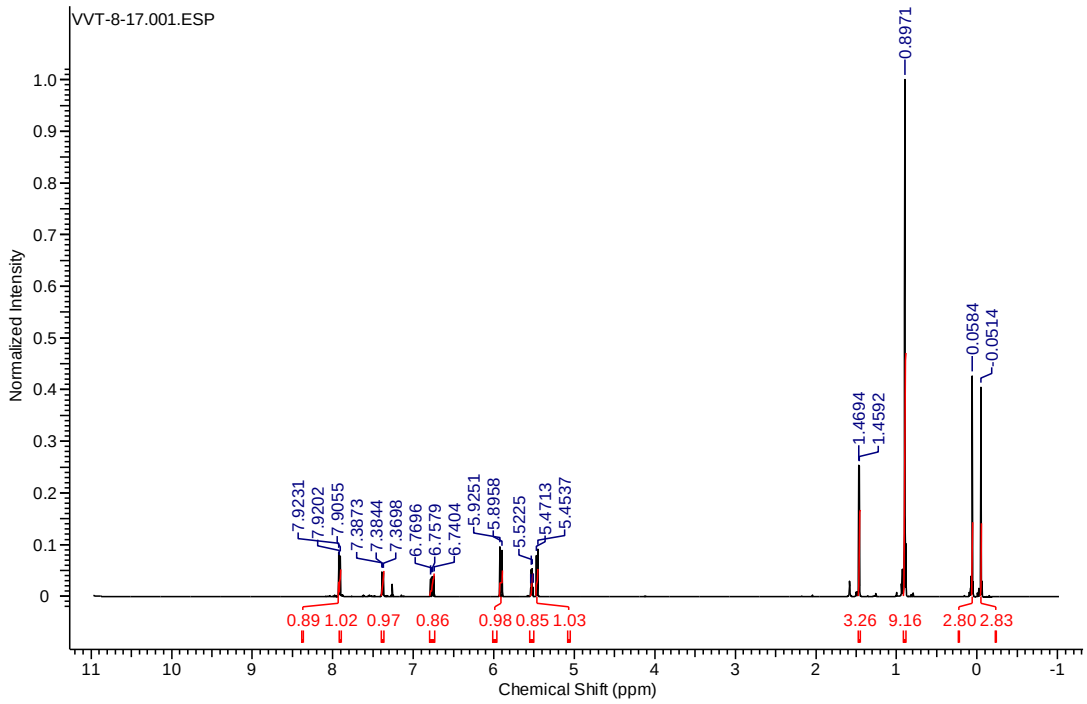


Figure 2.S22. $^{1}$H NMR spectrum of compound **12** in $CDCl_3$.

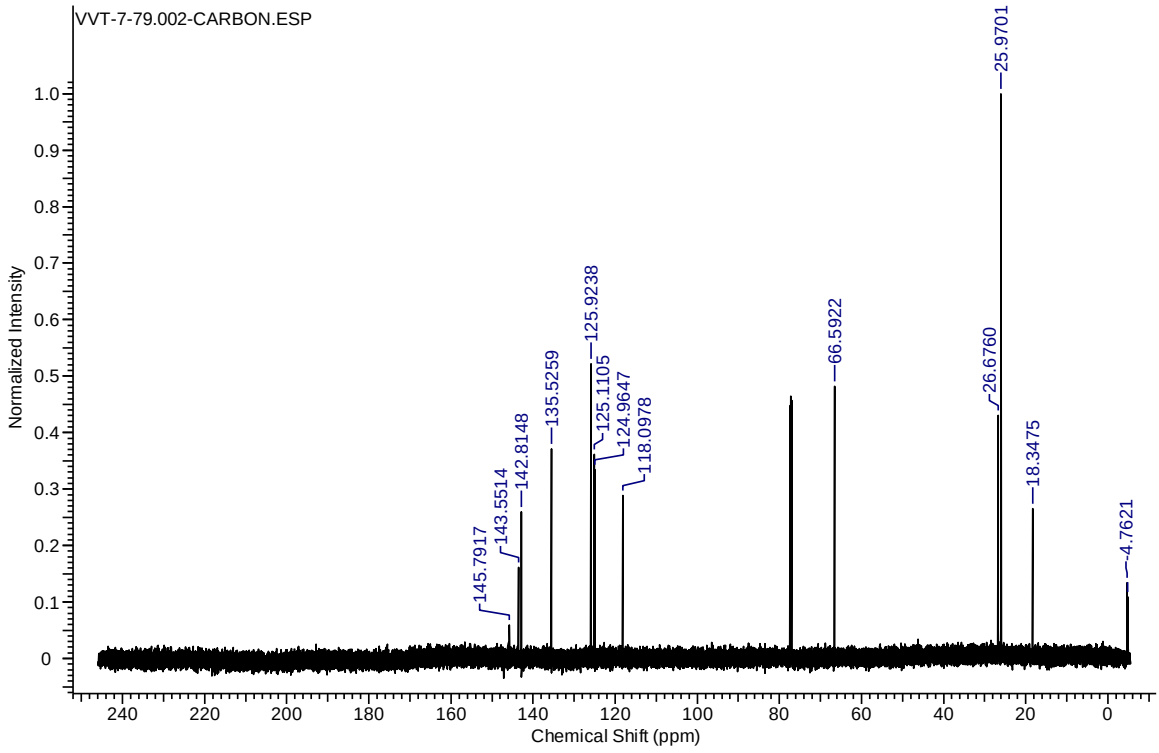


Figure 2.S23. $^{13}$C NMR spectrum of compound **12** in $CDCl_3$.

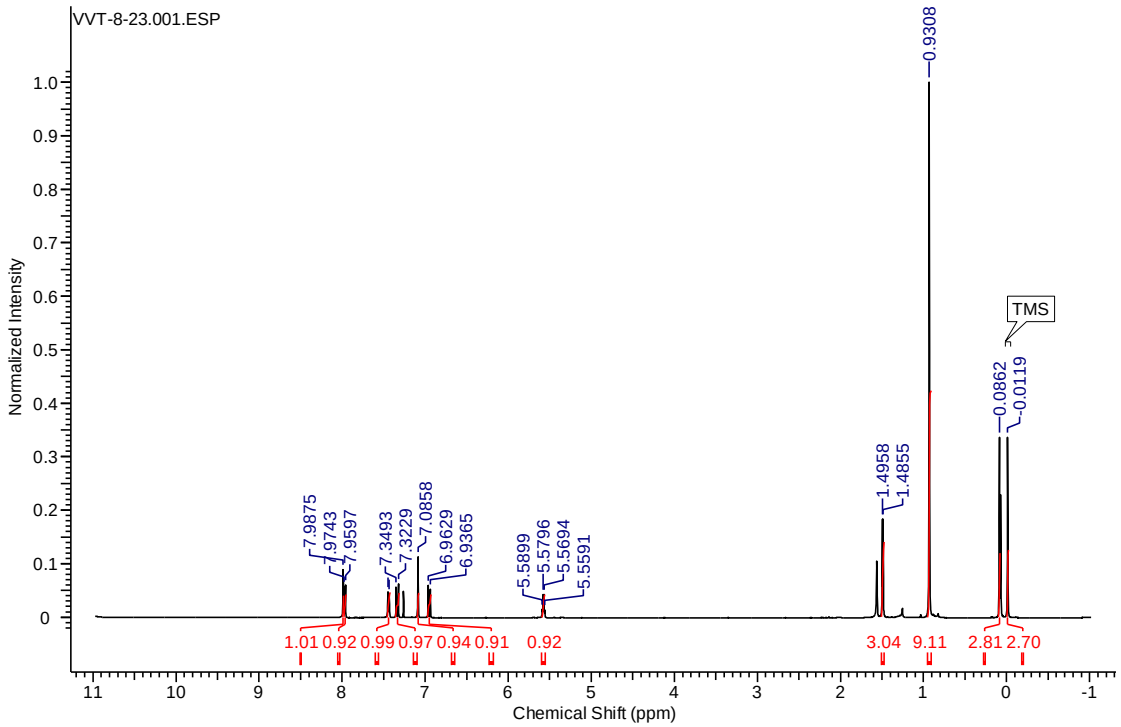


Figure 2.S24. $^{1}$H NMR spectrum of compound **13** in $CDCl_3$.

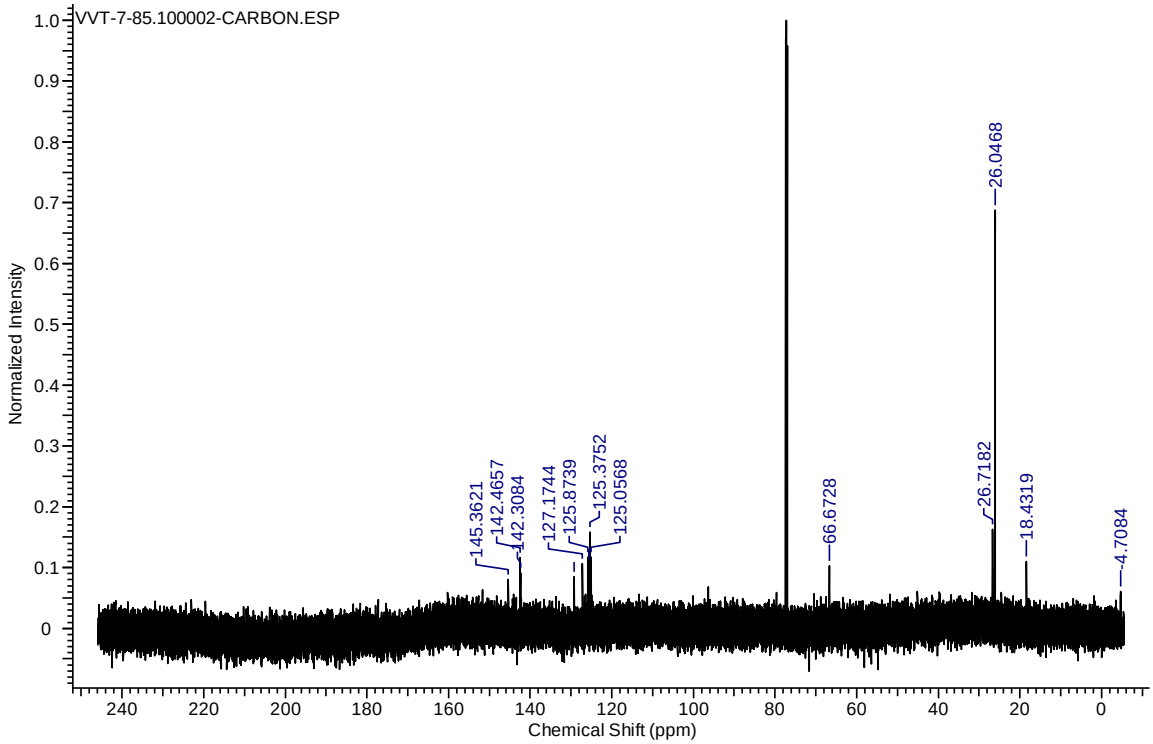


Figure 2.S25. $^{13}$C NMR spectrum of compound **13** in $CDCl_3$.

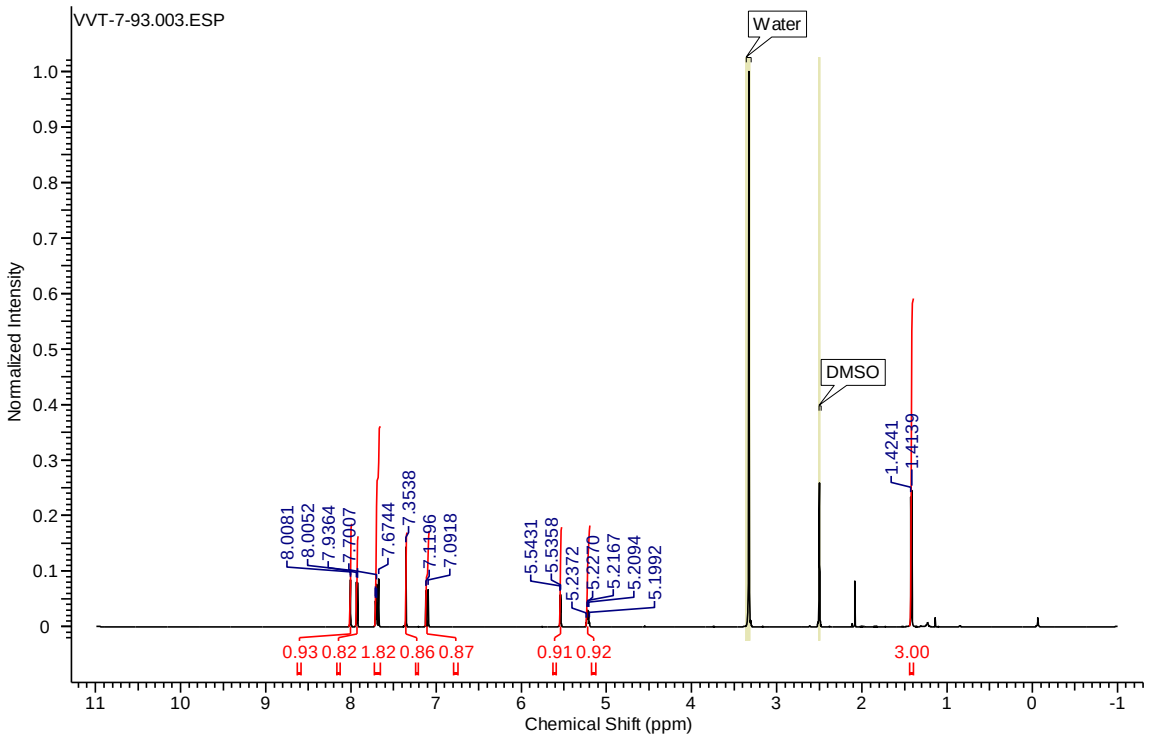


Figure 2.S26. $^{1}$H NMR spectrum of compound **14** in DMSO-$d_6$.

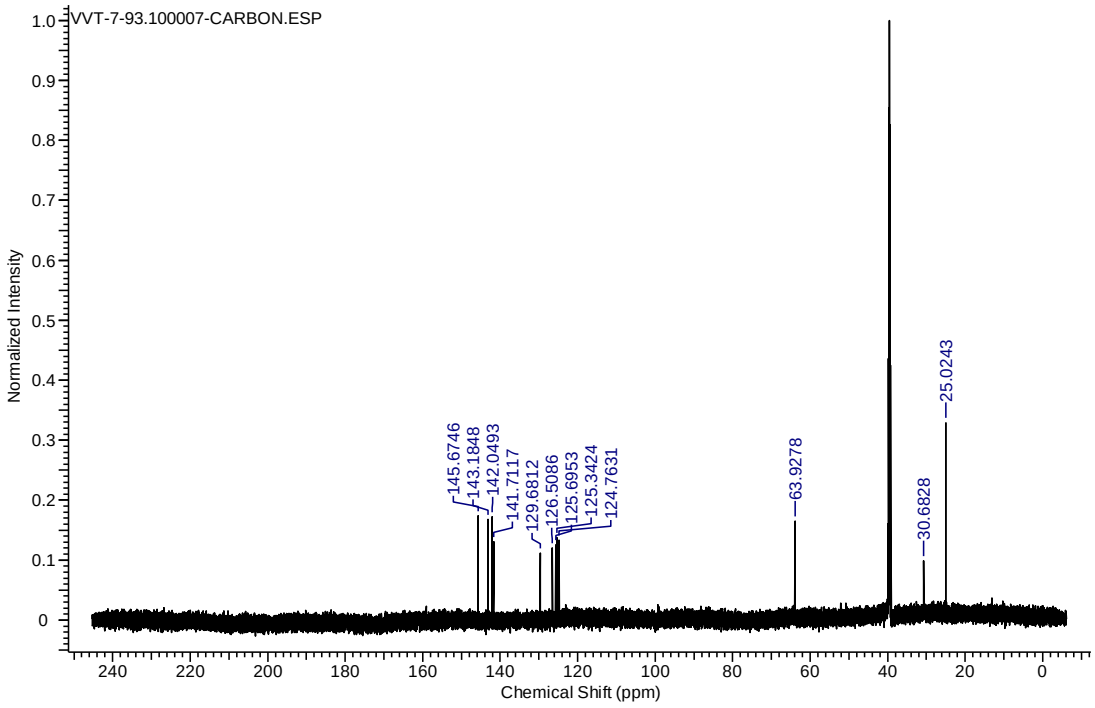


Figure 2.S27. $^{13}$C NMR spectrum of compound **14** in DMSO-$d_6$.

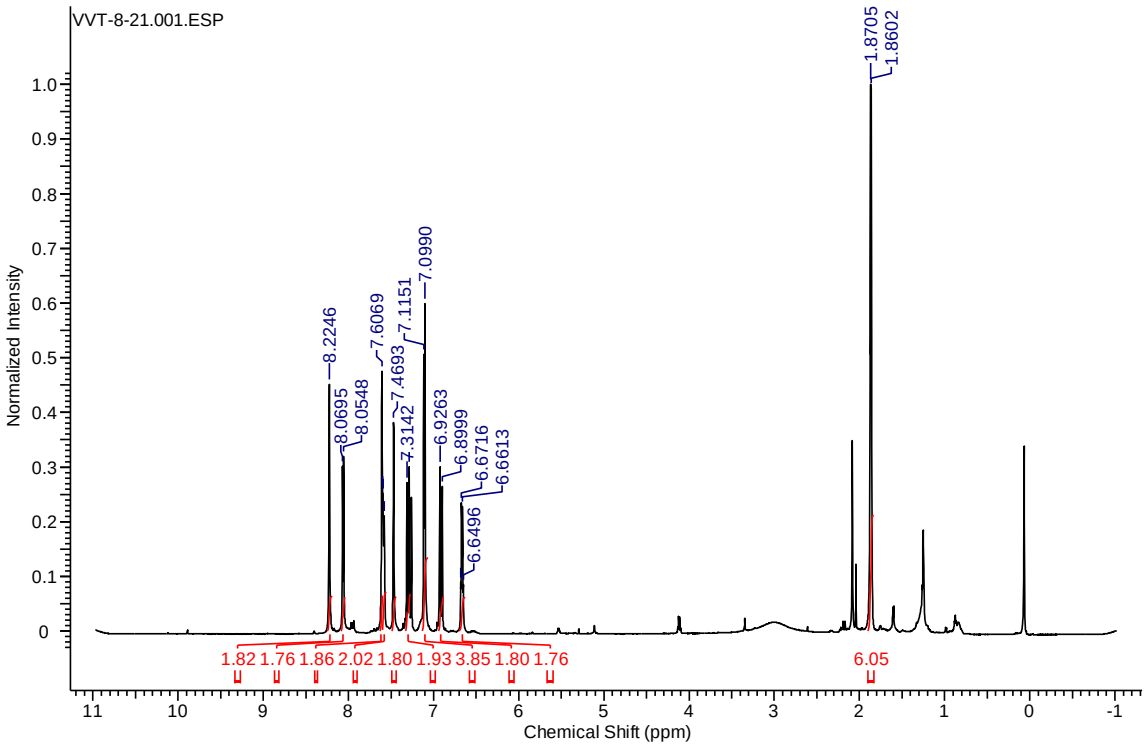


Figure 2.S28. $^{1}H$ NMR spectrum of monomer **2** in $CDCl_3$.

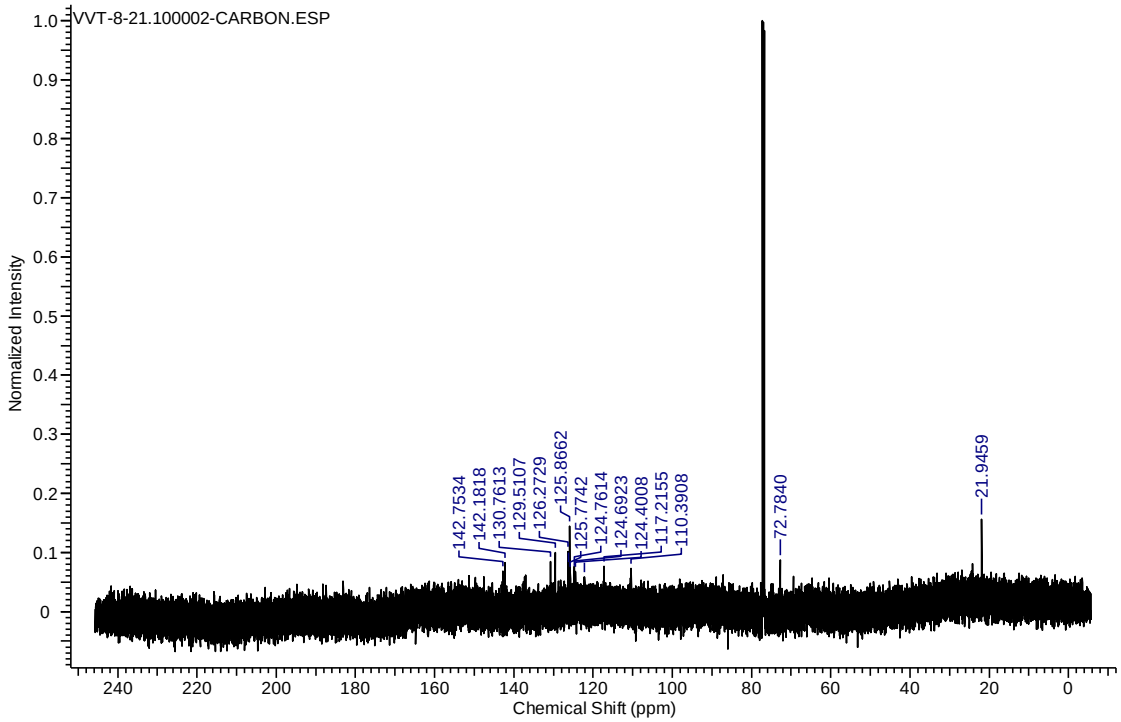


Figure 2.S29. $^{13}C$ NMR spectrum of monomer **2** in $CDCl_3$.

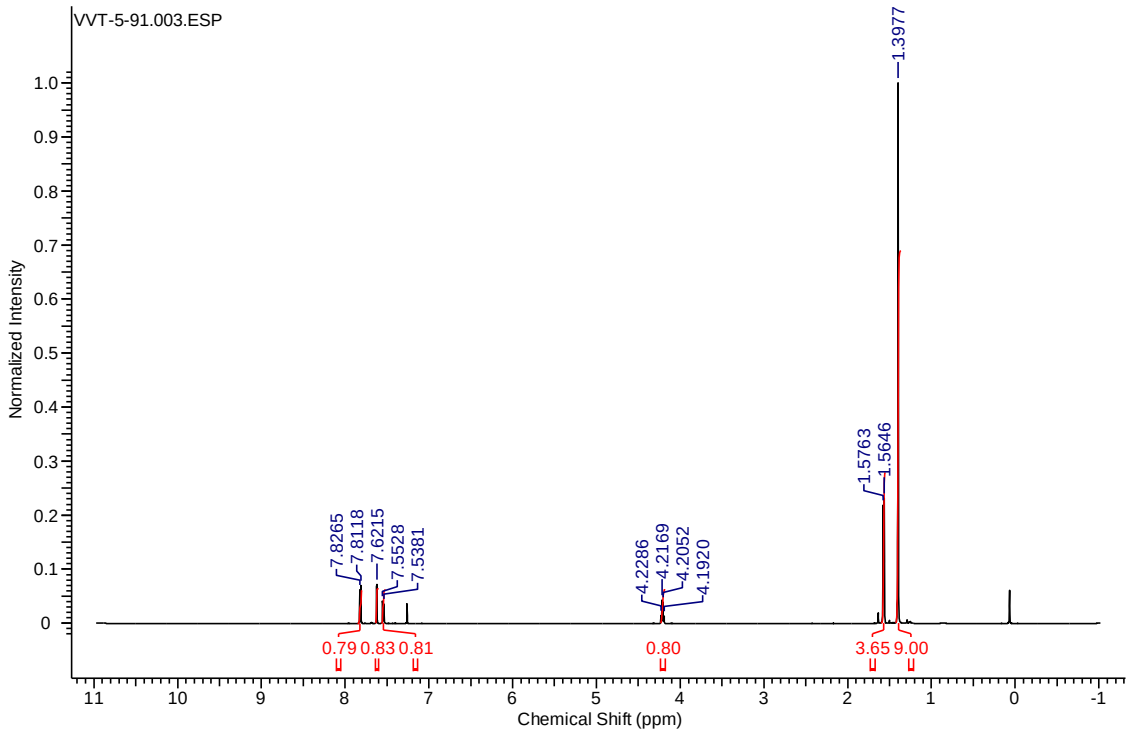


Figure 2.S30. $^{1}$H NMR spectrum of compound **16** in $CDCl_3$.

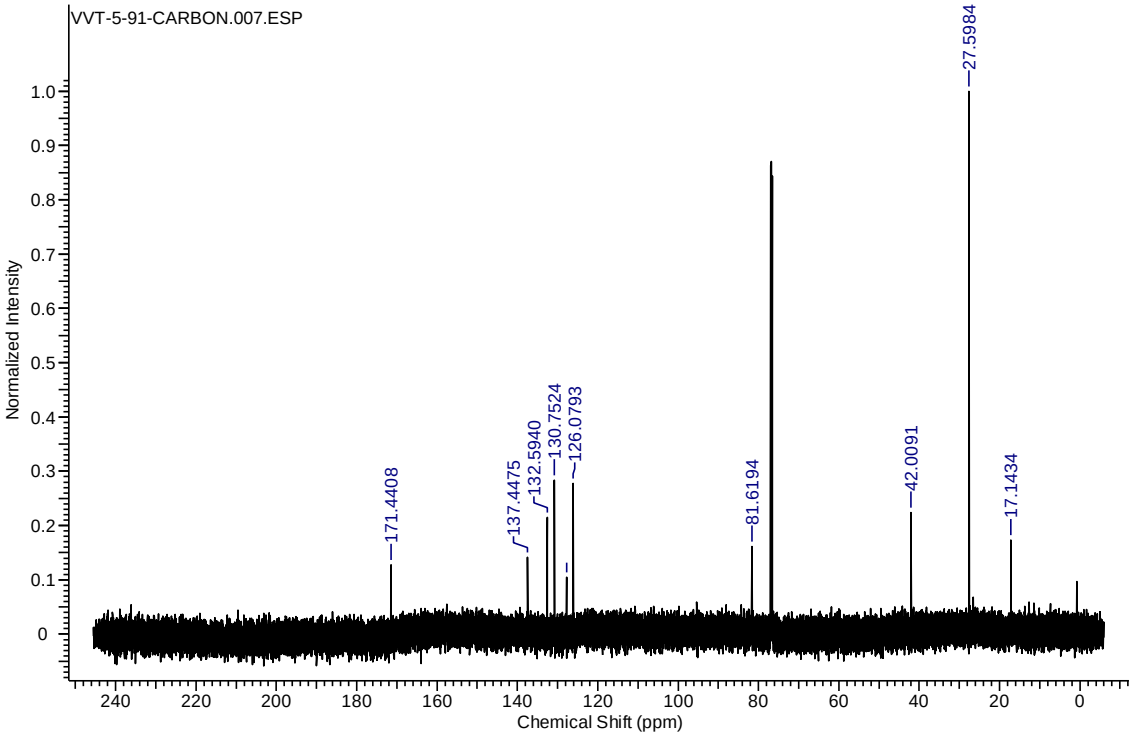


Figure 2.S31. $^{13}$C NMR spectrum of compound **16** in $CDCl_3$.

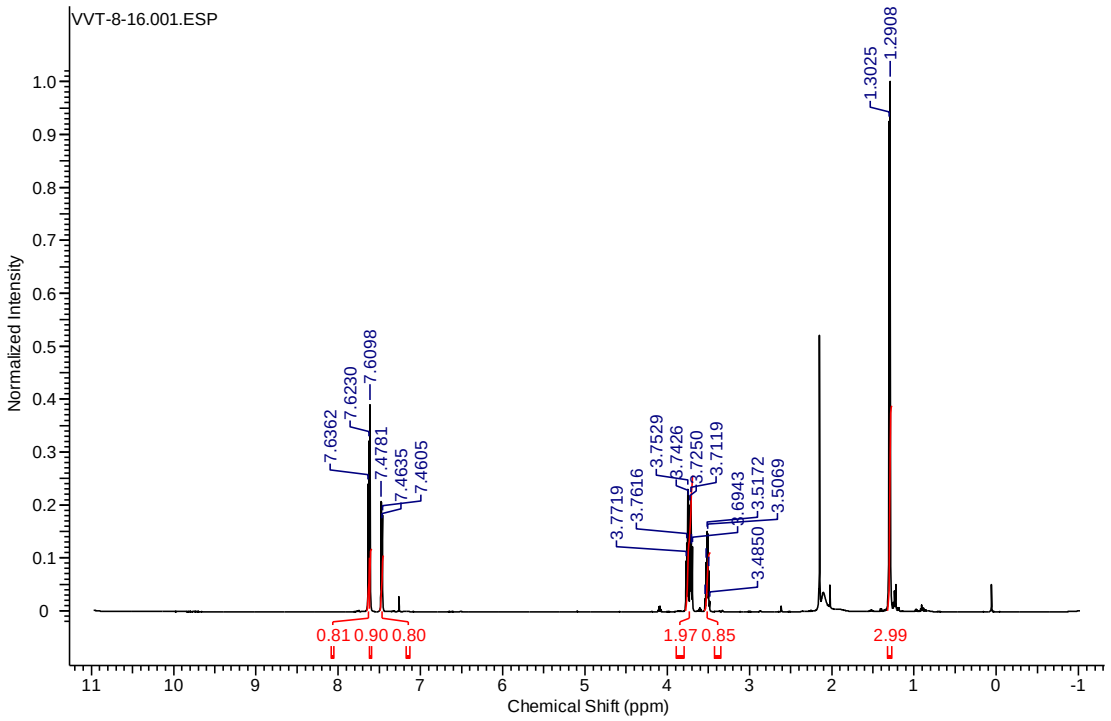


Figure 2.S32. $^{1}$H NMR spectrum of compound **17** in $CDCl_3$.

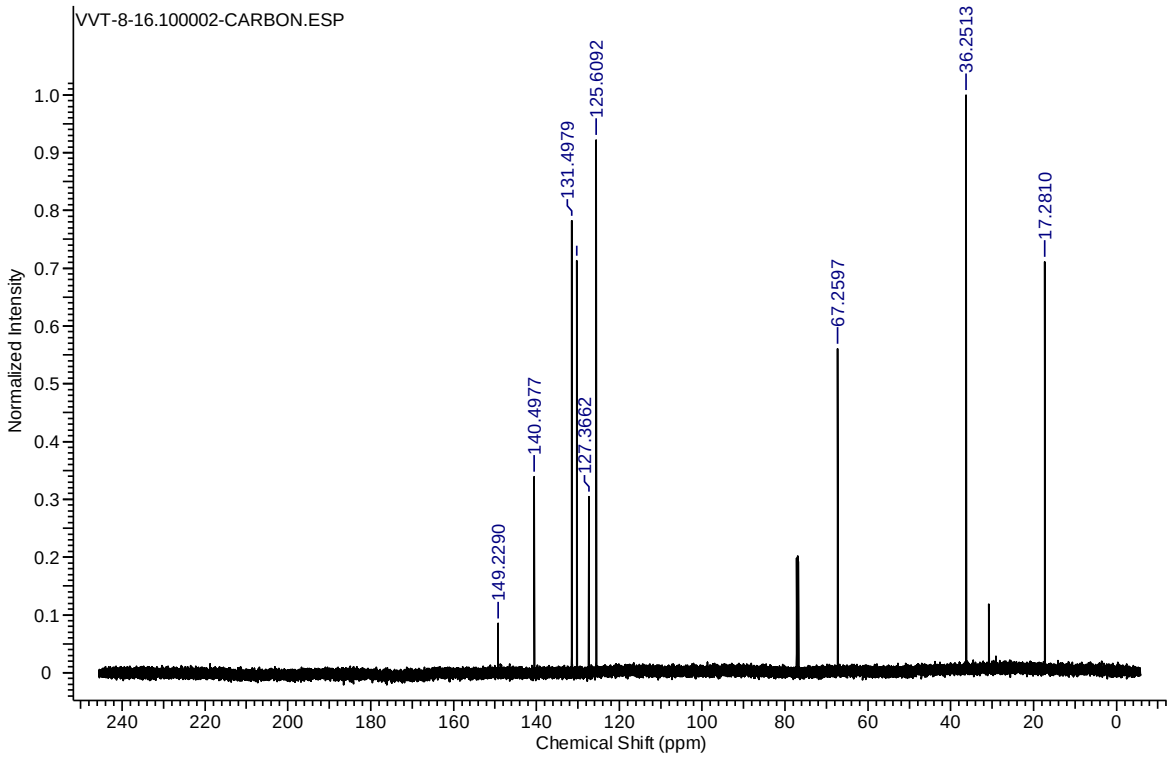


Figure 2.S33. $^{13}$C NMR spectrum of compound **17** in $CDCl_3$.

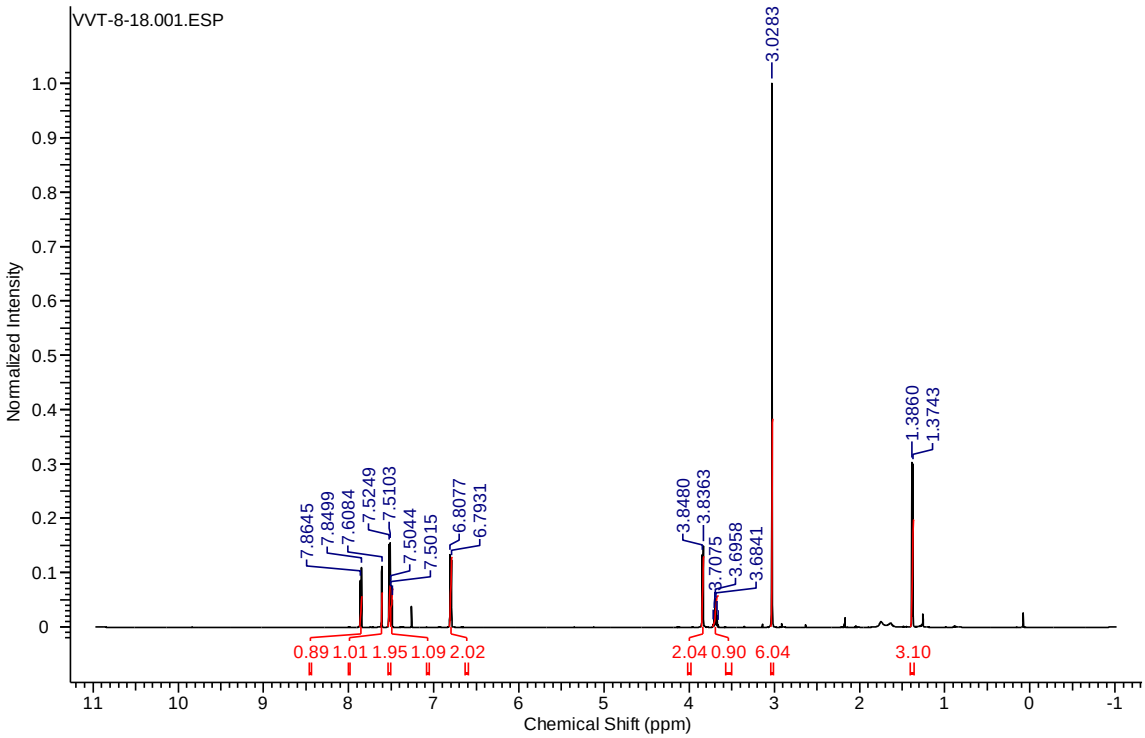


Figure 2.S34. $^{1}$H NMR spectrum of compound **18** in $CDCl_3$.

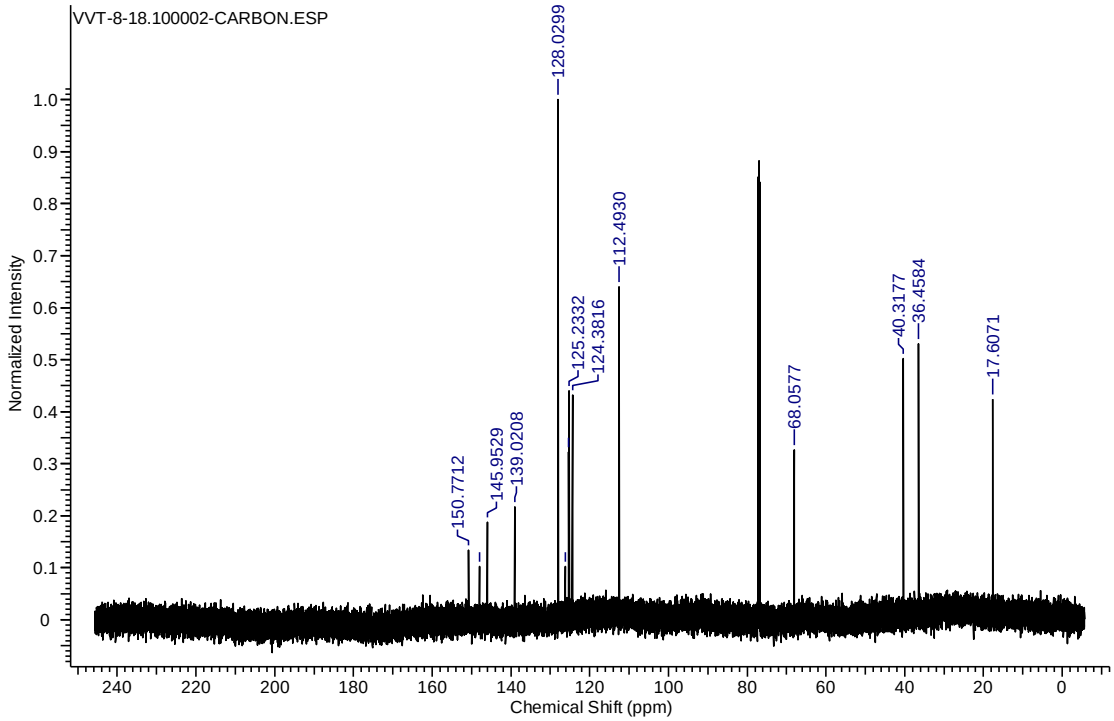


Figure 2.S35. $^{13}$C NMR spectrum of compound **18** in $CDCl_3$.

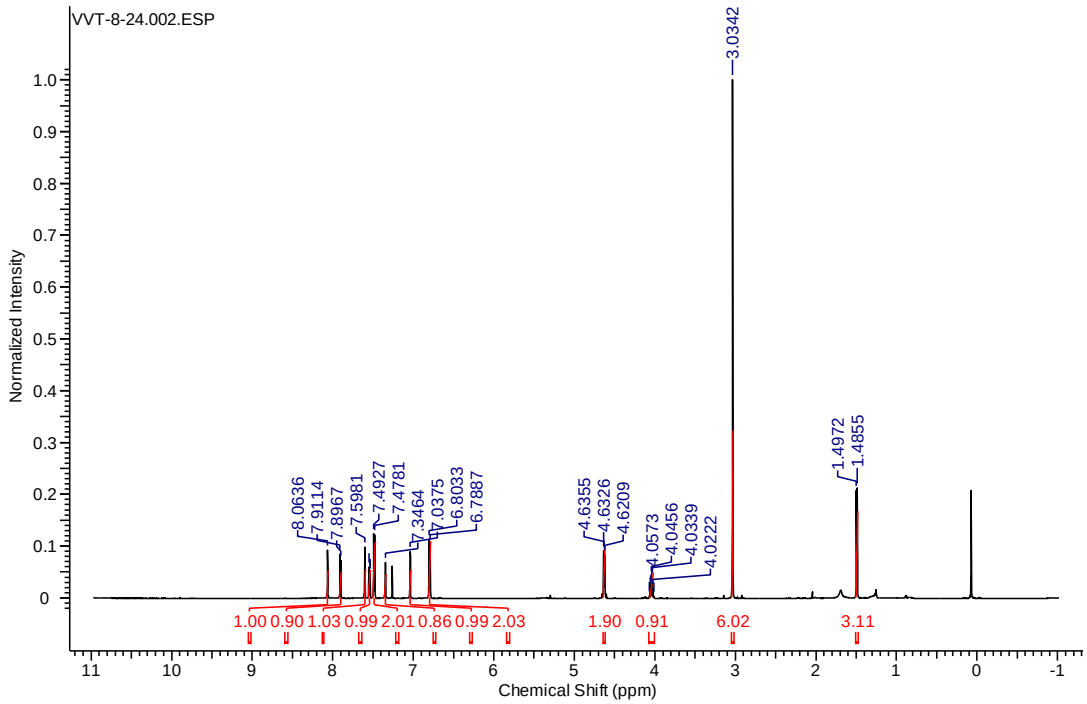


Figure 2.S36. $^{1}$H NMR spectrum of compound **19** in $CDCl_3$.

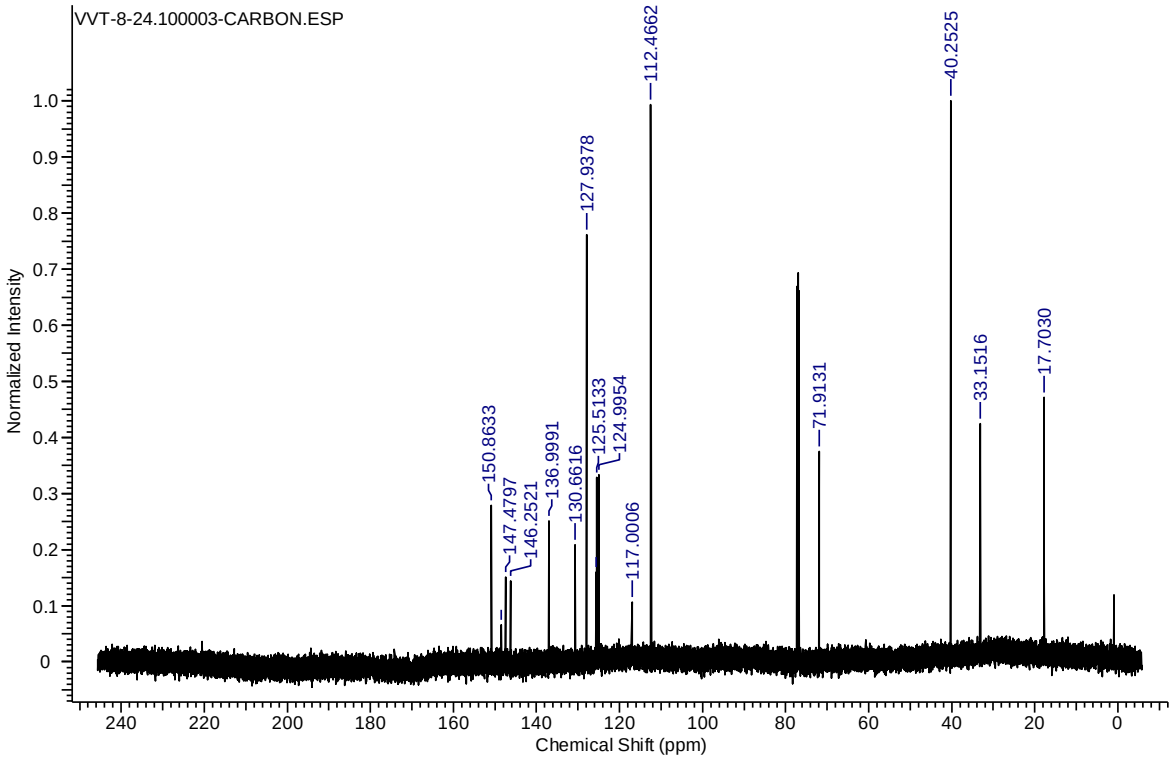


Figure 2.S37. $^{13}$C NMR spectrum of compound **19** in $CDCl_3$.

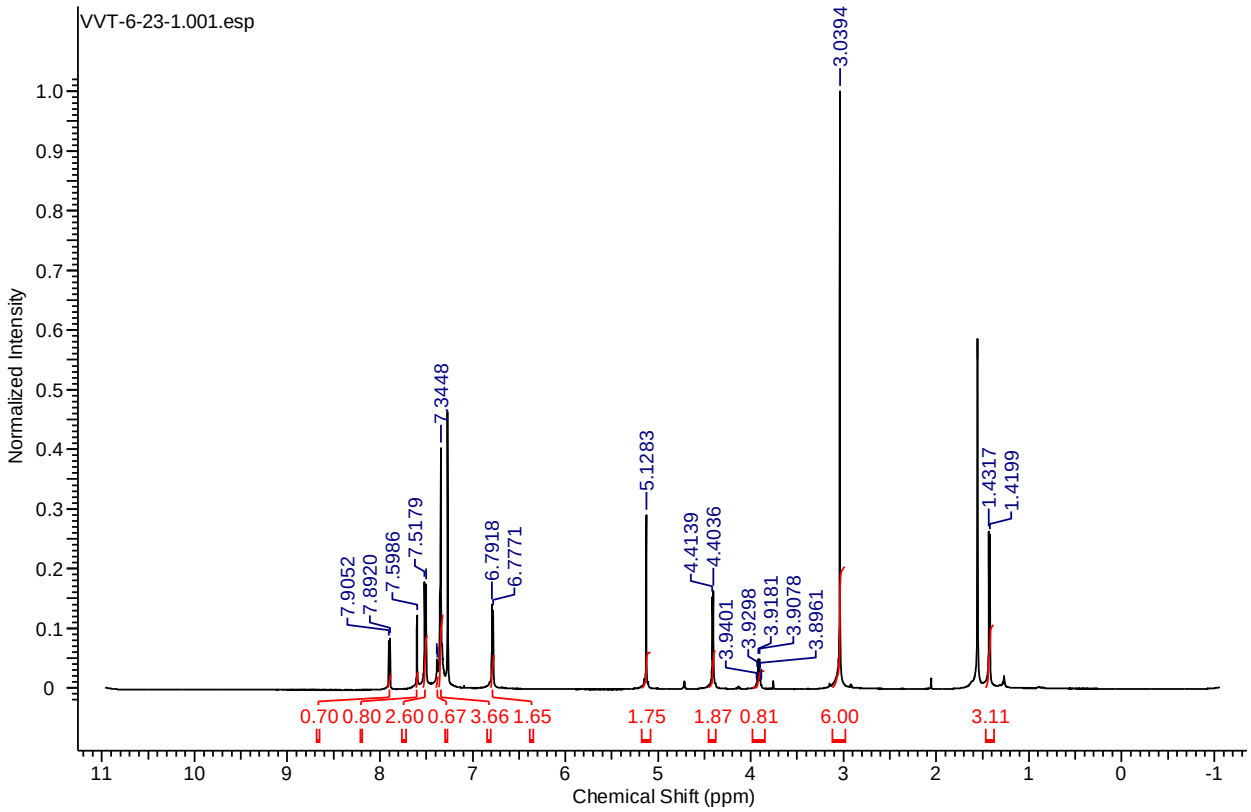


Figure 2.S38. $^{1}$H NMR spectrum of model compound **ANBP-Bn** in $CDCl_3$.

# CHAPTER 3

Visible Light Responsive Materials as Potential Blue Light Sunscreen Additives

## 3.1 Abstract

More research has shown that that deleterious health effects from prolonged sunlight exposure are not limited to just UVB/A wavelengths. Blue visible light has been shown to induce oxidative stress on your skin as well as pigmentation in those with darker skin types. Blue visible light has also been linked to melasma, a skin condition which causes unsymmetrical hyperpigmentation in the face and neck. Despite these concerns, most commercial sunscreens do not provide broad protection towards the visible wavelengths. Here, we discuss how effective blue visible light absorbing materials are at absorbing blue light from the sun. Three polymeric nanoparticles were formulated and their stability, absorbance capacity, and degradation potential were studied.

## 3.2 Introduction

Solar radiation which reaches the Earth's surface is comprised of: Ultraviolet B (UVB), Ultraviolet A (UVA), Visible (VL), and Infrared (IR) light. The deleterious effects of the high energy UV wavelengths have been well studied and documented. Both UVB (280-315nm) and UVA (315-400nm) are commonly characterized as the main culprits of sunlight induced skin cancers. DNA directly absorbs UVB wavelengths and causes mutations within the DNA strand, leading to tumor growth. UVA wavelengths damage DNA through a secondary pathway by generating radical Reactive Oxygenated Species (ROS) which damage and mutate DNA.[1] Although UV wavelengths are the most energetic, they only make up 5% of sunlight. 50% of sunlight consists of VL.[2] VL and IR radiation have long been considered to minimally impact the

skin apart from the heat sensation provided by IR irradiation. More recent research has found that this is no longer the case. High energy VL wavelengths contribute to about half of the skins free radical production due to sunlight which contribute to skin damage and that impact skin cancer.[3-5] It is clear that different wavelengths of sunlight cause skin cancer through different pathways and protection solely from UV is not enough.

The adverse effects of sunlight are not just limited to skin cancer. ROS generated from prolonged VL exposure can contribute to the degradation of the extracellular matrix in the skin, as well as collagen and elastin fibers.[6,7] Prolonged exposure to VL also induces erythema, the dilatation of the blood capillaries due to VL absorption by melanin, affecting those with darker skin types. Additionally, VL can induce persistent pigmentation. Pigmentation occurs in three different phases: immediate pigment darkening (IPD), persistent pigment darkening (PPD), and delayed tanning (DT). Each phase is characterized by how quickly they appear or persist. IPD occurs immediately after irradiation, PPD persists for 2-24 h, and DT occurs 5-7 days after irradiation and may last for weeks or months. IPD and PPD are suggested to result from oxidative stress and redistribution of melanin while DT results from the synthesis of new melanin. When people with Fitzpatrick skin types IV-VI were irradiated with UVA1 (340-400nm) and VL, it was found that both wavelengths induced pigmentation, but the VL induced pigmentation was much darker and more sustained.[8] It was later found that the higher energy blue-violet light caused significant hyperpigmentation lasting up to 3 months to those with skin types III and IV.[9] One study found that there are synergistic effects of combined low energy UVA and VL which will induce hyperpigmentation in skin types IV-VI that lasts over 14 days, sometimes lasting for over a month.[10] Additionally, VL has been linked to melasma, a skin condition under the umbrella of hyperpigmentation.[11] Melasma afflicts people with darker skin types and causes asymmetrical

pigmentation which leaves visible dark blotches throughout the face. This condition has adverse effects on the emotional well-being of those affected, so much so that specific quality of life scales were developed for melasma (MELASQoL and MASI) to better understand its emotional impact. Many melasma patients feel embarrassment, frustration, and unattractiveness all due to the hyperpigmentation caused by sunlight.[12] Current treatments for melasma include bleaching agents, oral treatments, and laser treatments, but a recent study found that the use of foundation powder that blocked sun exposure greatly improved pigmentation and produced positive MASI scores.[13]

Despite these growing concerns, most commercially available sunscreens do not protect against VL wavelengths. Sunscreens can be broken down into two classes: physical and chemical. Physical sunscreens consist of inorganic minerals that absorb and deflect light. Organic sunscreens utilize organic small molecules to absorb light. Currently, most commercially available sunscreens use organic filters as they are cheaper and easier to formulate into emulsions. However, a recent clinical trial found that four common sunscreen active ingredients (avobenzone, oxybenzone, octocrylene, ecamsule) were found in human plasma at concentrations exceeding 0.5 ng/mL under maximum use conditions.[14] The 0.5 ng/mL concentration was a threshold established by the FDA in a sunscreen guidance which stated that active ingredients below the threshold could waive some nonclinical toxicology studies. Many of these ingredients have exhibited endocrine disruption which can affect the body's natural hormonal balance.[15] Furthermore, avobenzone and oxybenzone have been seen to produce additional ROS on top of the ROS that is already produced by sunlight.[16]

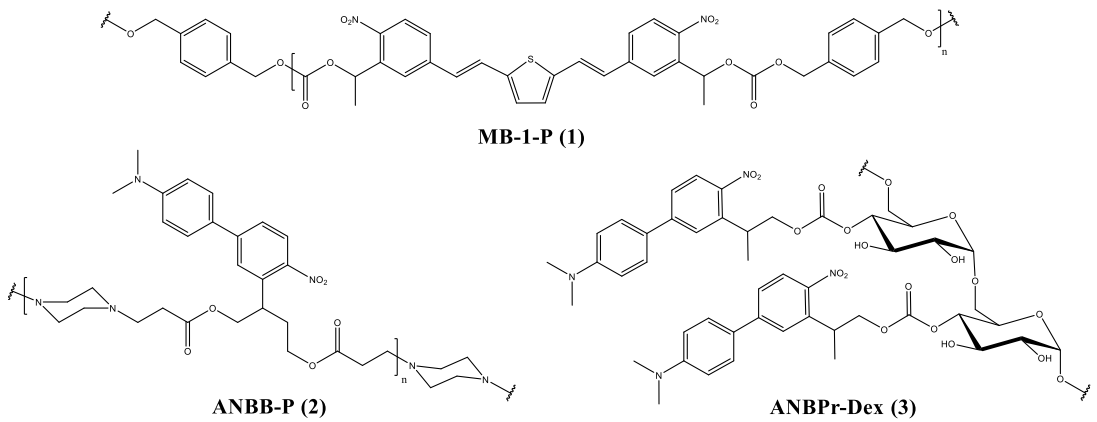


Figure 3.1. The three polymers containing the methyl-BIST and ANBB chromophores which will be formulated into nanoparticles using a single emulsion method.

As the negative effects of visible light and the inadequacies of commercially available sunscreens become more apparent, there is a clear need for an organic blue VL absorbing sunscreen that is photostable. To address this issue, the blue VL absorbance and photostability of three organic polymeric nanoparticles (MB-1-NP, ANBB-NP, ANBP-Dex-NP) will be assessed. MB-1-NP was formulated from an oligomer (**1**) containing a methyl-BIST chromophore.[17] The methyl-BIST chromophore was previously utilized in another project in hopes of developing a visible light responsive, nanoparticle drug carrier. ANBB-NP and ANBP-Dex-NP are formulated from polymers ANBB-P (**2**) and ANBP-Dex (**3**) (Figure 3.1). These polymers contain the 2-(4′-*N*-dimethyl**a**mino-4-**n**itro-[1,1′-**b**iphenyl]-3-yl)**b**utane-1,4-diyl dicarbonyl (ANBB) chromophore which also exhibits strong blue VL absorption.[18,19] UV-Vis spectroscopy will be used to assess each particle formulation's blue visible light absorbing capabilities without any irradiation and under blue light irradiation and exposure to ambient sunlight.

Furthermore, utilizing polymeric particles has many advantages over commercially available filters. First, over the course of 10 years of research in developing these optically active materials we observed a general trend that polymeric materials can undergo degradation however,

in general their commensurate particles do not. We always aimed to develop materials that degrade and observed that many of them didn't in certain formulations. As we do not expect our particles to degrade, we expect our sunscreen formulation will have limited absorption into the bloodstream. To assess if remains to be true with for the particles selected in this study, dynamic light scattering (DLS) will be used to evaluate their size before and after irradiation. Additionally, the formation of small molecule byproducts also needs to be assessed.

## 3.3 Methods

### *3.3.1 Polymer synthesis*

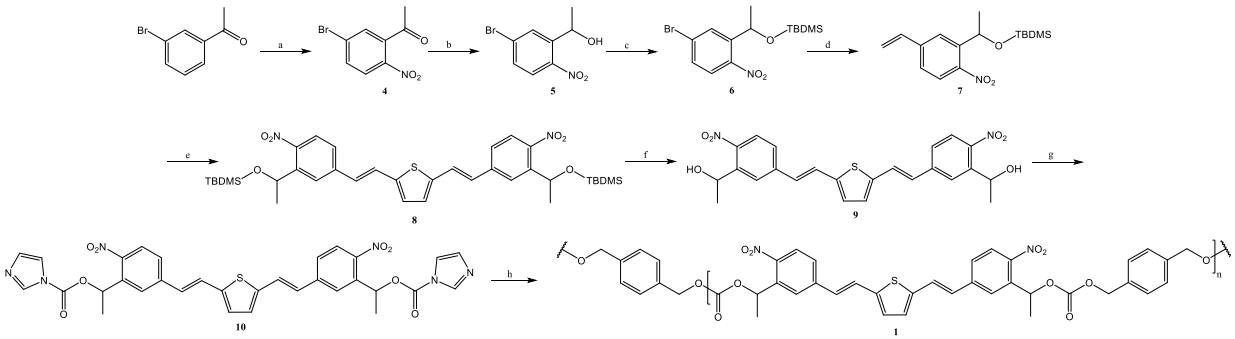

Scheme 3.1. Synthesis of MB-1 (1). (a) $HNO_3$, $H_2SO_4$; (b) $NaBH_4$, MeOH, 0 °C; (c) TBDMSCl, imidazole, DCM; (d) $Pd(PPh_3)_4$, 2,4,6-trivinyl-boroxin pyridine complex, $K_2CO_3$, DME, $H_2O$, 100 °C; (e) dibromothiophene, $Pd(OAc)_2$, LiCl, TBACl, $NaHCO_3$, DMF, 110 °C; (f) TBAF, THF, (g) CDI, DCM; (h) 1,4-benzenedimethanol, DMAP, DMSO, 80 °C.

MB-1-NP is composed of a polymer containing the methylBIST chromophore (**1**). Synthesis of monomer **10** (Scheme 1) started with the nitration of 3-bromobenzophenone, synthesized following the previously published procedure.[20] 5-Bromo-2-nitrobenzophenone (**4**) was reduced using $NaBH_4$ to the benzylic alcohol, compound **5.** The alcohol was then protected using TBDMS-Cl to form **6**. The protected alcohol was then vinylated using $Pd(PPh_3)_4$ and 2,4,6-trivinyl-boronxin pyridine complex following a procedure by Agarwal *et al*[17] to the styrene derivative, **7**. The BIST chromophore was synthesized by Heck coupling of **7** with

dibromothiophene to give **8**. The chromophore was deprotected using TBAF to yield the terminal diol, **9.** The final monomer (**10**) was prepared by transforming the terminal alcohols into an acyl imidazolide using CDI. **10** was polymerized with 1,4-benzenedimethanol as a linker with DMAP for 3 days, yielding **MB-1-P** ($M_w$: 2.8 kDa (PMMA Standard), PDI: 1.8).

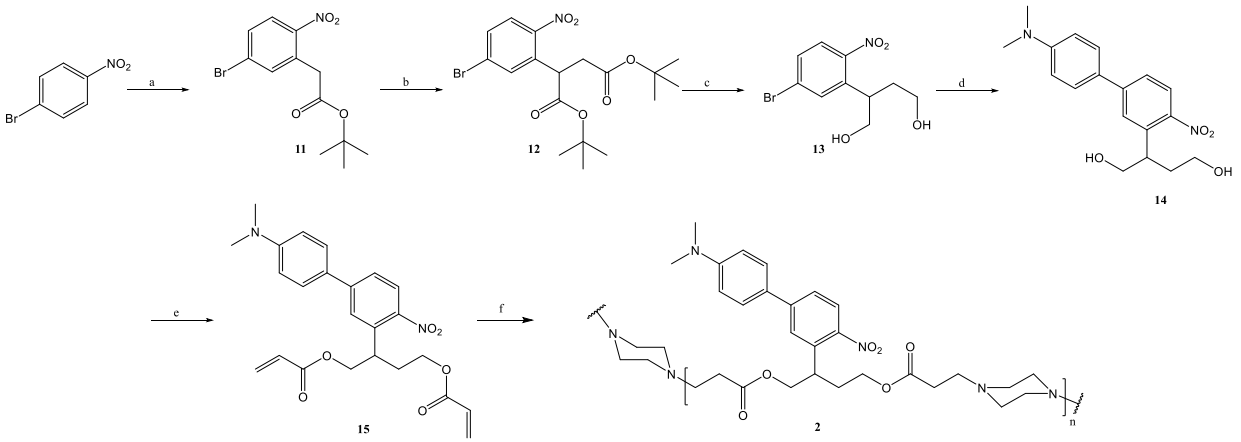

Scheme 3.2. Synthesis of ANBB (2). (a) $HNO_3$, $H_2SO_4$; (b) $NaBH_4$, MeOH, 0 °C; (c) TBDMS-Cl, imidazole, DCM; (d) $Pd(PPh_3)_4$, 2,4,6-trivinyl-boroxin pyridine complex, $K_2CO_3$, DME, $H_2O$, 100 °C; (e) dibromothiophene, $Pd(OAc)_2$, LiCl, TBACl, NaHCO3, DMF, 110 °C; (f) TBAF, THF.

ANBB-NP is composed of a polymer that was previously synthesized in the lab (Scheme 3.2). The polymer was made of an ANBB chromophore, linked together with piperazine using Michael Addition. ANBB-P (**2**) was synthesized over 7 steps to yield the polymer as an orange solid. ANBP-Dex (**3**), however, utilized a slightly modified version of the ANBB chromophore. ANBP (**18**) was following the published procedure by Donato *et al.* (Scheme 3.3).[18] To start, compound **11** was synthesized according to a published procedure.[22] **12** was then methylated using NaH and methyl iodide to form **17**. The *t*-butyl acetate group was reduced using DIBAL-H to form alcohol **18**. The final ANBP chromophore **18** was synthesized by Suzuki coupling of compound **17** with $Pd(PPh_3)_4$ and 4-dimethylphenylboronic acid. The alcohol on **18** was then

converted to the acyl imidazolide **20** with CDI and then conjugated onto dextran (9-10kDa) through a carbonate linker via CDI coupling following a procedure similar to Broaders et al.[21]

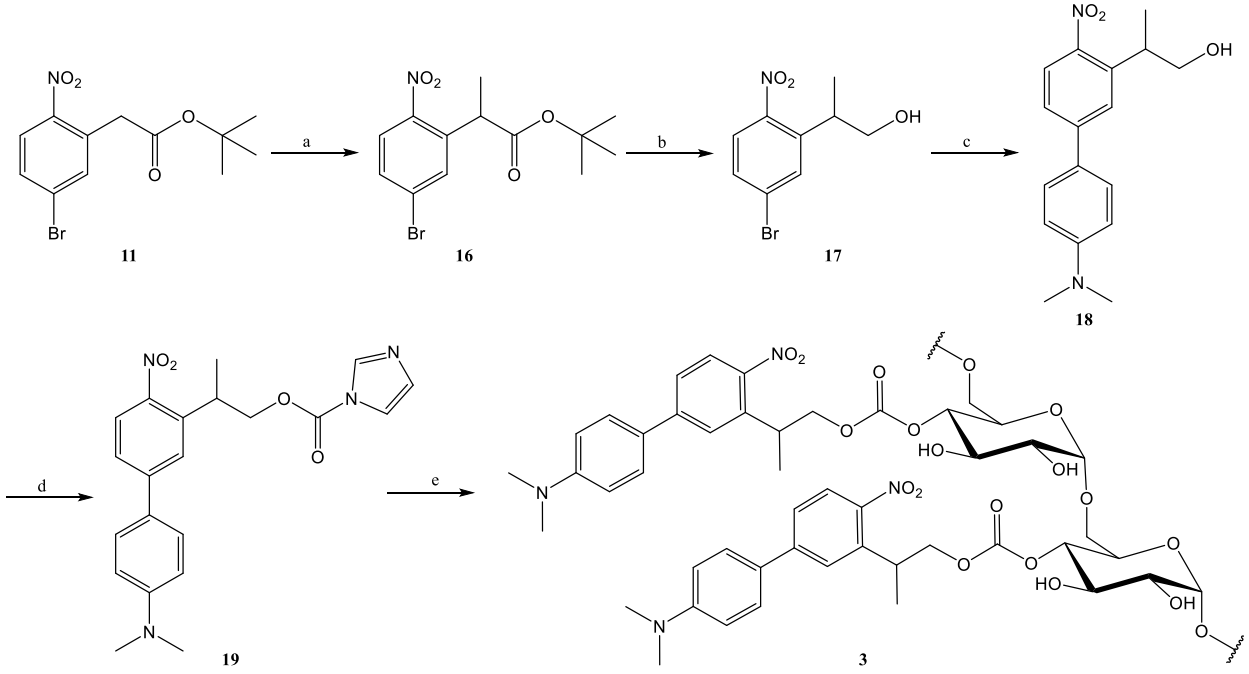


Scheme 3.3. Synthesis of ANBP-Dex (3). (a) NaH, MeI, DMF; (b) DIBAL-H, THF, 0 °C; (c) 4-(Dimethylamino)phenylboronic acid, $Pd(PPh_3)_4$, $Na_2CO_3$, toluene, EtOH, H2O, 90 °C; (d) CDI, DCM; (e) dextran, DMAP, DMSO, 80 °C.

*3.3.2 Particle Preparation*

All three polymers were formulated into empty nanoparticles using a single emulsion formulation method using sonication with PVA as a surfactant. 10 mg of each polymer was dissolved in 0.3 mL of DCM and was added to a 6 mL solution of 1% PVA w/v. The solution mixture was then sonicated (2400 J) over ice to form an emulsion. The organic solvent was removed from the particle solution *in vacuo* with stirring at 500-600 rpm. After about 3 hours under vacuum, the excess surfactants were removed by tangential flow using a 500 kDa membrane with water as an eluent. The solution was concentrated to 5 mL each time and solution was allowed

to run through the membrane 3 times before the particle solution was freeze-dried with 100 mg of mannitol as a cryoprotectant.

### *3.3.3 Preliminary Irradiation Studies*

Preliminary irradiation studies were done on the three nanoparticle formulations under both blue visible light irradiation and direct sunlight. The three nanoparticles were suspended in phosphate buffered saline (PBS, pH 7.4) at 0.05 mg $mL^{-1}$ and allowed to incubate at 37 °C for up to 24h. Each suspension was then exposed to blue VL using an OmniCure S2000 (Lumen Dynamics ($\lambda_{ex}$ = 400-500 nm, 0.9 W, 1.05 W $cm^{-2}$) at a distance of 8 cm away from the sample. Each suspension was irradiated at subsequent time points (15, 30, 60, 120 min.) and their UV-Vis absorbance measurements were taken after each time point using a dual beam Shimadzu UV-3600 UV-Vis-NIR Spectrophotometer. Sun exposure studies were done in a similar fashion, utilizing 0.05 mg $mL^{-1}$ suspensions of ANBB-P and ANBP-Dex-P in PBS (pH 7.4). The samples were exposed to direct sunlight on a clear summer day for up to 120 min in La Jolla, California. To determine if ambient UV light also affects blue VL absorbance, two samples of each suspension were tested simultaneously, one sample left in the open while the other behind an un-tinted, UV-blocking window. Like the BVL studies, the UV-Vis absorbance of each sample was taken after irradiation. The photostability of the suspensions was monitored by following changes in the area under the BVL spectral region (400-500 nm) as a function of exposure time.

### *3.3.4 Primary Irradiation Studies*

Based off the preliminary studies, the primary irradiation studies were done only on ANBP-Dex-NP and ANBB-NP for reasons which will be discussed below. Additionally, the preparation

of the suspensions was also changed. Due to issues with aggregate formation, DI water was used to prepare both suspensions instead of PBS. ANBP-Dex-NP suspensions were prepared by dissolving the dry NPs in DI $H_2O$ at 0.05 mg $mL^{-1}$ were incubated at 37 °C for up to 24 h. The preparation of ANBB-NP changed even more due to the presence of aggregates after incubation at 37 °C. Additionally, the original concentration of 0.05 mg $mL^{-1}$ did not absorb strongly enough in DI $H_2O$. To address these issues, 0.1 mg $mL^{-1}$ suspension were prepared with DI $H_2O$ and were hydrated at 4 °C for at least 24 hr. Both suspensions were irradiated with blue visible light at subsequent time points (15, 30, 45, 60, 90, 120, 150, 180 min) and the UV-Vis absorbance was measured after each time point.

For the sun irradiation studies, the samples were prepared in a similar fashion to the blue VL exposure stated above and the study was also done in triplicate. Two samples of each particle suspension were prepared, one to be exposed to direct sunlight (open) and one behind a car windshield (window) to block UV wavelengths at subsequent time points (15, 30, 45, 60, 90, 120, 150, 180 min) and the UV-Vis was measured after each irradiation time. In addition to UV-Vis, the count rate of the suspensions was measured using DLS. 0.05 mg $mL^{-1}$ suspensions of ANBP-Dex-NP were exposed to sunlight during the fall and winter seasons in La Jolla, California, reaching a maximum UV index of 4. For ANBB-NP, the particles were suspended in DI $H_2O$ at 0.1 mg $mL^{-1}$ and allowed to hydrate at 4 °C for 4 days. The samples were exposed to direct sunlight during the fall and winter seasons in La Jolla, California, reaching a maximum UV index of 3. The photostability of the suspensions was monitored by following changes in the area under the BVL spectral region (400-500 nm) as a function of exposure time. The count rate of the suspensions was also taken after each irradiation time using dynamic light scattering (DLS) using a Zetasizer Nano ZS (Malvern Panalytical Inc.)

*3.3.5 Stability of Non-Irradiated Suspensions*

The stability of the NP suspensions over time was also assessed using UV-Vis absorbance and dynamic light scattering. ANBP-Dex-NP (0.05 mg $mL^{-1}$) and ANBB-NP (0.1 mg $mL^{-1}$) suspensions were prepared in DI $H_2O$ and allowed to hydrate as previously discussed. The suspensions were kept in the dark at room temperature and their absorbance and DLS measurements were taken over a period of 31 days. The first measurements were taken after the suspensions were allowed to hydrate for the appropriate time and were noted as Day 0.

*3.3.6 Degradation Studies*

Alongside assessing the photostability of the NPs, it is important to assess the possible release of small molecules from the NP suspensions. One of the increasing concerns regarding current sunscreen formulations is their absorbance through the skin into the blood stream at concentrations that are considered toxic. To assess this leakage preliminarily, both NP suspensions were prepared with DI $H_2O$ and then irradiated with blue VL (400 – 500 nm) at subsequent time periods (0, 60, 180, 240 mins). After each hour of irradiation, 2 mL aliquots were taken filtered by centrifugal filtration using an Amicon Ultracel 3K filter made with regenerated cellulose at 15k rpm for 45 minutes. The supernatants were then analyzed by UV-Vis spectroscopy.

The release of small molecule photoproducts was also assessed under "sink conditions" by preparing the suspensions in DI water containing 1% w/v Pluronic® F127. In this case, no centrifuge filtration was done. Instead, the aliquots were centrifuged (15k, 45 min.) after irradiation and the UV-Vis absorbance of the supernatants were measured. Additionally, characterization of any small molecule photoproducts was done using MALDI-TOF (Agilent 6230

Accurate-Mass TOFMS). All supernatant aliquots were collected, lyophilized, then analyzed using MALDI-TOF, scanning from 450 m/z to 3500 m/z.

## 3.4 Results

### *3.4.1 Preliminary Irradiation Studies (BVL and Sun in PBS (pH = 7.4))*

To assess the affect blue visible light has on the absorbance on our nanoparticle suspensions, each polymer was formulated into nanoparticles and then subjected to blue visible light. MB-1-NP (size: 165 ± 0.3 nm (DLS)) exhibited an $Abs_{max}$ = 0.330 at $\lambda_{max}$ = 480nm but blue VL absorbance dropped to 51.8% after 120 min. of exposure (Figure 3.2c). Additionally, the MB-1-NP suspension displayed a color change upon irradiation, from a deep orange solution to a lighter solution with more irradiation (Figure 3.2c).

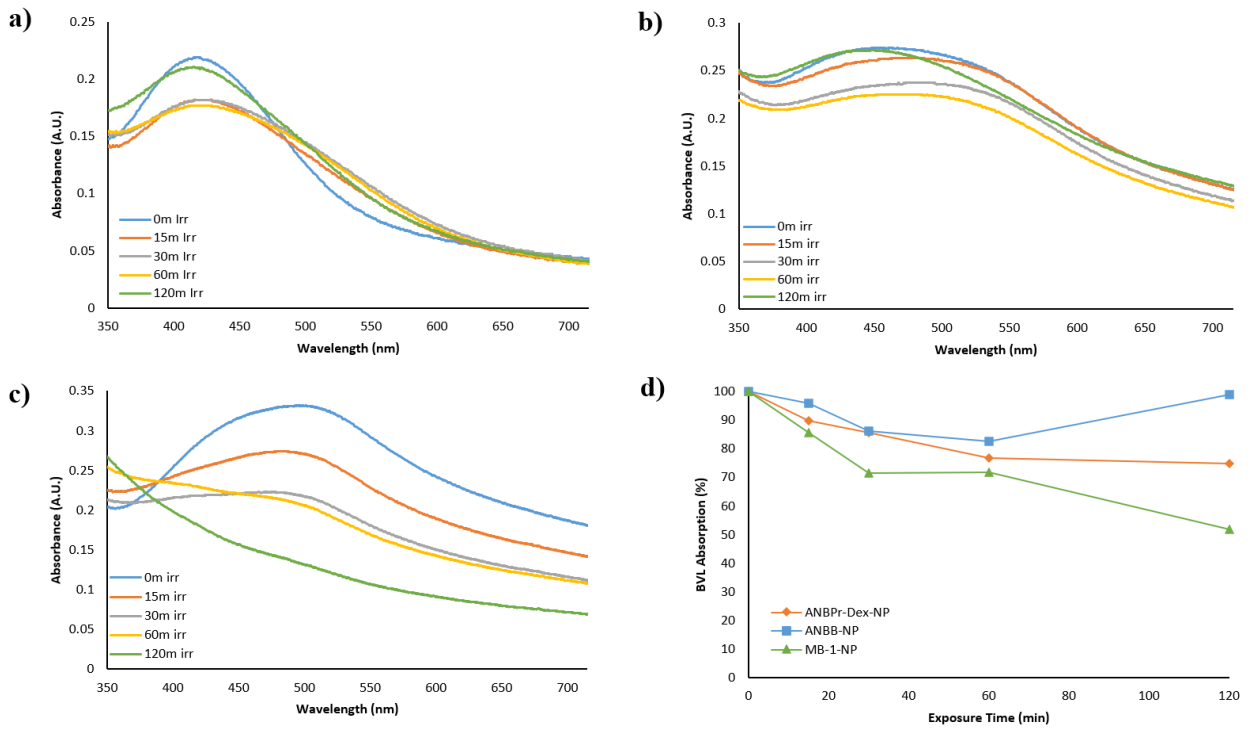


Figure 3.2. Preliminary absorbance profiles after blue visible light irradiation for (a) ANBP-Dex-NP, (b) ANBB-NP, and (c) MB-1-NP. (d) The change in BVL absorbance capacity after 15, 30, 60, and 120 minutes of BVL irradiation.

ANBB-NP (size: 166 ± 2.3 nm (DLS)) showed an $Abs_{max}$ of 0.274 at 438 nm. After 120 min. of blue VL exposure, the suspension's BVL absorbance capacity dropped to 98.9% (Figure 3.2b). ANBP-Dex-NP (size: 160 ± 1.1 nm (DLS)) showed similar results with an $Abs_{max}$ of 0.211 at 421nm. The BVL absorbance decreased to 75.0% after 120 min. of exposure (Figure 3.2a). Both suspensions also displayed a noticeable color change, changing from a yellow solution to a deep orange solution with more irradiation (Figure 3.3). These preliminary results suggest that the MB-1-NP may not be as photostable as the other two nanoparticle formulations and thus, MB-1-NP was excluded from studies with ambient sunlight.

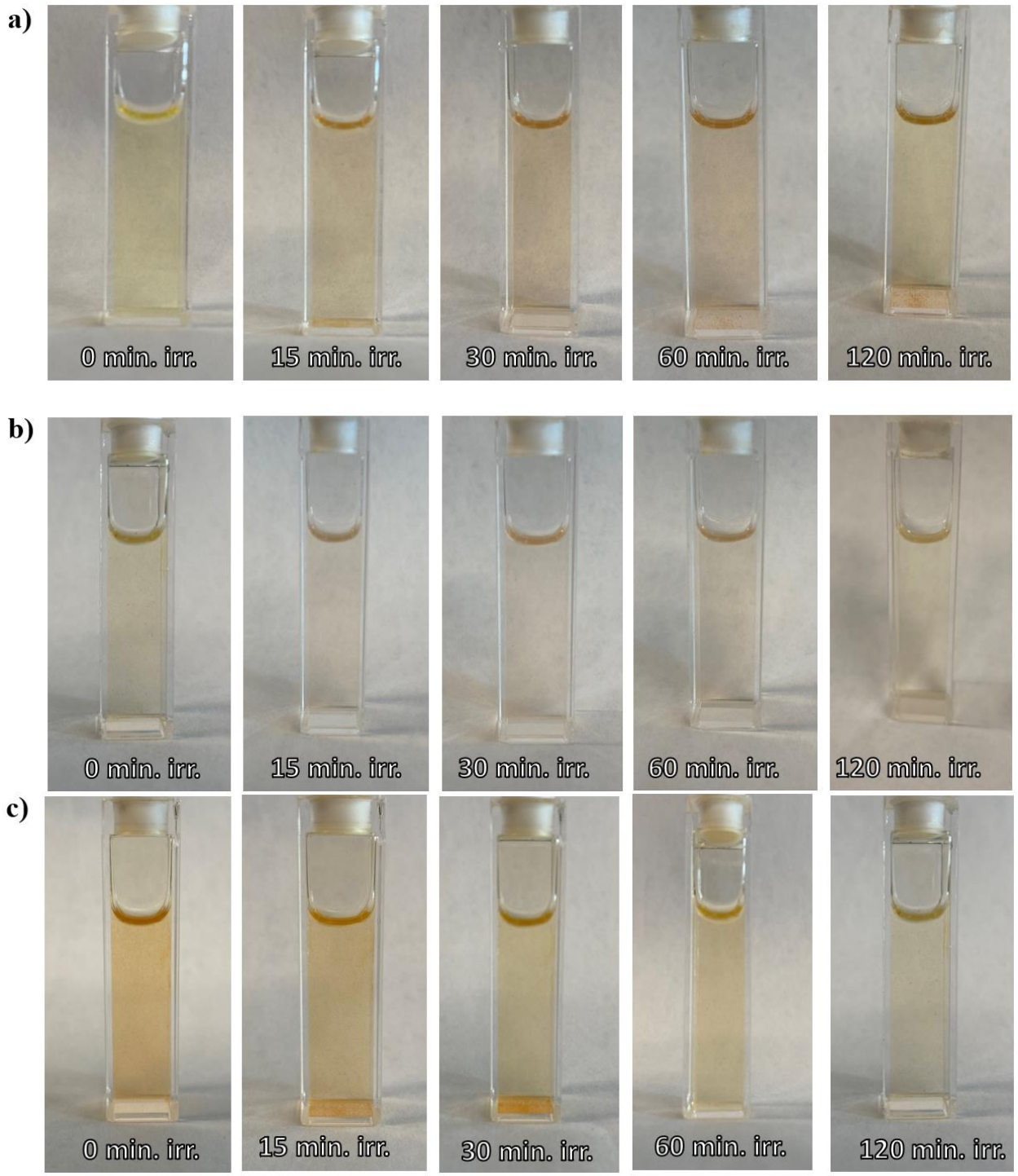


Figure 3.3. Photos of (a) ANBP-Dex-NP, (b) ANBB-NP, and (c) MB-1-NP suspensions after each irradiation time. ANBP-Dex-NP and ANBB-NP showed a similar color change, from yellow to orange. MB-1-NP displayed the opposite effect by starting from an orange suspension to yellow after 2 hours of BVL exposure.

To assess the potential of the NPs as a sunscreen additive, the effect of sunlight on the absorbance of the suspensions were also done. ANBB-NP also showed a similar result to its blue VL exposed counterpart. Both ANBB-NP open and window samples exhibited an $Abs_{max}$ of 0.286 and 0.291 at 412 nm and were exposed to unabated sunlight reaching a maximum UV index of 6. After 120 min. of exposure, the absorbance capacity of the open and window samples dropped to 73.9% and 72.8% compared to the non-irradiated samples (Figure 3.4 blue). Additionally, a color change was also observed that was like its blue VL exposed counterpart, going from a yellow solution to deep orange. The ANBP-Dex-NP samples exhibited an $Abs_{max}$ = 0.093 at 421 nm and were exposed to sunlight reaching a maximum UV index of 10. In contrast to ANBB-NP, both open and window samples of ANBP-Dex-NP suspensions still retained 96.2% and 94.3% of the original absorbance intensity, respectively (Figure 3.4 orange). Like the blue VL exposed samples, both the ANBP-Dex-NP suspensions displayed the same color change pattern.

Based on both the preliminary results, it appears as though the NPs containing the ANBB chromophore are relatively photostable to both blue VL and direct sunlight. However, there were a few issues with the preparation of the suspensions. First, using PBS to suspend the dry particles caused both ANBB-NP and ANBP-Dex-NP to aggregate, which was evident by initial DLS studies. Secondly, when ANBB-NP was incubated at 37 ℃, the solution formed aggregates that would not dissolve, even with sonication. To address these issues, water was used as a solvent instead of PBS and ANBB-NP was hydrated at 4 ℃ for 24hrs. With these slight changes, the two NPs were further analyzed as potential blue light absorbing sunscreen candidates.

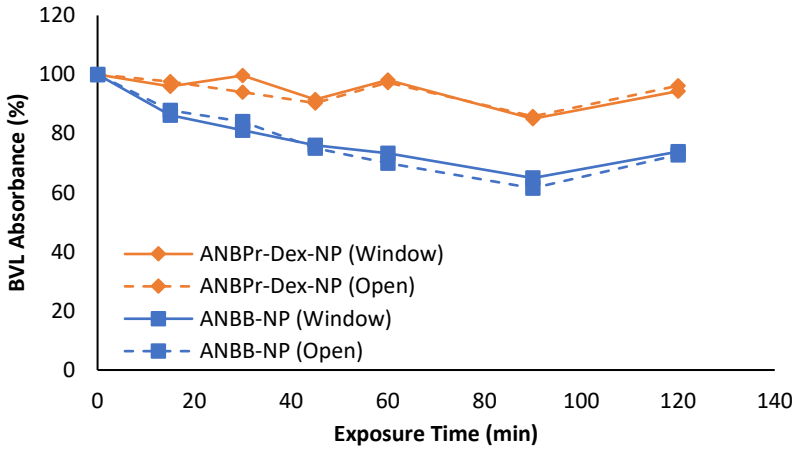


Figure 3.4. The preliminary BVL absorbance of ANBP-Dex-NP (orange) and ANBB-NP (blue) under direct sunlight. The absorbance capacity of samples exposed to sunlight in the open are shown with a dashed line while the samples behind a UV-blocking window are displayed with a solid line.

### *3.4.2 Primary Irradiation Studies (Blue VL and Sun in DI $H_2O$)*

Analysis of the preliminary irradiation data suggests that MB-1-NP was less photostable when compared to ANBB containing NPs. Therefore ANBB-NP and ANBP-Dex-NP were the only NPs that were further studied. These irradiation studies were done in triplicate, with more time points, and longer exposure. To start, ANBP-Dex-NP (0.05 mg $mL^{-1}$) suspensions were irradiated with blue visible light ($\lambda_{ex}$ = 400-500 nm, 0.9 W, 1.05 W $cm^{-2}$) at subsequent time points (15, 30, 45, 60, 90, 120, 150, 180 min) and the UV-Vis was taken after each time point. The initial average $Abs_{max}$ was 0.230 at $\lambda_{max}$ = 421 nm (Figure 3.5a) and the BVL absorbance capacity dropped to 94.3% after 180 min. of exposure (Figure 3.5b). A bathochromic shift in the $\lambda_{max}$ was observed as it shifted from 421 nm with no BVL exposure to 430 nm after 45 min. irradiation and steadily shifted back to 422 nm. These results coincide with the preliminary BVL study, and it appears that the extra hour of exposure did not affect the overall absorbance too drastically. In addition to absorbance studies, the effects of prolonged BVL exposure were also analyzed by DLS

and were compared to a non-irradiated sample. For the irradiated sample, the count rate did not decrease at all under aqueous conditions (Figure 3.5c).

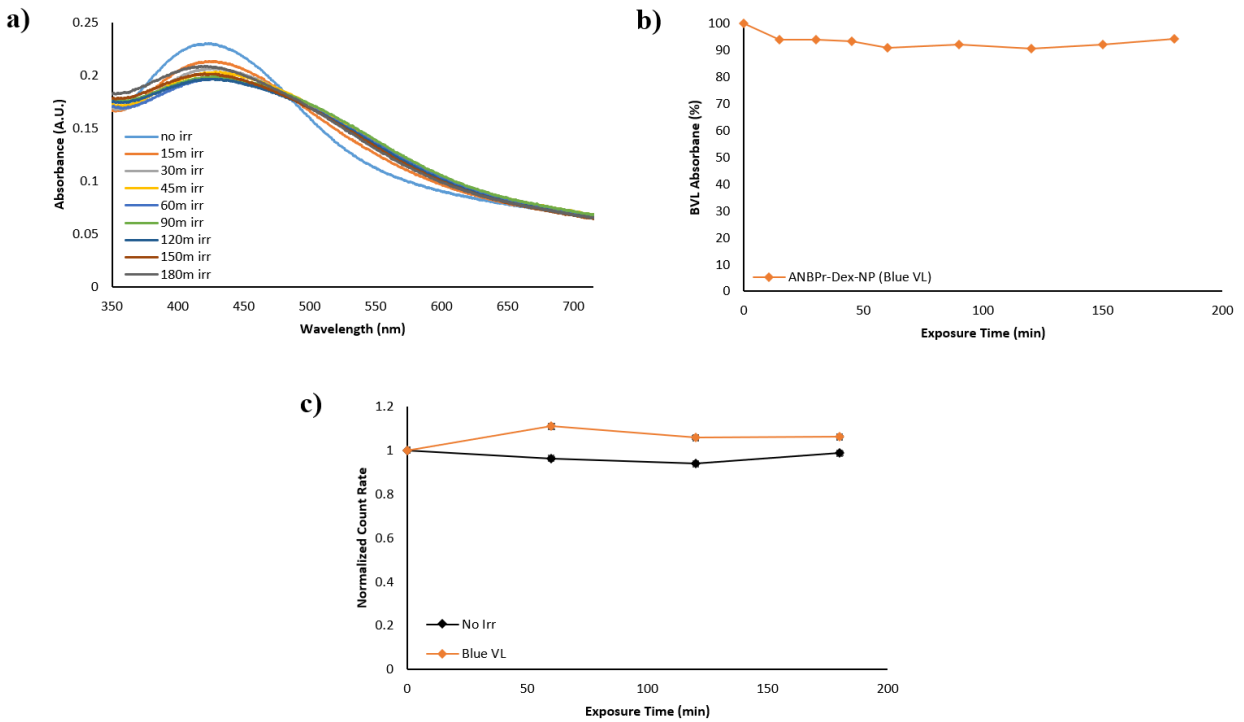


Figure 3.5. (a) The absorbance profile of ANBP-Dex-NP under BVL irradiation. The absorbance was measured at subsequent irradiation times (0, 15, 30, 45, 60, 90, 120, 150, 180 min). (b) The absorbance capacity of the suspension at each irradiation time point. The BVL absorbance capacity was measured by calculating the area under the curve from 400-500 nm. (c) The change in the count rate after each irradiation time point.

The absorbance of ANBB-NP changed the longer the NPs were hydrated. After 24 hours at 4 °C, the particles exhibited an $Abs_{max}$ = 0.303 with a $\lambda_{max}$ = 412 nm. The absorbance capacity decreased to as low as 86.7% after 180 min. exposure (Figure 3.6ac). Conversely, ANBB-NP suspensions that were hydrated for 7 days showed a lower $Abs_{max}$ = 0.160 at a different $\lambda_{max}$ = 450 nm (Figure 3.7b). However, the overall change in absorbance after irradiation seemed to be more stable, only dropping to 93.7% after 180 min (Figure 3.7c). Like ANBP-Dex-NP the $Abs_{max}$ wavelength for both the 0d suspension and 7d suspension both redshifted before shifting back to the original wavelength. The results from the preliminary studies were reproducible and the

changes in absorbance intensity coincided with what was expected, even at longer irradiation times. When compared to the non-irradiated suspension, the 7-day hydrated suspension count rate decreased to 79% of the original count after 180 min. of blue VL exposure while the non-irradiated sample dropped to just 94%.

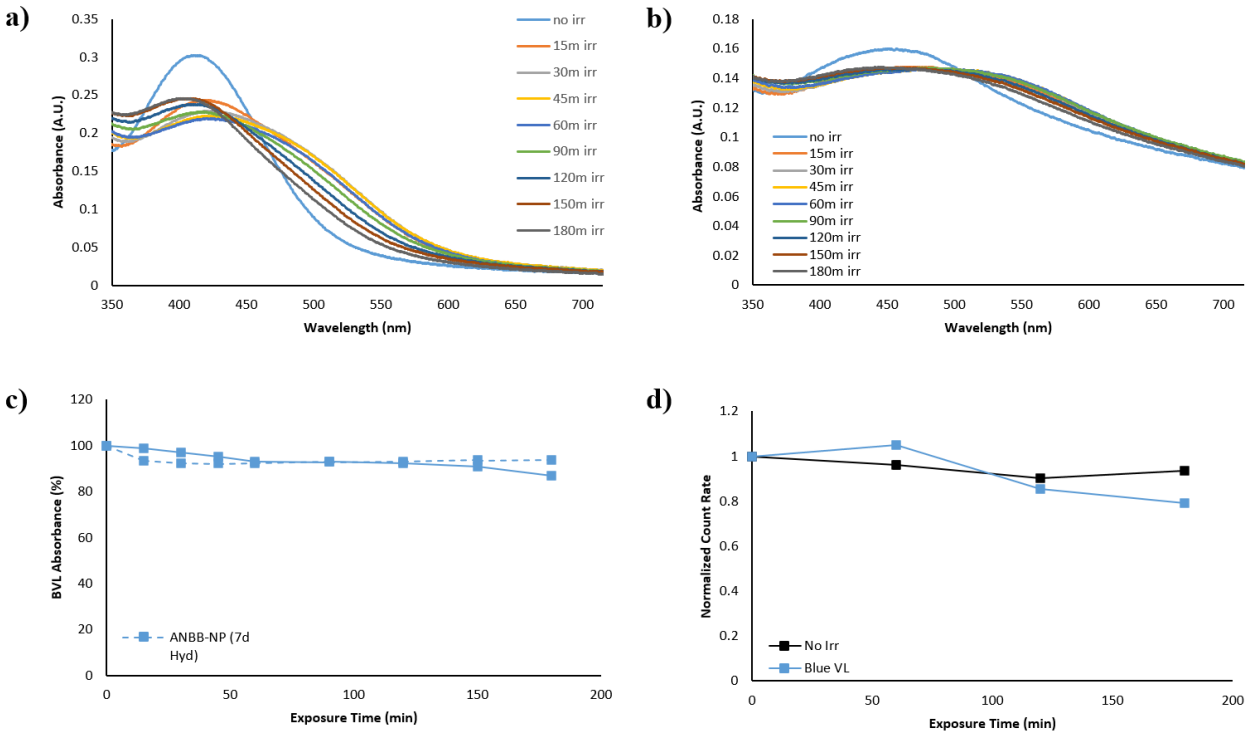


Figure 3.6. The absorbance profiles of ANBB-NP under BVL irradiation after (a) 1 day and (b) 7 days of hydration. (c) The absorbance capacity of the 1day hydration (solid) and 7-day hydration (dash) suspensions. (d) The change in the count rate for the 7-day hydration suspension after BVL exposure.

When comparing ANBB-NP (7-day hydration, 0.1 mg $mL^{-1}$) to ANBP-Dex-NP (24-hour hydration, 0.05 mg $mL^{-1}$) suspensions, both suspensions exhibit very similar blue VL absorbance capacities after 180 min. of exposure. However, over time, the ANBB-NP changes less over time while ANBP-Dex-NP appears to fluctuate.

Again, to go alongside the blue VL exposure, the ANBB particles were again exposed to ambient sunlight at subsequent time points (15, 30, 45, 60, 90, 120, 150, 180 min) and the UV-Vis

was taken after each time point. The window sample of ANBP-Dex-NP showed an average initial absorption of $Abs_{max}$ = 0.222 at $\lambda_{max}$ = 421 nm (Figure 3.7a). The absorbance capacity dropped to 95.8% of its original intensity after 180 min. of sunlight exposure (Figure 3.7c). The ANBP-Dex-NP open samples exhibited an initial $Abs_{max}$ = 0.218 at $\lambda_{max}$ = 421 nm (Figure 3.7b) with the absorbance capacity increasing to 104.1% after 180 min of open exposure (Figure 3.7c). Unlike the blue VL irradiated samples, the open and window exposed ANBP-Dex-NP samples exhibited a hypsochromic shift in $\lambda_{max}$ from 421 nm to 418 nm (open) and 413 nm (window) after 180 min. of exposure. Like the blue VL irradiated samples, there was a noticeable color change, changing from yellow to dark orange after just 30 min. of irradiation. The dark orange color was sustained even with prolonged exposure. For both open and window samples, the BVL absorbance never decreased below 95%. However, open exposed suspension increased in absorbance. This phenomenon was only seen in the open samples, and it is unclear as to why it occurs. The count rate for the open sample showed a slight decrease to 90% after 180 min. of exposure (Figure 3.7d).

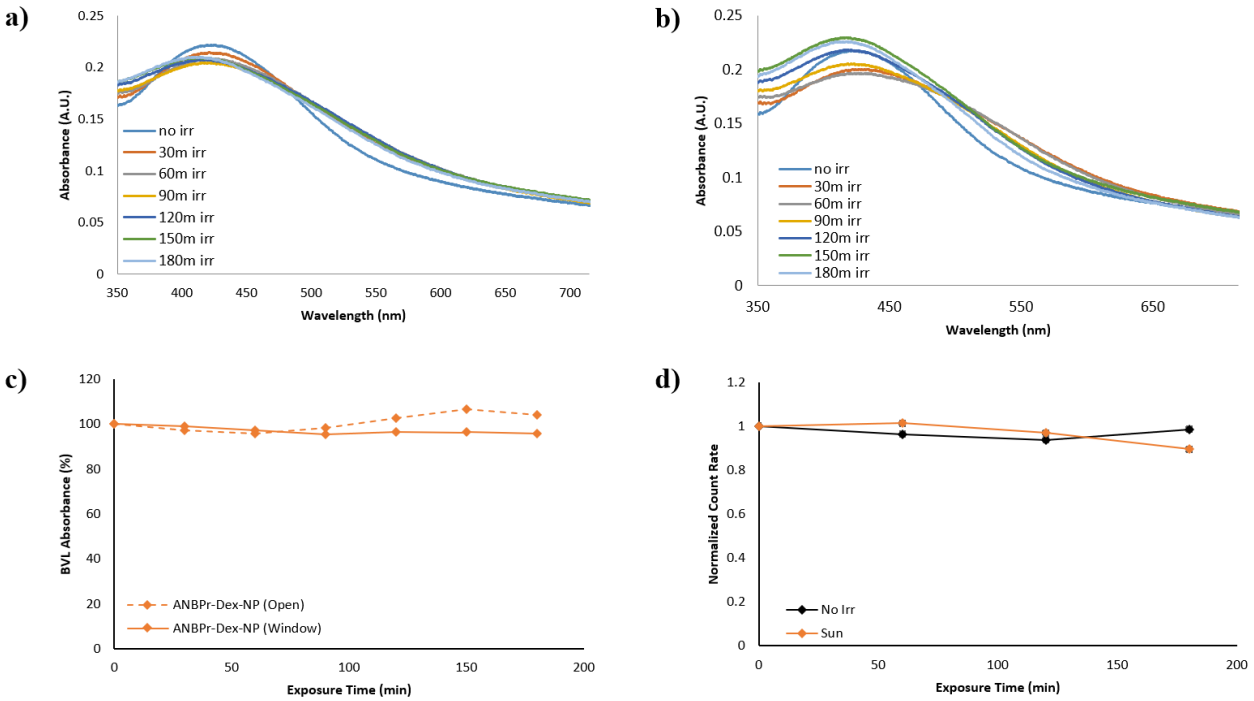


Figure 3.7. The absorbance profiles of ANBP-Dex-NP suspensions exposed to direct sunlight (a) behind a UV blocking window and (b) in the open. (c) The absorbance capacity of the window (solid) and open (dash) suspensions. (d) The change in the count rate for ANBP-Dex-NP exposed to open direct sunlight.

For ANBB-NP, the window sample exhibited an average $Abs_{max}$ = 0.229 at $\lambda_{max}$ = 430 nm (Figure 3.8a). The absorbance capacity decreased to 87.9% and exhibited a bathochromic shift to $\lambda_{max}$ = 436 nm after 90 min. of exposure but blue-shifted to $\lambda_{max}$ = 419 nm, further than the original wavelength (Figure 3.8c). The open samples exhibited an $Abs_{max}$ = 0.227 at $\lambda_{max}$ = 430 nm with the absorbance capacity dropping to 91.9% (Figure 3.8bc). Like the window samples, the open suspensions also exhibited a red-shift to $\lambda_{max}$ = 441 nm after 30 min. of exposure before undergoing a hypsochromic shift to $\lambda_{max}$ = 418 nm, past the original absorbance wavelength. When compared to a non-irradiated sample, ANBB-NPs that were exposed to the sun showed a steady decrease in count rate, dropping to 74% count rate after 180 min. of exposure (Figure 3.8d).

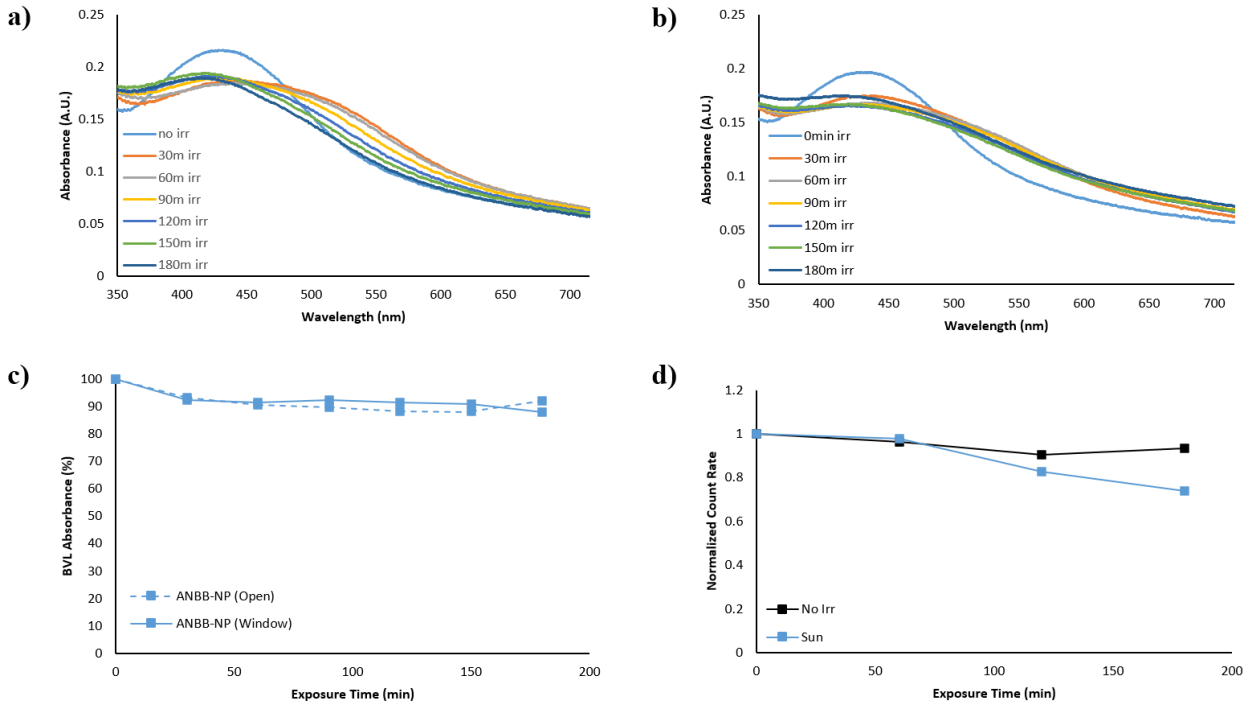


Figure 3.8. The absorbance profiles of ANBB -NP suspensions exposed to direct sunlight in sunlight (a) behind a UV blocking window and (b) in the open. (c) The absorbance capacity of the window (solid) and open (dash) suspensions. (d) The change in the count rate for ANBB-NP exposed to open direct sunlight.

When comparing ANBP-Dex-NP to ANBB-NP, the sun exposure had much more of an affect on the absorbance of ANBB-NP for both window and open samples. Similarly, the % count rate also decreased much more over time than ANBP-Dex-NP. However, the absorbance intensity and count rate did not drop below 80% after 3 hours of exposure, which may indicate the photostability of the NPs. Both NP formulations also displayed a similar color change pattern, going from a yellow suspension to deep orange after just 30 min. of exposure which appeared to get lighter the longer the sample was exposed (Figure 3.9).

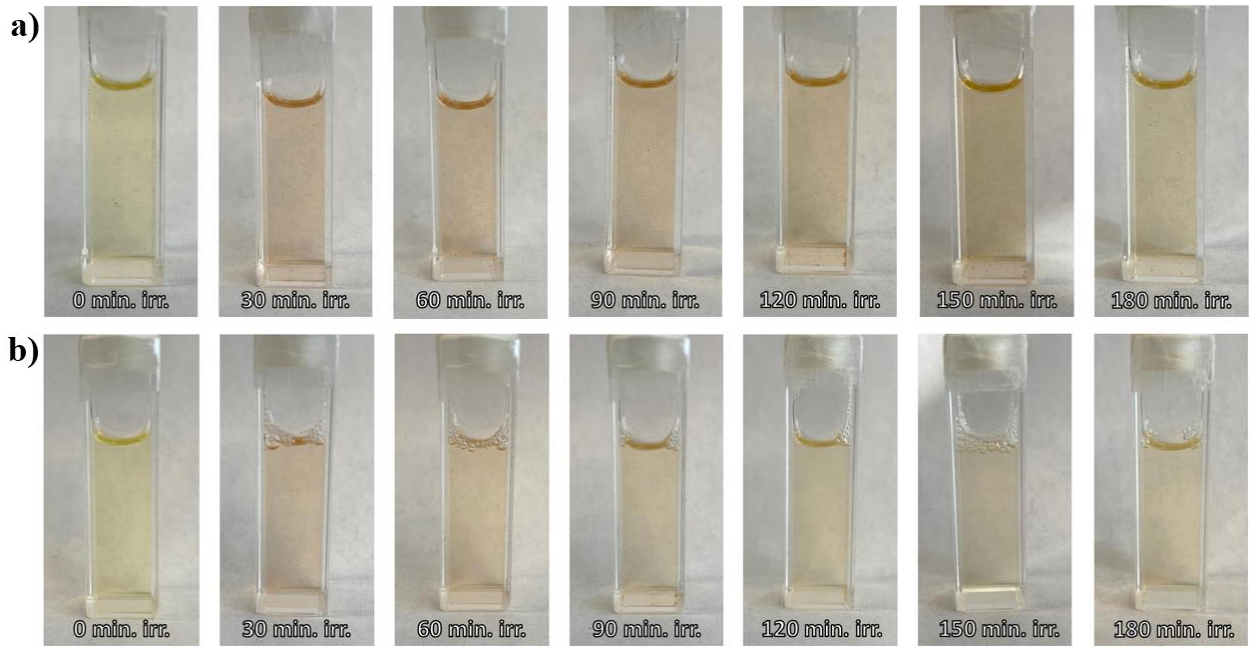

Figure 3.1. Photos of (a) ANBP-Dex-NP and (b) ANBB-NP after open sun exposure. Both suspensions showed a similar parttern of color change, from yellow to orange after just 30 minutes of exposure.

*3.4.3 Stability of Non-Irradiated NP Suspensions*

The stability of the non-irradiated NP suspensions was assessed by UV-Vis and DLS over a period of 31 days. The BVL absorbance capacity of ANBP-Dex-NP fluctuated over time, never dipping below 85%. but ended at 101.6% after 31 days. ANBB-NP exhibited a steady decline in absorbance capacity, dropping to 67.7% at the end of the study. The count rate of ANBP-Dex-NP decreased to 83% after 31 days but ANBB-NP displayed a more dramatic decrease, dropping to 62%. However, when looking at the change in size over the span of the study, ANBB-NP's increased over time to 110%, starting from 166 ± 2.3 nm and ending at 183 ± 3.0 nm. ANBP-Dex-NPs only saw a 4% loss in its size, from 160 ± 1.1 nm to 153 ± 1.3 nm (Figure 3.10).

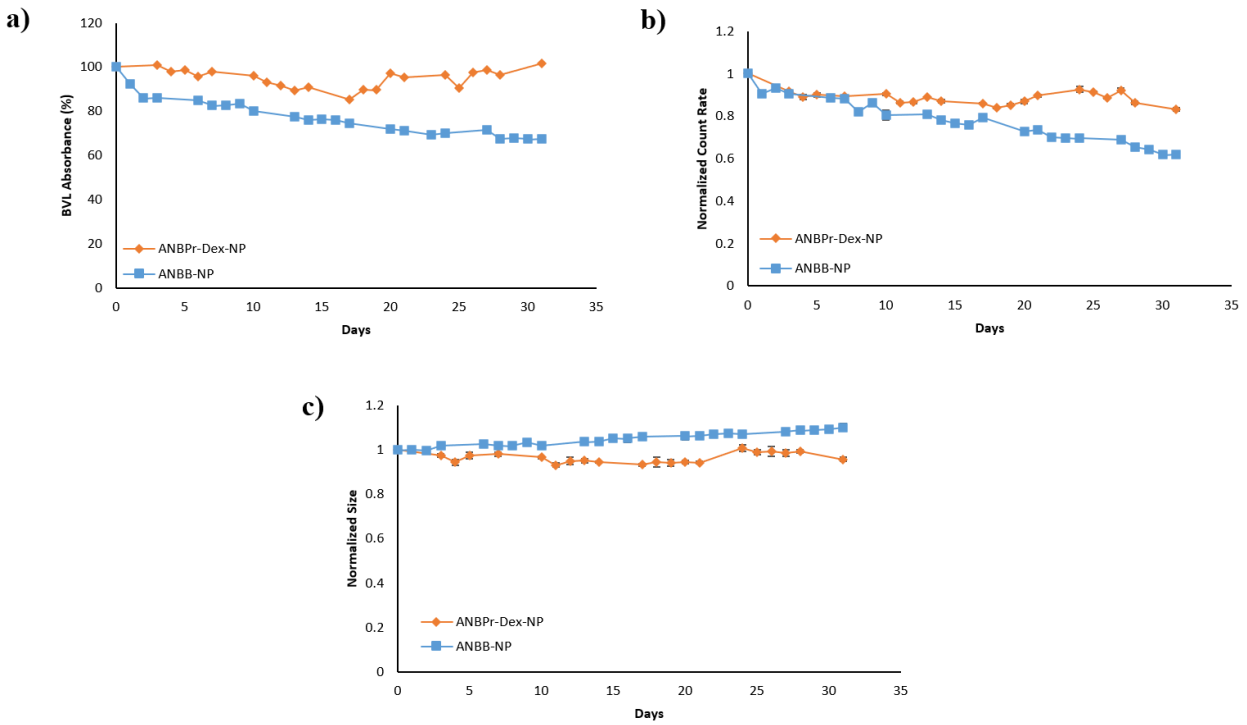


Figure 3.2. The stability of non-irradiated particles measured by (a) absorbance capacity, (b) change in count rate, and (c) change in particle size over a 31-day period.

### *3.4.4 Degradation Studies*

For ANBP-Dex-NP (0.05 mg $mL^{-1}$ in $H_2O$), the supernatant of the non-irradiated aliquot registered an $Abs_{max}$ = 0.002 at $\lambda_{max}$ = 409 nm which amounts to 1.4% of the absorbance capacity of the NP suspension. The absorbance capacity of the supernatants got as high as 3.4% after 180 mins. before ending at 1.5% (Figure 3.11c). By comparison, ANBB-NP (0.1 mg $mL^{-1}$ in $H_2O$, 4-day suspension) supernatants displayed a steady increase in BVL absorbance with prolonged irradiation. The non-irradiated sample exhibited an $Abs_{max}$ = 0.003 at $\lambda_{max}$ = 411 nm which amounts to 1.3% and getting as high as 6.0% after 240 min. exposure (Figure 3.12c).

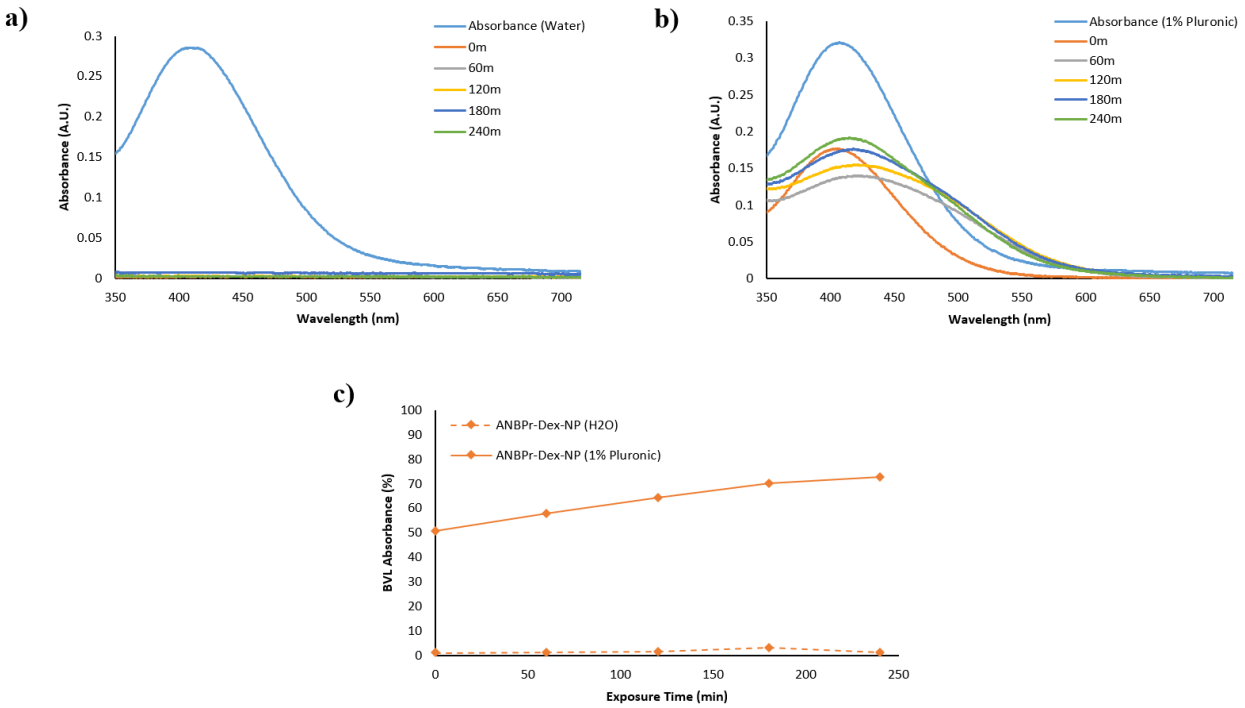


Figure 3.11. The absorbance profiles of ANBP-Dex-NP supernatants after centrifugation in (a) DI H2O and (b) 1% Pluronic F127. (c) The BVL absorbance capacity of the supernatants.

Although the NP suspensions do not leak small molecules under aqueous conditions, the lack of absorbance may be because the potential photoproducts are not soluble in the aqueous environment and are trapped inside the hydrophobic core of the NPs. To address the solubility issue, the suspensions were irradiated in 1% Pluronic® F127 and centrifuged. The supernatants of both suspensions exhibited a much stronger absorbance intensity than the DI $H_2O$ suspensions. The non-irradiated supernatant of ANBP-Dex-NP showed a significant absorbance intensity at $Abs_{max}$ = 0.176 (50.8%) at $\lambda_{max}$ = 407 nm. The absorbance capacity continued to increase with more exposure, getting to 72.6% after 240 mins. In contrast, the ANBB-NP supernatants exhibited a lower absorbance intensity with the non-irradiated aliquot $Abs_{max}$ = 0.043 (17.6%) at $\lambda_{max}$ = 411 nm. After 120 min. irradiation, the absorbance was at its highest at 16.5% before tapering out to 15.2% after 4 hours of BVL exposure (Figure 3.12c). Supernatants from both suspensions

displayed a bathochromic shift after irradiation. ANBP-Dex-NP shifted from $\lambda_{max}$ = 407 nm to 418nm while ANBB-NP shifted from $\lambda_{max}$ = 407 nm to 414 nm.

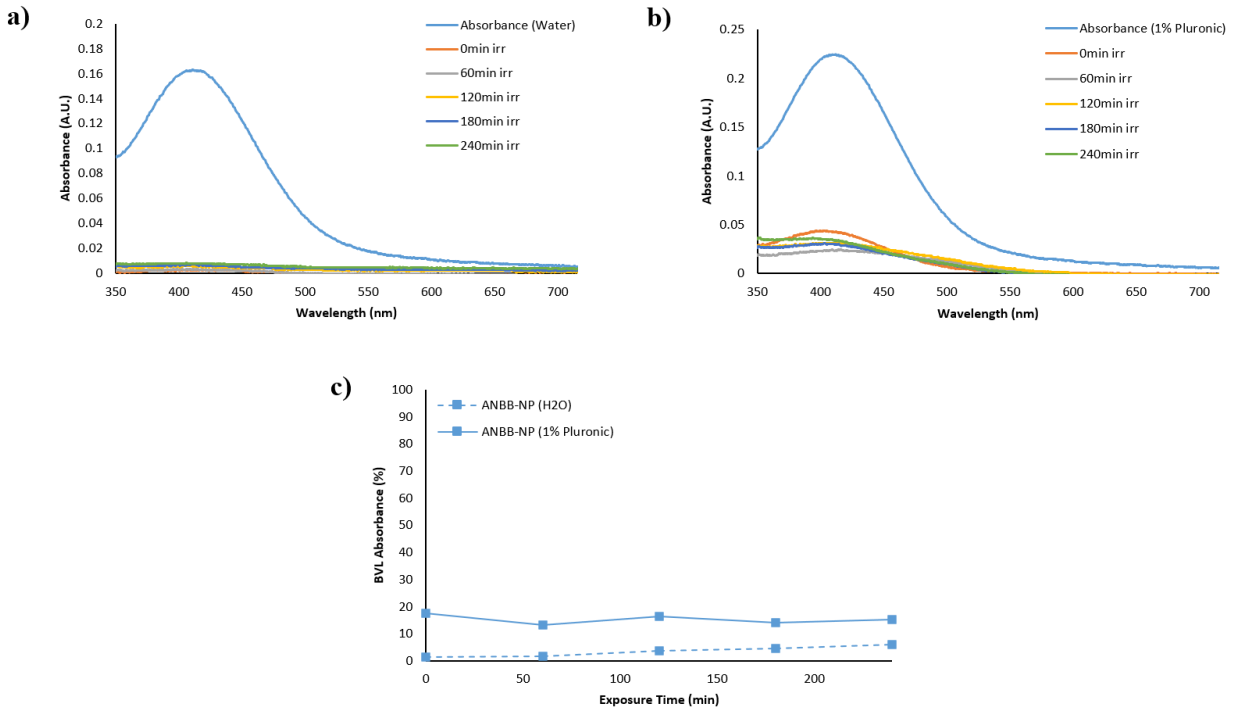


Figure 3.12. The absorbance profiles of ANBP-Dex-NP supernatants after centrifugation in (a) DI H2O and (b) 1% Pluronic F127. (c) The BVL absorbance capacity of the supernatants.

The supernatants were then lyophilized and analyzed by MALDI-TOF to check for the presence of any photodegraded small molecules. ANBB-NP irradiated supernatants appear to contain a photoproduct at 550.725 m/z. However, the peak does not correspond to the expected mass of the smallest theoretical photoproduct anticipated.

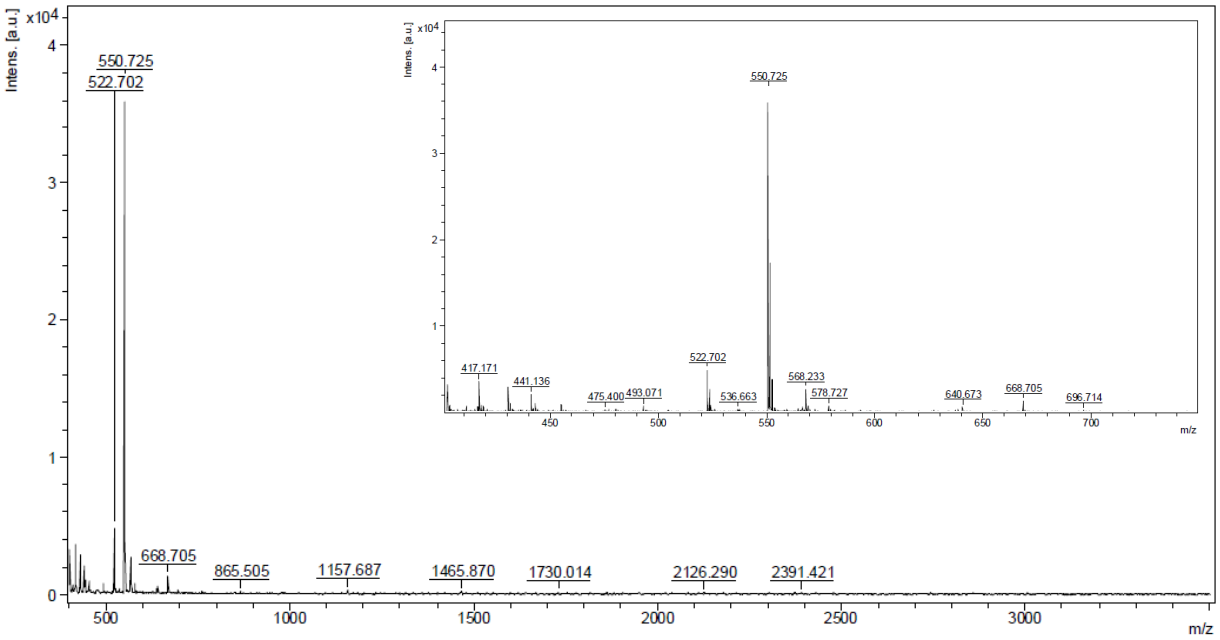


Figure 3.13. Analysis of the lyophilized supernatants of ANBB-NP using MALDI-TOF (Agilent 6230 Accurate-Mass TOFMS), scanning from 450 m/z to 3500 m/z.

### 3.5 Discussion

Studies have shown that some active chemical sunscreens lose their protective ability when exposed to UV radiation.[22,23] Sunscreens that utilize organic filters have displayed even greater photoinstability than their inorganic counterparts due to their absorption of UV light instead of scattering. Organic sunscreen filters absorb UV light, converting the molecules to their excited states which is later dissipated. If the energy release from the excited state is not effective, the organic molecules can undergo rearrangement, photocleave, and generate radicals. To ensure the molecules can be stabilized, many commercial sunscreen formulations have other organic additives, such as octocrylene, to either quench the excited states. Even still, most commercial sunscreens still include organic filters. One study compared the photostability of three commercial broad-spectrum sunscreens found in the US, containing 2-3% of avobenzone, 4-6% oxybenzone, and varying amounts stabilizers. The study found that a formulation containing 2% avobenzone

and 7.5% octinoxate was not photostable, due to the loss absorption in the UVB (20%) and UVA (42%) regions.[24] The other two formulations were considered more photostable with only minor losses of 1-5% across both UVB and UVA regions. In comparison, ANBP-Dex-NP's exposed to direct sunlight saw an increase in absorbance capacity from 400 nm – 500 nm. Conversely, the UV-blocked window samples only saw loss of 1.2-4.2% during the exposure time. However, ANBB-NP was not as photostable, showing a larger decrease in absorbance capacity in the open sample, losing 7.8% after just 30 min. of exposure to losing 12.1% at the conclusion of the study. Soley based on its absorbance profile, ANBP-Dex-NP would be a suitable additive for current sunscreen formulations as a blue visible light absorber. In contrast, due to its more significant loss of absorbance capacity, it would not be as suitable. However, compared to the one commercially available sunscreen, ANBB-NP still has a better absorbance capacity.

Regarding the stability of the stability of the non-irradiated NPs, ANBP-Dex-NP seems to fair better in terms of BVL absorbance capacity, count rate, and size. The noticeable difference in the absorbance capacity of ANBB-NP could be due to the aggregation of the particles in water, which is indicative in the increase of both size and PdI of the suspensions. Over time, the size of the non-irradiated particles increased alongside the PdI, going from 0.111 to 0.163 over 31 days, an increase of 47%.

Although its BVL absorbance capacity was lower than ANBP-Dex-NP, ANBB-NP does appear to be better in terms of releasing photodegradation products from the NPs under sink conditions with its supernatants only exhibiting 15.2% absorbance compared to ANBP-Dex-NP at 72.6%. However, under purely aqueous conditions, ANBP-Dex-NP seems to retain the possible photoproducts better than ANBB-NP, with the supernatants exhibiting 1.4% absorbance compared to ANBB-NP's 6.0%. The MALDI-TOF data only displayed one major peak corresponding to

550.7 m/z. The mass of the smallest theoretical photoproduct of ANBB-P is expected to be 525.3 m/z. The segment found in the MALDI-TOF does not match any of our suspected photoproduct. The cytotoxic effect of the irradiated NPs still needs to be investigated.

### 3.6 Conclusion

With concerns of the deleterious effects of prolonged blue visible light exposure on the rise, there is a growing need for sun protection that goes beyond UVB/A wavelengths. Here we introduce blue light absorbing NP formulations as a potential additive to current sunscreen formulations. Two of our formulations, ANBB-NP and ANBP-Dex-NP, are shown to be photostable as their absorbance intensity does not decrease with prolonged irradiation. However, ANBB-NP seems to produce small molecules after blue light exposure. There are a lot of improvements that could be made to make this a more thorough study. First, clearer characterization of the polymers would be much more beneficial towards making conclusions about the NP formulations discussed above. Second, for the degradation of the NPs, size exclusion chromatography should be utilized to separate all the components that make up the polymeric nanoparticles. However, the use of a Franz diffusion cells with skin like membranes would result in a much more conclusive study.

### 3.7 Abbreviations

UV, ultraviolet; VL, visible light; IR, infrared; ROS, reactive oxygenated species; DNA, deoxyribonucleic acid; IPD, immediate pigment darkening; PPD, persistent pigment darkening; DT, delayed tanning; BVL, blue visible light; MELASQoL, melasma quality of life scale; MASI, melasma area and severity index; FDA, Food and Drug Administration; ANBB, 2-(4′-*N*-

dimethylamino-4-nitro-[1,1′-biphenyl]-3-yl)butane-1,4-diyl dicarbonyl; ANBP, (2-(40-(N,N-dimethylamino)-4-nitro-[1,10-biphenyl]-3-yl) propyl carbonyl); MB-1-P, methyl BIST polymer; BIST, dinitro derivative of bisstyrylthiophene; DLS, dynamic light scattering; TBDMS-Cl, tert-Butyldimethylsilyl chloride; TBAF, tetra-n-butylammonium fluoride; DCM, dichloromethane; DME, dimethoxyethane; TBACl, tetrabutylammonium chloride; DMF, dimethyl formamide; THF, tetrahydrofuran, LC-MS, liquid chromatography-mass spectroscopy; NMR, nuclear magnetic resonance; NP, nanoparticle; PVA, polyvinyl alcohol; CDI, 1,1′-carbonyldiimidazole; PBS, phosphate buffered saline; DI, deionized; MALDI-TOF, matrix-assisted laser desorption ionization time-of-flight;

### 3.8 Acknowledgements

NMR spectra were acquired at the UCSD Skaggs School of Pharmacy and Pharmaceutical Sciences NMR Facility. Mass spectroscopy data was acquired at the UCSD Department of Chemistry and Biochemistry Molecular Mass Spectrometry Facility. Gel Permeation Chromatography data was acquired at the UCSB Materials Research Laboratory Polymer Characterization Facility and the Godula Research Laboratory at UCSD.

This chapter was coauthored with Dr. Adah Almutairi. The dissertation author was the principal researcher and author of this chapter.

### 3.9 References

1) Cadet, J., Douki, T., *Photochem. Photobiol. Sci.*, **2018**, 17, 1816.

2) Krutmann, J., Bouloc, A., Sore, G., Bernard, B.A., Passeron, T.; *J. Dermatol. Sci.*, **2017**, 85 152–161.

3) Liebmann, J., Born, M., Kolb-Bachofen, V. *J. Invest. Dermatol.*, **2010**, 130, 259-269

4) Tonoli, P.N., Chiarelli-Neto, O., Santacruz-Perez, C., Junqueira, H.C., Watanabe, I.S., Ravagnani, F.G., Martins, W.K., Baptista, M.S.; *J. Invest. Dermatol.*, **2017**, 137, 2447-2450.

5) Zastrow, L., Meinke, M.C., Albrecht, S., Patzelt, A., Lademann, J.; *Adv. Exp. Med. Biol*., **2017**, 996, 311-318.

6) Panich, U., Sittithumcharee, G., Rathviboon, N., Jirawatnotai, S.; *Stem. Cells. Int*., **2016**, 2016, 7370642.

7) Schalka, S., de Paula, C.M., Sawada, L.Y., Canale, C.C., de Andrade, T.N.; Clin. *Cosmet. Investig. Dermatol*., **2019**, 12, 605-616.

8) Mahmoud, B.H., Ruvolo, E., Hexsel, C.L., Yang, L., Owen, M.R., Kollias, N., Lim, H.W., Hamzavi, I.H.; *J. Invest. Dermatol*., **2010**, 130, 2092-2097.

9) Duteil, L., Cardot-Leccia, N., Queille-Roussel, C., Maubert, Y., Harmelin, Y., Boukari, F., Ambrosetti, D., Lacour, J.P., Passeron, T., *Pigment Cell Melanoma Res*., **2014**, 27, 822-826.

10) Kohli, I., Chaowattanapanit, S., Mohammad, T.F., Nicholson, C.L., Fatima, S., Jacobsen, G.,Kollias, N., Lim, H.W., Hamzavi, I.H.; *Br. J. Dermatol.*, **2018**, 178, 1173-1180.

11) Misun, K., Shibata, T., Kwon, S., Park, T.J., Kang, H.Y.; *Sci. Rep*., **2018**, 8, 4235; D'mello, S.A.N., Finlay, G.J., Baguley, B.C., Askarian-Amiri, M.E.; *Int. J. Mol. Sci.*, **2016**, 17, 1144.

12) Handog, E.B., Enriquez-Macarayo, M.J., "Melasma and Vitiligo in Brown Skin", Springer India, 2017; Leeyaphan C., Wanitphakdeedecha, R., Manuskiatti, W., Kulthanan, K..; *BMC Dermatol.*, **2011**, 11, 16.

13) Castanedo-Cazares, J.P., Hernandez-Blanco, D., Carlos-Ortega, B., Fuentes-Ahumada, C., Torres- Alvarez, B.; *Photodermatol. Photoimmunol. Photomed.*, **2014**, 30, 35-42.

14) Matta, M.K., Zusterzeel, R., Pili, N.R.; *JAMA*, **2019**, 321, 2082-2091.

15) Krause, M., Klit, A., Jensen, M.B., Soeborg, T., Frederiksen, H., Schlumpf, M., Lichtenseiger, W., Skakkebaek, N.E., Drzewiecki, K.T.; *Int. J. Androl.*, **2012**, 35, 424-43.

16) Damiani, E., Baschong, W., Greci, L.; J. *Photochem. Photobiol. B,* **2007**, 87, 95-104; Hanson, K.M., Gratton, E., Bardeen, C.J.; *Free Radical Biology & Medicine*, **2006**, 41, 1205-1212.

17) Agarwal, H.K., Janicek, R., Chi, S.H., Perry, J.W., Niggli, E., Ellis-Davies, G.C.; *J. Am. Chem. Soc.*, **2016**, 11, 3687-3693.

18) L. Donato, A. Mourot, C. M. Davenport, C. Herbivo,D. Warther, J. Leonard, F. Bolze, J. F. Nicoud, R. H. Kramer, M. Goeldner and A. Specht, *Angew. Chem.*, **2012**, 51, 1840.

19) Carling, C.J., Viger, M.L., Huu, V.A.N., Garcia, A.V., Almutairi, A.; *Chem. Sci.*, **2015**, 6, 335-34.

20) Peters, M., Trobe, M., Tan, H., Kleineweischede, R., Breinbauer, R.; *Chem. Eur. J.*, 2013, 19, 2442-2449.

21) Broaders, K. E.; Grandhe, S.; Frechet, J. M. J. *J Am Chem Soc*, **2011**, 133, 756.

22) N. Serpone, A. Salinaro, A.V. Emeline, S. Horikoshi, H. Hidaka, J. Zhao, *Photochem.Photobiol. Sci.*, **2002**, 1, 970–981.

23) N. Tarras-Wahlberg, G. Stenhagen, O. Larko, A. Rosen, A.M. Wennberg, O.Wennerstrom, *J. Investig. Dermatol*., **1999**, 113, 547–553.

24) Beasley, D.G., Meyer, T.A., *Am. J. Clin. Dermatol.*, **2010**, 11, 413-421.